Modulation of Proteostasis for the Efficient Intracellular Transport of the F508 Mutant of Cystic Fibrosis Transmembrane Conductance Regulator

Thesis

Modulation of proteostasis for the efficient intracellular transport of the ΔF508 mutant of cystic fibrosis transmembrane conductance regulator

Ramanath Narayana Hegde

MSc

Thesis submitted for the Degree of Doctor of Philosophy

Life and Biomolecular Sciences

The Open University

Date of Submission; 24 September 2013
Date of Award; 30 April 2014

Affiliated Research Centre: Telethon Institute of Genetics and Medicine, Naples, Italy

September 2013

To my Late Grandfather

You wanted me to become an artist

I chose science

You know, they say

"SCIENCE IS AN ART"

I have not become an artist till now

But trying to become one

To my loving family and relatives

Abstract

The cystic fibrosis transmembrane conductance regulator (CFTR) ΔF508 mutant (ΔF508CFTR) contributes to 70% cystic fibrosis cases, and it undergoes aberrant proteostasis, misfolding, intracellular retention and degradation. Targeting ΔF508CFTR proteostasis components has been successful in the partial rescue of ΔF508CFTR at the plasma membrane. Drug screening has identified correctors which rescue a fraction of the ΔF508CFTR at the plasma membrane. However, all these correctors are marginally effective and are not therapeutically viable.

This thesis project used a systems-biology-based meta-analysis approach of gene expression induced by corrector drugs to infer their mechanisms of action, and this led to the identification of a group of genes that are commonly regulated by many of these drugs. These groups of genes were used to determine the networks/ pathways/ molecules that might be correlated with their correction. These include components of RNA processing, the cell cycle, ubiquitin ligases, and kinases, many of which have led to partial rescue of ΔF508CFTR when they have been depleted by RNA interference. Furthermore, two of these pathways are characterised here: the MAP3K11-JNK cascade and the CaM kinase (CAMKK2) cascade. Several members of these cascades rescued ΔF508CFTR. The MAP3K11-initiated pathway has a role in ER-associated degradation and plasma-membrane stability of ΔF508CFTR. MAP3K11 also appears to link oxidative stress and inflammation to intracellular proteostasis of ΔF508CFTR. Some upstream activators and downstream targets of MAP3K11 can also rescue ΔF508CFTR. Drugs that inhibit the MAP3K11-JNK cascade rescued functional ΔF508CFTR at the plasma membrane. Combinations of these drugs with the previously clinically studied corrector pharmacochaperone VX-809 led to a high level of correction of ΔF508CFTR, which was much greater than for VX-809 alone. Many candidate genes and drugs that are identified in the current study open the way to the development of the new efficient therapeutic agents for cystic fibrosis caused by the ΔF508 mutation.

Acknowledgements

One of the joys of completion is to look over the journey past and remember all the people who have helped and supported me along this long but fulfilling road.

As I re-find them, here I am assembling the ones who meant most to me.

I would like to express my heartfelt gratitude to my director of studies, Dr. Alberto Luini for his constant guidance, support, motivation and untiring help during the course of my PhD. He has given me enough freedom during my research, and he has always been nice to me. I will always remember his calm nature, and the words "is there anything new". I would like to express my sincere regards to Prof. David Stephens, University of Bristol for his kind guidance as an external supervisor. I would like to thank Dr. Antonella De Matteis and Dr. Giancarlo Parenti for advising me as my thesis committee members.

My special thanks to Seetharaman Parashuraman for all the discussions and support during this PhD research project. Moreover when I came to Naples his help was outstanding in making my stay comfortable. I extend my gratitude to the people who helped with the bioinformatic analysis, especially Francesco Iorio, Fabrizio, Fabiana, Veer and the all the people at the bioinformatic core TIGEM. Special thanks to Dr Diego di Bernardo for collaboration on the bioinformatic part of the present study. I extend my gratitude to Dr. Luis Galietta and colleagues at his laboratory and Dr. D Y Thomas and his colleagues for the help they provided with functional assays.

This research was not possible without support from all the senior members of the laboratory: Anita, Antonella, Jorge, Juan, Maria, Riccardo and junior members of laboratory; Advait, Altea, Laura, Rosaria. They also provided the nice and friendly atmosphere at the laboratory that I will carry in my memory for a long time. Heartfelt thanks to Dr. Daniela Corda for her encouragement during my PhD research. I would like to thank all the colleagues at Dr. Daniela Corda's laboratory, Dr. Antonella De Matteis laboratory, Dr. Giovanni D'Angelo and members of his laboratory, Dr. Antonino Colanzi and members of his laboratory, Dr. Roman Polishchuk and members of his laboratory for help with reagents, discussions and friendship. I extend my gratitude to Dr. Christopher Berrie for help with language editing.

I would also like to thank my examiners: Dr. David Sheppard and Dr. Enrico Maria Surace and chair of the examination committee and co-ordinator of The Open University PhD programme Dr. Sandro Banfi for reviewing the thesis.

I gratefully acknowledge the Telethon Foundation and other the funding sources that made my PhD work possible. I acknowledge all the scientific staff, and office staff at TIGEM and IBP for their support.

I am thankful to my former research advisor, Dr. Lalitha R Gowda and her lab members: Dr. Santosh Kanade, Dev, Lings, and other colleagues. I am grateful to Prof. R R Dighe who provided an opportunity to work at his laboratory; I thank Mandar, Krishnamurthy, Gaurav, Satarupa, Ankur and other colleagues form Dr. R. R. Dighe's laboratory. The periods at these laboratories were helpful to develop my knowledge and research skill. I express my gratitude to Dr. Ramachanadra, for his unconditional support during my stay at IISc. I thank all my teachers at school, lecturers at collage and professors at the university without their contribution the journey on this road would have been tougher.

I especially thank my wife Rajeshwari, mum Savitha, dad Narayana, and sister Shubha for the support they provided me in all my pursuits for their unconditional love and care. Most importantly, Rajeshwari supported, encouraged me with patience and love which were undeniably the bedrock upon which the past few years of my life have been built. I would not have made it this far without their support. I thank my in-laws, Vijaya, Subray, and Shankar for being supportive and caring. I am grateful to Ananth, Annie, V. G. Hegde and his family, G. R. Janyath, G.S. Ranganath and Mangala for their care, all my cousins and relatives for their support in these years. I extend my gratitude to Dr. G. S. Amur and family, G.M. Hegde and family for their support during my postgraduate study.

I thank my best friend Ravish for being so caring, helpful and supporting which contributed greatly to my progress. I am grateful to Ravish also for those wonderful years of company from collage days to beyond and continuing. I will cherish the weekend outings the discussions, critics, shopping and dinners. I extend my gratitude to Nagaraj Halkani, Ventakraman, Ramachandra and Suresh Bhat for their care.

I also thank all my friends for providing support and friendship and making my life at large an enjoying journey.

Table of Contents

List of abbreviations

ADP -adenosine diphosphate

AMP- adenosine monophosphate

APS - ammonium persulphate

ATP- adenosine triphosphate

cDNA- complementary deoxyribonucleic acid

CF- cystic fibrosis

CFBE -cystic fibrosis bronchial epithelia

CFTR -cystic fibrosis transmembrane conductance regulator

CHIP - carboxyl-terminus of Hsp70-interacting protein

CHX -cyclohexamide

COPII -coat protein complex II

ΔF508CFTR- CFTR mutant with deletion of phenylalanine at position 508

DMEM –Dulbeco's modified Eagle's medium

DNA- deoxyribonucleic acid

DPBS- Dulbecco`s phosphate buffered saline

E1- ubiquitin-activating enzyme

E2- ubiquitin-conjugating enzyme

E3- ubiquitin-protein ligase

ECL -enhanced chemiluminescent substrate

EDEM- ER degradation enhancing α-mannosidase-like protein

EDTA- ethylenedinitrilo-tetraacetic acid disodium salt

EndoH^r -EndoH resistant

EndoH^s -EndoH sensitive

ER -endoplasmic reticulum

ERAD –ER-associated degradation

ERQC -ER quality control system

FBS - foetal bovine serum

HA- haemagglutinin

Hop- Hsp organiser protein

Hsc- heat shock cognate

Hsp- heat-shock protein

HSR-heatshock response

ICL- intracellular loop

IP- immunoprecipitation

IPACA-ingenuity pathways analysis core analysis

MAPK- mitogen-activated protein kinase

MEM- minimum essential medium

MEM-NEAA- MEM non-essential amino acid

mRNA- messenger ribonucleic acid

MSD –membrane-spanning domain

NBD- nucleotide-binding domain

PBS - phosphate-buffered saline

PDE- phosphodiesterase

pH- potential of hydrogen

PI- protease inhibitor cocktail

PM- plasma membrane

PQC- peripheral quality control

RIPA- Radio-immunoprecipitation analysis

RMA1- RING membrane associated 1

RNF1- RING finger protein 1

RT-PCR reverse transcriptase-polymerase chain reaction

SAPK- stress-activated protein kinase

SDS- sodium dodecylsulphate

SDS-PAGE- SDS polyacrylamide gel electrophoresis

siRNA- small-interfering RNA

TEMED - tetramethylethylenediamine

UPR-unfold protein response

IPACA Network Legends


Cytokine/Growth factor


Enzyme


G-protein coupled receptor


Ion channel


Kinase


Ligand-dependent nuclear receptor


Peptidase


Phosphatase


Transcription regulator


Translation regulator


Transmembrane receptor


Transporter


Micro-RNA


Complex/ group


Other

— Direct relation

--- Indirect relation

List of figures

List of Tables

Chapter 1

General Introduction

1.1. Cystic fibrosis

Cystic fibrosis (CF) was recognised in 1938 as a cystic fibrosis of the pancreas (Andersen 1938). The mucus was plugging the glandular ducts during the autopsy studies of malnourished infants. This disease had the hallmarks of malabsorption, growth failure, and pulmonary infection. The thick, sticky mucus that clogs the ducts of mucus glands throughout the body gave rise to the alternative designation of "mucoviscidosis" (Farber 1944).

In 1946, CF was recognized as a genetic disease that is transmitted in an autosomal recessive pattern (Andersen and Hodges 1946). The important discovery by Dr. Paul di Sant'Agnese in 1948 demonstrated a five-fold excess of sodium and chloride in the sweat of patients with CF (di Sant'Agnese et al. 1953). This study established elevated sweat chloride concentration as one of the first diagnostic tests for CF. The elevated chloride levels in all CF patients hinted that the basic defect may not be mucus related, and further in 1983 chloride transport was established as the primary defect in CF, using the sweat duct (Quinton 1983).

In 1989 the gene responsible for CF was discovered, cloned, characterised, and named the cystic fibrosis transmembrane conductance regulator (CFTR) (Kerem et al. 1989; Riordan et al. 1989; Rommens et al. 1989). Several tissues, like the kidney, pancreas, intestine, heart, vas deferens, sweat duct and lung, express the CFTR channel at the apical membrane of epithelia (Bradbury 1999; Bertrand and Frizzell 2003). Loss of function of CFTR is responsible for CF, the most common inherited disease in Caucasians (Riordan et al. 1989). In molecular genetic terms CF is caused by the presence of two CF-causing mutations one in each parental *CFTR* gene, in physiological terms CF is a disorder of electrolyte transport across epithelial membranes resulting from absence or anomaly of the CFTR protein (Bombieri et al. 2011). There is an extensive variation in range and severity of symptoms and organs involved between and within individuals. CF is characterised by elevated sweat chloride concentrations, lung bacterial infections and bronchiectasis, pancreatic insufficiency, intestinal obstruction, biliary cirrhosis, and congenital

bilateral absence of the vas deferens, and fatal lung disease (Davis 2006). In contrast, the hyperactivity of CFTR channels can lead to secretory diarrhoeas (Al-Awqati 2002).

The lung phenotype in CF is characterised by a ferocious cycle of obstruction, inflammation and infection that progressively damages the airway tissue, which lead to respiratory failure and death (Lubamba et al. 2012). The CF lung and its airways are susceptible to chronic infection by *Staphylococcus aureus, Hemophilus influenzae, Pseudomonas aeruginosa, Burkholderia cepacia* complex organisms, *Stenotrophomonas maltophilia,* and *Achromobacter xylosoxidans* (Chmiel et al. 2013) which form biofilms and activate persistent inflammatory signals (Chmiel and Davis 2003). As part of the host defence strategy, neutrophils are recruited to prevent infection, but ultimately this inflated inflammatory response worsens lung function and leads to lung failure (Chmiel et al. 2013).

Patients with CF have increased levels of oxidative stress in the airways compared to unaffected individuals (Hull et al. 1997), which can be due to inflammation in the lungs or to decreased glutathione levels (Berube et al. 2010). The most common cause of death in CF is lung failure that is typically triggered by acute bacterial infections, which promote the progressive loss of the tissue architecture in lungs (bronchiectasis) (Chmiel and Davis 2003). In 1938 70% of babies with CF died within the first year of life (Andersen, 1938). Today the median life expectancy of patients with CF in the USA has improved, to 41 years in 2012 (http://www.cff.org/UploadedFiles/research/ClinicalResearch/PatientRegistryReport/2012-CFF-Patient-Registry.pdf). CF affects 1 in 2500 new-borns (Collins 1992), and hence there are tremendous efforts to find a therapy to cure CF.

1.2. Cystic fibrosis transmembrane conductance regulator

Cystic fibrosis transmembrane conductance regulator (CFTR) is a protein that functions as a chloride channel in the plasma membrane (PM) (Riordan et al. 1989). CFTR is the only member of the ATP-binding cassette (ABC) transporter family that forms a regulated chloride channel, ATP binding and hydrolysis by the nucleotide-binding domains acts a timing mechanism to control the duration of channel openings (Hwang and Sheppard 2009). driven by the electrochemical gradient across the cell membrane CFTR allows the passage of several molecules across cell membranes,

mainly chloride, and including iodide, HCO_3^-, and others (Illek et al. 1999). The CFTR channel allows the passage of negatively charged chloride ions into and out of cells, and this helps to control the movement of water in tissues, which is necessary for the production of thin, freely flowing mucus (http://ghr.nlm.nih.gov/gene/CFTR).

CFTR single-channel conductance have been thoroughly characterised and established as an apical epithelial chloride channel (Venglarik et al. 1994) and demonstrated to behave as an ohmic low-conductance channel (Hanrahan et al. 1998). Although the primary function of CFTR is anion conductance, it is also known to have regulatory effects on other molecules. When stimulated by cAMP agonists, CFTR inhibits the amiloride sensitive epithelial Na^+ channel (Stutts et al. 1997). Additionally CFTR regulates the outwardly rectifying chloride channel (ORCC) that can only be activated by protein kinase A (PKA) and ATP when CFTR is functionally active (Jovov et al. 1995). CFTR has been shown to control many other ion channels, such as the Ca^{2+}-activated chloride conductance (CaCC) channel, the renal outer medullar K^+ (ROMK) channel, the sodium/ proton exchanger NHE3, and an aquaporin channel (Stutts et al. 1995; Mall et al. 1996; Mall et al. 1996; McNicholas et al. 1996; Schreiber et al. 1997). Moreover, CFTR has been shown to be expressed in intracellular vesicles, where it might have a role in intracellular and intravesicular pH regulation (Lukacs et al. 1992). CFTR also appears to control exocytosis/ endocytosis processes (Jouret et al. 2007), and to regulate proinflammatory cytokine expression, and possibly other cellular functions (Vandivier et al. 2009).

The coding gene for the CFTR protein is located on the long arm of chromosome 7 at position 31.2 (http://ghr.nlm.nih.gov/gene/CFTR), which translates into a 1480-amino-acid protein with a predicted molecular mass of 168,138 Da (Riordan et al. 1989). The predicted structure has two repeated motifs, each of which contains a hydrophobic domain of six helices that span the membrane (membrane-spanning domain, MSD; or transmembrane domain, TMD) and are linked by a hydrophilic cytosolic ATP-binding domain (nucleotide-binding domain, NBD), followed by a large and highly charged cytoplasmic domain, known as the R domain. The second MSD is followed by another NBD on the C-terminus (Figure 1.2). The R domain consists of 241 amino acids arranged in alternating clusters of positive and negative charges, and there are several consensus sequences for phosphorylation by PKA and PKC (Riordan et al. 1989).

a

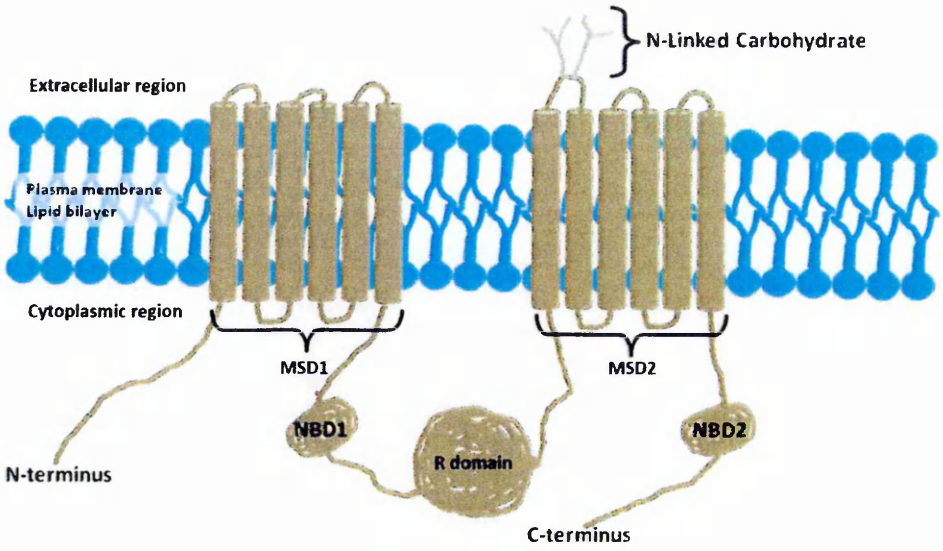

b

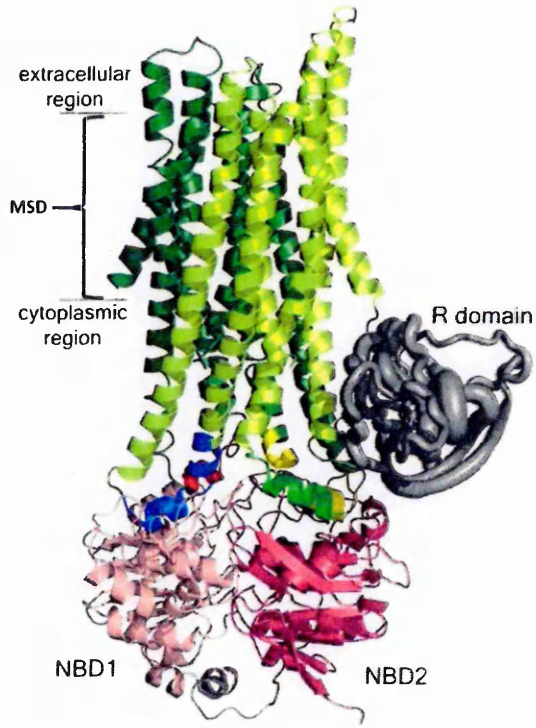

Figure 1.2. Model of proposed domain structure of CFTR.

a. Model of CFTR primary structure containing two nucleotide-binding domains (NBD1 and NBD2), two membrane-spanning domains (MSD1 and MSD2), and a regulatory region (R domain). b. Homology model of CFTR constructed from Sav1866 exporter (Serohijos et al. 2008).

The domains of CFTR assemble to form the channel across the membrane, which is gated by cAMP dependent PKA phosphorylation of the R domain (Gadsby et al. 2006). There are two glycosylation sites, between the 7th and 8th membrane-spanning helices, at amino acids 894 and 900. CFTR is core glycosylated in the endoplasmic reticulum (ER), which is an immature form that is also called "band B". After folding, CFTR leaves the ER, progresses through the secretory pathway, and passing through the Golgi complex it attains the complex glycosylation to the mature form that is usually found on the PM, also known as "band C". This band C moves at a higher molecular weight than band B on SDS-PAGE; there is also a third form of CFTR that has mobility on SDS-PAGE slightly faster than band B, which is referred to as "band A" (Gregory et al. 1990), which might be the non-glycosylated form.

The R domain is a target of protein kinases, including PKA, PKC and AMP-activated protein kinase (AMPK) (Ostedgaard et al. 2001). There were 10 PKA sites identified *in vitro* (Picciotto et al. 1992; Gadsby and Nairn 1999), and six of these sites are phosphorylated on full-length CFTR purified from cells (Picciotto et al. 1992). Many of these phosphorylation sites stimulate channel activity in an additive/ synergistic way, although phosphorylation at S737 and S768 were reported as inhibitory under certain conditions (Wilkinson et al. 1997). Mutating as many as four (Ostedgaard et al. 2000) or more (Chang et al. 1993) of these phosphorylation sites can abolish the function of the CFTR channel. There are also five PKC phosphorylation sites located in the R region, four of which have been studied *in vitro*, with one verified in the full-length protein (Picciotto et al. 1992; Jia et al. 1997; Chappe et al. 2004). PKC phosphorylation on the R region does not stimulate the channel activity by itself, but might be involved in enhancing the effects of PKA phosphorylation (Bozoky et al. 2013). The cellular-energy-level-activated kinase, AMPK, phosphorylates the R region on inhibitory site (s768), this phosphorylation can fix CFTR into a state that is insensitive to PKA and PKC phosphorylation (King et al. 2009), which might decrease the channel open probability. It has been also noted that cAMP-dependent stimulation and PKA phosphorylation can overcome the inhibitory effect of AMPK phosphorylation. (Kongsuphol et al. 2009), The phosphatase 2 (PP2) isoforms, PP2A, PP2B and PP2C, and alkaline phosphatase can dephosphorylate CFTR (Thelin et al. 2005), and they can also reduce most of the CFTR channel activity (Hallows et al. 2000).

Once CFTR is phosphorylated, channel gating is tightly regulated by cycles of ATP binding and hydrolysis. Phosphorylated CFTR channels can be opened by a broad range of nucleoside triphosphates, including ATP, GTP, ITP, UTP, CTP, The frequency of CFTR-channel opening increases with ATP concentration, at saturating concentrations of ATP, a channel waits in the closed state for a second or so (depending on the temperature) before opening. This means that binding of ATP limits channel opening at low concentrations, but at saturating ATP concentrations some other slow step controls how quickly the channel can open once ATP has bound (Gadsby et al. 2006). On the assembled CFTR the ATP is known to bind tightly to ATP-binding site 1 (site 1; formed by the Walker A and B motifs of NBD1 and the LSGGQ motif of NBD2), but is not hydrolysed at this site. Contrastingly, ATP is hydrolysed rapidly at the other ATP-binding site 2 (site 2; formed by the Walker A and B motifs of NBD2 and the LSGGQ motif of NBD1) (Hwang and Sheppard 2009). The ATP hydrolysis at ATP-binding site 2 is known to controls the channel closure, whereas ligand binding at ATP-binding site 1 might modulate the rate of channel closure and the anion flow through the CFTR channel aperture is believed to be gated by the interaction of ATP with sites 1 and 2 powering NBD dimerisation and hence conformational changes in the MSDs (Hwang and Sheppard 2009). Opening of a CFTR channel was viewed as triggered by a pincer-like drawing together of ATP-bound NBD1 and ATP-bound NBD2, channel closing would follow hydrolysis of the ATP at the NBD2 composite site, loss of the liberated phosphate and subsequent disruption of the heterodimeric NBD1–NBD2 interaction (Gadsby et al. 2006).

1.3. Mutations of CFTR

There have been about 1900 mutations reported in the gene encoding CFTR (http://www.genet.sickkids.on.ca/cftr/StatisticsPage.html). Based on the type of the defect caused, the *CFTR* mutations have been categorised into six classes (Welsh and Smith 1993; Zielenski and Tsui 1995; Haardt et al. 1999; Lubamba et al. 2012), as follows.

Class I: Mutations that interfere with protein synthesis: These mutations include the introduction of a stop codon in the mRNA, or nonsense (p.Gly542X), or a frame shift (394DelTT), or severe splicing mutations (1717-1G>A), which result in truncated proteins that are unstable, and hence these proteins do not reach the apical membrane.

Class II: Mutations that affect protein maturation. These mutations result in the production of a protein that is incorrectly folded and cannot be trafficked to its site of function on the apical membrane (p.Phe508del (ΔF508), p.Ile507del, p.Asn1303Lys).

Class III: Mutations that alter channel regulation. The mutation produces a protein that is correctly trafficked and localised to the apical membrane, but cannot be activated to function as a chloride channel (p.Gly551Asp).

Class IV: Mutations that affect chloride conductance. These mutations produce a CFTR protein that is correctly trafficked to the apical membrane, but functionally this CFTR has a reduced level of chloride ion flow (p.Arg117His, p.Arg334Trp).

Class V: Mutations that reduce the level of the normally functioning CFTR at the apical membrane (partially aberrant splicing mutation or inefficient trafficking) (c.1210-12T (5T allele), c.3140-26A>G (3272-26A>G), c.3850-2477C>T (3849+10kbC>T)).

Class VI: Mutations that decrease the stability of the synthesised CFTR (Q1412X, S1455X).

Class I, II, III and VI mutations confer insignificant or no functional level of CFTR at the apical membrane, and they lead to the severe and classic CF phenotype, with pancreatic insufficiency and severe lung damage, whereas class IV and V mutations make a protein that can retain some residual channel activity, and might thus lead to a milder phenotype. Patients with at least one mild CF allele of CFTR have sufficient digestion, and less severe lung disease (The Cystic Fibrosis Genotype-Phenotype Consortium 1993). Individuals with CFTR mutations that can give rise to about 10% of the normal level of CFTR mRNA can present only one symptom, such as congenital bilateral absence of the vas deferens in males (Anguiano et al. 1992). Some individuals who are heterozygous for a CFTR mutation have increased risk for characteristic CF pathophysiology, such as pancreatitis, or allergic bronchopulmonary aspergillosis (Casals et al. 2004). Each class of mutation has the potential to have a significant role in the development of CF (Frizzell 1999); however, class I, II and V mutations with defects in early biosynthesis and folding are the major contributors to CF disease. Single CF mutation might have multiple mechanisms of CFTR dysfunction like ΔF508 (see section 1.4).

1.4. The ΔF508 mutation of CFTR

Among the identified CF patients, approximately 90% have an allele where phenylalanine at the 508 position of the protein is deleted (Phe508del; the Phe508 deletion mutant; ΔF508) (Welsh and Smith 1993; Amaral 2005). ΔF508 accounts for nearly 70% of CF cases (Collins 1992). Patients with CF who have the ΔF508 mutation have no functional channel at the PM (Cheng et al. 1990). The ΔF508 mutation causes a protein folding defect that prevents its intracellular transport and delivery to the plasma membrane (Kartner et al. 1992), but a partial amount can reach the PM and function as a chloride channel (Drumm et al. 1991; Li et al. 1993). It was also noted that the ΔF508CFTR trafficking defect is temperature sensitive, as the channel function was partially restored at the PM by expressing ΔF508CFTR in insect cells or in *Xenopus* oocytes that were grown at low temperature (Drumm et al. 1991; Li et al. 1993), which was further confirmed in mammalian cells (Denning et al. 1992).

The ΔF508 mutation leads to multi-level defects, like misfolding (Qu and Thomas 1996), ER retention, degradation (Kopito 1999), reduced channel function (Dalemans et al. 1991), increased membrane instability (Lukacs et al. 1993), and reduced levels of transcripts (Ramalho et al. 2002). ΔF508CFTR is also known to lead to many other changes at the molecular level that can contribute to the outcome of CF. The CF foetus with homozygous ΔF508 mutation has excess inflammation-relevant molecules, like COX2, ICAM1, MMP1 and NF-κB, in the lung without any histological signs of inflammation (Verhaeghe et al. 2007). It has been demonstrated that loss of function of CFTR can be the major trigger of inflammation and NF-κB activation (Venkatakrishnan et al. 2000; Weber et al. 2001) in cellular models of CF with ΔF508 and other non-functional CFTR mutations. There is also evidence of hyperactivation of p38 MAPK in the lungs of ΔF508 CF patients, and when challenged with *Pseudomonas aeruginosa* diffusible material, cellular models of ΔF508 led to IL6 synthesis that was dependent on reactive oxygen species (ROS) and p38 activation (Berube et al. 2010). Primary CF cells with the ΔF508 mutation also have hyperactive AMPK (Hallows et al. 2006), which might be an adaptive response to reduce inflammation, because pharmacological activation of AMPK reduces inflammatory mediators like IL6, IL8 and TNFα. Also, AKT is hyperphosphorylated in CF model cells, and its inhibition can suppress IL8 expression (Bhattacharyya et al. 2011). The ΔF508CFTR condition also leads to

growth factor receptor (e.g., EGFR) phosphorylation and increased production of vascular endothelial growth factor (VEGF)-A (Martin et al. 2013). Several other gene products, like TNFα, TGF-β1, and others, can influence CF disease progression by acting as modifiers (Collaco and Cutting 2008). ΔF508 mutation causes the CFTR protein to misfold (Qu and Thomas 1996), and it might also cause up-regulation of the unfolded protein response (UPR) (Bartoszewski et al. 2008).

1.5. Biogenesis of wtCFTR and ΔF508CFTR

The biogenesis of a functional protein has been proposed to depend on the cell control of the concentration, conformation, binding interactions and location of individual proteins, often through transcriptional and translational changes referred as "proteostasis" (Balch et al. 2008). Proteostasis can be influenced by the chemistry of protein folding and misfolding, and by numerous regulated networks of interacting and competing biological pathways, called the proteostasis network, which influence protein synthesis, folding, trafficking, disaggregation, and degradation (Balch et al. 2008). CFTR biogenesis has a complex folding, degradation and membrane trafficking itinerary that is managed by the proteostasis network.

There are documented transcriptional control programmes that can affect the biogenesis of CFTR. Very few copies of CFTR mRNA have been found in airway epithelial cells (Trapnell et al. 1991), which might affect the amount of CFTR protein at the PM. The micro-RNAs miR-101 miR-144, miR-145 and miR-494 have been reported to directly target the CFTR 3′-UTR and to suppress the expression of the CFTR protein (Gillen et al. 2011; Hassan et al. 2012). IL-1β was demonstrated to increase CFTR mRNA and to induce the CFTR promoter in Calu-3 cells using NF-κB (Brouillard et al. 2001). TGF-β1 was shown to inhibit CFTR biogenesis by reducing its mRNA levels and protein abundance in primary differentiated human bronchial epithelial cells, and to also inhibit biogenesis and impair the functional rescue of ΔF508CFTR in primary differentiated human bronchial epithelial cells from patients who were homozygous for the ΔF508 mutation (Snodgrass et al. 2013). Additionally, ER stress is reported to contribute via the UPR, to decrease CFTR expression at the transcriptional, translational, and maturational levels (Bartoszewski et al. 2011). The β-adrenergic receptor has also been demonstrated to modulate expression of CFTR via the elevation of cAMP, which leads to activation of the PKA and, subsequently, of cAMP

responsive element binding protein 1 (CREB1) and activating transcription factor 1 (ATF-1)-dependent transcription of CFTR (McDonald et al. 1995; Pittman et al. 1995; Matthews and McKnight 1996). The endogenous CFTR protein is only expressed at the apical membranes of well-differentiated epithelial cells (Puchelle et al. 1992). The targeting of CFTR to the apical PM appears to be tightly linked to the process of epithelial differentiation and polarisation (Hollande et al. 1998).

The *CFTR* gene is translated into a large integral membrane glycoprotein and the N-terminus is inserted into the ER membrane co-translationally (Lu et al. 1998). Generally, the co-translational insertion of integral membrane secretory proteins involves the ER-membrane-localised translocation machinery complex (Shao and Hegde 2011). Although the structures and functions of many members of this complex are poorly understood and their roles in translocation or membrane insertion are essentially unexplored, the components of the complex are known and they include the heterotrimeric Sec61 complex, the ribosome, and the accessory proteins, such as TRAP, TRAM, RAMP4, Sec62, Sec 63 and p180 (Shao and Hegde 2011). In association with the translocation machinery, the ribosome correctly inserts the transmembrane domains and the ER luminal domains via polypeptide chain elongation (Fedorov and Baldwin 1997).

The translation of the CFTR protein is estimated to be completed in about 9 min (Ward and Kopito 1994). During the translation of CFTR on the ribosome, the insertion to the ER membrane takes place by combining the translocation mechanism of the signal and stop transfer signals (Skach 2000). The NBD1 folds largely co-translationally, but the native structure of NBD2 and the full channel is attained post-translationally (Du et al. 2005; Kleizen et al. 2005; Lukacs and Verkman 2012). Furthermore, the formation of the complete functional channel requires interactions between the two MSDs (Ostedgaard et al. 1997). CFTR folding appears to be inefficient in many heterologous expression systems, where only 20% to 40% of nascent synthesised wtCFTR polypeptide chains attain the terminal native conformation and a functional channel (Lukacs and Verkman 2012). However, in endogenous cells this is reported to be highly efficient, where nearly 100% of the nascent polypeptides attained the native confirmation and reach the PM (Varga et al. 2004). On the contrary, ΔF508CFTR is almost completely absent on the PM due to its misfolding, and ER retention and degradation (Amaral 2005).

The CFTR has a large portion exposed on the cytosolic side, and the folding is known to involve both cytosolic and ER luminal chaperones and ER membrane proteins (Yang et al. 1993; Pind et al. 1994; Meacham et al. 2001). The chaperones that can influence the significant folding of the cytosolic sub-domains are members of the Hsp family, Hsp/Hsc70, Hsp90 and the co-chaperones STIP1, AHSA1 (Aha1), and Hsp40 proteins; Hdj1 and Hjd2, and JB1 (Yang et al. 1993; Strickland et al. 1997; Meacham et al. 1999; Farinha et al. 2002; Koulov et al. 2010; Grove et al. 2011). From the luminal side, there are calreticulin, calnexin and ERp29 (Pind et al. 1994; Chanoux and Rubenstein 2012).

The Hsp70 family of proteins have been shown to reversibly bind nascent, unfolded, or partially unfolded proteins in an ATP-dependent manner, and to prevent inappropriate interactions and facilitate protein folding (Gething and Sambrook 1992). The Hsp70 family chaperones are ~70 kDa proteins, and when they are bound to ATP they can open the substrate-binding pocket for non-native polypeptides (Mayer and Bukau 2005). Hsp70 ATPase activity is known to be regulated by interacting proteins, called co-chaperones (Cyr et al. 1992). Hsc70, Hdj1 and Hdj2 interact with CFTR immediately following insertion of MSD1 (Meacham et al. 1999). The HSP70-Hdj2 interaction with CFTR is high with the expression of the CFTR N-terminal and cytoplasmic sub-domains, but it is reduced when MSD2 is translated, which suggests the importance of Hdj2 activity in the folding of the CFTR sub-domains (Meacham et al. 1999). Importantly, the Hsc70-Hdj2 association with ΔF508CFTR is stronger than that with wtCFTR and functions to prevent aggregation and to promote CFTR folding (Meacham et al. 1999). ΔF508CFTR might be aggregation prone and might expose the structure to Hsc70-Hdj2 molecular chaperone system similar to a wtCFTR translation intermediate (Meacham et al. 1999). Overexpression of Hsp70 cannot alter wtCFTR or ΔF508CFTR turnover; however, Hdj-1 (Hsp40) and Hsp70 co-overexpression led to the stabilisation of wtCFTR, but not of ΔF508CFTR, without any apparent alteration in the efficiency of maturation (Farinha et al. 2002).

The Hsp90 family of proteins are ~90 kDa cytosolic proteins that assist in the folding of nascent CFTR, their inhibition blocks CFTR maturation and increases CFTR degradation (Loo et al. 1998). Hsp90 interacts with Hsp70 via the Hsp organiser protein (HOP) (also known as Stress induced phosphoprotein 1-STIP1) (Chen and Smith 1998), to form a multi-chaperone complex that

might allow the transfer of substrates between the chaperones, most likely from Hsp70 to Hsp90 (Prodromou et al. 1999). HOP can link the nascent protein and the Hsp40/ Hsc70 complex to Hsp90 in the ADP state and later the co-chaperone regulator p23 in the presence of ATP, which displaces Hsc-Hsp40/70 and HOP, to form the protein-Hsp90-p23 complex in the ATP-bound state (Wang et al. 2006). Aha1 or AHSA1, an Hsp90 ATPase regulator, has also been shown to contribute to the folding of CFTR, and depleting Aha1 can also lead to partial rescue of ΔF508CFTR at the PM (Wang et al. 2006). Co-immunoprecipitation followed by mass spectrometry determination of both wtCFTR and ΔF508CFTR interactors have defined many proteins that bind to either wtCFTR or ΔF508CFTR (Wang et al. 2006). While some of the ΔF508CFTR and wtCFTR interactors are common to these two proteins, there are a significant number of proteins that are specific to each (Wang et al. 2006). One such interacting chaperone is Hsp105, which was later on found to be important in the folding and biogenesis of ΔF508CFTR, and overexpression of Hsp105 led to increase in folding of ΔF508CFTR, which then reached the PM (Saxena et al. 2012).

On the ER luminal side, calnexin is an ER transmembrane lectin with chaperone activity that was demonstrated to interact with newly synthesised and immature forms of both wtCFTR and ΔF508CFTR (Pind et al. 1994). Calnexin-ΔF508CFTR complexes were shown to last longer than for wtCFTR (Pind et al. 1994); moreover, calnexin overexpression led to the destabilisation of only immature ΔF508CFTR, and not of wtCFTR (Farinha and Amaral 2005). In the ER, CFTR is core glycosylated at Asn894 and Asn900, which forms an immature form of the protein (band B). This glycosylation is used to assess the folding by the lectin/ chaperone calnexin, and the defect at this stage can be recognised, with the resulting proteins subjected to degradation through the mannosidase (EDEM1,2,3)-driven ER-associated degradation (ERAD) pathway (Olivari and Molinari 2007) wtCFTR, but not ΔF508CFTR, appears to undergo EDEM1-dependent ERAD (Farinha and Amaral 2005). Core glycosylation has an important influence on CFTR folding and stability, as it enhanced the folding efficiency by chaperone-dependent and chaperone-independent mechanisms (Glozman et al. 2009). CFTR appears to be negatively regulated by calreticulin, as CFTR expression and function are enhanced by depletion of calreticulin in both cultured cells and

mouse models (Harada et al. 2006; Harada et al. 2007). Another luminal chaperone, ERp29, has been demonstrated to promote biogenesis of both ΔF508CFTR and wtCFTR (Suaud et al. 2011).

At the end of the folding process, CFTR attains the domain assembly to form a functional channel. When assembled correctly, intracellular loop (ICL) 2 interacts with NBD2, ICL4 interacts with NBD1, and ICLs 1 and 3 interact with both NBD1 and NBD2 (Patrick and Thomas 2012). Importantly, the F508 position in NBD1 is predicted to lie near the interface between NBD1 and ICL4. The F508 residue interfaces with the coupling helix of cytoplasmic ICL4 and ICL1 in MSD2 and MSD1, respectively (Lukacs and Verkman 2012). These NBD and ICL interactions serve to transmit ATP-dependent conformational changes involved in the chloride channel gating, and also appear to have a crucial role in CFTR biogenesis (Lukacs and Verkman 2012).

1.6. Trafficking of CFTR

Once CFTR is folded, assembled and core glycosylated, it exits the ER in a COPII dependent manner (Yoo et al. 2002; Wang et al. 2004). COPII consists of the Sar1 GTPase, the cargo-selection protein complex Sec23 (a Sar1-specific guanine-nucleotide-activating protein), the cargo-binding Sec24, and a coat polymer assembly factor, Sec13/31 (Antonny and Schekman 2001). The GTPase Sar1 is recruited and activated by the ER-localised transmembrane protein Sec12, a Sar1-specific guanine nucleotide exchange factor. Sar1 activation is necessary for recruitment of the Sec23/24 complex to the ER membrane, to select the cargo and initiate COPII coat assembly. CFTR exit from the ER has been shown to be dependent on Sar1 (Yoo et al. 2002); moreover, wtCFTR has been demonstrated to bind to Sec24, and ΔF508CFTR binding to Sec24 was reduced (Wang et al. 2004). This binding to Sec24 was dependent on the di-acidic motif present on CFTR (YKDAD; residues 563 to 567) (Wang et al. 2004). Studies using CFTR expressed in *Saccharomyces cerevisiae* have demonstrated that COPII regulates the delivery of wtCFTR to the ERAD pathway (Fu and Sztul 2003). Immunoelectron microscopic studies have indicated that there is a limited amount of wtCFTR and no ΔF508CFTR in the Golgi and complex and other anterograde compartments (Bannykh et al. 2000). There are also studies that have reported ΔF508CFTR in the ER-Golgi intermediate compartment (ERGIC) in CF cells (Gilbert et al. 1998). So there is a proposed retention and retrieval mechanisms (i.e., selective anterograde and

retrograde trafficking) that might exert the quality control of CFTR in the early secretory compartments (Amaral 2004).

CFTR passes through the Golgi complex, where it is processed by multiple Golgi glycosyltransferases, to create the fully mature form of CFTR (band C) (Farinha et al. 2013). However, the glycosylation does not alter the channel function, although it was very important for the stability of the protein after its ER exit (Morris et al. 1993; Chang et al. 2008). Indeed, the complex glycosylation in the Golgi is used as a measure of the extent of conformational maturation and ER export of CFTR (Chang et al. 2008). Fully glycosylated CFTR exits the Golgi complex using post-Golgi carriers that transport it to the PM (Amaral and Farinha 2013).

The functional pool of CFTR is maintained on the PM by its continuous recycling from early endosomes to the PM using Rab11 and Myo5b-driven recycling endosomes (Swiatecka-Urban et al. 2007; Silvis et al. 2009). The trafficking of CFTR from the PM to early endosomes is controlled by Rab5 (Gentzsch et al. 2004). Rab4 and Rab27a might help CFTR in the restraining of its localisation to intracellular compartments, and thus limiting the channel expression at the PM (Saxena and Kaur 2006; Saxena et al. 2006). CFTR was demonstrated to co-distribute with annexin V, which affects the functional localisation of CFTR at the PM (Trouve et al. 2007), probably due to a scaffolding function of annexin V (Faria et al. 2011). More recently, pleiotropic casein kinase 2 (CK2) was demonstrated to interact and phosphorylate CFTR, which has positive influences on the trafficking of wtCFTR, whereas CK2 inhibition leads to decrease in the PM CFTR levels (Luz et al. 2011); however, the relevant mechanism of the CK2 phosphorylation that regulates the trafficking has not been defined.

Although recycling is considered as the main mechanism for sustaining a functional pool of CFTR at the PM, up to 50% of the surface CFTR has been demonstrated to exist in an immobile pool, using its PDZ interactions (Haggie et al. 2006). NHERF-1 has an important function in the targeting of endosome-associated CFTR to the apical membranes, and the anchoring of CFTR at the PM to the apical actin cytoskeleton using ezrin (Short et al. 1998; Swiatecka-Urban et al. 2002; Haggie et al. 2006). N-WASP inhibition and actin cytoskeleton disruption led to a sharp decrease in the surface CFTR pool, highlighting the role of the actin cytoskeleton in the CFTR recycling and

immobilisation at the PM (Ganeshan et al. 2007). WASP proteins are known to promote actin polymerisation in response to signalling molecules like the Rho family of small GTPases (Benesch et al. 2005). One such Rho family of small GTPases, protein TC10 (a member of the Cdc42 subfamily) increases CFTR levels at the cell surface; moreover, activated TC10 promotes the binding of NHERF-1 to the C-terminus of CFTR, and reduces CFTR degradation, preventing its binding to CFTR associated ligand (CAL) (Cheng et al. 2005; Wolde et al. 2007).

At the TGN level, the PDZ protein CAL facilitates the trafficking of CFTR to lysosomes, which is prevented by NHERF-1 overexpression (Cheng et al. 2004; Cheng et al. 2005; Wolde et al. 2007). Overexpression of NHERF1 also promotes the apical expression of the ΔF508CFTR mutant channel, and rescues chloride secretion in bronchial epithelial cell lines (Guerra et al. 2005). In contrast, NHERF1 depletion enhances the degradation of temperature-rescued ΔF508CFTR from the PM (Kwon et al. 2007). The effect of NHERF-1 overexpression on CFTR might be dependent on the activation of Rac1 signalling, to promote ezrin-mediated PM anchoring of CFTR, and RhoA stimulation to favour CFTR recycling to the PM (Moniz et al. 2013). The CFTR movement to late endosomes and lysosomes, away from recycling endosomes, is regulated by Rab7, whereas Rab9 mediates transport from late endosomes back to the *trans*-Golgi (Gentzsch et al. 2004).

CFTR has also been demonstrated to use unconventional transport to the PM. CFTR was not detected in the central region of Golgi cisternae (Bannykh et al. 2000), moreover it was insensitive to blocking of the conventional ER-to-Golgi trafficking pathway by Arf1, Rab1a/Rab2 GTPases, and syntaxin 5 (Yoo et al. 2002). There was a block in CFTR maturation that was dependent on syntaxin 13 function, which indicates the importance of Golgi-to-endosome recycling for CFTR maturation (Yoo et al. 2002). Later on, CFTR was also identified in a novel compartment, known as the intermediate compartment, on its way to the PM (Marie et al. 2009). When conventional ER-to-Golgi transport is blocked by syntaxin 5 overexpression, Sar1- and Arf-dominant negative mutants, CFTR and ΔF508CFTR can reach the PM in its core-glycosylated form, unconventionally, using PDZ interactions with GRASP55 (Gee et al. 2011).

1.7. Degradation of CFTR

Around 70% of wtCFTR and nearly all of ΔF508CFTR cannot fold (Ward and Kopito 1994), and so fails the ER quality control (ERQC), and is retained in the ER and to be subsequently degraded by the proteasome (Cheng et al. 1990; Yang et al. 1993; Lukacs et al. 1994; Ward and Kopito 1994; Ward et al. 1995). CFTR degradation was not affected by the treatment of lysosomal degradation inhibitors (Lukacs et al. 1994), but proteasome inhibitors lead to the accumulation of CFTR (Ward et al. 1995). Thus, CFTR was proposed as a substrate of ERAD and the proteasome.

Nascent wtCFTR and ΔF508CFTR are selected for proteasomal degradation with the assistance of the molecular chaperones. The ER membrane resident E3 ubiquitin ligase RMA1 or RNF5 in association with Derlin-1 and the E2 ubiquitin ligase Ubc6e promotes the ubiquitination of wtCFTR or ΔF508CFTR (Younger et al. 2006). RMA1 has a critical role in the selection of ΔF508CFTR for premature degradation, and RMA1 depletion leads to the partial rescue of the CFTR protein at the PM. RMA1 interacts with the transmembrane quality control component Derlin-1, and knock-down of Derlin-1 enhances the cell-surface expression of ΔF508CFTR (Sun et al. 2006). Over-expression of Derlin-1 promotes ER retention and proteasomal degradation of wtCFTR and ΔF508CFTR, through the complexes it forms with MSD1 of CFTR (Sun et al. 2006; Younger et al. 2006). Later on, DNAJB12 (JB12), which is an Hsp-40, was demonstrated to act with Hsc70 and RMA1 to facilitate proteasomal degradation of wtCFTR and ΔF508CFTR. JB12 forms a complex that contains RMA1 and Derlin-1, which increases JB12 levels, and enhances the association of Hsc70 and RMA1 with immature forms of CFTR (Grove et al. 2011). Depletion of JB12 increased the folding efficiency of CFTR and led to the partial escape of ΔF508CFTR from the ER (Grove et al. 2011). Hsc70 down-regulation by the drug matrine increased protein levels of ΔF508CFTR, and promoted its localisation to the PM (Basile et al. 2012).

Additionally, CHIP is an E3 ubiquitin ligase that interacts with Hsc70 and Hsp70, to form a quality control machine that uses the polypeptide-binding activity of Hsc70 to target misfolded CFTR for proteasomal degradation (Meacham et al. 2001). The selection mechanism of CFTR for degradation by the RMA1 machinery and the CHIP complex are not entirely clear (Grove et al. 2011). However, RMA1 has been demonstrated to act early, to coincide with translation to

recognize folding defects in CFTR that involve the misfolding and defective assembly of NBD1 into a complex with the R-domain, while the CHIP E3 (Figure 1.7a) might act post-translationally to recognize misfolded regions of CFTR, which include NBD2 (Younger et al. 2006; Rosser et al. 2008). HspBP1and BAG2 co-chaperones have been shown to inhibit CHIP ubiquitin ligase activity, to promote maturation of the CFTR (Alberti et al. 2004; Arndt et al. 2005). FKBP8 is a co-chaperone that is involved in modulating the activity of the core Hsp70 and Hsp90 proteins, and it also demonstrates an important function in folding and stability of both wtCFTR and ΔF508CFTR. Absence of FKBP8 promotes more degradation of both of the proteins, whereas overexpression of FKBP8 leads to partial rescue of ΔF508CFTR to the mature form (Hutt et al. 2012). Ubiquitinated CFTR is usually translocated and delivered to the proteasome, which involves Gp78 (Morito et al. 2008), Sec61, BAP31 (Wang et al. 2008) and p97 (Dalal et al. 2004).

Gp78 has also been shown to facilitate the degradation of ΔF508CFTR by enhancing both its ubiquitination and its interaction with p97/VCP, and the silencing of gp78 leads to the stabilisation of ΔF508CFTR, preventing its degradation (Ballar et al. 2010). Valosin-containing protein (VCP)/p97 and gp78 have been shown to form complexes with CFTR, and interference in the VCP-CFTR complex using shRNA to VCP promoted the accumulation of immature CFTR in the ER and the partial rescue of functional chloride channels at the PM (Vij et al. 2006). Gp78 has been shown to assist ubiquitin chain extension, whereas UCH-L1, Usp19, Usp25 stabilise the ΔF508CFTR nascent chain by catalysing ubiquitin cleavage (Hassink et al. 2009; Henderson et al. 2010; Blount et al. 2012). BAP31 or BCAP31 an endoplasmic reticulum protein-sorting factor was also found to associate with the N-terminus of newly synthesised ΔF508CFTR, to promote its retrotranslocation from the ER (Wang et al. 2008). Depletion of BAP31 reduced the proteasomal degradation of ΔF508CFTR, and partial amounts also reached the PM. The cytosolic E3 ubiquitin ligases Nedd4-2 and Fbs1 have also been implicated in the ERAD of ΔF508CFTR (Yoshida et al. 2002; Caohuy et al. 2009). Many other proteins, like UBE4A, ERDJ5, XTP3-B, UBXD2, and others, have been shown to contribute to the degradation of ΔF508CFTR (Christianson et al. 2012) although the mechanism is still unknown. ΔF508CFTR over expression and proteasomal inhibition leads to the formation of aggresomes (Johnston et al. 1998) which indicates the tendency of misfolded proteins to aggregate if they are not degraded by the proteasome. In yeast, this

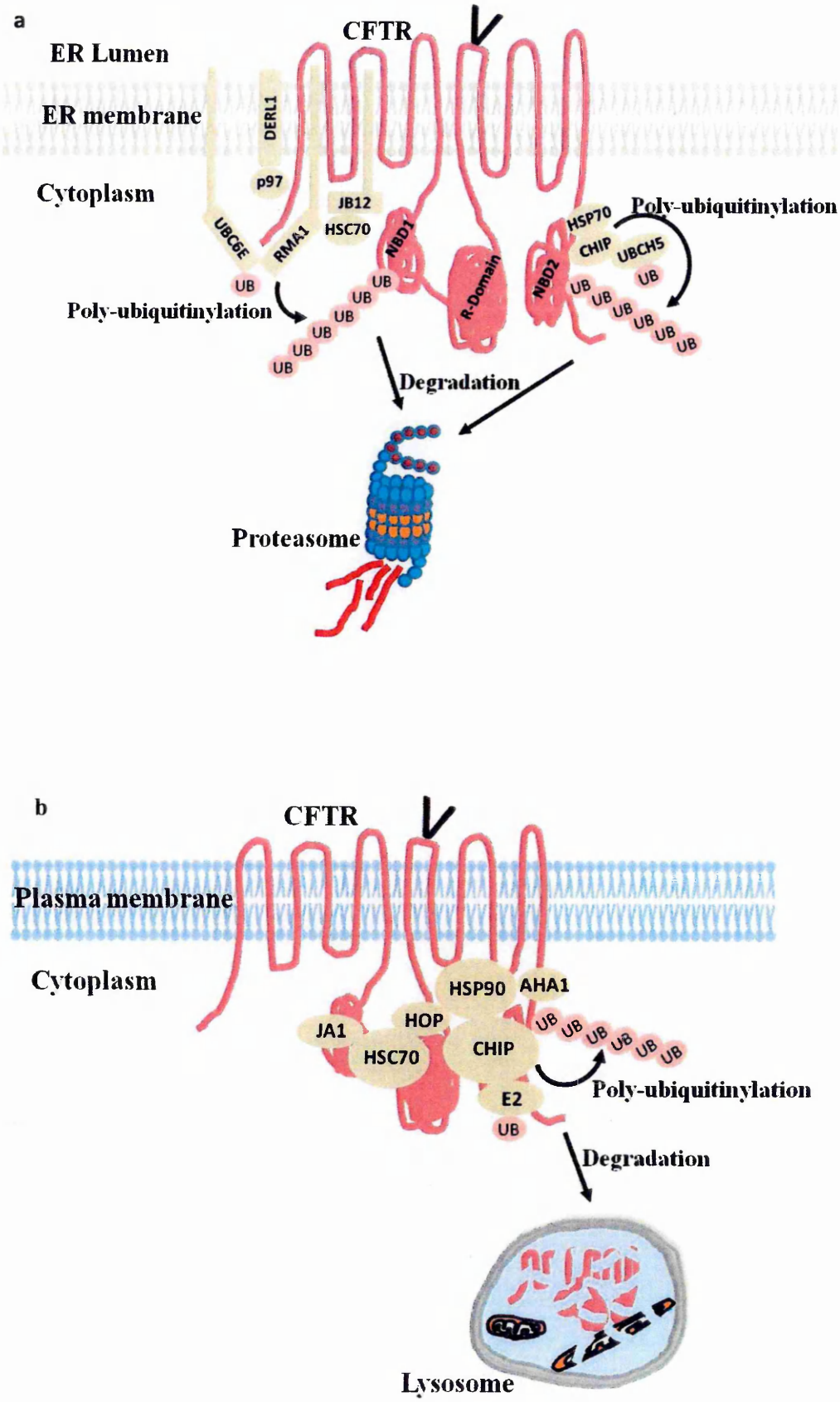

Figure 1.7. The models of ΔF508CFTR degradation.

a. ER associated degradation. **b.** Peripheral quality control from the plasma-membrane.

aggregated CFTR was shown to be degraded by autophagy (Fu and Sztul 2009). Either rapamycin treatment or serum starving BHK cells stably expressing CFTR led to decreased levels of total ΔF508CFTR but not of wtCFTR (Kaushal 2006). Rapamycin and serum starvation are known to induce autophagy in various cells, although there is no strong evidence for CFTR or ΔF508CFTR degradation by autophagy.

Even though ΔF508CFTR can be rescued at the PM, it was highly unstable and degraded at a faster rate (Okiyoneda et al. 2010). The rapid degradation of ΔF508CFTR is dependent on ubiquitination similar to that of several other conformationally defective PM proteins (Okiyoneda et al. 2011). CHIP and gp78 ubiquitin ligases were responsible for the removal of rescued ΔF508CFTR from the PM (Okiyoneda et al. 2010). This process required Hsc70 and Hsp90 a subset of co-chaperones, as DNAJ1 (Hdj2), Bag1, HOP and Aha1, for rapid ubiquitin-dependent endocytosis and lysosomal degradation (Figure 1.7b). The lysosomal delivery of rescued ΔF508CFTR from endosomal recycling was dependent on the endosomal sorting complex ESCRT0-III (Sharma et al. 2004; Okiyoneda et al. 2010). Degradation of wtCFTR can be regulated by a multifunctional protein, c-Cbl, which acts as an adaptor protein to facilitate CFTR endocytosis by a ubiquitin-independent mechanism, and also to ubiquitinate CFTR in the early endosomes, and thereby facilitate the lysosomal degradation of CFTR (Ye et al. 2010). It was also demonstrated that activation of the deubiquitinating Usp10 enzyme stabilises wtCFTR by facilitating its recycling (Bomberger et al. 2009). CFTR at the PM interacted with COMMD1, which appears to protect it from ubiquitination and to sustain its surface expression (Flattau et al. 2011).

1.8. Therapies for cystic fibrosis

There has been a tremendous effort to find therapies for cystic fibrosis; first, to treat the pathogenic mechanisms of CF as a disease, and secondly, to correct the underlying basic defects responsible for CFTR loss-of-function. In the early 1950s, at the CF centre in Cleveland, USA, Matthews and co-workers established three pillars of treatment: nutritional repletion, relief of airway obstruction, and antibiotic therapy of the lung infection, which in a few years improved survival and quality of life without the knowledge of the basic CF defect (Davis 2006). Indeed, 85% of these patients with CF showed pancreatic insufficiency at birth, and the others gradually

lost this function over time, with pancreatic enzyme supplements administered to prevent some of the malnutrition. Later, in the 1980s, more sophisticated methods were developed to administer pancreatic enzymes. Calorie-dense oral supplements to enteral feedings were adapted to overcome the malnutrition (Davis 2006). Another severe problem in CF is the plugging of airways with thick and sticky airway secretions, and clearance of these secretions assumed a prominent role in therapy early in the history of the disease (Davis 2006). Postural drainage and clapping (the "ketchup-bottle" method), and other mechanical devices have been used as effective methods to clear the thick and sticky airway secretions. DNA-cleaving agents were also demonstrated to reduce the viscosity of airway secretions (Davis 2006). Administration of hypertonic saline aerosols resulted in a modest increase in pulmonary function through the temporary hydration and clearing of airway secretions (Wark and McDonald 2003). Since the optimal strategies of therapy have not been established, culture-specific antibiotics have been a mainstay of CF therapy for many years. More antibiotic aerosol formulations are currently being developed specifically for CF patients with *Pseudomonas*, and other bacterial infections. Inflammation is elevated in the CF patients and its pharmacological suppression reduced the pulmonary destruction in the healthy patients with CF. However, even after these many interventions, many patients face the threat of respiratory failure that requires lung transplantation to survive. According to the CF Foundation data registry, there are more than 100 patients with CF who receive lung transplantation every year. This leads to the survival of about 80% at the 1-year mark, and 50% by 4 years, so this is not yet a perfect therapy (Davis 2006). Further refinements of conventional care continue to drive the median survival age upwards. Children with CF have to take multiple pills and aerosols daily, eat extra food, exercise vigorously, while incurring medical costs upwards of $25,000 a year (Davis 2006).

Since the discovery of the gene responsible for CF, gene therapy has been explored (Rosenecker et al. 2006), although in the few trials to date, no clinical benefit has been recorded (Griesenbach and Alton 2011). The underlying mutations resulting in CF are being uncovered since the discovery of the gene, and the recent focus has been towards new and better pharmacotherapies directed at either the pathogenic mechanisms or the correction of CFTR loss-of-function. Another method is to by-pass defective CFTR using alternative chloride channels. Some efforts have been undertaken to activate the alternative TMEM16 chloride channel (Namkung et al. 2011). There are

several other identified candidates for alternative anion conductance, and the relevant pharmacological candidates to activate and potentiate these are in consideration (Lubamba et al. 2012).

Class I mutations with a premature stop codon can be treated with gentamicin, which induces the read through of stop codons, and this has been shown to be beneficial in patients with CF (Clancy et al. 2001). Another drug, Ataluren, which acts in a similar manner, has also been shown to be beneficial in a phase II clinical trial for patients with CF (Kerem et al. 2008). If proved further, these drugs may offer a therapeutic option to a very limited number of patients with CF, as class I mutations are highly prevalent only in Israel, while seen in the rest of the population at only about 5%. Relatively rare class III mutations, which reduce the PKA-dependent open probability of the CFTR channel, can be treated with compounds that enhance ATP-dependent channel gating once CFTR has been activated by PKA-dependent phosphorylation (potentiators)(Sheppard 2011). Classic class III and the third most common (2%-3%) mutation G551D can be treated with ivacaftor or VX770, to potentiate chloride transport in epithelial cells expressing G551D CFTR (Van Goor et al. 2009). The less common class V and VI mutations affect mRNA and CFTR stability, and hence treatment for increasing mRNA and maximal activation of the normal CFTR, such as 4-phenylbutyrate, milrinone or genistein combinations, might prove useful (Lubamba et al. 2012).

On the other hand, the major CF causing mutation, ΔF508, accounts for about 70% of cases, and so this is the major area where therapeutic efforts have been focused more recently. This is one of the class II mutations; they need drugs that increase the transport of the channel to the PM. ΔF508CFTR poses more challenges because of its multiple level problems; namely, defective channel activity, rapid degradation from the PM, and defective recycling. Therefore, an ideal drug for this mutation should increase the surface expression, gating, surface stability and recycling of ΔF508CFTR. People with CFTR gene mutations that produce only 10% of the normal levels of CFTR at the functional level due to reduced mRNA levels have no lung and pancreatic complications, although they do show the congenital bilateral absence of the vas deferens (Anguiano et al. 1992). These observations lead to the belief that the rescue of about 10% of the

ΔF508CFTR protein might be sufficient to reduce the pathophysiological complications in patients with CF. Although there is varied estimates of the amount of ΔF508-CFTR rescue believed to ameliorate the decline of lung function in CF patients ranging from 5-30% of wt-CFTR (Van Goor et al. 2006). There are many proposed drugs that allowed a certain amount of ΔF508CFTR to traffic to the PM in different cells and that can rescue partial chloride conductance, these are termed correctors, while some compounds have been reported to increase the chloride channel open probability (potentiators).

The temperature-sensitive nature of the ΔF508 mutant has led to trials of chemical chaperones like glycerol (Brown et al. 1996), to induce the "rescue", or to restore the functional channel at the PM, at least partially. However, the concentrations that need to be used in patients might be toxic (Gelman and Kopito 2002). Studies with chemical chaperones (Brown et al. 1996) and on the temperature-sensitive folding (Denning et al. 1992) have suggested that modification of the cellular environment that favour the folding of the proteins might help ΔF508CFTR to fold and to reach the cell surface, and to function as a channel that might ultimately rescue the CF phenotype.

There have been great efforts to understand the molecular basis of ΔF508CFTR dysfunction and the difference in the quality control components compared to wtCFTR, on the basis that, this might lead at some stage to better therapies. These efforts have put forward the protein quality control systems and the folding and degradation machinery activity for ΔF508CFTR as complementary approaches to rescue the functional channel. It has been demonstrated that inhibitors of histone deacetylases, like 4-phenylbutyrate (Rubenstein et al. 1997), suberoylanilide hydroxamic acid (SAHA), and trichostatin A (TSA) (Hutt et al. 2010), and inhibitors of Hsc70 (Cho et al. 2011) can partially rescue ΔF508CFTR. Miglustat has also been shown to rescue ΔF508CFTR in different CF models, including mice with suspected disruption of calnexin and ΔF508CFTR (Lubamba et al. 2009; Norez et al. 2009). Miglustat is undergoing a clinical trial for CF caused by the ΔF508 mutation (Leonard et al. 2012). Simultaneously, there have also been searches for possible correctors and potentiators using the available large-scale chemical and drug libraries using high-throughput screening (Pedemonte et al. 2005; Van Goor et al. 2006; Carlile et

al. 2007; Robert et al. 2010). There was also a reported computational model-based screening approach that yielded several corrector compounds (Sampson et al. 2011).

As a result of these screening efforts, several compounds and drugs have been identified, namely Corr4a, VRT325, VRT422, chlorzoxazone, glafenine, sildenafil, and others, that appear to increase the trafficking of ΔF508CFTR to the PM, whereas VRT532 increases the gating of ΔF508CFTR. Vertex Pharmaceuticals has further developed a corrector, VX-809, which increases the stability and folding of ΔF508CFTR and can establish about 15% of the channel activity at the cell surface in primary CF cells, compared to non-CF cells (Van Goor et al. 2009). VX-809 underwent a clinical trial, but it was found to be ineffective (Clancy et al. 2012), and now VX-809 in combination with ivacaftor are undergoing a trial to induce effective channel activity of ΔF508CFTR at the cell surface. Current efforts to identify correctors, which have been based largely on phenotype screens, have not been successful in identifying highly efficient molecules (Lukacs and Verkman 2012). A recent discoveries has demonstrated that multiple defects, including ΔF508-NBD1 energetic and the NBD1-MSD2 interface stabilization are required for wild-type-like folding, processing and transport function of ΔF508CFTR, correction of either individual process is only partially effective. (Mendoza et al. 2012; Rabeh et al. 2012). Thus, with the exception of the symptomatic therapy, there still remains no therapy for the basic defect in CF caused by the ΔF508 mutation, and thus this remains an urgent need.

1.9 Hypothesis and aim of the study.

There have been as many as many as 90 corrector molecules reported to date. Each one of these drugs shows very low efficacy, and moreover, except very few, the modes of action of these corrector molecules are yet to be identified (Riordan 2008; Sheppard 2011; Lukacs and Verkman 2012). They have been shown to correct the trafficking of ΔF508CFTR with the help of cell-based high-throughput screening. A few of these molecules, like Corr4a, VX-809, VRT325, have been shown to directly bind to ΔF508CFTR (Wang et al. 2007; Ren et al. 2013) and to help in its folding and trafficking, whereas other molecules, such as thapsigargin, curcumin (Wang et al. 2007), TSA, SAHA, A3, C1, F1 (Hutt et al. 2010; Calamini et al. 2012) might not contribute to folding and trafficking of ΔF508CFTR through direct interactions. Instead, these molecules might modulate the proteostasis network, which, in turn, might contribute to the correct positioning of ΔF508CFTR at the cell surface. Correct folding, trafficking and restoration of function are proposed to be achieved through several mechanisms. First, there appears to be a direct energetic stabilisation of the protein through its folding upon use of therapeutics, generally referred to as pharmacological chaperones (pharmacochaperones) (Balch et al. 2011) exemplified by Corr4a and VX-809, which rescue the ΔF508CFTR trafficking to the PM (called correctors). A few pharmacochaperones can just increase the gating of ΔF508CFTR, like VX770 or ivacaftor (called potentiators) (Balch et al. 2011). There are very few molecules which have both CFTR corrector and CFTR potentiator actions, or dual-acting molecules, despite the intensive efforts to develop such molecules (Sheppard 2011). Secondly, an alternative to the pharmacochaperones, there is a another approach to achieve the folding and trafficking, using proteostasis regulators (Balch et al. 2011).

The general belief is that defects in protein conformation like ΔF508CFTR can be rescued by: (i) stabilising protein folding with pharmacochaperones that bind directly; and/or (ii) enhancing the protein folding efficiency of the cells using proteostasis regulators (Lukacs and Verkman 2012). It is also possible that a combination of the various classes of pharmacochaperones (correctors, potentiators) and proteostasis regulators might act synergistically. Recently it has been shown that a proteostasis regulator molecule cystamine combined with the pharmacochaperone potentiator VX770 synergised in the restoration of the channel function (Luciani et al. 2012). A few studies have also shown that addition of combinations of different correctors can provide additive effects

(Wang et al. 2007; Okiyoneda et al. 2013). Combinations of corrector drugs targeting NBD1-MAD2 interface (like VX-809) and NBD1-NBD2/ NBD2-MSD1/2 interface targeting drugs (like Corr4a) with pharmacochaperones (like glycerol) led to enhanced ΔF508-CFTR plasma membrane expression to ~60–110% that of the wild type in BHK cells (Okiyoneda et al. 2013).

It has been proposed that the proteostasis network is constituted by about a thousand contributing components (Balch et al. 2011). These include the Hsp/Hsc70 and Hsp90 chaperone systems, the normal activities of which are regulated by numerous signalling pathways that sense folding and metabolic stress, as well as the UPR, the HSR, calcium sensing, and inflammatory pathways (Balch et al. 2011). The proteostasis network is also complemented by the components of the ubiquitin sumoylation proteasome system in the cytosol, and the lysosomal and autophagic degradation pathways, which are also sensitive to multiple stress pathways. CFTR folding requires extensive support from the proteostasis network, moreover, wtCFTR and ΔF508CFTR appear to interact with the proteostasis network differentially (Wang et al. 2006), and modulation of the proteostasis network function might contribute significantly to the treatment of CF (Balch et al. 2011). It has been proposed that efforts to identify CF drugs through biological analyses of the proteostasis network function might strongly support the possibility to find the compounds that alter the folding proteostasis network of ΔF508CFTR, which might have great potential for the generation of a more wild-type-like function, and hence, might have significant benefit in the clinic (Balch et al. 2011). Many of the reported drugs do not have a known mechanism of action for the rescue, and many among them might act as proteostasis regulators that target the proteostasis network, which might be responsible for the rescue of ΔF508CFTR.

Even though with lower efficacies, all of these drugs are doing one thing in common, they allow the partial trafficking of ΔF508CFTR to the PM. Apart from this, the majority of drugs are not known to bind directly to ΔF508CFTR; moreover, a few of them, like TSA and SAHA, have been proposed as proteostasis regulators (Hutt et al. 2010). The proteostasis regulators might change the proteostasis network component or its regulators through transcription (Hutt et al. 2010); moreover, depletion of proteostasis network components like Aha1 or RMA1 partially restores functionality of ΔF508CFTR in CF models. So targeting the proteostasis network and related components might yield better candidates to be targeted than by drugs. It has also been

shown that expression of ΔF508CFTR leads to the UPR and further activation of ATF6, and depletion of ATF6 can partially rescue the ΔF508 to the cell surface (Kerbiriou et al. 2007). A recent study showed that ATF6 controls the proteostasis network (Shoulders et al. 2013). It might be a logical argument that ATF6-controlled proteostasis network components are helping in the degradation; on the other hand, ATF6 depletion might decrease the proteostasis network components, which results in a decrease in the ERAD and an increase in the trafficking of ΔF508CFTR. Although CFTR has been well studied and many proteostasis network components are known, it is still not clear how ΔF508CFTR is retained and degraded by the ERAD; moreover, the regulation of these proteostasis network components is completely unknown.

The many previously discovered ΔF508CFTR corrector drugs might be proteostasis regulators. The assumption that needed to be tested was whether most of these reported drugs commonly affect some gene network/ pathway by modulating gene expression, such as those including the known proteostasis network genes and those proteostasis network genes that are yet to be determined, or by modulating proteostasis network regulators. In other words, the hypothesis was to look at the mechanism of action of drugs that can help rescue ΔF508CFTR to the cell surface. This is possible, as drug induced changes in gene expression can be easily and reliably detected using microarray or gene expression profiling, and moreover, the gene expression profiles of many corrector drugs are available (Lamb et al. 2006; Zhang et al. 2012). So the aim of the project was as follows:

a) Determination of the genes that are commonly regulated among most of the available gene expression profiles of corrector drugs.
b) Accessing the commonly regulated genes to dissect out the networks/ pathways/ molecules that are involved in the rescue of ΔF508CFTR to the cell surface, using a systems biology approach and a literature-based survey.
c) Testing the networks/ pathways/ molecules found as described earlier and specifically targeting those using genetic tools or new drugs, to confirm their involvement in the rescue of ΔF508CFTR to the cell surface.
d) Testing the efficacy of the combinations of different pathways/ networks/ molecules found to be effective for the rescue of ΔF508CFTR.

Chapter 2

Mechanism of action common to most of the drugs affects the proteostasis of ΔF508CFTR.

Introduction

It has become more common in recent times to use genome-wide gene expression studies to infer drug mechanisms of action (Lamb et al. 2006; Iorio et al. 2009). It has been proposed that monitoring of genome-wide gene expression is likely to reveal insights into the actions of drugs and the prediction of additional drug targets (Iskar et al. 2010). The drug-induced gene expression has been used to assign new functions to existing drugs using systems-biology-based drug repositioning (Iorio et al. 2010). Using this method, the Rho-kinase inhibitor Fasudil that was used for treatment of cerebral vasospasm (Tanaka et al. 2005) was shown to act as an enhancer of cellular autophagy (Iorio et al. 2010). A study using genome-wide gene expression of breast cancer, myelogenous leukemia and prostate cancer and anti-correlating these with the drug-induced genome-wide gene expression (comparing the most up-regulated genes in the cancer tissue against the most down-regulated genes by the each drug treatment) was able to predict drugs for these cancers. This study was able to reposition four FDA-approved cancer drugs that are in use, and 22 FDA-approved drugs that were in clinical trials for the treatment of these cancers (Shigemizu et al. 2012). The study of the mechanism of action of the antiulcer drug cimetidine by gene expression concluded that the gene expression changes are almost opposite to that of lung adenocarcinoma gene expression, this observation has led to use of cimetidine as a candidate therapeutic in the treatment of lung adenocarcinoma (Sirota et al. 2011).

The investigation of mechanism by the studying the gene expression have also been successfully used for diseases like cancer, where the gene expression from different cancers are used to infer the common mechanism among the many types of cancer tissue (Rhodes et al. 2002; Iskar et al. 2010). Comparisons of large numbers of microarrays from different cancer samples showed that there are commonly regulated genes among all of these different cancer samples that might drive neoplastic transformation and progression, and also suggested that there might be

common molecular mechanisms by which cancer cells progress and avoid differentiation (Rhodes et al. 2004). More recently, dissecting out drug mechanisms of action using drug-induced gene expression led to the discovery of HSF1 as an important mediator of malignancy, and its inhibition was shown to reduce tumours (Santagata et al. 2013). So, in principle, genome-wide gene-expression profiles can be used to predict the mechanisms of action of drugs. So, it might be logical to use genome-wide gene-expression methods to define the mechanisms of action of ΔF508CFTR corrector drugs.

Among the numerous (~90) drugs that have been shown to be correctors of ΔF508CFTR, gene-expression profiles of the 23 drugs were available, but their mechanisms of action were unclear. As described earlier in the section 1.9, many of these drugs might be affecting the proteostasis network indirectly, but rather than acting as pharmacochaperones. Although gene-expression profiles of the few known pharmacochaperones were available, they were not considered for the present analysis. It was decided to analyse gene-expression-based mechanisms of action of the drugs that might act by regulating the proteostasis network of ΔF508CFTR. Using the global gene-expression profiles, common pathways/ networks/ genes affected by most of the drugs were identified and the involvement of many of these pathways/ networks/ genes in proteostasis and the correction of ΔF508CFTR was confirmed. The targeting of different pathways simultaneously, or the addition of pharmacochaperones, was additive or synergistic, and rescued ΔF508CFTR more efficiently than previously reported.

Results

2.1. Corrector drugs induce transcriptional changes for the rescue of ΔF508CFTR

There are several corrector compounds that allow ΔF508CFTR to overcome the ERQC and reach the PM (Pedemonte et al. 2005; Van Goor et al. 2006; Carlile et al. 2007; Hutt et al. 2010; Zhang et al. 2012). These drugs might act by direct binding, thereby promoting ΔF508CFTR folding/ trafficking, or they might act by modulation of the proteostasis network of the cell, which includes the ERQC, to allow the rescue of ΔF508CFTR. The known binders of ΔF508CFTR, like Corr4a and RDR1 (Wang et al. 2007; Sampson et al. 2011) were not included here, and 24 probable proteostasis modulators were chosen for this analysis, as listed in Table 2.1a. There were

no apparent chemical similarities among these modulators, nor any similarities in the characterised targets. If the drugs had any transcriptional action which is responsible for the correction then the correction must be suppressed by inhibiting the transcription. So simultaneously the drugs and transcription inhibitor actinomycin D was treated to the cells. It was noted that the effects of many corrector drugs on ΔF508CFTR were sensitive to actinomycin D (Figure 2.1), which suggested that the correctors have a transcriptional component in their mode of action. It was decided to correlate the mechanisms of action of these drugs on the proteostasis network, through an analysis of their effects on cellular gene expression profiles (the gene signature), which included both transcriptional and post-transcriptional (mRNA stability) effects.

Specifically, the gene signatures of two sets of drugs were used. The first set was made up of 11 correctors for which the gene signatures were available as Prototype Ranked Lists, as published by Iorio et al 2010. These were based on the drug gene signature database created using the Affymetrix platform (www.broadinstitute.org/cMap) (hereafter referred to as the cMap dataset; see Table 2.1a). The second set was made up of 13 correctors for which the gene signatures were obtained using the Agilent platform through treating immortalised CF bronchial epithelial (CFBE41o$^-$ cells stably transfected with ΔF508CFTR [a widely accepted cellular model for CF (Bebok et al. 2005)]) for 24 hours (hereafter referred to as the CFBE dataset; Table 2.1a). The CFBE dataset gene signature was obtained through the Thomas Laboratory in the Department of Biochemistry, McGill University, Montréal, Canada, in a collaboration with our Laboratory, and a part of these microarray data has already been published (Zhang et al. 2012). The microarray data from the CFBE cells were then processed to obtain ranked lists (see section 6.18). Glafenine was common between the cMap and CFBE datasets, and when probed using the database (www.broadinstitute.org/cMap), there was a significant similarity between the glafenine profiles found in both of the datasets (Table 2.1b), although glafenine was not one the top hits based on similarity. Nevertheless, the profiles of 13 corrector drugs obtained in the CFBE cell lines and those of the 11 drugs obtained from the cMap database were analysed separately.

2.2. Meta-analysis of the gene signatures to obtain commonly regulated genes

To extract information about the commonly regulated genes from gene signatures, a fuzzy intersection analysis of the microarray data was used, which was similar to methods published

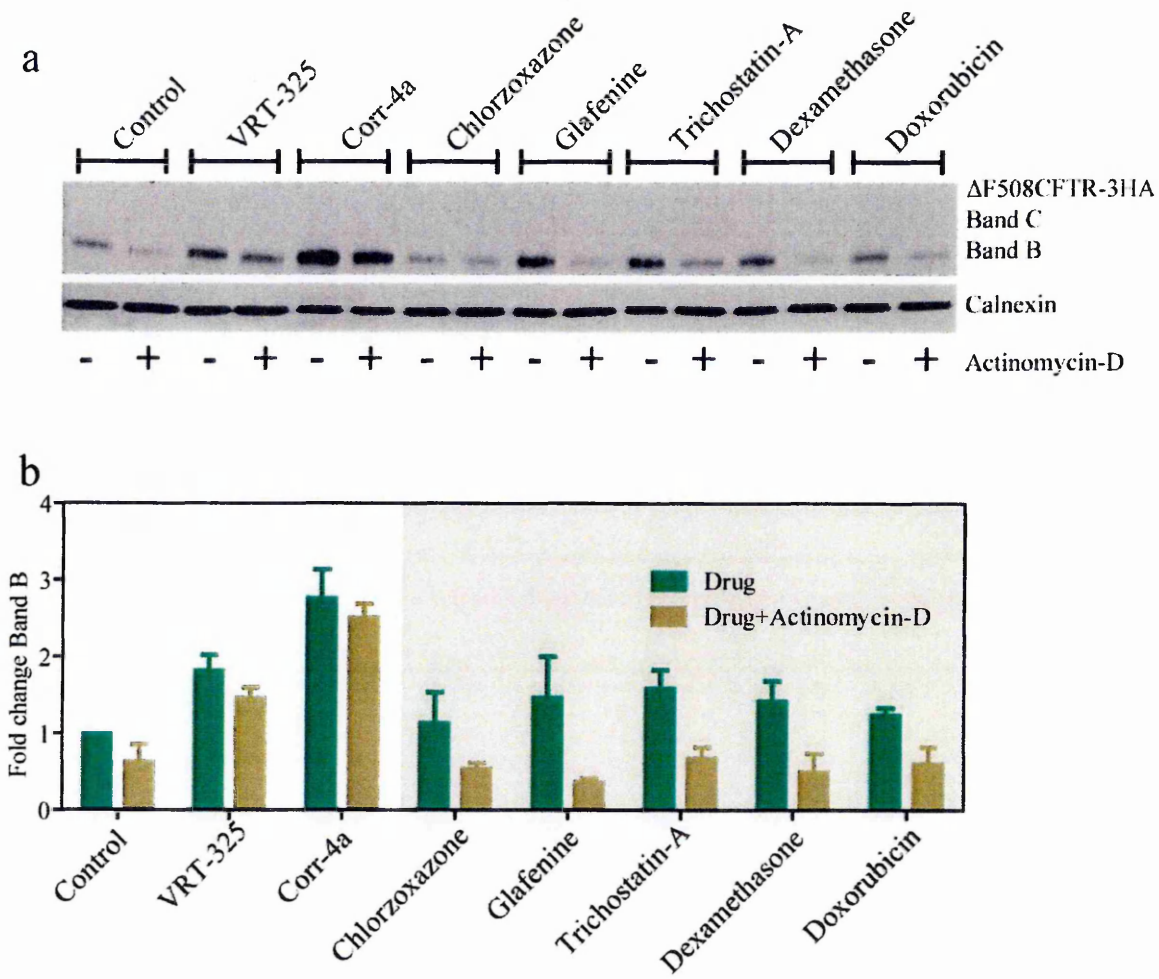

Figure 2.1. Corrector drugs act through transcription.

a. HeLa cells expressing ΔF508CFTR-3HA were treated with the drugs alone or with 10μg/ml actinomycin-D for 6 hours, lysed and proteins were immunobloted for CFTR. **b.** The levels of band B were quantified from immunoblots (like a, n=3) and expressed as fold change compared to control (DMSO treatment). Data represent mean ± SD. The Corr-4a and VRT325 (not known to act by transcriptional changes) were used as controls.

Table 2.1a. The corrector drugs used for the analysis of the gene signatures.

The CFBE dataset microarray obtained from treating drugs to the CFBE cells for 24 hour, the cMap dataset was made up of correctors for which the gene signatures were obtained from Iorio et al. 2010. The low temperature treatment was used as a positive control for correction in the CFBE dataset. The reference indicate the source where the corrector was originally identified.

Drugs of the CFBE dataset	Drugs of the cMap dataset
4-AN, PARP1 inhibitor (Anjos et al. 2012) ABT888 (Anjos et al. 2012) Glafenine (Robert et al. 2010) GSK339 (D Y Tomas lab unpublished) Ibuprofen (Robert et al. 2010) JFD03094 (Robert et al. 2008) KM11060 (Robert et al. 2008) Latonduine (Carlile et al. 2012) Minocycline H (D Y Tomas lab unpublished) Ouabagenin (Zhang et al. 2012) Ouabain (Zhang et al. 2012) PJ34(Anjos et al. 2012)	Chloramphenicol (Carlile et al. 2007) Chlorzoxazone (Carlile et al. 2007) Dexamethasone (Caohuy et al. 2009) Doxorubicin (Maitra et al. 2001) Glafenine (Robert et al. 2010) Liothyronine (Carlile et al. 2007) MS-275 (Hutt et al. 2010) Scriptaid (Hutt et al. 2010) Strophanthidin (Carlile et al. 2007) Thapsigargin (Egan et al. 2002) Trichostatin-A (Hutt et al. 2010)
Positive control Low temperature (Denning et al. 1992)	

Table 2.1b. Glafenine has similar effects on the CFBE with cMap dataset.

Top 200 and Bottom 200 ranked genes from CFBE cells treated with glafenine were queried with the cMap (http://www.broadinstitute.org/cMap/) database to infer the similarity between the two gene expression profiles.

cMap Name	Enrichment (similarity score)	p-Value
quinostatin	0.993	0.00004
emetine	0.815	0.00223
sulfafurazole	0.812	0.00058
dequalinium chloride	0.785	0.0041
glafenine	0.761	0.00615
fluspirilene	0.752	0.00726
simvastatin	0.744	0.00806
cephaeline	0.724	0.00368

earlier (Rhodes et al. 2002; Rhodes et al. 2004; Ramasamy et al. 2008; Clarke et al. 2013). This was based on the hypothesis that the rescue effect that is common to all of these drugs would be associated with common gene expression changes that are induced by most or all of these drugs. Keeping the cMap and CFBE gene-signature datasets independent, the down-regulated and up-regulated gene probes were intersected separately to obtain the probes that were commonly regulated by the correctors. To do this, the fuzzy intersection algorithm (Iorio et al. 2010) was used with a series of cut-offs, starting from a cut-off number the same as the number of drugs in each dataset (see section 6.18). The number of microarray probes present in the intersection increased sharply as the fuzzy intersection cut-off was decreased. For instance, in the case of the cMap dataset, 24 probes were commonly down-regulated when the fuzzy cut-off was set to 9; i.e., a probe commonly down-regulated by at least 9 out of the 11 drugs. This increased to 108 when the fuzzy cut-off was reduced to 8. The expected number of probes to be obtained by such an intersection of random drug profiles was also calculated and compared to the specific corrector drug profiles in each dataset (Figure 2.2a-h).

This fuzzy analysis yielded several sets of genes that were statistically significant both for the up-regulated and down-regulated probes of the CFBE dataset, and the down-regulated probes of the cMap dataset. There was no statistically significant gene sets obtained from the intersection of up-regulated probes from the cMap dataset. Even a very low fuzzy intersection cut-off of 5 yielded statistically significant numbers of probes in the intersections (Figure 2.2a-h). Moreover, at such low cut-offs, the enrichment over the randomly obtained probes was comparatively very low being false positives more than 50%). Even though statistically significant, at a cut-off of 5, the cMap down dataset has 2,687 probes, although 1,903 probes might have come up just at random, whereas the CFBE-down dataset had 7,093 probes, out of which 4,064 might have occurred at random (Figure 2.2a, c, e, g). Moreover, the hypothesis was to look at genes that are common to most of the drugs. So an optimal cut-off point for the fuzzy intersection was set to 8 in the case of the cMap dataset, and 9 in the case of the CFBE dataset, where the random probes (false positives) were below 30%. Moreover, the probes obtained from the intersection at cut-offs of 8 and 9 for cMap and CFBE, respectively, were also the optimal cut-offs where some biological functions by gene ontology were enriched. This enrichment might mean that at this cut-off it is more likely that a

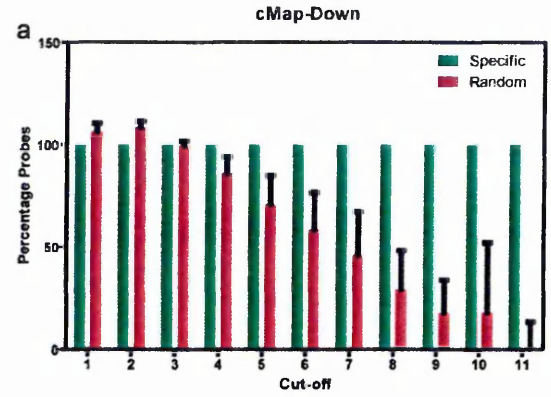

e

Cut-off	P-Value	Specific	Random	
			Mean	SD
1	0.918	17900	19082.5	770.3
2	0.989	12880	13982.7	509.3
3	0.389	8735	8706.7	180.364
4	0.062	5248	4514.8	449.5
5	0.031	2687	1903.2	381.3
6	0.023	1086	636.5	200.7
7	0.013	356	164.4	75.2
8	0.005	108	31.59	20.53
9	0.002	24	4.297	3.98
10	0.066	2	0.365	0.69
11	0.015	1	0.015	0.12

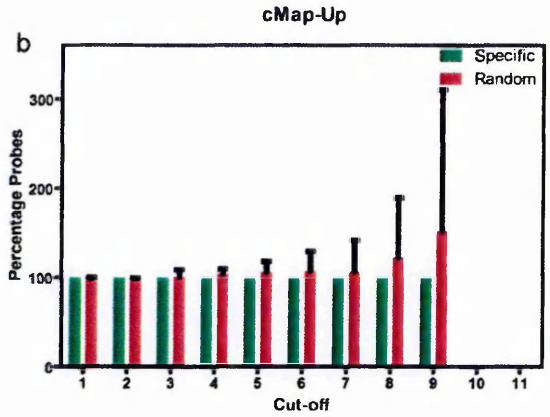

f

Cut-off	P-Value	Specific	Random	
			Mean	SD
1	0.308	20167	20027.5	251.68
2	0.187	14919	14705.9	246.85
3	0.835	8464	8524.81	68.25
4	0.833	3712	3885.87	191.35
5	0.674	1310	1392	166.29
6	0.586	364	390.83	83
7	0.534	79	84.17	28.29
8	0.604	11	13.45	7.37
9	0.726	1	1.52	1.58
10	1	0	0.107	0.31
11	1	0	0.003	0.054

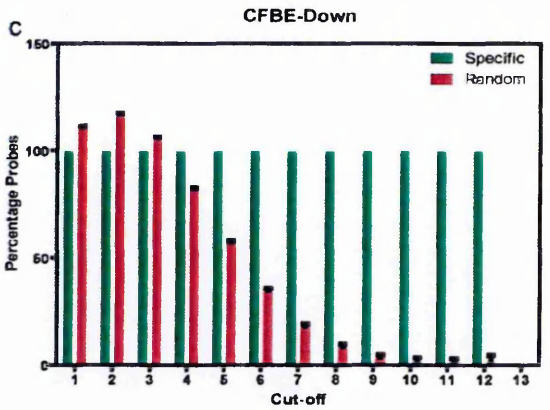

g

Cut-off	P-Value	Specific	Random	
			Mean	SD
1	>0.05	34858	38746.2	41.7922
2	>0.05	26835	31420.7	61.0181
3	>0.05	19273	20432.8	59.1375
4	<0.05	12587	10358.7	55.0638
5	<0.05	7093	4064.48	46.4943
6	<0.05	3527	1231.58	30.961
7	<0.05	1591	286.975	16.034
8	<0.05	592	51.0129	7.03208
9	<0.05	191	6.8076	2.59168
10	<0.05	44	0.6588	0.808568
11	<0.05	8	0.0431	0.207948
12	<0.05	1	0.002	0.044677
13	>0.05	0	0	0

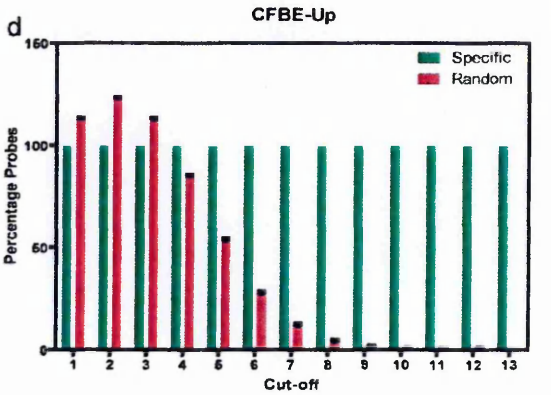

h

Cut-off	P-Value	Specific	Random	
			Mean	SD
1	>0.05	34233	38746.5	41.576
2	>0.05	25533	31420.9	61.5034
3	>0.05	18107	20432	58.2331
4	<0.05	12192	10359.2	54.071
5	<0.05	7596	4064.51	47.1841
6	<0.05	4465	1231.22	31.2179
7	<0.05	2439	287.139	16.2045
8	<0.05	1245	51.0595	7.09941
9	<0.05	541	6.7871	2.60929
10	<0.05	200	0.6561	0.814268
11	<0.05	43	0.0426	0.207811
12	<0.05	5	0.0013	0.036032
13	<0.05	1	0	0

Figure 2.2. Summary of the intersection of the probes at the different cut-offs.

(**a, b, c, d**) Percentage of the probes in specific and random drugs of each down-regulated or up-regulated gene set, as indicated above the figure. (**e, f, g, h**) The respective number of probes in each gene set, as tables.

Table 2.2a. CFBE -Up regulated genes.

The commonly up-regulated genes at a cut off of 9 (genes up-regulated in any 9 drugs out of 13 CFBE data set) were computed using the fuzzy algorithm.

ABCA12	C14orf147	CRNKL1	FIP1L1	KCND2
ABCG1	C14orf49	CTDSP2	FNBP1L	KCNJ2
ACPL2	C18orf18	CUL3	FOXO1	KCNMB4
ACPP	C1D	CXCL10	FRAS1	KDM3A
ACYP1	C1GALT1C1	CYBRD1	FSIP1	KIAA0182
ADAM28	C20orf3	CYP4B1	G3BP2	KIAA1033
AHI1	C20orf30	DIDO1	GABARAPL2	KIAA1107
AKAP9	C3orf14	DNAJA1	GBP2	KIAA1370
AKD1	C4orf34	DPY19L2	GEMIN8P4	KIF1B
ALOX5	C5orf53	DRAM2	GK	KL
ALS2CR8	C6orf35	DSC3	GNA13	KLF12
AMOT	C9orf44	DTX4	GNAQ	KLHL24
ANKRA2	C9orf68	DUOX2	GNPTAB	KTN1
ANXA4	CAND1	ECEL1P2	GPR110	KYNU
ARAP2	CASC2	ECT2	GRAMD1C	LAMTOR3
ARFGAP3	CCDC113	EFCAB7	GTF2I	LAPTM4A
ARID5B	CCDC121	EIF3H	H2AFJ	LCA5
ARMCX1	CCDC126	EIF4E	HBP1	LGALS3
ARMCX3	CCDC148	ELF2	HCG26	LGALS8
ARRDC3	CCDC57	ENTPD4	HNRNPR	LGR6
ATG5	CCNT2	EP300	HOOK1	LHX9
ATP6V1C2	CCPG1	EPM2AIP1	HPSE	LMO7
ATP7A	CD109	ERLIN2	HS2ST1	LNX1
AUH	CDC37L1	ETV1	HS3ST5	LOC100129794
BACH1	CDC73	ETV5	HSPA4	LOC100169752
BACH2	CEACAM1	ETV7	IBTK	LOC100287803
BANK1	CEP44	EVI5	IFIH1	LOC100505930
BAZ2A	CH25H	FAM122C	IGFL2	LOC100505956
BBS12	CHD7	FAM131B	IL20RA	LOC100506012
BBS2	CIITA	FAM150A	IMMP2L	LOC100506046
BCL2L11	CISD2	FAM171B	INPP5D	LOC100506262
BCL6	CLCA2	FAM18B1	INTU	LOC100506398
BDH2	CLDN16	FAM198B	ITFG1	LOC100506538
BET1	CLIC4	FAM47E	ITIH5	LOC100507197
BLNK	CLIC5	FAM59A	IVNS1ABP	LOC100507398
BRWD1	CLK1	FAM65B	JRKL	LOC100507524
C11orf54	CNGA1	FAM84A	KAT6B	LOC220594
C12orf23	COL20A1	FANCM	KATNAL2	LOC286161
C12orf26	COL21A1	FAS	KBTBD2	LOC401098
C12orf48	CPEB3	FASTKD1	KBTBD3	LOC401320

Table 2.2a. CFBE -Up regulated genes (continued).

LOC541467	PAFAH1B1	RASEF	STK31	WDR33
LOC541473	PAIP2	RB1	STK38L	WDR78
LOC728978	PAIP2B	RBAK	STON1	WNT8B
LPIN2	PAPOLG	RBBP4	STX11	XRN1
LRP1B	PBX1	RBMXL1	SUV420H1	YIPF5
LUC7L3	PCDH7	REV3L	SYNPO2	YPEL1
LZTFL1	PCDHB10	RFPL2	TBX20	YPEL2
MAFB	PCDHB18	RFX3	TET2	YPEL5
MARCKS	PCMTD1	RIC3	TFRC	ZBED5
MAT2B	PCMTD2	RRM2B	THAP2	ZBTB26
MBD2	PDCD2	SAT1	TIGD7	ZBTB38
MBD5	PDE4B	SCAF8	TLL1	ZC3H11A
MCEE	PDE4D	SDR16C5	TLR1	ZFAND6
MCM9	PDE5A	SEC62	TLR3	ZFPM2
METTL7A	PDGFD	SEL1L	TLR6	ZNF10
MEX3B	PDK4	SEPSECS	TMEM106B	ZNF184
MFSD4	PFKFB2	SERTAD4	TMEM123	ZNF214
MIA3	PHC3	SGSM1	TMEM18	ZNF217
MLF1	PIK3C2G	SHPRH	TMEM20	ZNF230
MLLT4	PIK3C3	SIRT4	TMEM237	ZNF233
MME	PITX2	SLAIN2	TMEM39A	ZNF323
MMP13	PIWIL4	SLC11A2	TMEM59	ZNF404
MMP7	PLEKHA7	SLC15A2	TMEM86A	ZNF449
MRE11A	PLRG1	SLC16A7	TNFRSF11A	ZNF483
MRPL50	PLSCR4	SLC19A2	TNNT2	ZNF525
MXRA5	PPIE	SLC1A3	TP53INP1	ZNF546
MYO6	PPIL6	SLC25A27	TRAK2	ZNF571
N4BP2L1	PPM1D	SLC35A1	TRIM22	ZNF577
N4BP2L2	PPP1CB	SLFN12	TSPAN12	ZNF586
NBR1	PPP6C	SLFN13	TSPAN2	ZNF606
NEK1	PPT1	SMARCA5	TSPAN6	ZNF613
NIPBL	PRPF4B	SMPDL3A	TTC23L	ZNF649
NLGN4X	PSD2	SNX16	TTC28-AS1	ZNF780A
NOTCH2NL	PTPLAD2	SOS2	TTC30A	ZNF850
NPNT	PTPN4	SPATA18	TTC33	
NR1D2	PTPRR	SPATA19	TUB	
NUDCD1	PXDNL	SPDYE1	UBE2D1	
NUP62CL	QPCT	SPDYE5	USP25	
OK/SW-CL.58	RAD21	SPG20	UST	
OPRK1	RALGPS1	SRSF1	VTCN1	
OR2L13	RAPGEF2	STEAP4	WDR17	
OXGR1	RAPGEF5	STIM2	WDR19	

Table 2.2b. CFBE and cMap down regulated genes.

The commonly down-regulated genes of CFBE drugs at cut-off 9 and cMap drugs at cut-off 8 (genes down-regulated in any 9 drugs of CFBE data set or any 8 drugs of cMap data set) were computed using the fuzzy algorithm.

CFBE-Down regulated genes			cMap-Down regulated genes		
ABCG5	GJC3	OSMR	AKAP1	GTSE1	SLC25A6
ADAMTS19	GNB4	PALMD	AKAP8	HMGXB4	SLC4A1AP
ADAMTS9	GRIN2B	PCP4	ANKLE2	HPS4	SMCR7L
ALPK1	GSC	PDE11A	ARID1A	HYAL3	SNAPC4
ARHGEF25	GYG2	PDE3A	ASB8	JRK	STAG2
ATN1	HLA-DRB4	PDZD7	C10orf26	KIF20A	TAX1BP3
ATP13A4	HNF4G	PIF1	C11orf61	LMF1	TBC1D13
BASP1	HYDIN	PLIN5	C14orf106	LMNB1	TDP1
BIN2	IL25	POLR3D	CAMKK2	MAP3K11	TMEM115
C14orf162	ILDR1	PXN	CCDC59	MED1	TMEM121
C16orf45	INO80B	RAX2	CD2BP2	MED13	TOP3A
C7orf69	IVL	REG1B	CENPA	MEPCE	TROAP
CAPN6	KRT34	RGL3	CENPE	METTL3	UNKL
CISD3	LAIR1	RNF215	CHPF2	MKI67	VPS72
CLDN17	LCN15	S100A2	COIL	MPPE1	WDR6
COL14A1	LIMS3	S100A7	COMMD4	MRFAP1L1	WDR74
CRCT1	LOC100132234	SAGE1	COMMD9	MYB	WTAP
CTSC	LOC100505915	SHC3	CTDSP1	NCAPH2	XYLT2
DCD	LOC100506328	SLC22A3	DGCR8	NOL3	YWHAH
DCLK1	LOC100510044	SLC47A1	DHX30	NR2F2	ZC3H3
DLL3	LOC388796	SOSTDC1	DHX38	NSUN5P2	ZCCHC10
DNALI1	LOC729059	SPRR1A	DICER1	NUP50	ZNF443
DPCR1	LRRC31	SPRR1B	DNAJC2	ORC1L	
EFHD2	MAL	ZFP36L2	DSN1	PAQR4	
EHD1	MATN2	SPRR3	EHMT2	PATZ1	
EPB41L4A	MBL2	SULT1C2	ENDOG	PDCD6	
ERBB4	MDGA1	TCEB3C	EXOSC4	PPAP2B	
EVI2B	METTL21A	TCTN1	FAM111A	PRPF4B	
FAM101B	METTL7A	TECRL	FAM120A	PRPF8	
FAM131C	MGC10814	TEP1	FAM128B	RAB17	
FAM49B	MIR210HG	TLN2	FARSA	RABIF	
FAM83A	MITF	TMPRSS1	FBXO7	RBM7	
FANCD2	MRPL24	5	FOSL1	RGS19	
FCRL4	NCRNA00319	UBOX5	GATAD1	SAFB	
FERMT1	NOG	VHL	GEMIN4	SAP30L	
FGFBP1	NPRL3	VNN1	GLT8D1	SART1	
FLJ45340	NUDT22	VPS13D	GNPTAB	SCO2	
FLNB	ODF3L2	ZAP70	GPATCH1	SENP6	
FOXK1	ONECUT1		GPRC5C	SETDB1	
FUT6	OR8J1		GTF3C4	SH2B1	

particular associated biological function can be affected by many of these drugs commonly, and that this common process might be somehow relevant to ΔF508CFTR correction. So with both the "biological criterion" and the "statistical criterion" the cut-off was set to 8 for the cMap down-regulated probe set and to 9 for the CFBE up-regulated and down-regulated probe set.

For the CFBE dataset, these fuzzy intersections resulted in 541 up-regulated probes (corresponding to 402 genes, hereafter referred to as CFBE-Up) (Figure 2.2d) and 191 down-regulated probes (corresponding to 117 genes, hereafter referred to as CFBE-Down) (Figure 2.2c). For the cMap dataset, there were 108 down-regulated probes (corresponding to 102 genes, hereafter referred to as cMap -Down) (Figure 2.2a). Statistical analyses revealed that close to 7 probes were obtained at random in the CFBE dataset, and that in the case of the cMap -Down dataset, this was close to 30 probes (Figure 2.2e). The cMap -Up dataset did not show significant probes at the selected cut-off (Figure 2.2b, f). It should be noted here that the statistical tests with the CFBE datasets yielded a relatively low number of randomly obtained probes due to the statistical method used (see section 6.18). Three genes were present in both the up-regulated and down-regulated gene sets (considering CFBE and cMap together). This might be caused by the disagreement between the two or more probes for the same gene, and also due to the distinct platforms used (Agilent *vs* Affymetrix); nevertheless, this is very low compared to the total number of genes obtained (close to 600) (Table 2.2a, 2.2b).

To summarise, three sets of genes were collected: CFBE-Up, as 402 genes; CFBE-Down, as 117 genes; and cMap -Down, as 102 genes, and these are called the commonly regulated genes (Table 2.2a, 2.2b). These intersected common sets of up-regulated or down-regulated genes of the microarray profiles of the corrector drugs will lead to the identification of a common pathway(s) targeted by most of these corrector drugs. However, as the drugs or a subset of the drugs might also target specific idiosyncratic pathways other than the common ones, the results obtained from the above-described analyses might be limiting.

2.3. Analyses of commonly regulated genes to obtain commonly regulated pathways/ networks

The commonly regulated genes obtained were then analysed using a series of bio-informatic tools to extract the commonly regulated molecular pathways/ networks that were embedded in the gene lists. The gene ontology enriched biological processes were analysed in the different

commonly regulated gene lists. The biological processes that had the false discovery rate (FDR) below 5 were considered for the analysis. The cMap -Down dataset was enriched in mitotic or cell-cycle and mRNA processing machineries, CFBE-Down was enriched in keratinocyte differentiation processes, while the CFBE-Up was enriched, in transcriptional processes (Figure 2.3). As the numbers of commonly regulated genes were relatively low, a manual inspection of the list was carried out to look for genes/ proteins involved in processes that were shown to be involved in ΔF508CFTR proteostasis or others like regulatory proteins (kinases and phosphatases), ubiquitin pathway components, and chaperones. There were several kinases, phosphatases and other associated proteins present in the commonly regulated gene list. From a literature analysis of the accumulated knowledge about these proteins, an observation that stands out is that many proteins that are modulated affect the stress-activated MAPK pathway (p38 and JNK).

Specifically there were a few proteins in the CFBE-Up dataset that are known negative regulators of the SAPK pathway, including INPP5D (An et al. 2005), PPM1D (Hickson et al. 2007), PPP6C (Kajino et al. 2006) and PTPRR (Su et al. 2013), while among the down-regulated proteins there were FLNB, an adaptor involved in promoting JNK signalling (Jeon et al. 2008), and MAP3K11 (also known as MAP3K11), an upstream activator of JNK signalling (Brancho et al. 2005). Among the ubiquitin pathway components as described earlier, USP25, a deubiquitinase involved in the regulation of ΔF508CFTR proteostasis (Blount et al. 2012) is up-regulated, and so is an E2 ubiquitin ligase UBE2D1 (UbcH5a), which is involved in the ERAD of ΔF508CFTR (Younger et al. 2006). Among the chaperones, surprisingly, not many were modulated by the corrector drugs. The most important was HSP70 (HSPA4), which has been shown to rescue ΔF508CFTR when overexpressed (Trzcinska-Daneluti et al. 2009), and is present in the CFBE-Up dataset, along with DNAJA1, which is known to increase the degradation of ΔF508CFTR (Okiyoneda et al. 2010).

To gain further insight, the datasets were then analysed for various biologically relevant characteristics, including protein-protein interactions, ingenuity pathway building analysis, and also manual inspection, to identify interesting CFTR proteostasis-relevant molecules in the dataset. The results of these analyses are summarised below.

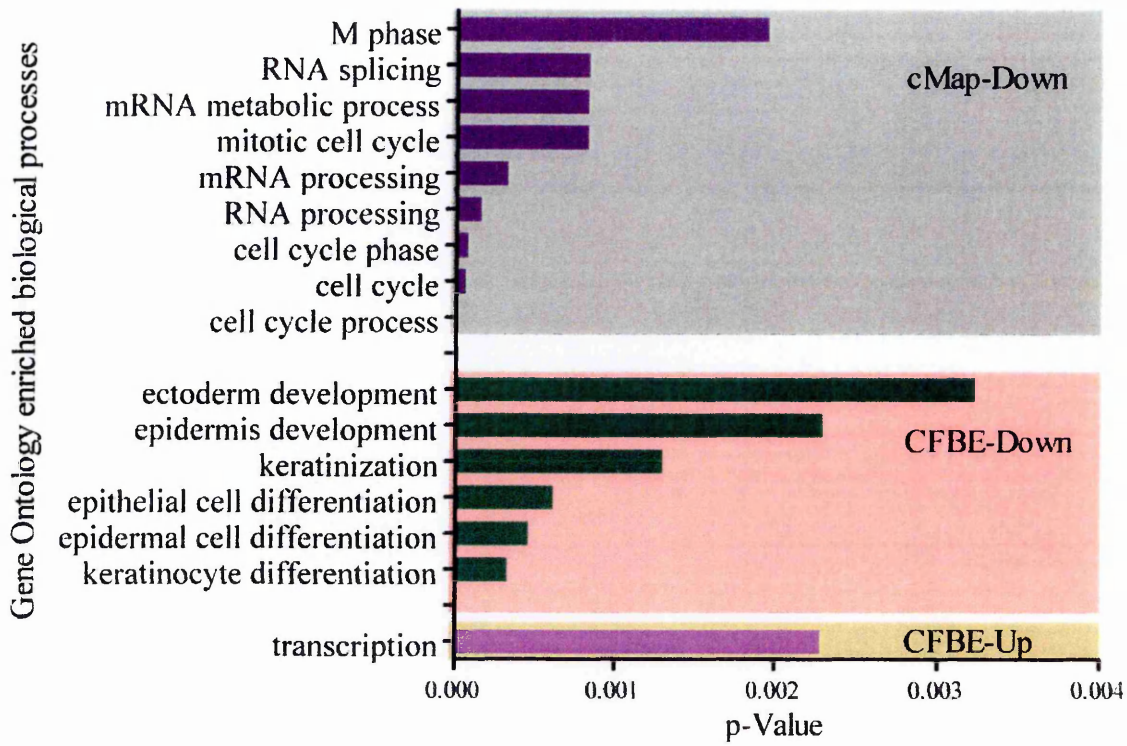

Figure 2.3. Gene ontology enrichment in the commonly regulated gene lists.

The p-Values were plotted for each of the enriched biological processes (false discovery rate bellow 5) computed using DAVID (http://david.abcc.ncifcrf.gov/) gene ontology for each indicated gene set.

2.4. Commonly regulated genes form macromolecular interaction complexes

STRING database identifies protein-protein interactions among the commonly regulated genes:

To analyse the protein-protein interactions (PPIs) among the commonly regulated genes, the STRING database was used (http://string-db.org/) (Franceschini et al. 2013). Among the total of 618 proteins (all of the commonly regulated proteins combined) that were provided as input (see section 6.18), significant interactions based on a cut-off score of >0.7, were seen between 166 proteins, with a total of 166 interactions among them (Figure 2.4a). Upon manual inspection of the network, sub-networks relating to the components of the centromere/ kinetochore/ cohesin, RNA processing machinery, transcription factors, phosphodiesterases, collagen and keratinocyte differentiation markers were found. In addition, several genes from both the up-regulated and down-regulated datasets interacted among themselves, suggesting that similar pathways are targeted by both up-regulated and down-regulated genes, mainly in the network of the RNA processing machinery and phosphodiesterases. For one of the phosphodiesterases present in the network, PDE3A (present in the cMap -Down dataset), its inhibition is known to promote CFTR-mediated chloride conductance (Penmatsa et al. 2010).

Ingenuity pathway analysis identifies embedded commonly regulated pathways/ networks among commonly regulated genes:

To dissect the pathways/ networks from the identified commonly regulated genes Ingenuity Pathway analysis (IPA), a well-characterised pathway-building tool (web-based software application) was also used (http://www.ingenuity.com/products/ipa) (see section 5.20). IPA is based on prior published knowledge and has been used extensively by the scientific community to analyse large datasets, to understand the biological mechanisms embedded in them. The commonly regulated gene sets were analysed using the core analysis application of IPA (hereafter referred to as IPACA). IPACA helps to assess the enrichment for canonical signaling/ metabolic pathways, builds molecular networks with the dataset of interest, and also identifies upstream regulators of the given gene set.

When the CFBE-Up, CFBE-Down and cMap-Down commonly regulated genes were analysed together using the IPACA application, this identified 7 upstream regulators, among which

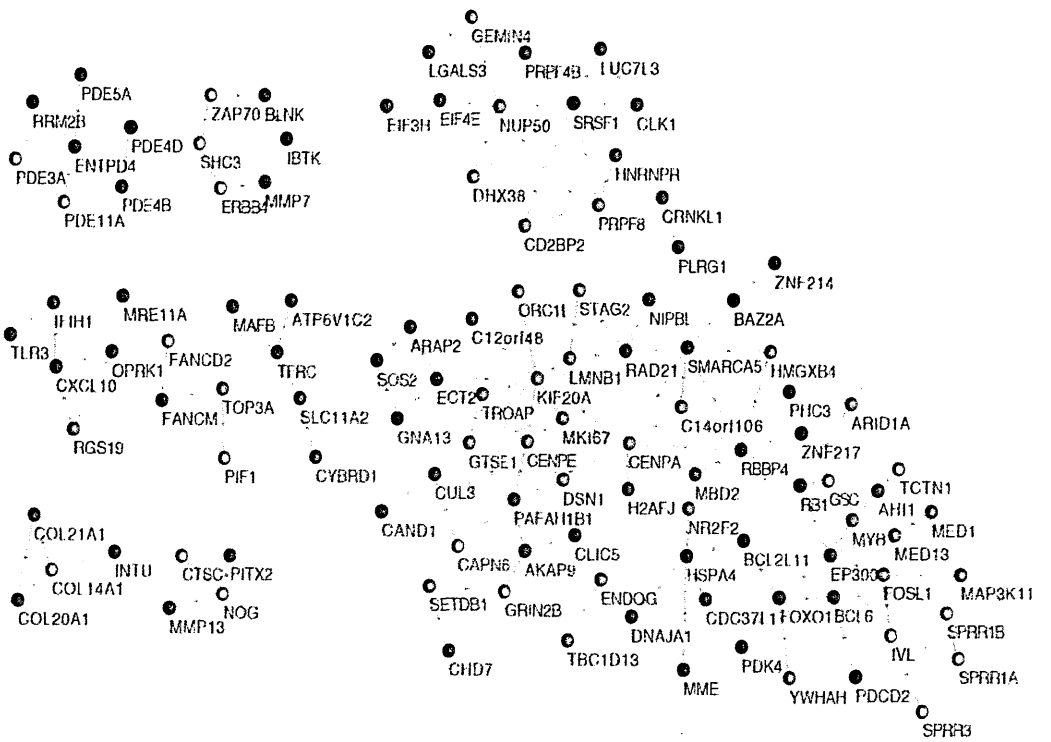

Figure 2.4a. String network of the commonly regulated genes.

The protein-protein interaction among the commonly regulated genes were derived from the String database (http://string-db.org/). The interaction network with at least four proteins are presented. Nodes ○ CFBE-Down, ◎ cMAP-Down, ● CFBE-Up.

5 were predicted to be activated and 2 were inhibited in the commonly regulated gene sets (Table 2.4a). Among the activated category there was SLC29A1, a nucleoside transporter, colony stimulating factor (CSF2), STAT4, oncosuppressor p73 (TP73), and interferon regulatory factor-1 (IRF-1), while in the inhibited category there were TAB1 and miR-155. TAB1 binds to TAK1 and is involved in the TGF-β signalling pathway, while miR-155 has been shown to be up-regulated in lung epithelial cells of CF patients, and has been linked to the hyper-inflammatory phenotype of CF (Bhattacharyya et al. 2011). This analysis also identified canonical pathways in which the commonly regulated genes were enriched, which included chondroitin/ dermatan sulphate biosynthesis, PKA signalling, ERK/MAPK signalling, p53 signalling, β-cell receptor signalling, GPCR signalling, integrin signalling, signalling via pattern-recognition receptors, prostate cancer signaling, and hereditary breast cancer signalling (Table 2.4b).

Analysis of IPACA also yielded 25 networks that consisted of 35 nodes each. It is important to note here that IPA builds networks not only with the genes provided, but it also predicts potential interacting nodes to build the networks. The networks with close to two-thirds of the nodes included from the list of commonly regulated genes were considered for further analysis. This resulted in 8 networks (Figure 2.4.b) with the number of nodes taken from commonly regulated genes varying from 22-30, out of the 35 nodes in each network. The top functions associated with these networks included several developmental disorders, the cell cycle, DNA recombination/ repair, RNA post-transcriptional modifications, cell death and survival, lipid metabolism, and infectious diseases (Table 2.4c, Figure 2.4.b). RNA processing was also found earlier by gene ontology analysis. Then 117 down-regulated, 402 up-regulated genes of the CFBE dataset and 102 cMap down-regulated genes were subjected to IPACA analysis separately to test whether these datasets particularly affect some other specific pathways or functional networks other than the common (CFBE-Up, CFBE-Down and cMap -Down commonly regulated genes analysed together) pathways or network functions, as described above. The resulting canonical pathways and networks with associated functions are summarised in Table 2.4d, e, f and Figure 2.4c, d, e. No dataset had any significantly inhibited or activated upstream regulators. The CFBE-Up dataset yielded 40 top canonical pathways affected, which included p53 signalling, PDGF signalling, insulin receptor signalling, β-cell receptor signalling and others, and also yielded 22 networks; interestingly, two

Table 2.4. IPACA of the commonly regulated genes.

CFBE-Up, CFBE-Down and cMap-Down commonly regulated gene sets analysed using IPACA. **a.** Upstream regulators. **b.** Identified enriched canonical pathways. **c.** Top 8 networks, and their associated scores and functions.

a

Upstream regulator	Molecule type	Predicted activation state	p value
TAB1	Enzyme	Inhibited	9.65E-04
mir-155	MiRNA	Inhibited	2.30E-02
SLC29A1	Transporter	Activated	1.93E-03
CSF2	Cytokine	Activated	2.73E-03
STAT4	Transcription regulator	Activated	9.27E-03
TP73	Transcription regulator	Activated	1.46E-02
IRF1	Transcription regulator	Activated	2.79E-02
STAT1	Transcription regulator	Activated	5.22E-02
TP53	Transcription regulator	Activated	6.41E-02

b

Ingenuity canonical pathways	-log(p value)
tRNA splicing	3.51E00
Cardiac β-adrenergic signalling	2.97E00
p53 signalling	2.96E00
Relaxin signalling	2.89E00
Chondroitin sulphate biosynthesis	2.47E00
Dermatan sulphate biosynthesis	2.39E00
Protein kinase A signalling	2.36E00
cAMP-mediated signalling	2.1E00
ERK/MAPK signalling	1.83E00

c

Network	Score	Top diseases and functions
1	46	Developmental disorders, hereditary disorders, neurological diseases
2	39	Infectious diseases, cardiovascular diseases, dermatological diseases and conditions
3	37	Organ morphology, skeletal and muscular system development and function, connective tissue disorders
4	36	Cell cycle, cellular assembly and organisation, DNA replication, recombination and repair
5	30	Cell death and survival, connective tissue development and function, RNA post-transcriptional modification
6	29	Lipid metabolism, small molecule biochemistry, infectious diseases
7	29	Post-translational modification, lipid metabolism, molecular transport
8	28	Gene expression, RNA damage and repair, RNA post-transcriptional modification

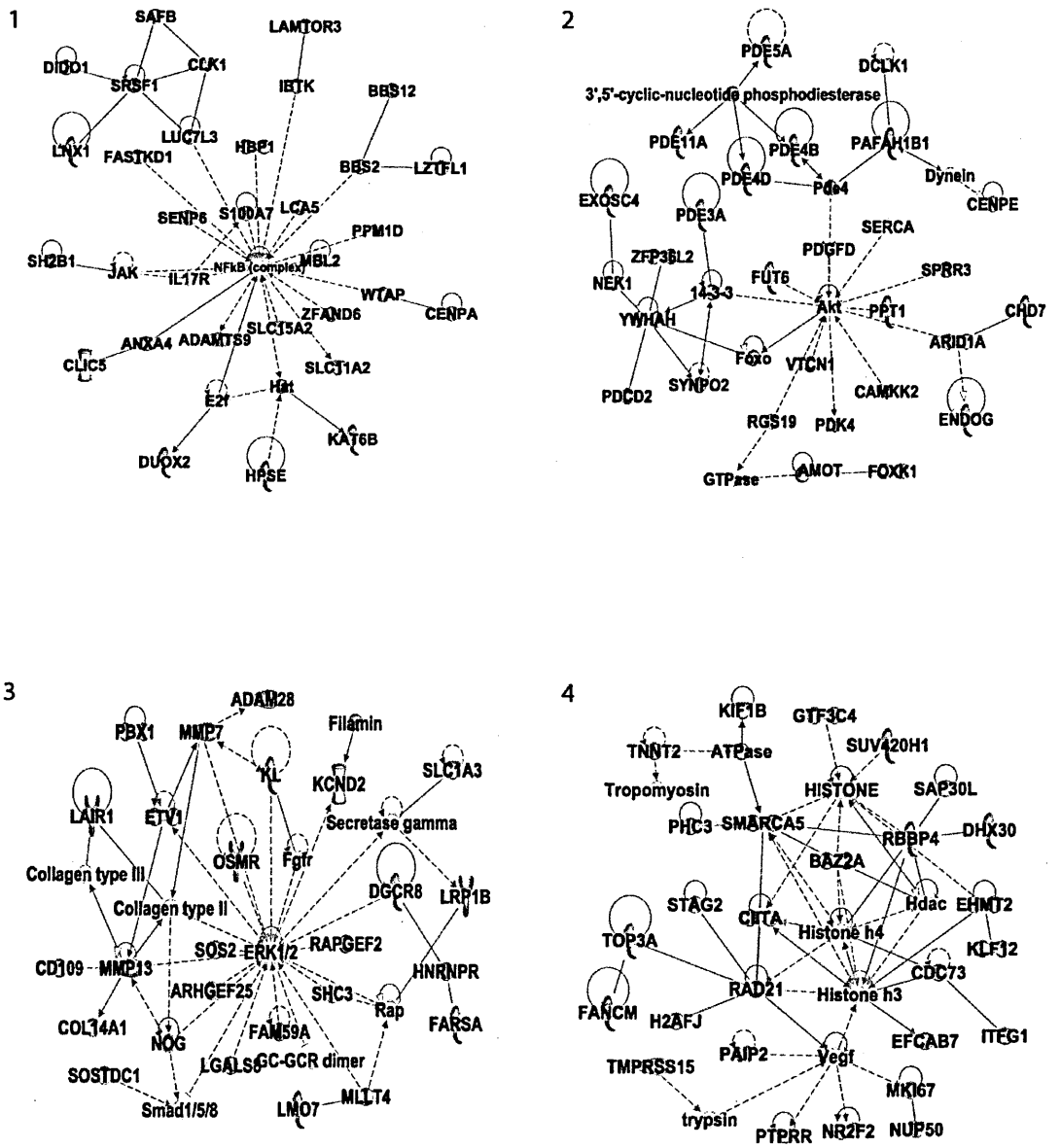

Figure 2.4b. IPACA networks of the commonly regulated genes.

1-4 Networks of CFBE-Up, CFBE-Down and cMap-Down commonly regulated genes analysed together using IPACA. The networks contain Green nodes which are down-regulated genes; red nodes which are up-regulated genes and white nodes which are IPACA genes.

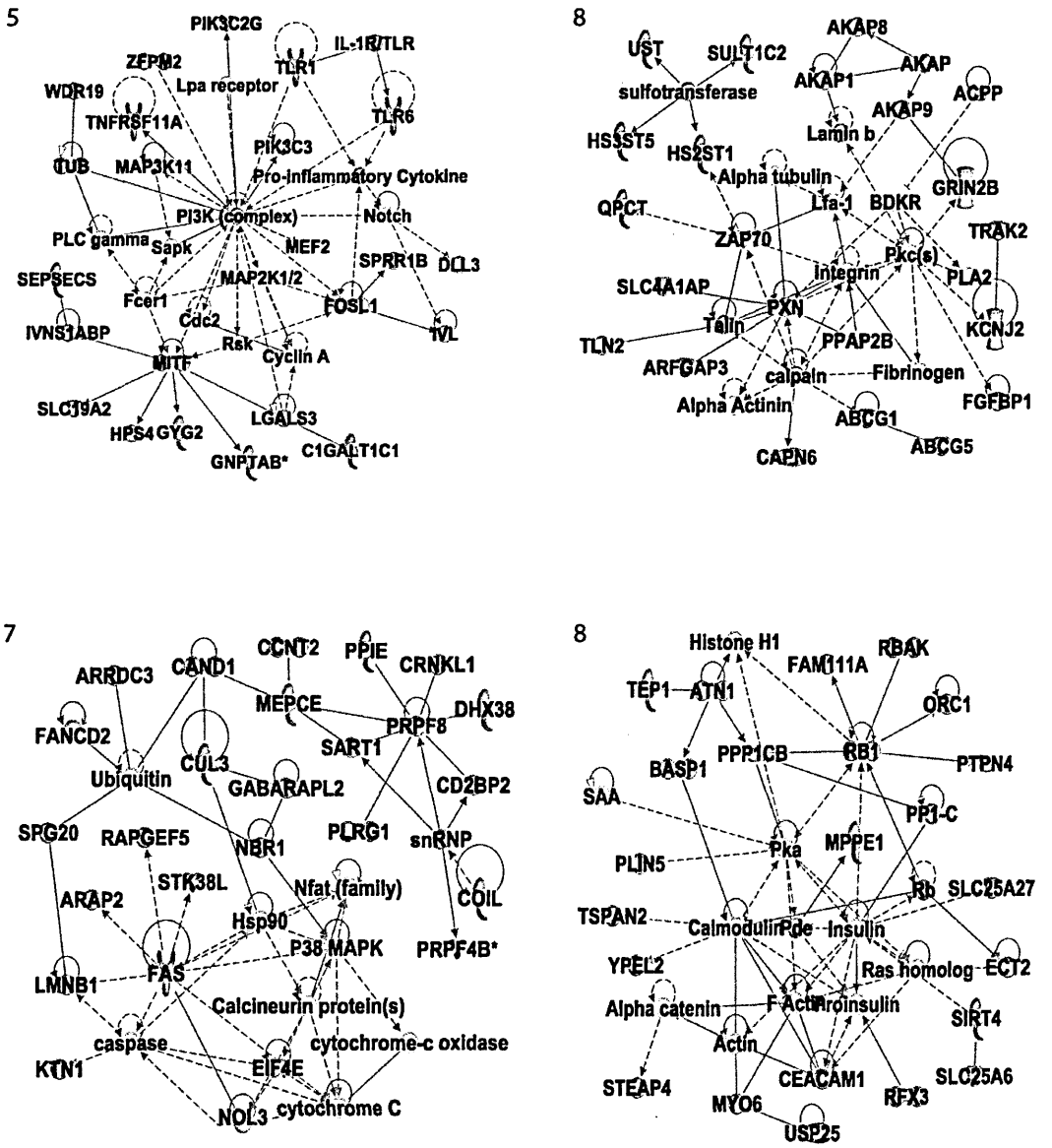

Figure 2.4b. IPACA networks of the commonly regulated genes (continued).

5-8 Networks of CFBE-Up, CFBE-Down and cMap-Down commonly regulated genes analysed together using IPACA. The networks contain Green nodes which are down-regulated genes; red nodes which are up-regulated genes and white nodes which are IPACA genes.

networks have one of their top associated functions as "molecular transport" although information about the specific kind of molecular transport these networks may be associated was not clear. There were also other network-associated functions, like the cell cycle, and DNA replication, recombination, and repair, among others. The CFBE-Down dataset yielded 7 canonical pathways, which included regulation of cellular mechanics by calpain protease, FAK signalling, tRNA splicing, nNOS signalling, relaxin signalling and cardiac β-adrenergic receptor signalling. The CFBE-Down dataset also yielded only 6 significant networks that are associated with functions like cellular movement, connective tissue development and function, embryonic development, cell morphology, haematological system development and function, gene expression, cell death and survival, cell cycle, and others. The cMap-Down dataset again yielded 7 canonical pathways, which included granzyme B signalling, systemic lupus erythematosus signalling, cardiac β-adrenergic receptor signalling, chondroitin sulphate biosynthesis, chondroitin and dermatan biosynthesis, dermatan sulphate biosynthesis, glycoaminoglycan-protein linkage region biosynthesis, and ERK5 signalling, and also yielded 6 significant networks that are associated with functions like cell signalling, gene expression, the cell cycle, DNA replication, recombination, and repair, and lipid metabolism.

To summarise, the IPA analysis identified many processes present in the commonly regulated genes that were identified earlier, reiterating the possible importance of these pathways in the regulation of CFTR proteostasis. This analysis also identified several other pathways, including molecular transport, lipid metabolism, integrin signalling and GPCR signaling, as potential proteostatic regulators. Apparently these networks or canonical pathways excluded previously validated ΔF508CFTR proteostasis genes (Table 2.5), this may mean that the commonly regulated genes are novel regulators of ΔF508CFTR proteostasis which need further validation. Moreover, networks of the commonly regulated genes when analysed particularly yielded connections between the many commonly regulated genes and few regulatory kinases and transcription factors. The kinases included AKT, CK2, ERK1, ERK2, MAPK, and MEKs, transcription factors HNF4A, TP53, and NF-κB, the cytokine TGFβ1, the growth factor VEGF, which were connected to many commonly regulated genes. These genes may regulate the many commonly regulated genes, and they are also important candidates to be tested for their roles towards ΔF508CFTR proteostasis.

Table 2.4d. IPACA of the cMap-Down genes.

The cMap-Down gene sets analysed using IPACA. **1.** Identified enriched canonical pathways. **2.** Networks with associated scores and functions.

1

Ingenuity canonical pathways	-log(p value)
Granzyme B signalling	2.59E00
Systemic lupus erythematosus signalling	1.68E00
Cardiac β-adrenergic signalling	1.61E00
Chondroitin sulphate biosynthesis	1.58E00
Chondroitin and dermatan biosynthesis	1.55E00
Dermatan sulphate biosynthesis	1.55E00
Glycoaminoglycan-protein linkage region biosynthesis	1.48E00
ERK5 signalling	1.44E00

2

Network	Score	Top functions
1	53	Cell signalling, cell cycle, gene expression
2	30	Cellular assembly and organization, DNA replication, recombination and repair, cell cycle
3	27	Cellular function and maintenance, cardiovascular system development and function, dermatological diseases and conditions
4	23	Dermatological diseases and conditions, developmental disorders, hereditary disorder
5	22	Metabolic disease, lipid metabolism, small molecule biochemistry
6	16	Developmental disorders, skeletal and muscular disorders, molecular transport

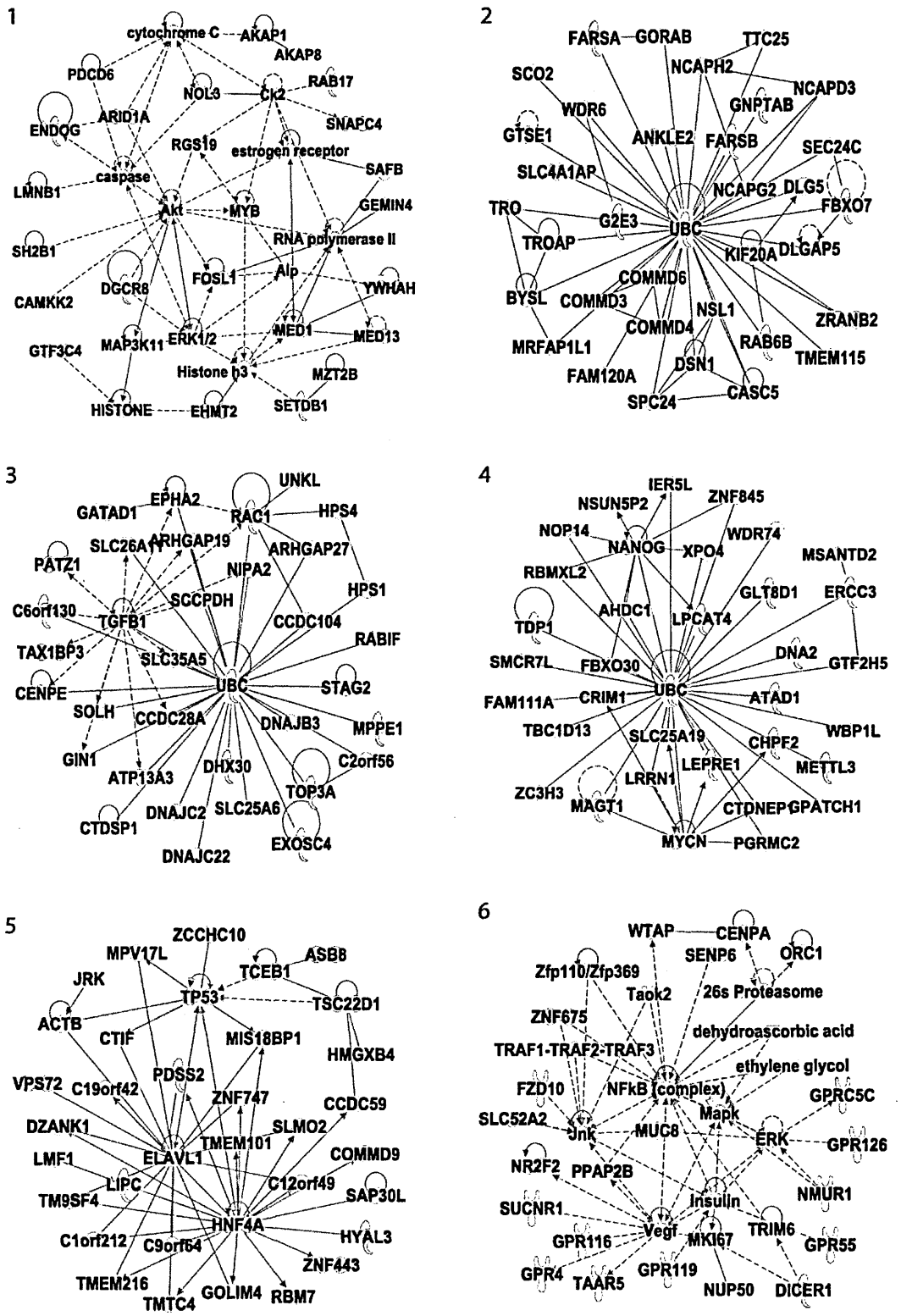

Figure 2.4c. IPACA networks of the cMap -Down genes

1-6 Networks of cMap -Down genes analysed using IPACA. The networks contain Grey nodes which are cMap down-regulated genes and white nodes which are IPACA genes.

Table 2.4e. IPACA of the CFBE-Up genes.

CFBE-Up gene sets analysed using IPACA. **1.** Identified enriched canonical pathways. **2.** Networks with associated scores and functions

1

Ingenuity canonical pathways	-log(p value)
p53 signalling	2.87E00
FLT3 signalling in haematopoietic progenitor cells	2.7E00
Prostate cancer signalling	2.47E00
FcγRIIB signalling in B lymphocytes	2.23E00
Role of pattern recognition receptors in recognition of bacteria and viruses	2.14E00
B Cell receptor signalling	2.13E00
Insulin receptor signalling	2.03E00
Relaxin signalling	2E00
PDGF signalling	1.92E00

2

Network	Score	Top functions
1	52	Cellular function and maintenance, haematological system development and function, humoral immune response
2	31	Connective tissue development and function, embryonic development, organ development
3	31	Cell cycle, cellular assembly and organization, DNA replication, recombination and repair
4	29	Molecular transport, cellular assembly and organisation, haematological disease
5	28	Infectious disease, cardiovascular diseases, dermatological diseases and conditions
6	23	Carbohydrate metabolism, lipid metabolism, small molecule biochemistry
7	21	Amino acid metabolism, nucleic acid metabolism, small molecule biochemistry
8	21	Molecular transport, developmental disorders, hereditary disorders
9	19	Cell-to-cell signalling and interaction, reproductive system development and function, cellular assembly and organisation
10	19	Hereditary disorder, metabolic disease, cell morphology
11	18	Post-translational modification, cardiac fibrosis, cardiovascular diseases
12	18	Cell morphology, cellular function and maintenance, infectious diseases

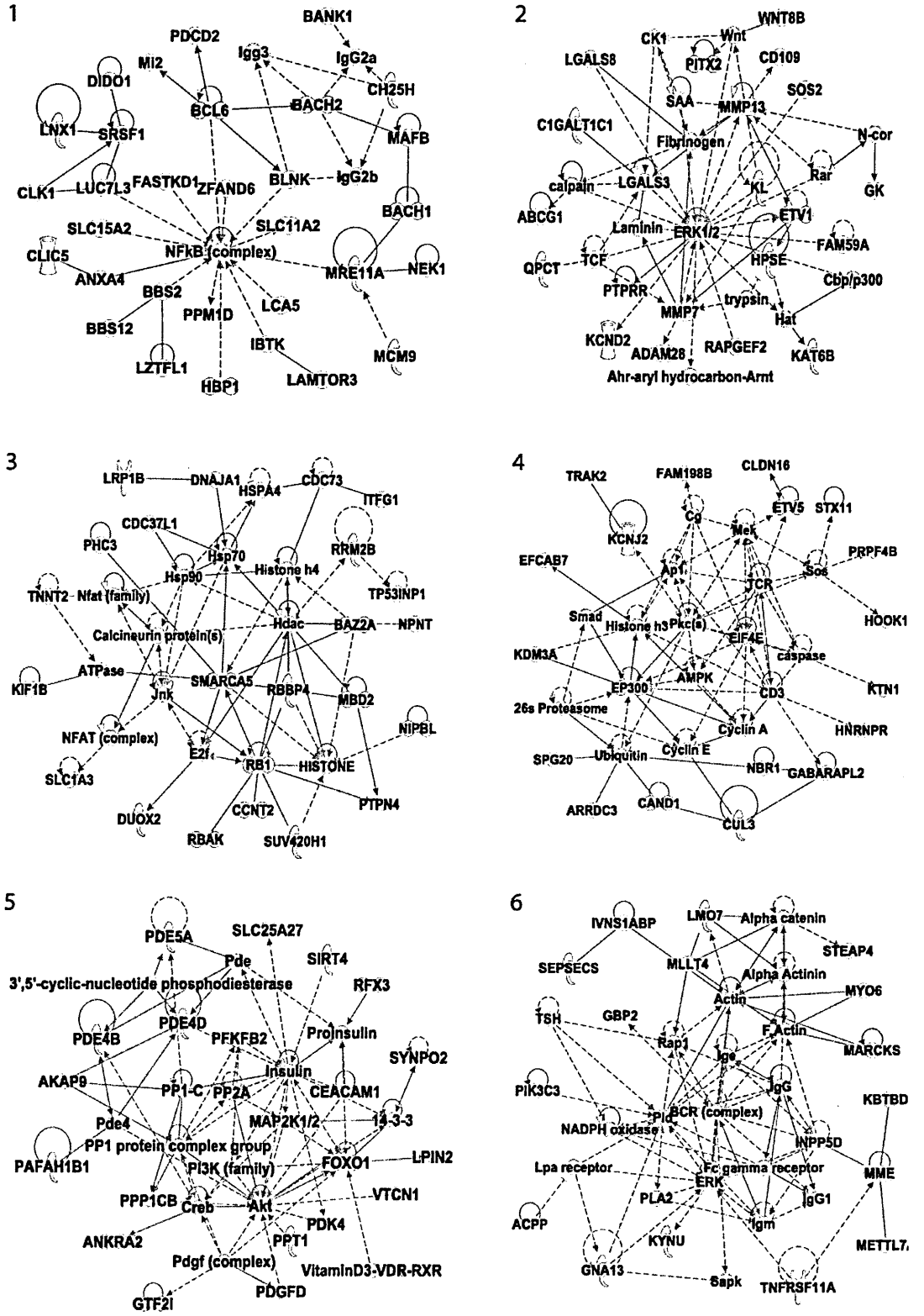

Figure 2.4d. IPACA networks of the CFBE-Up genes.

1-6 Networks of CFBE-Up genes analysed using IPACA. The networks contain Grey nodes which are CFBE up-regulated genes and white nodes which are IPACA genes.

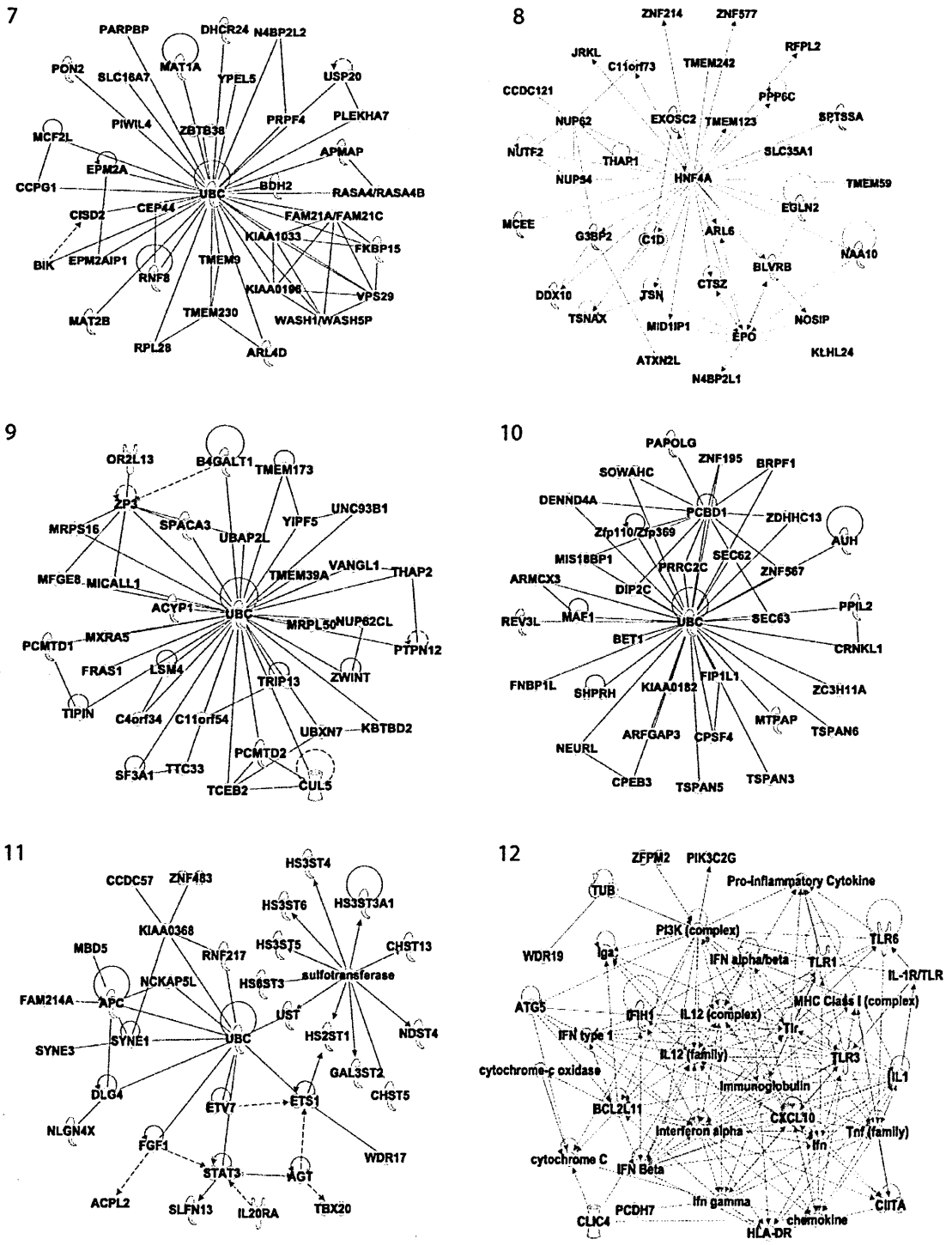

Figure 2.4d. IPACA networks of the CFBE-Up genes (continued).

7-12 Networks of CFBE-Up genes analysed using IPACA. The networks contain Grey nodes which are CFBE up-regulated genes and white nodes which are IPACA genes.

Table 2.4f. IPACA of the CFBE-Down genes.

CFBE-Down gene sets analysed using IPACA. **1.** Identified enriched canonical pathways. **2.** Networks with associated scores and functions.

1

Ingenuity canonical pathways	-log(p value)
Regulation of cellular mechanics by calpain protease	2.48E00
FAK signalling	1.96E00
tRNA splicing	1.85E00
nNOS signalling in neurons	1.58E00
Glycogen biosynthesis II (from UDP-D-glucose)	1.5E00
Cardiac β-adrenergic signalling	1.48E00
Relaxin signalling	1.46E00

2

Network	Score	Top functions
1	36	Cellular movement, connective tissue development and function, embryonic development
2	28	Developmental disorders, hereditary disorder, neurological disease
3	26	Cell morphology, haematological system development and function, Gene expression
4	23	Cell morphology, cell death and survival, cell cycle
5	23	Cell death and survival, cellular compromise, neurological diseases
6	21	Infectious diseases, cardiovascular diseases, dermatological diseases and conditions

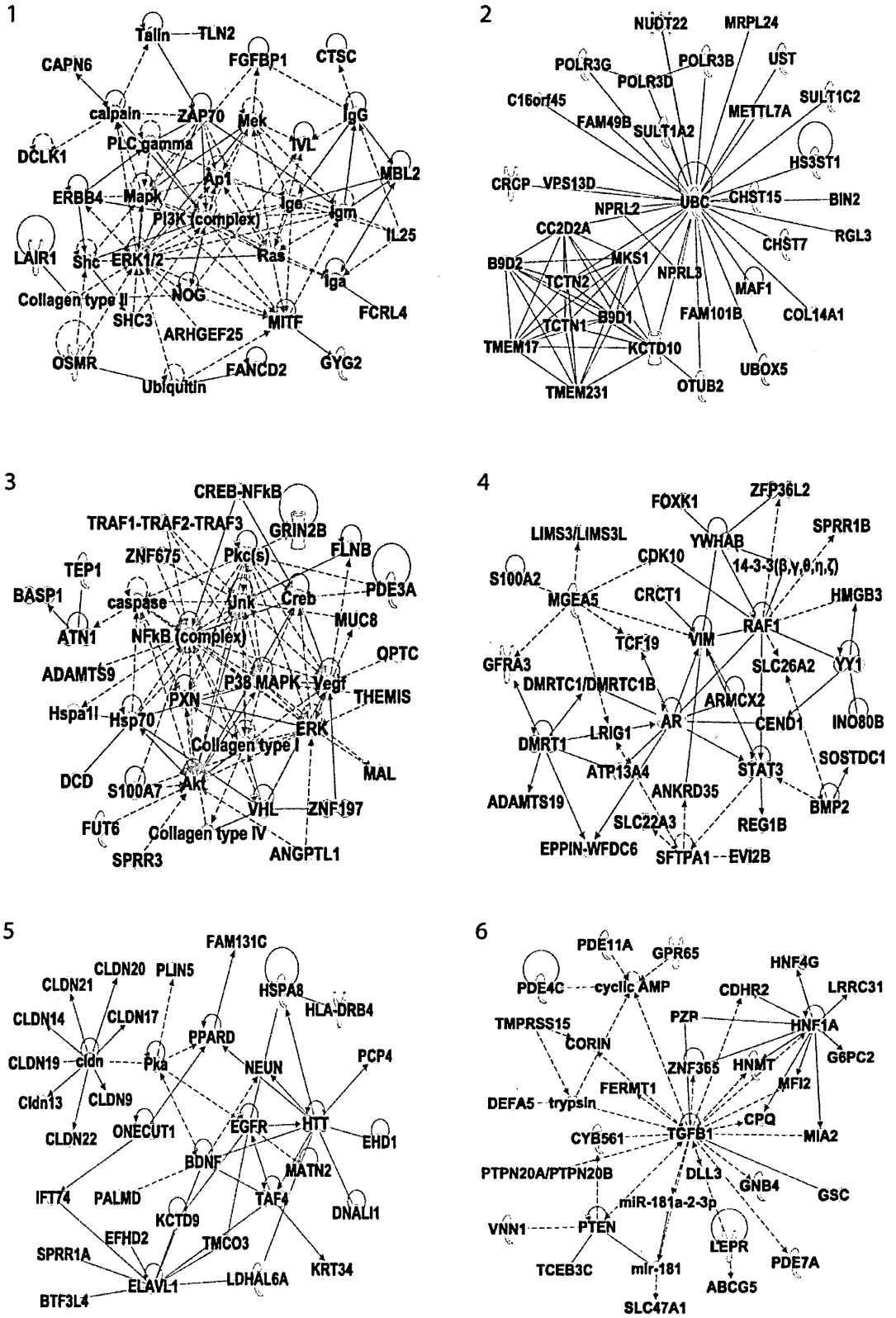

Figure 2.4e. IPACA networks of the CFBE-Down genes.

1-6 Networks of CFBE-Down genes analysed using IPACA. The networks contain Grey nodes which are CFBE down-regulated genes and white nodes which are IPACA genes.

2.5. Commonly regulated genes/ networks interact with CFTR proteostasis network components

To understand if the commonly regulated genes/networks are indeed related to regulators or components of CFTR proteostasis, the dataset of known CFTR proteostasis regulators was collected (the CFTR proteostasis network) (Table 2.5). Then the relationship between the commonly regulated genes and the CFTR proteostasis network were studied. The CFTR proteostasis network dataset that was built included known proteostatic regulators of CFTR; i.e., proteins for which their expression/ activity level changes have been shown to rescue ΔF508CFTR proteostasis. In spite of the presence of some CFTR proteostasis network components in the commonly regulated gene lists, there was no statistically significant intersection between the two lists. IPACA analysis of several molecular networks of the commonly regulated genes described was tested for any relationships with known CFTR proteostasis network genes. To this end, the networks were allowed to grow and connect to the CFTR proteostasis network genes. This demonstrated that many of the networks of commonly regulated genes had extensive connections with the CFTR proteostasis network components, which suggested that although many were not part of the CFTR proteostasis network itself, they either regulated or were regulated by CFTR proteostasis network components (Figure 2.5a). Using the other method, where the commonly regulated genes were combined with the CFTR proteostasis network and subjected to IPACA analysis, this demonstrated that there is also an interaction between CFTR proteostasis network genes and commonly regulated genes when both are analysed together (Figure 2.5b).

2.6. Commonly regulated genes/ networks control ΔF508CFTR proteostasis

To experimentally validate the down-regulated commonly regulated genes for their effect on ΔF508CFTR proteostasis, a biochemical assay was used (see section 6.12). The assay has been shown to be robust and very sensitive to small changes in the ΔF508CFTR proteostasis (Farinha et al. 2004). To monitor the effects of the drugs on ΔF508CFTR, CF bronchial epithelial (CFBE41o$^-$) cells stably expressing ΔF508CFTR (hereafter referred to as CFBE (Bebok et al. 2005)) were used. To test the commonly down-regulated genes that belong to the different gene ontology groups or pathways/ networks (mRNA processing, the cell cycle, MAPK pathway, and others), the analysis was restricted to those genes that satisfied any one of the following criteria: (i) down-regulated

Table 2.5. CFTR-Proteostasis Network gene set.

The CFTR proteostasis genes (ΔF508CFTR correctors/ERAD inhibitors) were collected from literature. They were based on either siRNA-based knock-down or cDNA-based over-expression.

CFTR Proteostasis Network genes					
siRNA-based knock-down effects				Overexpression-based effects	
Gene	Reference	Gene	Reference	Gene	Reference
NEDD4L	(Caohuy et al. 2009)	PARK2	(Okiyoneda et al. 2010)	USP10	(Bomberger et al. 2009)
AUP1	(Christianson et al. 2012)	PPID	(Okiyoneda et al. 2010)	SGK1	(Caohuy et al. 2009)
DERL3	(Christianson et al. 2012)	PPIL2	(Okiyoneda et al. 2010)	ANXA2	(Trzcinska-Daneluti et al. 2009)
DNAJC10	(Christianson et al. 2012)	SIAH1	(Okiyoneda et al. 2010)	AP2M1	(Trzcinska-Daneluti et al. 2009)
EDEM1	(Christianson et al. 2012)	STAM	(Okiyoneda et al. 2010)	AQP3	(Trzcinska-Daneluti et al. 2009)
ERLEC1	(Christianson et al. 2012)	STIP1	(Okiyoneda et al. 2010)	C20orf7	(Trzcinska-Daneluti et al. 2009)
ESYT1	(Christianson et al. 2012)	STUB1	(Okiyoneda et al. 2010)	Cav2	(Trzcinska-Daneluti et al. 2009)
FOXRED2	(Christianson et al. 2012)	SYVN1	(Okiyoneda et al. 2010)	CCBL1	(Trzcinska-Daneluti et al. 2009)
HERPUD1	(Christianson et al. 2012)	TRIP12	(Okiyoneda et al. 2010)	CCK	(Trzcinska-Daneluti et al. 2009)
KIAA0090	(Christianson et al. 2012)	TSG101	(Okiyoneda et al. 2010)	CCL2	(Trzcinska-Daneluti et al. 2009)
NGLY1	(Christianson et al. 2012)	UBE2D3	(Okiyoneda et al. 2010)	CRYAB	(Trzcinska-Daneluti et al. 2009)
PSMD2	(Christianson et al. 2012)	UBE2N	(Okiyoneda et al. 2010)	DNAJC10	(Trzcinska-Daneluti et al. 2009)
SELS	(Christianson et al. 2012)	UBE3A	(Okiyoneda et al. 2010)	DUSP3	(Trzcinska-Daneluti et al. 2009)
TTC35	(Christianson et al. 2012)	UBE4B	(Okiyoneda et al. 2010)	DYDC2	(Trzcinska-Daneluti et al. 2009)
TXNDC16	(Christianson et al. 2012)	UBE4A	(Okiyoneda et al. 2010)	EDN1	(Trzcinska-Daneluti et al. 2009)
UBAC2	(Christianson et al. 2012)	AHSA1	(Okiyoneda et al. 2010)	FAM195A	(Trzcinska-Daneluti et al. 2009)
UBXN4	(Christianson et al. 2012)	UBE2J1	(Okiyoneda et al. 2010)	GAPDH	(Trzcinska-Daneluti et al. 2009)
VCP	(Christianson et al. 2012)	AMFR	(Okiyoneda et al. 2010)	GORASP1	(Trzcinska-Daneluti et al. 2009)
VCPIP1	(Christianson et al. 2012)	COPS5	(Tanguy et al. 2008)	HSPA4	(Trzcinska-Daneluti et al. 2009)
DERL1	(Christianson et al. 2012)	BCAP31	(Wang et al. 2008),	HSPB8	(Trzcinska-Daneluti et al. 2009)
KRT18	(Davezac et al. 2004)	RNF5	(Younger et al. 2006)	HSPBP1	(Trzcinska-Daneluti et al. 2009)
DNAJB12	(Grove et al. 2011)			LGALS3	(Trzcinska-Daneluti et al. 2009)
CALR	(Harada et al. 2006)			Park7	(Trzcinska-Daneluti et al. 2009)
HDAC7	(Hutt et al. 2010)			PFDN2	(Trzcinska-Daneluti et al. 2009)
ATF6	(Kerbiriou et al. 2007)			PPARG	(Trzcinska-Daneluti et al. 2009)
SQSTM1	(Luciani et al. 2010)			PRG2	(Trzcinska-Daneluti et al. 2009)
BAG1	(Okiyoneda et al. 2010)			PRKCI	(Trzcinska-Daneluti et al. 2009)
CDC37	(Okiyoneda et al. 2010)			REG3A	(Trzcinska-Daneluti et al. 2009)
DNAJA1	(Okiyoneda et al. 2010)			S100A8	(Trzcinska-Daneluti et al. 2009)
DNAJA2	(Okiyoneda et al. 2010)			STAT1	(Trzcinska-Daneluti et al. 2009)
DNAJA3	(Okiyoneda et al. 2010)			TCEB2	(Trzcinska-Daneluti et al. 2009)
DNAJB2	(Okiyoneda et al. 2010)			TCP10L	(Trzcinska-Daneluti et al. 2009)
DNAJC27	(Okiyoneda et al. 2010)			TFG	(Trzcinska-Daneluti et al. 2009)
DNAJC3	(Okiyoneda et al. 2010)			TRIM31	(Trzcinska-Daneluti et al. 2009)
DNAJC5	(Okiyoneda et al. 2010)			TRNAU1AP	(Trzcinska-Daneluti et al. 2009)
DNAJC7	(Okiyoneda et al. 2010)			UBXN1	(Trzcinska-Daneluti et al. 2009)
HGS	(Okiyoneda et al. 2010)			USP19	(Hassink et al. 2009)
Hsp90AA1	(Okiyoneda et al. 2010)			UCHL1	(Henderson et al. 2010)
HSPA8	(Okiyoneda et al. 2010)			AnxA5	(Le Drevo et al. 2008)
MARCH2	(Okiyoneda et al. 2010)			BECN1	(Luciani et al. 2012)
MARCH4	(Okiyoneda et al. 2010)			UVRAG	(Luciani et al. 2012)
MDM2	(Okiyoneda et al. 2010)			CANX	(Norez et al. 2006)

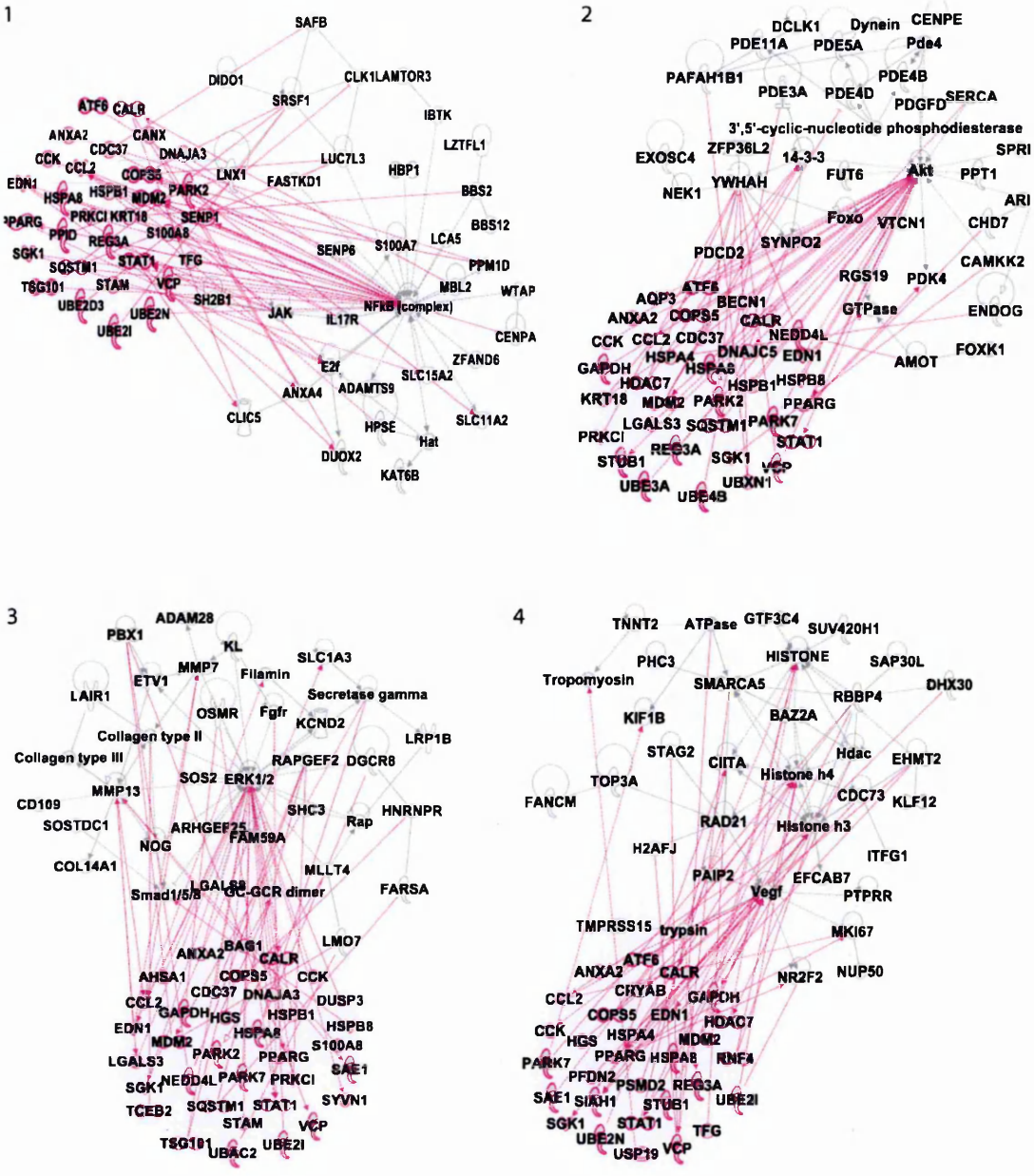

Figure 2.5a. IPACA predicted interactions between commonly regulated gene IPACA networks and CFTR proteostasis network genes.

Each of the top four IPACA network of commonly regulated genes (white nodes) has a predicted interaction (purple line) with many CFTR proteostasis network genes (grey nodes with purple border).

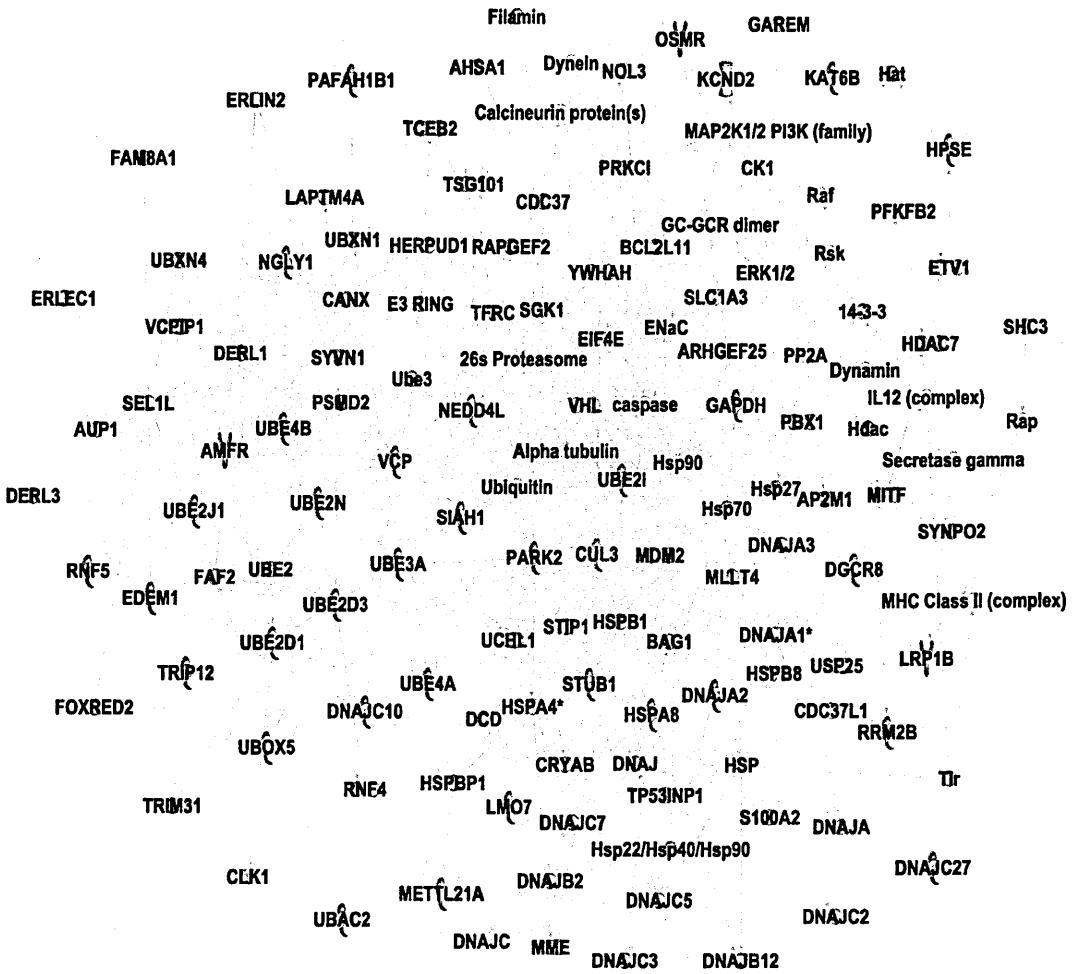

Figure 2.5b. IPACA predicted interactions between CFTR proteostasis network genes and commonly regulated genes.

The network contains the commonly regulated genes (green) that have a predicted interaction with many CFTR proteostasis network genes (red).

commonly regulated genes that belong to the enriched biological processes in gene ontology; (ii) part of the separate PPI network of cMap and CFBE down-regulated genes obtained from STRING; (iii) regulatory components, like kinases and transcription factors, that have connections to at least three commonly regulated genes in the networks from the separate IPACA of the cMap -Down and CFBE-Down gene sets; (iv) down-regulated commonly regulated genes that were of general interest because of their regulatory nature, including signalling molecules (kinases-phosphatases) and ubiquitination process related components.

Down-regulated genes were considered for validation instead of the up-regulated genes simply because of the available efficient small-interfering (si) RNA-based knock-down technology, whereas the optimal overexpression of genes at a large scale was limiting for validating the up-regulated genes. Finally, this amounted to 107 genes (Table 2.6), among which 69 were commonly regulated down-regulated genes (from both the CFBE-Down and cMap -Down groups), and 47 were selected using IPACA analysis; 9 genes were common between the selected commonly regulated genes and the IPACA genes. The CFBE cells were treated with siRNAs targeting each of the 107 selected genes, and after 72 h, the effects on ΔF508CFTR proteostasis were monitored by Western blotting. A commonly regulated gene was considered a CFTR proteostasis modulator or a hit if at least 2 out of the 3 siRNAs targeting the gene resulted in a significant change in the band C levels compared to the control siRNAs. The results of the screen are summarised in Figure 2.6 a, b. Among the 107 genes screened, 74 were found to be CFTR proteostasis regulators, where 32 of them increased the levels of band C (correctors or positive modulators) (Figure 2.6c, f), compared to the controls, and 42 of them decreased the levels of band C (negative modulators).

The corrector genes elevated the level of both band B and band C (Figure 2.6 f), which might reflect a nonspecific transport out of the ER because of the increased endoplasmic reticulum load of ΔF508CFTR. If there is a nonspecific transport then the ratio of amount of band C to band B would be simply proportional (Hutt et al. 2010) in control and specific gene siRNA-treated cells. It was tested whether the increase in band C was a consequence of a nonspecific effect or of an increased trafficking by calculating the ratios of bands C/B. The ratio of band C to band B has been be used to indicate the level of post-endoplasmic reticulum glycoforms of CFTR relative to ER pool (Hutt et al. 2010). Interestingly, the ratio of bands C/B was higher for most of the corrector

Table 2.6. Gene list for validating the effects on ΔF508CFTR proteostasis.

Genes shortlisted from commonly regulated (cMap-Down and CFBE-Down) genes and IPACA of (cMap-Down and CFBE-Down) genes for further testing their influence on the proteostasis of ΔF508CFTR.

Shortlisted Genes			
Commonly down regulated genes		**IPACA genes**	
RNF215	RGS19	CSNK2A1	MAP2K3
SART1	PPAP2B	CSNK2A2	MAP2K4
UBOX5	SPRR1A	CSNK2B	MAP2K5
NUP50	WTAP	MAPK3	MAP2K6
STAG2	TROAP	MAPK1	MAP2K7
C14orf106	DICER1	MAPK6	
DSN1	EHD1	MAPK7	
GTSE1	S100A7	MAPK15	
FBXO7	TOP3A	CYC1	
MED1	LMNB1	CYCS	
CD2BP2	FARSA	MED1	
SENP6	DCLK1	TP53	
YWHAH	BIN2	HNF4A	
CTDSP1	EXOSC4	VEGFR3	
MED13	SPRR3	VEGFR1	
MAP3K11	ZC3H3	KDR	
OSMR	RBM7	PDGFRB	
CAMKK2	DNAJC2	PDGFRA	
TEP1	NOL3	PROKR1	
PRPF8	CENPA	PROKR2	
ASB8	ERBB4	ZAP70	
SPRR1B	AKAP8	SHC3	
SCO2	ALPK1	OSMR	
GEMIN4	MKI67	ERBB4	
IVL	SHC3	AKT1	
ZAP70	PRPF4B	AKT3	
PDE3A	FGFBP1	AKT2	
PXN	AKAP1	MITF	
WDR6		PXN	
DGCR8		RELB	
CENPE		RELA	
ONECUT1		NFKB2	
MAL		NFKB1	
KRT34		PDE3A	
KIF20A		PDE11A	
PDE11A		PIK3CB	
MITF		PIK3CD	
DHX38		PIK3CG	
VHL		PIK3CA	
FLNB		MAP2K1	
PATZ1		MAP2K2	

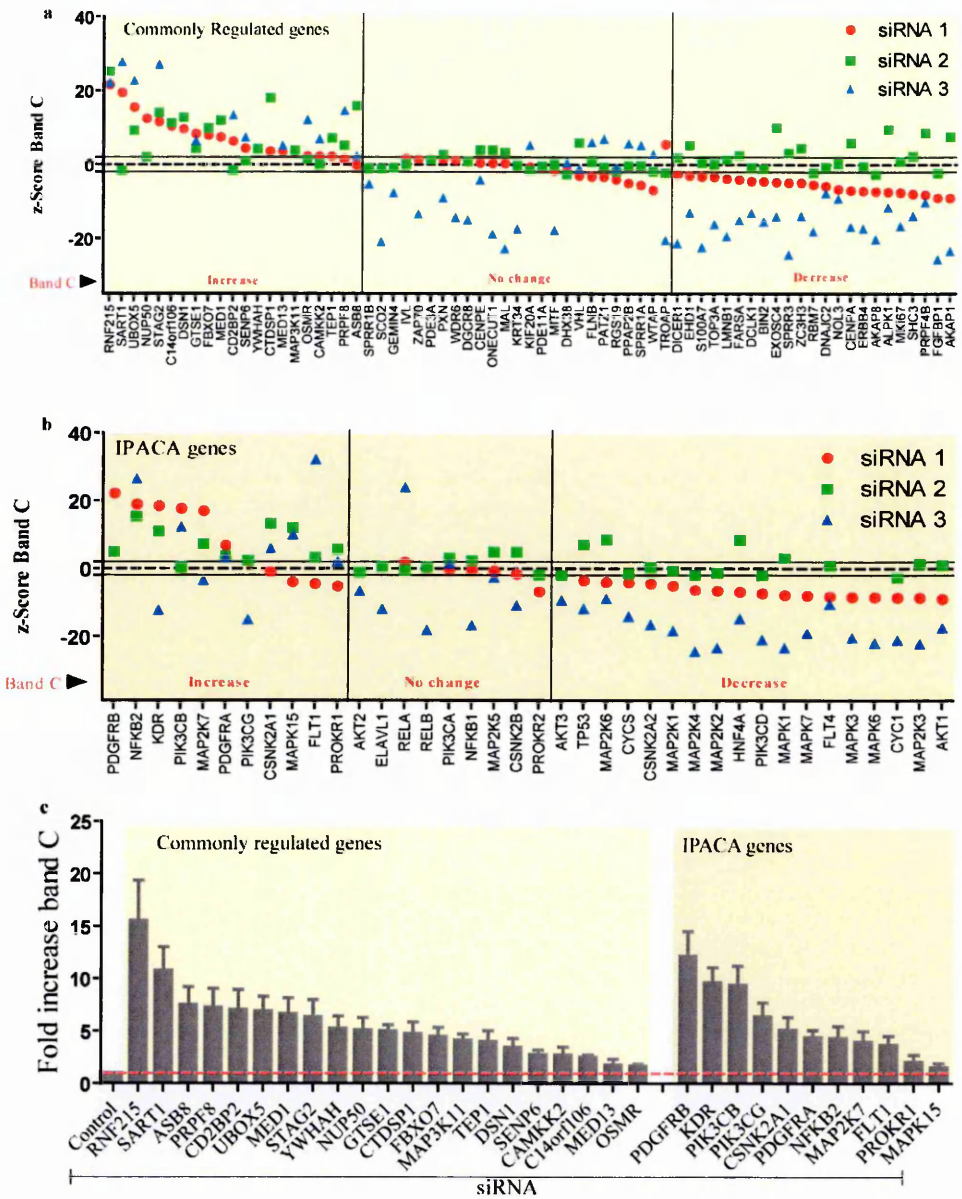

Figure 2.6. siRNA screening of selected genes.

CFBE cells were transfected with each of the 3 silencer select siRNAs for indicated genes for 72 hours and then the cells were lysed and total proteins were immunoblotted. **a.** z-Scores of the immunoblot-quantified band C corresponding to each single siRNA for selected CR genes. **b.** z-Scores of the immunoblot-quantified band C corresponding to each single siRNA for selected IPACA genes. The different partitions of the background represent the indicated changes in band C. **c.** CFBE cells were transfected with mix of three silencer select siRNAs targeting the indicated positive hit genes (cut-off of the z-score (2) to classify the positive hits) for 72 hours, lysed, and proteins were immunoblotted and fold-increases in band C plotted compared to control siRNA treatment (data represent mean ± SEM, n=3).

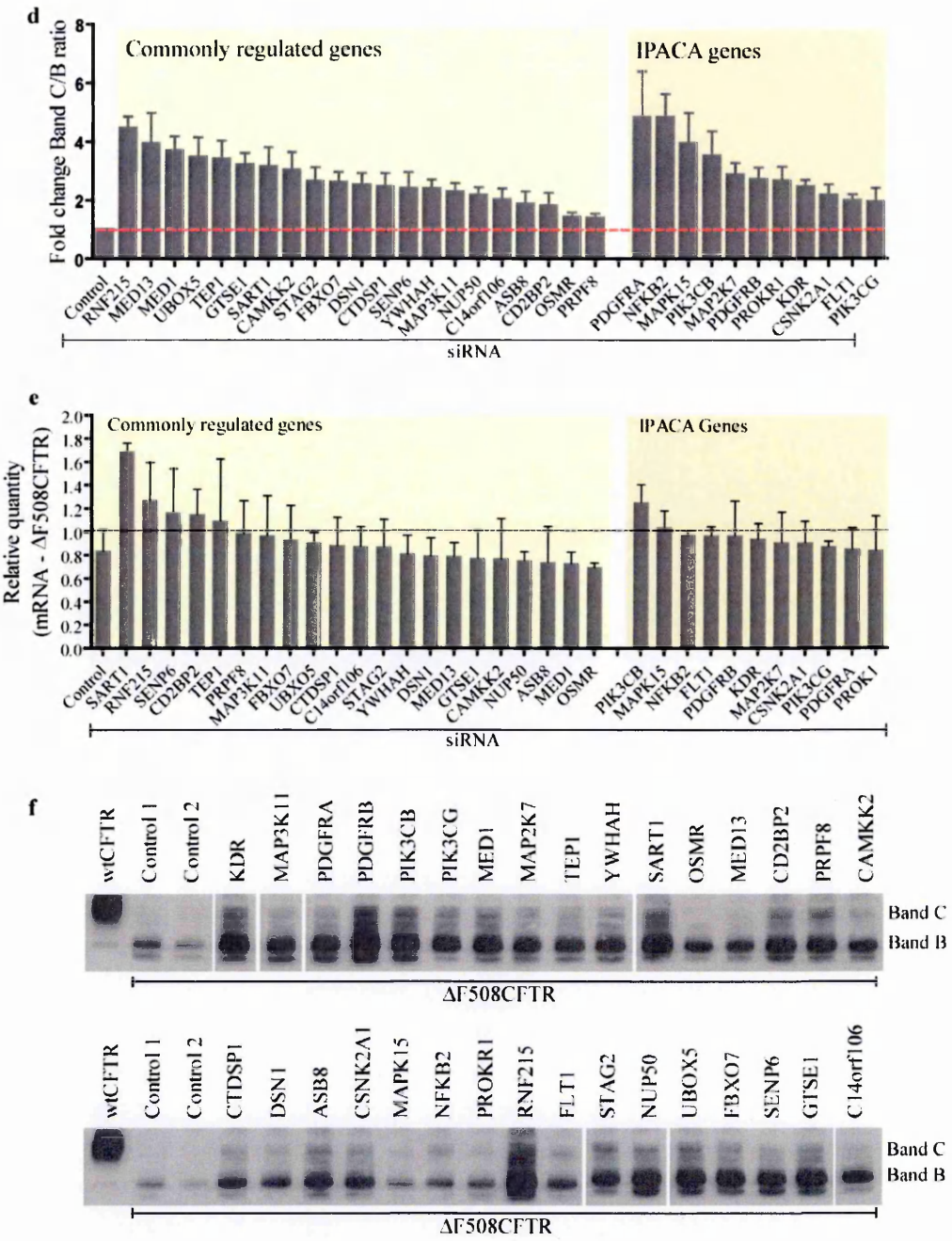

Figure 2.6. siRNA screening of selected genes (continued).

CFBE cells were transfected with mix of three silencer select siRNAs targeting the indicated positive hit genes for 72 hours, **d.** Quantified fold-changes in the band C/B ratio compared to control siRNA treatment was plotted after cell lysis and protein immunoblot. (Data represent mean ± SEM, n=3). **e.** Relative quantity of ΔF508CFTR mRNA normalised to HPRT1 mRNA is determined using the qRT-PCR is plotted comparing to control siRNA treatment (Data represent mean ± SD, n=4). **f.** Immunoblot of CFTR after the treatment with mix of three silencer select siRNAs for the classified positive hits (representative of three separate experiments).

genes (Figure 2.6d), which indicated that the correctors might increase the trafficking of ΔF508CFTR, and so the increased ER load of ΔF508CFTR is not solely responsible for the increased trafficking. The siRNAs used in the study were able to deplete the mRNA of respective gene to about 50-70% (Figure 6.3). The relative mRNA levels of ΔF508CFTR were not changed greatly by the treatment of siRNAs for classified positive hits except for the SART1 (Figure 2.6e).

When commonly regulated gene hits were mapped onto the commonly regulated pathways obtained earlier, to see which pathways were effective in regulating CFTR proteostasis, the commonly regulated genes mapped onto all the three identified commonly regulated pathways/ networks: cell-cycle processes (kinetchore/ centromere components), mRNA processing network, and regulation of JNK cascade. Among the three down-regulated commonly regulated pathways analysed, the mRNA processing network, cell-cycle processes, and JNK pathway (or stress activated protein kinase SAPK) regulators/ components included hits that increased as well as decreased the levels of band C. There were five ubiquitin ligases that are found in commonly regulated genes and VHL and PATZ1, they were associated with positive hits, corrected the ΔF508CFTR, RNF215 was one of the strongest corrector among the screening. While in the cases of the keratinocyte differentiation network and the mediator complex network, the former was uniformly present in the negative hits with the latter in the positive.

To summarise, screening confirmed that commonly regulated RNA processing, cell-cycle related and SAPK networks/ pathways that were monitored were indeed involved in controlling the proteostasis of ΔF508CFTR, and in addition, a few ubiquitin ligases were also found; RNF215 is a strong candidate ubiquitin ligase that controls the proteostasis of ΔF508CFTR.

Discussion

The present study has identified several CFTR proteostasis modulators and validated a set of molecular pathways/ networks/ genes that are commonly down-regulated by corrector drugs that can partially rescue the folding/ trafficking defects of ΔF508CFTR. The identified correction relevant commonly regulated pathways/ networks provide a novel link between RNA processing, cell-cycle components, the JNK cascade and a few novel ubiquitin ligases to ΔF508CFTR proteostasis. Among the RNA processing, cell-cycle components, kinases and ubiquitin ligases that

were screened, many of these were distributed equally between the positive and negative hits, except the ubiquitin ligases, which were distributed almost exclusively to the positive hits. This suggests that the ubiquitin ligases present in the commonly regulated genes might be in some way required for the retention/ degradation of ΔF508CFTR.

The commonly regulated genes included a few known proteostasis regulators of ΔF508CFTR, like USP25 and HSPA4 (HSP70), which were present in the up-regulated genes, and these are known to help in the rescue of ΔF508CFTR (Trzcinska-Daneluti et al. 2009; Blount et al. 2012). On the other hand, there were also UBE2D1 and DNAJA1, which were also present in the up-regulated commonly regulated genes, and these are known to be required for degradation of ΔF508CFTR (Younger et al. 2006; Okiyoneda et al. 2010). These examples show that although the commonly regulated gene list contained a few known proteostatic regulators of CFTR, it did not always correlate the "correction" effect of the drugs with the known action of these proteostatic regulators. The screened commonly regulated genes yielded both positive and negative regulators of ΔF508CFTR proteostasis, which might explain the modest correction of ΔF508CFTR obtained by treatment with these drugs; however, the net effect of the correctors was detectable at the level of the correction of ΔF508CFTR. Moreover, our approach identified that depletion of PIK3CB, PIK3CG, PDGFRA, PDGFRB and the kinase insert domain receptor (KDR or VEGFR2) rescues ΔF508CFTR.

Recently, a kinase inhibitor screening strategy showed that targeting these genes or pathways by inhibitors rescues ΔF508CFTR not only in CFBE cells, but also in primary human CF cells (Trzcinska-Daneluti et al. 2012). This evidence confirms the strength of the meta-analysis of the microarray data used as combined with the bio-informatic analysis strategies to find the novel proteostasis regulators of ΔF508CFTR. In the CF patients VEGF-A has been reported to be over produced (Martin et al. 2013), which was a known major transducer of signalling through the KDR or VEGFR2 (Terman et al. 1992). VEGF is also known to be over produced under conditions of ER stress and aberrant calcium homeostasis (Abcouwer et al. 2002). Both ER stress and aberrant calcium homeostasis are very much known to be present in CF models, so it was interesting to find the KDR or VEGFR2 as a rescuer of ΔF508CFTR, although the mechanistic insight is still to be defined. Casein kinase 2 (CSNK2A1 or CK2) depletion also rescued ΔF508CFTR, although

previous studies have shown that the CK2 phosphorylation of wtCFTR is necessary for its trafficking to the PM, it has no role in ΔF508CFTR (Luz et al. 2011). CK2 inhibition was also reported to attenuate ER-stress-induced XBP1 cleavage (Hosoi et al. 2012), and moreover, as inferred from IPACA, it has interactions with many CFTR proteostasis network genes, which indicates that CK2 also might be an important molecule in co-ordinating ER stress to CFTR proteostasis network genes, whereby its inhibition has a positive influence on ΔF508CFTR proteostasis. ΔF508CFTR was also known to have increased the levels of NF-κB (Bodas and Vij 2010), and that this might contribute to the aberrant proteostasis. This study has also found that depletion of NF-κB 2 can rescue ΔF508CFTR. In addition, depletion of CAMKK2 (activator of the CAMK cascade), and MAP3K11 (involved in the JNK cascade) also rescues ΔF508CFTR. Further characterisation of the MAP3K11 and CAMKK2 pathways is described in Chapter 3 and 4, respectively.

The RNA-processing molecules like SART1, CD2BP2, NUP50 and PRPF8, and the cell-cycle components GTSE1, STAG1 and C14orf106 depletion also rescued ΔF508CFTR. The molecular mechanism through which these genes affect proteostasis remains to be elucidated. Although the rationales behind the correction by these RNA-processing cell-cycle components are unknown, depletion of a few of them has been implicated in the prevention of misfolding and the aggregation of the Huntingtin and SOD1 proteins (Doumanis et al. 2009; Silva et al. 2011). Recently, the RNA-processing protein TDP-1 was shown to regulate protein homeostasis in *Caenorhabditis elegans* (Zhang et al. 2012), which is dependent on the proteostasis regulator DAF-16. So it might be that these RNA processing molecules regulate the levels of different RNAs, which in turn might affect some of the pathways that control proteostasis. The genes belonging to the biological functions of RNA splicing or cell-cycle processes might also be involved in the control of ΔF508CFTR proteostasis, although the mechanisms and rationale is a further avenue for study. Depletion of the mediator complex molecules MED13 and MED1 was associated with rescue, and the mechanism by which they influence proteostasis is not clear. The mediator complex is known to serve as a bridge to convey information from gene-specific regulatory proteins to the basal RNA polymerase II transcription machinery (Malik and Roeder 2005), so depletion of mediator molecules might selectively change the transcription in the cell to influence proteostasis.

The reduction in band C levels upon down-regulation of AKAP1, AKAP8 or ERBB4, which are related to the cAMP/PKA pathway and its molecules, might indicate that the up-regulation of this pathway might be necessary for correction, and indeed the drug up-regulated commonly regulated genes have members of the cAMP/PKA pathway. Many of the spliceosomal components rescue of ΔF508CFTR upon down-regulation but PRPF4B, a kinase that is associated with the spliceosome which functions during the assembly of the spliceosomal complex decreased the ΔF508CFTR upon down-regulation. The PRPF4B was an apparent contrast to the effects of other spliceosomal components that show a rescue of ΔF508CFTR upon down-regulation. Few of the keratinocyte differentiation-related genes were included in the screening, none of them rescued ΔF508CFTR, interestingly keratin 8 and 18 have been shown to rescue ΔF508CFTR (Davezac et al. 2004; Colas et al. 2012). A desumoylation enzyme, SENP6, also rescued ΔF508CFTR. As mentioned above, all of the ubiquitin ligases tested, except VHL and PATZ1, were associated with positive hits. Among the ubiquitin ligases, RNF215 was a strong corrector and increased band C levels to around 10-fold the control levels. Not much is known about the function or localisation of RNF215. Including RNF215, the ubiquitin ligases have strong effects on the control of ΔF508CFTR proteostasis. This opens a new avenue for studying their roles in ΔF508CFTR degradation.

In conclusion the results of this study have rationalised the mechanism of action of the known correctors that can rescue ΔF508CFTR from the ERQC. The drugs appear to act as proteostatic correctors, although they do not appear to have one or a few direct genes/ networks/ pathways as specific targets, but to induce mild changes in expression of multiple gene leading to the ΔF508CFTR correction. Many of the drugs affected commonly modulated genes are indeed novel components of ΔF508CFTR proteostasis or its regulators. This study also opens the avenue for targeting the identified individual genes or pathways in combination to achieve a highly potent correction of the basic trafficking defects of ΔF508CFTR.

Chapter 3

The stress-activated MAPK pathway controls ΔF508CFTR proteostasis

Introduction

In general, proteostasis is believed to be influenced by the chemistry of protein folding/ misfolding and by numerous regulated networks of interacting and competing biological pathways that manipulate protein synthesis, folding, trafficking, disaggregation and degradation (Balch et al. 2008). Proteostasis is also regulated by many signalling pathways, like the UPR, HSR, calcium signalling, and inflammatory pathways (Balch et al. 2011). It has been postulated that activation of stress responsive signalling pathways in particular cellular compartments results in the synthesis and/or activation of regulators that orchestrate programmes to enhance the proteostasis capacity (Lindquist and Kelly 2011). The production of misfolded proteins that exceeds the degradation ability leads to the UPR (Liu and Ye 2011), which increases the ER protein-folding capacity through broad transcriptional up-regulation of ER protein-folding and lipid biosynthesis, and coordinates the ERAD machinery with a decrease in the folding load through selective mRNA degradation and translational repression (Gardner et al. 2013). The UPR is known to be dependent on IRE1, PERK and ATF6 (Hartl et al. 2011), and signal transduction includes MAPKs, p38 and JNK (Kim et al. 2008). The HSR is involved in sensing abnormally high levels of misfolded or aggregated proteins in the cytosol and nucleus, and it coordinates signalling to lead to the reduction in the load on the proteostasis network. Thus, at the same time as blocking non-essential protein synthesis and degrading mRNA, there is an increase in the concentration of proteostasis network components through transcription and translation (Lindquist and Kelly 2011). The HSR involves well-established transcriptional regulators, like the HSF-1 and FOXO transcription factors (Hartl et al. 2011), and rapid signal-transduction events dependent on the stress-activated protein kinases JNK and p38 (Dorion and Landry 2002). Recently, the JNK pathway and *Slpr* (a MAP3K) phosphorylation have been shown to be required for the *Drosophila* HSR (Gonda et al. 2012). It has also been shown that HSR controlled mechanisms regulate the proteostasis network, which can in turn lead to the rescue of ΔF508CFTR (Calamini et al. 2012).

The MAPKs p38 and JNK are referred to as stress activated protein kinases (SAPKs), because they are preferentially activated by inflammatory cytokines and cell stress, including UV light, X-rays, hydrogen peroxide, heat and osmotic shock, and withdrawal of growth factors (Ichijo 1999). The MAPK signalling cascade (Figure 3) is also activated following growth factor activation (Wagner and Nebreda 2009), and this system has been evolutionarily conserved from yeast to humans (Ichijo 1999). This cascade regulates the expression of cytokines and proteases, cell-cycle progression, cell adherence, motility and metabolism, and influences cell proliferation, differentiation, survival, apoptosis and development, and hence it is critical for cellular homeostasis (Cuevas et al. 2007). The canonical architecture of the MAPK pathway includes three kinases, MAP3K, MAP2K and MAPK, whereby MAP3K phosphorylates MAP2K, which in turn phosphorylates MAPK (Ichijo 1999) (Figure 3).

In the MAPK cascade, MAP3Ks are differentially activated by upstream stimuli, including cytokines, antigens, toxins, stress and MAP4Ks, and they provide a mechanism to merge the activation of different downstream MAP2Ks and MAPKs with the cellular responses to each stimulus (Qi and Elion 2005; Cuevas et al. 2007). The p38 pathway has the upstream activator of MAP2Ks as MKK3 and/or MKK6, and of the JNK pathway, MKK4 or MKK7. The knock-out of p38 alpha is embryonically lethal in mice (Risco and Cuenda 2012). By contrast the knock-out of a single JNK isoform is not lethal, although the knock-out of JNK1 and JNK2 together is embryonically lethal (Yamasaki et al. 2012). This indicates that SAPKs are essential for normal growth and development. Hog1 is a yeast homologue of SAPK, and it has been demonstrated to be activated at late stages of UPR and to maintain ER homeostasis (Bicknell et al. 2010). Stress induction in the ER of mammalian cells by perturbations that lead to accumulation of misfolded proteins was demonstrated to activate JNKs (Urano et al. 2000). There is also evidence from different model systems that accumulate misfolded protein, like the poly Q mutant huntingtin (HTT), and in Alzheimer's disease (AD), and Parkinson's disease (PD), leads to activation of JNK and p38 (Savage et al. 2002; Borsello and Forloni 2007; Klegeris et al. 2008; Morfini et al. 2009; Reijonen et al. 2010). It was also shown that the ERAD substrate rhodopsin P23H mutant in *Drosophila* also results in activation of JNK and p38 (Galy et al. 2005). More recently, stress-induced activation of the p38 pathway has been shown, which, in turn, leads to phosphorylation of

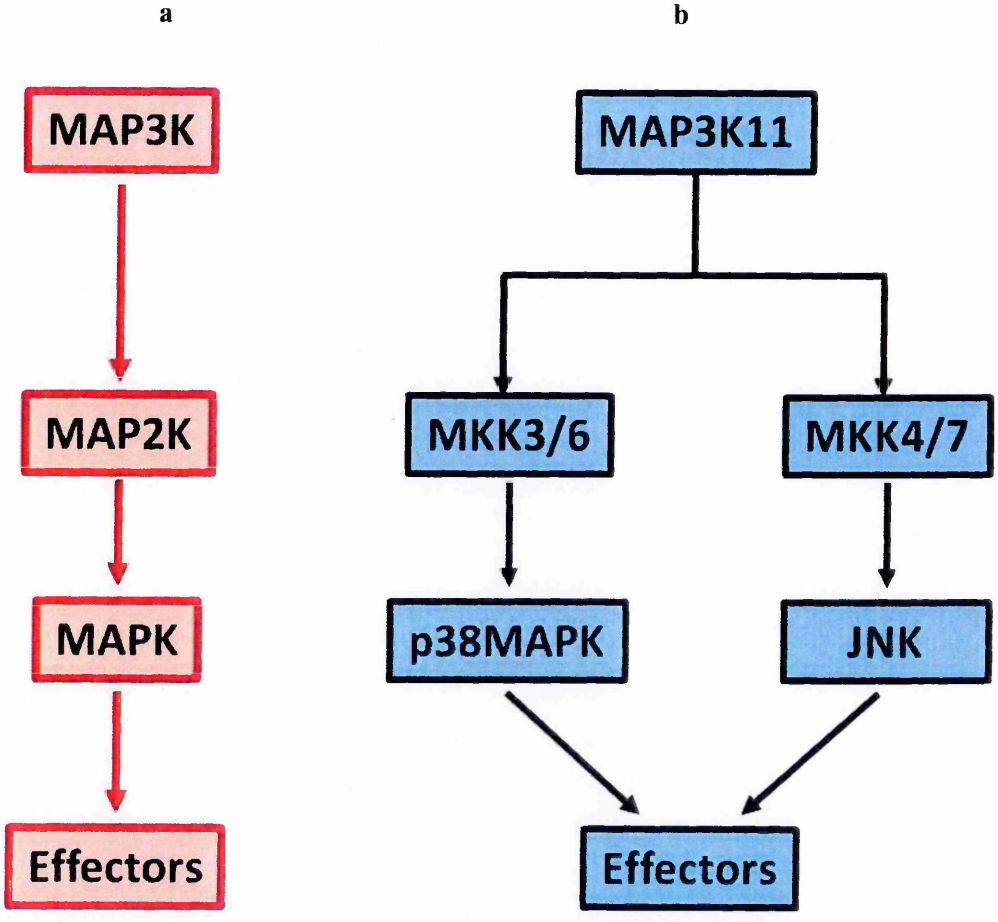

Figure 3. MAPK cascade.

a. The hierarchical organization of canonical MAP kinase cascade. **b.** MAP kinase cascade that was hypothesised to control proteostasis of ΔF508CFTR.

Ubc6e (Menon et al. 2013). However, whether the activation of these SAPKs is necessary for the degradation of these stress-causing proteins is not known.

Interestingly, in *C. elegans*, it has been shown that the RAS-MAPK pathway participates in EGF-induced proteostasis and activation of proteasomal signalling (Liu et al. 2011; Rajalingam and Dikic 2011). There is also well-documented evidence of SAPKs being activated upon oxidative stress (Son et al. 2011). Taken together, these data indicate that the SAPK pathways which responds to various stresses, might integrate the proteostasis network with the general stress response, to form integrated stress-response pathways. This pathway has been targeted for anti-inflammatory treatment in several clinical trials (Bogoyevitch and Arthur 2008; Graczyk 2013) (http://clinicaltrials.gov/ct2/show/NCT01630252) successfully, with little or no apparent side effect.

Initial studies that analysed the mechanisms of action of the corrector drugs led to the identification SAPK signalling in the correction of ΔF508CFTR (section 2.6). So the role of the SAPK pathway in regulating the proteostasis of ΔF508CFTR was investigated further. This led to the discovery of several SAPK pathway components that when depleted by siRNA acted as correctors of ΔF508CFTR. The present study also discovered that the SAPK pathway has a potent effect on the ERAD and proteostasis of ΔF508CFTR. SAPK pathway has many characterised inhibitors (Bogoyevitch and Arthur 2008) that are interesting to be tested for ΔF508CFTR correction. Several inhibitor drugs of this pathway were tested some of them acted as novel correctors of ΔF508CFTR proteostasis. One of the SAPK pathway upstream kinase MAP3K11, has been shown to be activated by upstream activators, like TGF-β (Kim et al. 2004) and TNF-α (Brancho et al. 2005), which are known CF genetic modifier (Collaco and Cutting 2008), and also by ROS (Hong and Kim 2007), which are known to be involved in CF pathogenesis (Luciani et al. 2010). The presence of pro-inflammatory cytokines and stress such as oxidative stress and ROS are documented in CF pathology (Brown et al. 1996; Mitola et al. 2008; Luciani et al. 2010). The present study also demonstrates that oxidative stress and inflammatory cytokines like TNF-α and TGF-β can activate this SAPK pathway, to lead to increased ERAD of ΔF508CFTR. This indicates that SAPK pathway links inflammation and oxidative stress to ΔF508CFTR proteostasis.

Results

3.1. The MAP3K11–JNK pathway controls the proteostasis of ΔF508CFTR

Meta-analysis of ΔF508CFTR corrector-drug-induced microarrays led to the identification of several regulatory genes/ networks/ pathways that control CFTR proteostasis (section 2.6). The demonstrated positive hits included MAP3K11 and MAP2K7 (MKK7). These indicate a kinase cascade, which are of great interest because there are well-developed kinase inhibitors that are available for many kinases, and they have provided particularly interesting targets for therapy (Cohen 2002; Sawyer et al. 2013). Thus, an interesting hit was MAP3K11, and when tested, these published siRNAs to MAP3K11 (Swenson-Fields et al. 2008; Chen et al. 2010) also reproduced the correction effect seen with the siRNAs used in the screening. All of the five siRNAs that were tested had an effect on the ΔF508CFTR proteostasis, as monitored by the biochemical assay (see section 6.12) that showed a clear increase in the Golgi processed band C (Figure 3.1a,b), thus demonstrating that the effect of these siRNAs on the ERQC is most probably mediated by MAP3K11. The best results here in terms of correction were obtained with siRNA1 which was used in the further analysis described below.

MAP3K11 is part of the validated commonly regulated pathway that is known to activate at least four pathways, including JNK (Brancho et al. 2005), p38 (Kim et al. 2004), ERK (Chadee and Kyriakis 2004) and NF-κB (Hehner et al. 2000) under various conditions, and it is also known to have kinase-independent functions in the regulation of signalling to RhoA (Swenson-Fields et al. 2008). Downstream of MAP3K11 in JNK cascade, MAP2K7 (which is also upstream of JNK) can rescue ΔF508CFTR levels and promote its proteostasis (see section 2.6), while the other two arms downstream of MAP3K11, as the ERK and p38 pathways, cannot rescue ΔF508CFTR levels upon down-regulation. It has been reported that the down-regulation of MAP3K11 leads to a reduction in the levels of I-κB, an inhibitor of NF-κB hence, activating NF-κB (Cole et al. 2009). Interestingly, the present study identified NF-κB among the positive hits (rescue of ΔF508CFTR upon down-regulation), along with MAP3K11, which suggests that the MAP3K11–NF-κB axis might not be relevant in the correction by MAP3K11.

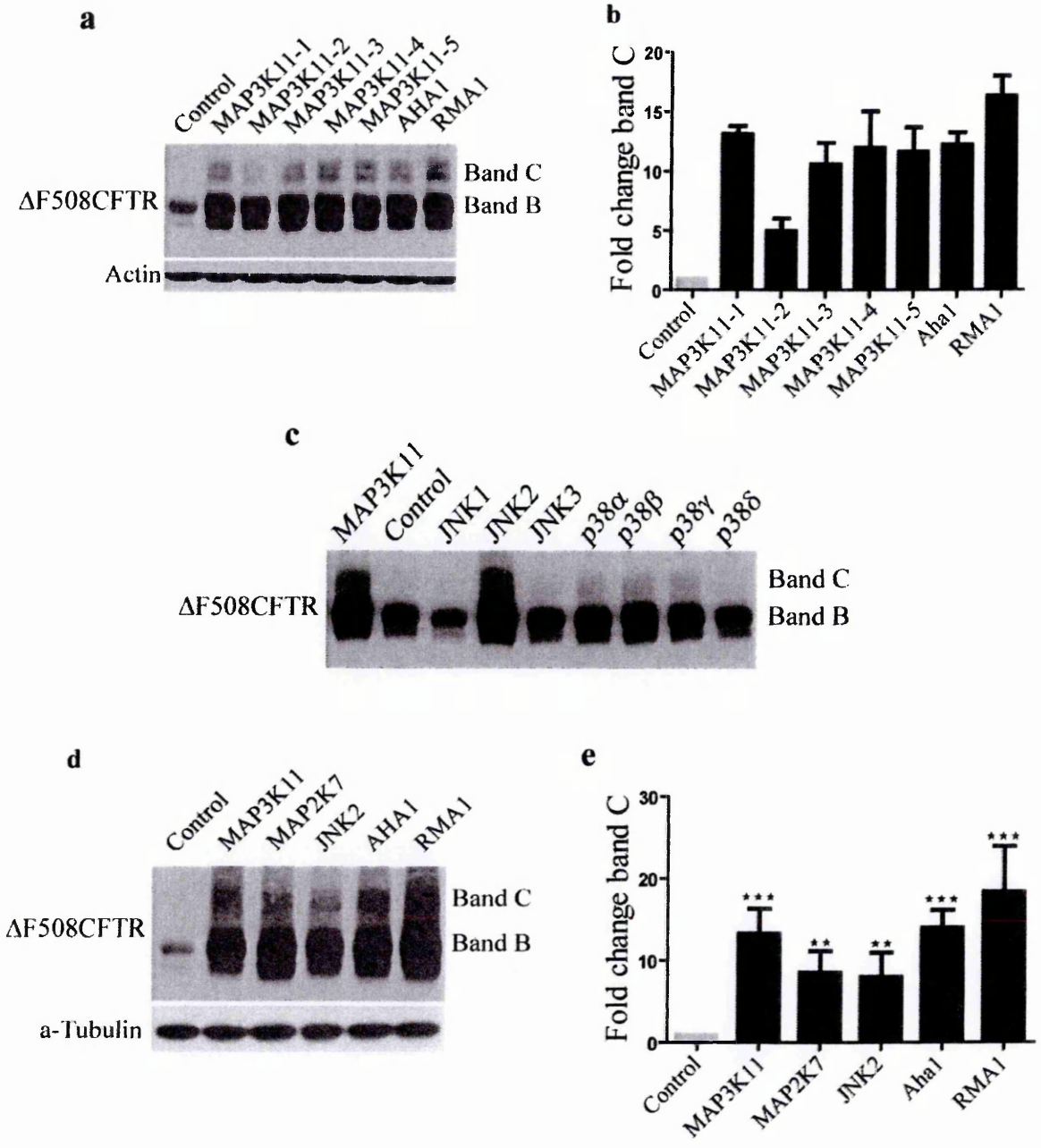

Figure 3.1. The MAP3K11–JNK pathway controls ΔF508CFTR proteostasis.

CFBE cells were transfected with indicated siRNA for 72 hours, lysed and immunoblotted. **a.** Representative immunoblot of the experiments shown in (b) **b.** Fold-change of band C quantified from immunoblot (n=3) shown in (a). **c.** Immunoblot of depletion of different JNK and p38 family proteins, depletion of MAP3K11 was used as positive control for correction. **d.** Representative immunoblot of the experiments shown in (e). **e.** Fold-change of band C quantified from immunoblots (n=3) shown in (d) Aha1 and RMA1 siRNAs were used as positive control for the correction. Data represent mean ± SD (**P ≤ 0.01, ***P ≤ 0.001).

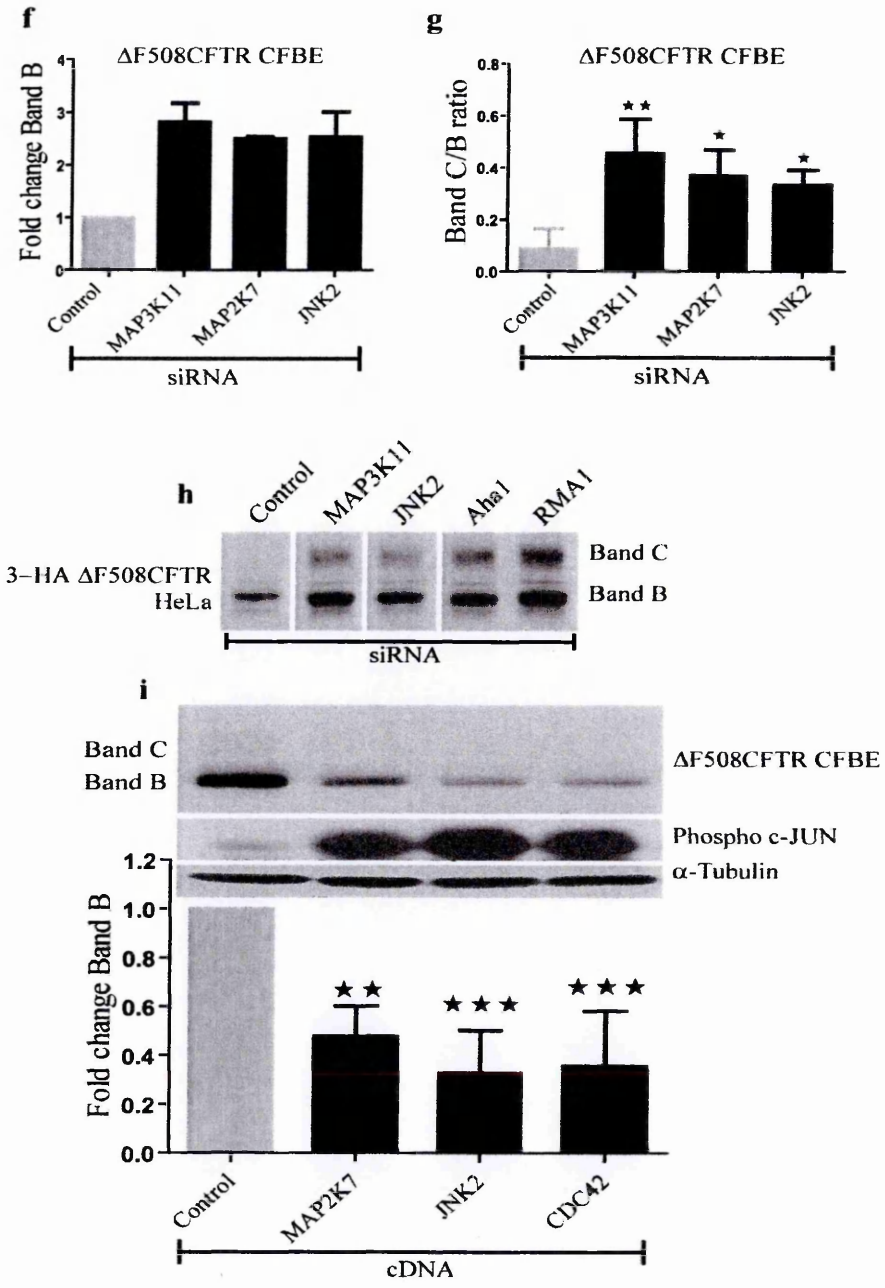

Figure 3.1. The MAP3K11–JNK pathway controls ΔF508CFTR proteostasis (continued).

CFBE cells were transfected with indicated siRNA for 72 hours, lysed, proteins immunoblotted for CFTR and quantified **f.** Fold-change in band B is plotted compared to control siRNA treatment (n=3). **g.** Quantified C/B ratio is plotted (n=3). **h.** HeLa cells were transfected indicated siRNA for 72 lysed and proteins were immunoblotted for CFTR (representative of five separate experiments). **i.** CFBE cells were transfected with indicated cDNA for 24 hours, lysed, proteins were immunoblotted for CFTR, fold-change band B quantified and plotted (n=3), with representative immunoblot shown in the insert. Data represent mean ± SD (*P ≤ 0.05, **P ≤ 0.01, ***P ≤ 0.001).

To further validate the involvement of the MAP3K11–JNK pathway in the correction of ΔF508CFTR, three JNK family of proteins were depleted using siRNA approach in CFBE cells. Down-regulation of JNK2 led to ΔF508CFTR rescue (Figure 3.1c), while JNK1 or JNK3 did not lead to significant increases in band C. As there is extensive cross-talk between the p38 and JNK pathways, siRNAs against p38 family of proteins were also tested in the assay, and there was no significant increase in band C levels when each of the p38 family of proteins were depleted (Figure 3.1c). Therefore, in the MAP3K11–JNK pathway, MAP3K11, MAP2K7 and JNK2 depletion lead to the rescue of ΔF508CFTR (the efficacy of depletion of gene is presented in the section 6.3), and biochemically, the rescue levels were comparable to those obtained by down-regulation of the known rescuers RMA1 and Aha1 (Figure 3.1d, e). An expression database (http://biogps.org) has shown that JNK2 is highly expressed in bronchial epithelial cells compared to other cells, which probably explains the strong effects observed with JNK2 compared to other JNK isoforms. Although the increase in band C levels was also accompanied by an increase in band B levels (Figure 3.1e), there was a significant change in the band C/B ratio of ΔF508CFTR (Figure 3.1f), which suggests increased export or decreased peripheral quality control. If the amount of band c is due to a nonspecific transport then the ratio of amount of band C to band B would be simply proportional in control and specific gene siRNA-treated cells. (Hutt et al. 2010). Hence the rescue seen above may not be due to the nonspecific increase in the transport.

To further test the effects of the JNK pathway on ΔF508CFTR, the activity of the pathway was enhanced to see whether this indeed controls ERQC. If the pathway controls or enhances ERQC, up-regulation of the pathway components should have the opposite effect, and reduce the levels of ΔF508CFTR. To achieve this, cDNA of the upstream activators of the SAPK pathway CDC42 (activator of MAP3K11), MKK7 (activator of JNK) and active JNK2 fused to MKK7 were transfected into CFBE cells. The activators activated JNK, as examined by phosphorylated cJUN (Figure 3.1h), and this was accompanied by a reduction in the levels of band B of ΔF508CFTR (Figure 3.1g, h). Thus, the reduction in the JNK pathway activity led to a stabilisation and enhanced export of ΔF508CFTR from the ER, and the activation of the pathway led to a reduction in the levels of ΔF508CFTR. This demonstrates that the JNK pathway, or specifically the MAP3K11-mediated JNK pathway, is indeed a regulator of ΔF508CFTR proteostasis.

3.2. The MAP3K11–JNK pathway regulates the ER-associated degradation of ΔF508CFTR

An observation that stands out from the experiments described above and in the siRNA screening was that the rescue of ΔF508CFTR is invariably accompanied by an increase in the levels of band B. Furthermore, this was also accompanied by an increase in the band C/B ratio. The increase in band B levels associated with the depletion of the MAP3K11–JNK pathway components might be caused by either an increase in the synthesis or a decrease in the rate of degradation of ΔF508CFTR at the ER level. Quantitative RT-PCR after the siRNA treatment against the MAP3K11–JNK pathway showed no changes in the levels of CFTR mRNA (Figure 3.2a), which indicated that the increased band B levels were apparently not due to increased mRNA synthesis of ΔF508CFTR. However, the possibility of increased translation of CFTR mRNA cannot be excluded.

To determine whether the down-regulation of the MAP3K11–JNK pathway decreases the ERAD of ΔF508CFTR, a cycloheximide chase assay was performed, to measure the half-lives ($t_{½}$) of proteins (Okiyoneda et al. 2010; Alvarez-Castelao et al. 2012). ΔF508CFTR is continuously subjected to degradation in the ER, so when protein synthesis is blocked, the kinetics of the reduction in the levels of ΔF508CFTR (band B) monitored by Western blotting reflects the kinetics of ERAD of ΔF508CFTR. This reduction in the levels of the ER-associated protein (band B of ΔF508CFTR) is due to a combined effect of ERAD and the exit of the protein from the ER to the Golgi complex. Both of these processes can be monitored by measuring the changes in the levels of band B and the Golgi processed band C. Control CFBE cells and CFBE cells treated with siRNAs targeting the MAP3K11–JNK pathway were treated with cycloheximide for 20, 40 and 60 min, and the changes in the levels of band B were monitored by Western blotting (Figure 3.2b). During the chase, there was no increase in the band C levels, which suggested that during this period, there was no significant export of ΔF508CFTR out of the ER, while the band B levels gradually decreased with a $t_{½}$ of ~7 min in the control cells. In the case of the siRNA-treated cells, the reductions in the levels of band B was much less than that of the control cells, and the $t_{½}$ was about ~13 min for the JNK knock-down, to about 24 min for the MAP3K11 knock-down cells. Thus, the effect on the reductions in the rates of ERAD of ΔF508CFTR was more prominent for The MAP3K11–JNK pathway does not affect the activity of the proteasome itself, as the depletion of

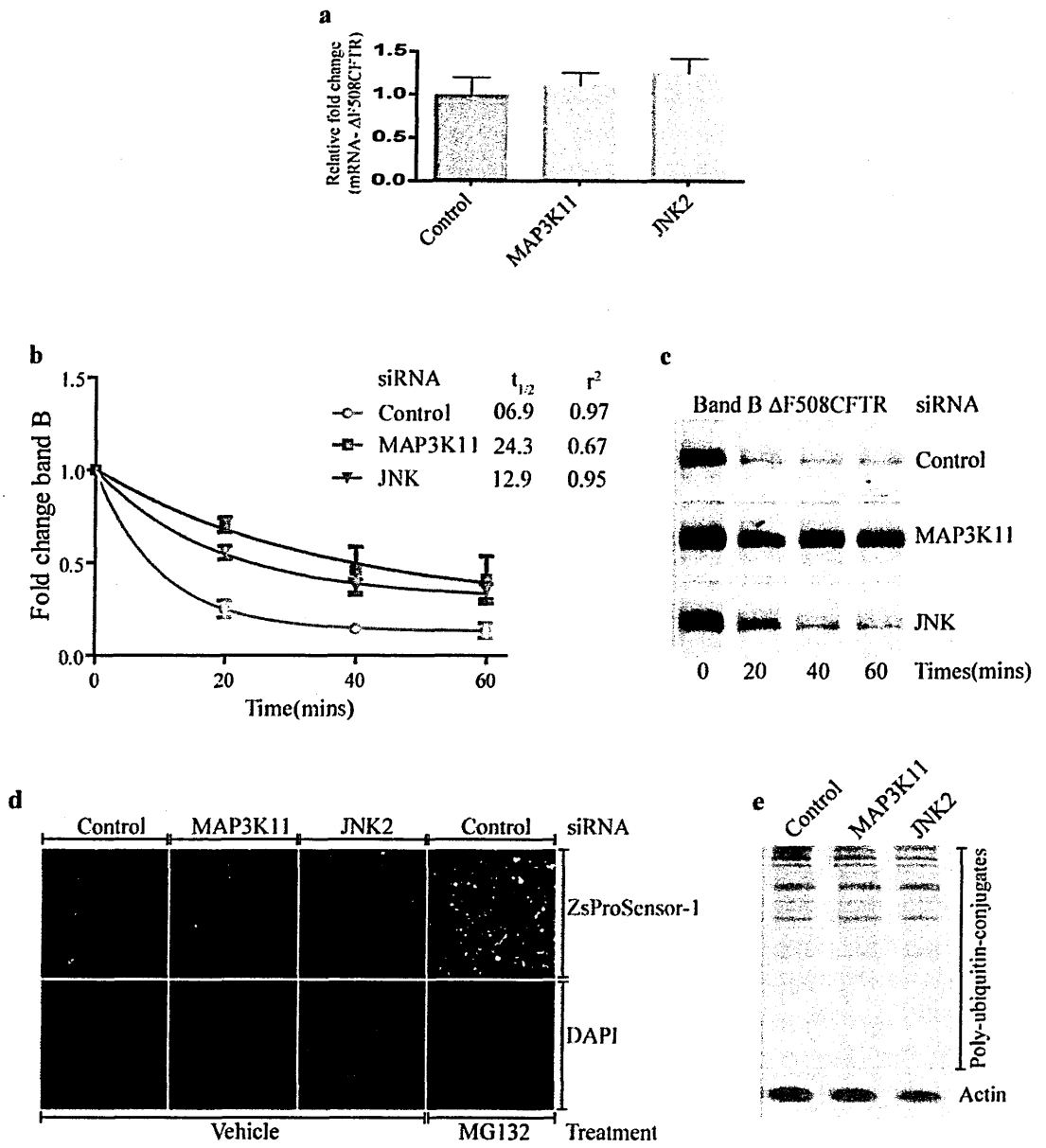

Figure 3.2. MAP3K11-JNK pathway regulates the ERAD of ΔF508CFTR.

CFBE cells were transfected with indicated siRNA for 72 hours before processing the sample for analysis. **a.** Relative levels of ΔF508CFTR mRNA quantities determined by RT-PCR (n=3). **b.** Kinetics of CFTR band B disappearance was quantified from immunoblot after cycloheximide chase (100mg/ml) at indicated times and expressed as fold change to the initial amount (time 0) from the experiments shown in (c) (n=3). **c.** Representative immunoblot after cycloheximide chase (100mg/ml) at different times as indicated. **d.** ZsProSensor-1 transfected and expressed for 24 h after 48 h of depletion of the indicated genes. MG132 is used as positive control for inhibition of proteasome. **e.** Immunoblot of the ubiquitin conjugated proteins analysed from indicated siRNA treated cells (representative of three separate experiments). Data represent mean ± SD.

MAP3K11, JNK2 did not lead to accumulation of ZsProSensor-1 whereas MG132 (proteasome inhibitor) treatment for 3 hours led to evident accumulation of ZsProSensor-1 (Figure 3.2d). Then to test whether the pathway affects the ubiquitination process itself, the ubiquitin conjugates were monitored in the total protein isolated from the cells depleted with MAP3K11 and JNK2. If there is any change in ubiquitin conjugation to the proteins (down regulation of ubiquitin ligases) there will be a decrease in the poly-ubiquitin conjugates in the cell (Xu et al. 2010; Oh et al. 2013). There was no change in the poly-ubiquitin conjugates in the MAP3K11 and JNK2 depleted cells (Figure 3.2e) suggesting that the ubiquitination process and the proteasome were unaffected.

3.3. The MAP3K11–JNK pathway does not affect folding of ΔF508CFTR or exit from the ER

As noted before, the down-regulation of the SAPK pathway induces an increase in the band C/B ratio of ΔF508CFTR (Figure 3.1f), which suggests that either the folding/ export of ΔF508CFTR is enhanced, or the stability of band C at the PM is increased. To determine whether ΔF508CFTR folds better when the MAP3K11–JNK pathway is down-regulated, the trypsin sensitivity of ΔF508CFTR was monitored (Rosser et al. 2008; Glozman et al. 2009) after knock-down of MAP3K11, a key component of the SAPK pathway. As expected, NBD1 and NBD2 of wtCFTR were resistant to trypsin-mediated digestion compared those of ΔF508CFTR (Figure 3.3a), similar to what has been shown before (Rosser et al. 2008). Down-regulation of MAP3K11 did not significantly change the trypsin sensitivity of ΔF508CFTR, which suggests that the increase in the intensity of band C should not be ascribed to a detectable increase in folding of ΔF508CFTR. It is important to note that increased folding of ΔF508CFTR by low temperature treatment (26 °C for 24 h) led to a visible change in the folding of ΔF508CFTR as measured by trypsin sensitivity of the NBD1 domain, which demonstrated that the assay was sensitive for the detection of changes in folding (Figure 3.3a). At this stage, it is not possible to rule out the subtle improvements in folding that were below the sensitivity levels of the assay used, but improved folding appears to contribute little towards the increased levels of band C.

With no apparent change in folding as measured by the trypsin sensitivity, there is the possibility that the export of ΔF508CFTR might be enhanced. The kinetics of transport of cargoes out of the ER was then measured using VSVG-GFP transport to the Golgi complex under control

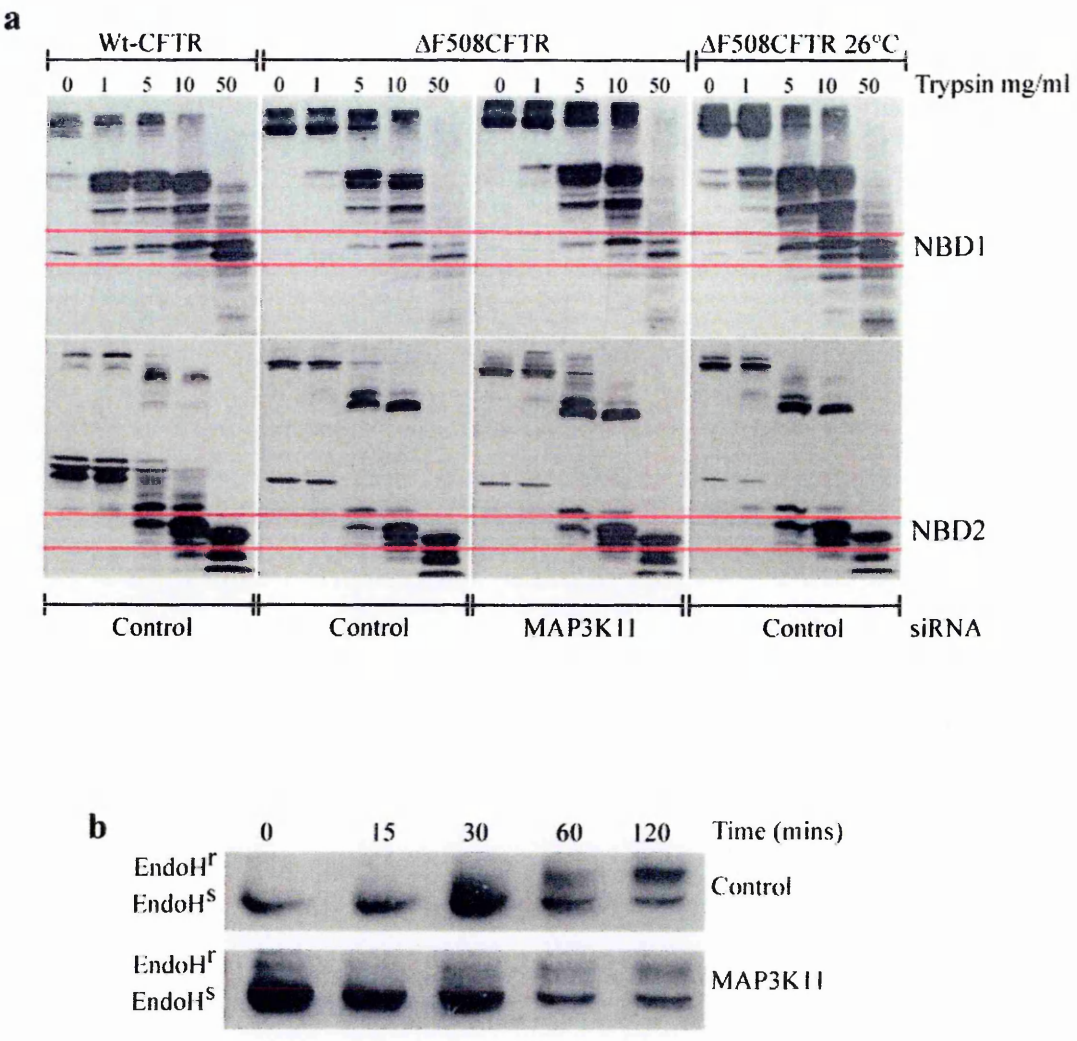

Figure 3.3. The MAP3K11–JNK pathway does not affect folding or exit from the ER.

a. Immunoblot of limited proteolysis of wtCFTR and ΔF508CFTR treated with siRNAs. Cell lysates were subjected to immunoblotting with the indicated antibodies (either anti-NBD1 or anti-NBD2 CFTR) (representative of three separate experiments). The low temperature 26°C was used as positive control for folding of ΔF508CFTR. **b.** Kinetics of VSVG transport. VSVG-GFP was transfected for 24 h at 40 °C after 48 h of siRNA treatments, as indicated, and then transferred to 32 °C. The cells were lysed for biochemical assay (section 6.9) at indicated time, and the lysates were treated with endoH and immunoblotted for VSVG (representative of two separate experiments).

and MAP3K11 knock-down conditions. VSVG has been used extensively as a marker to study the biochemical and molecular basis for transport along the secretory pathway both *in vivo* (Tisdale et al. 1992) and *in vitro* (Davidson and Balch 1993). VSVG is a type I transmembrane protein that has two N-linked carbohydrate chains and is transported from the ER to the Golgi apparatus. Its transport through the Golgi can be followed by the processing of two oligosaccaride chains from the high mannose endoH-sensitive form (which is found in the ER and pre-Golgi compartments) to the endoH-resistant form (which is found in the Golgi). The processing intermediates can be easily distinguished by SDS-PAGE (Davidson and Balch 1993). The first endoH-resistant form corresponds to the transport of VSVG from the ER to the early Golgi compartment where one or both of the oligosaccaride chains becomes endoH resistant by the action of the resident 1,2-mannosidases and glycosyltransferases (Davidson and Balch 1993); (Tisdale et al. 1992). The subsequent transport of VSVG to the TGN results in the appearance of the fully processed form, which contains two complex endoH-resistant oligosaccarides (Davidson and Balch 1993), (Tisdale et al. 1992). The appearance of sequential processing intermediates allows the direct examination of the effects of treatments on both ER-to-Golgi and intra-Golgi transport in the same experiment (Davidson and Balch 1993); (Tisdale et al. 1992). When the endoH resistance was examined (as described section 6.9) and the kinetics of VSVG-GFP was calculated there was no significant change in the kinetics of the tested cargo up on MAP3K11 depletion (Figure 3.3b).

3.4. The MAP3K11–JNK pathway regulates the peripheral quality control of ΔF508CFTR

As the MAP3K11–JNK pathway does not control either the folding of ΔF508CFTR or its exit out of the ER, as inferred from above set of experiments, an alternative possibility to explain the increased band C/B ratio is the stabilisation of the mutant protein at the PM. ΔF508CFTR that arrives at the PM is known to undergo peripheral or PM-associated quality control, where the mutant protein is recognized by the quality control system of chaperones and ubiquitin ligases and is ubiquitinated and degraded (Okiyoneda et al. 2010). Moreover, the quality control system operating at the PM level overlaps significantly with that operating at the ER, and given that the ERQC of ΔF508CFTR is affected under the conditions examined, there was a high probability of a compromise in the peripheral quality control too. To determine the effects of the MAP3K11-directed siRNAs on the degradation of PM-associated ΔF508CFTR an established procedure was

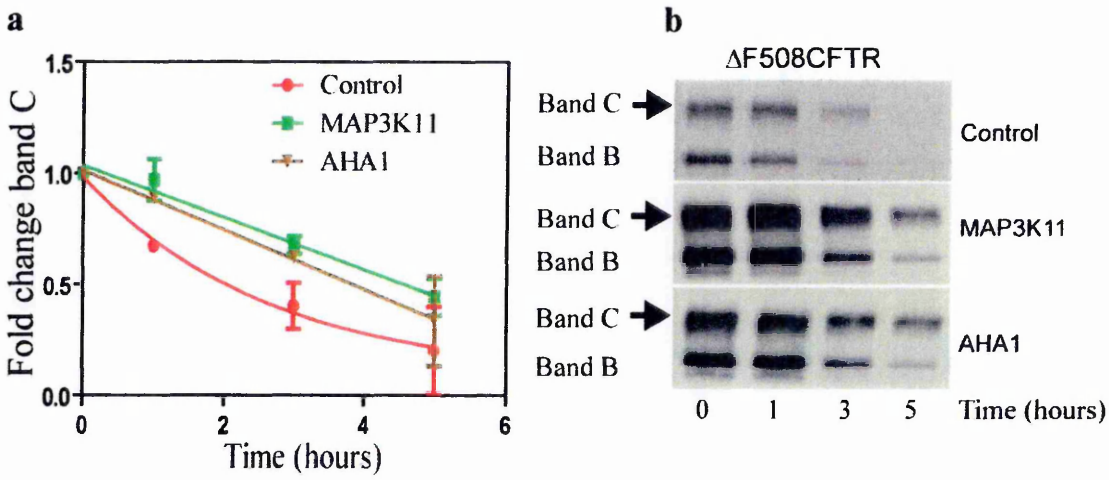

Figure 3.4. The MAP3K11–JNK pathway regulates the peripheral quality control of ΔF508CFTR.

CFBE cells were treated with siRNAs as indicated and were kept at 26 °C for 36 h. Then the cells were shifted to 37 °C for 1.5 h with 100 μg/ml cycloheximide, before being were lysed, as indicated, at 37 °C and immunoblotted. **a.** Kinetics of the degradation of band C as fold change to initial amount (Time-0) in the experiments shown in (b) (n=3) **b.** Representative immunoblot with the treatment of the siRNAs indicated. Aha1 was used as positive control for peripheral quality control. Data represent mean ± SD.

used (see section 6.10) (Okiyoneda et al. 2010). Degradation of band C occurred with a $t_{½}$ of approximately 2 h, and the depletion of MAP3K11 increased the half-time of degradation to about 4 h (Figure 3.4a,b), which suggested that the peripheral quality control of ΔF508CFTR is compromised in the absence of the MAP3K11-initiated pathway. In conclusion, inhibiting the MAP3K11-mediated pathway markedly reduces the efficiency of the both the ER-associated and the PM-associated quality control and degradation machineries, which results in relatively large increases in the mutant protein at the PM.

3.5. Upstream activators and downstream targets of the of MAP3K11–JNK pathway participate in the control of ΔF508CFTR proteostasis

MAP3K11 is known to be phosphorylated and activated by different MAP4Ks: HPK1/MAP4K1 (Arnold et al. 2005), GCK/MAP4K2 (Chadee et al. 2002), and GSK3B (Mishra et al. 2007), and by direct binding to the CDC42/Rac (Zhao et al. 2007) family proteins. Thus, to investigate the upstream MAP4K involved in the activation of the MAP3K11–JNK pathway, each of these upstream regulators were down-regulated using siRNAs and the effects on ΔF508CFTR were monitored using the biochemical assay (see section 6.12). Here, down-regulation of MAP4K1, CDC42 and Rac2 led to increases in the band C levels, with CDC42 showing the strongest response (Figure 3.5a).

The JNK pathway that forms a part of the SAPK pathway has been well studied, with several known downstream targets reported. Therefore, to understand the possible targets of this pathway, the details of several characterised substrates were collected from the published literature. This list included transcription factors, proteostatic components, and those involved in apoptosis regulation. Then these components were down-regulated using siRNA-mediated knock-down, to determine their effects on ΔF508CFTR proteostasis.

Among the targets BAG3 and HSF1 down-regulations were especially strong for the rescue of ΔF508CFTR, while the ATF1 led to modest but significant rescue (Figure 3.5b). Thus BAG3 appeared to be an ideal target of the MAP3K11–JNK pathway for the rescue of ΔF508CFTR. Although BAG3 was not identified in the CFTR interactome study performed (see section 3.9), other studies have shown an interaction (Wang et al. 2006), which suggests that BAG3 can

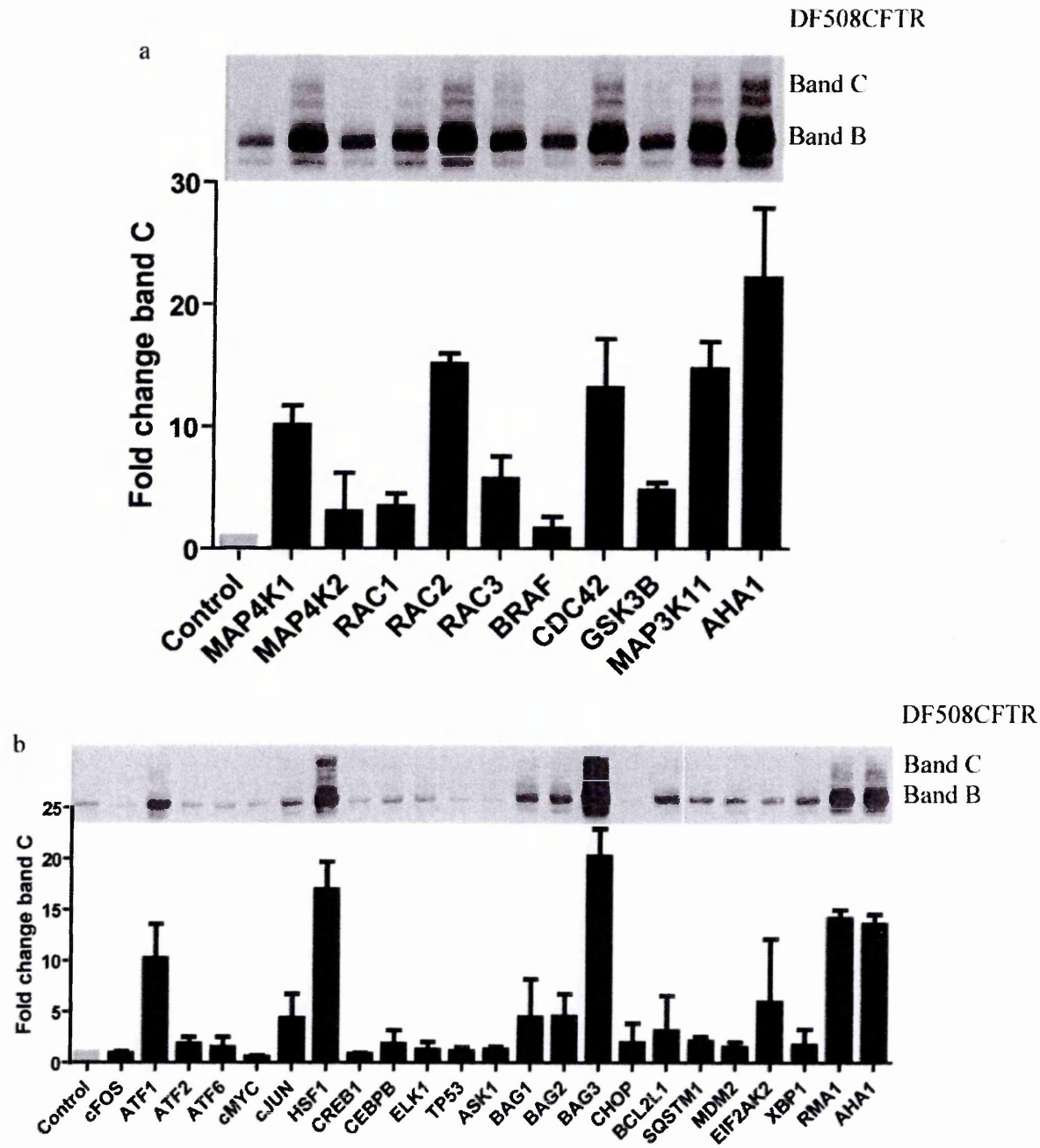

Figure 3.5 Upstream activators and downstream targets of the MAP3K11–JNK pathway also correct ΔF508CFTR.

CFBE cells were treated with siRNAs, as indicated, for 72 h and lysed and immunoblotted. **a.** Fold-increase in band C quantified from the immunoblots (n = 3) of the tested upstream activators, with representative immunoblot. **b.** Fold-increase band C of the tested downstream targets quantified from immunoblots (n =3), with representative immunoblot. Aha1 and RMA1 siRNAs were used as positive control for the correction. Data represent mean ± SD.

probably act indirectly to achive ΔF508CFTR rescue. Another interesting observation was that the knock-down of HSF1, which is a known proteostasis regulator (Balch et al. 2008), also led to partial correction of ΔF508CFTR, and previous studies have correlated the HSF1 activation to CFTR correction (Calamini et al. 2012). The other transcription factors c-JUN and ATF1 individually contributed to the rescue, indicating a transcriptional component in the action of the MAP3K11–JNK pathway. These observations thus opened an avenue to further explore the transcriptional effect of this pathway.

3.6. Inflammatory cytokines and ROS enhance ΔF508CFTR degradation

To understand the physiological relevance of the SAPK pathway that regulates the ERQC, the physiological upstream activators of the pathway were explored. MAP3K11 is known to be involved in the activation of JNK by TNF-α, TGF-β and ROS. Interestingly, TGF-β and TNF-α have been suggested to be genetic modifiers of CF (The Cystic Fibrosis Genotype-Phenotype Consortium 1993). If these cytokines indeed control the ERQC via MAP3K11, then in the case of overexpression of the SAPK activators (Figure 3.1i), the activation of the cytokine receptors by their respective ligands would activate a pathway that enhances the degradation of ΔF508CFTR.

To study the action of cytokines, CFBE cells were treated with TNF-α or TGF-β levels of band B for ΔF508CFTR were examined. As shown in figure 3.6, addition of TNF-α or TGF-β led to immediate decreases in the levels of band B of ΔF508CFTR. These reductions were maximal at 15 min after the addition of TNF-α or TGF-β, and by 60 min, the levels of band B of ΔF508CFTR recovered to the pretreatment levels (Figure 3.6a, b). To understand whether the MAP3K11-mediated pathway is indeed involved in this cytokine-mediated effect, the cells pretreated with MAP3K11-directed siRNAs were exposed to TNF-α or TGF-β. While the control cells showed reductions in the levels of ΔF508CFTR after these cytokine treatments, the siRNA-treated cells did not show any changes in the levels of ΔF508CFTR after the TNF-α or TGF-β treatments, which suggested that the MAP3K11-mediated pathway is indeed required for the regulation of ΔF508CFTR proteostasis by TNF-α and TGF-β (Figure 3.6b, c). As the levels of TNF-α and TGF-β recovered by 60 min after the start of this treatment, it was next analysed whether chronic administration of TNF-α or TGF-β also leads to changes in ΔF508CFTR proteostasis. To this end,

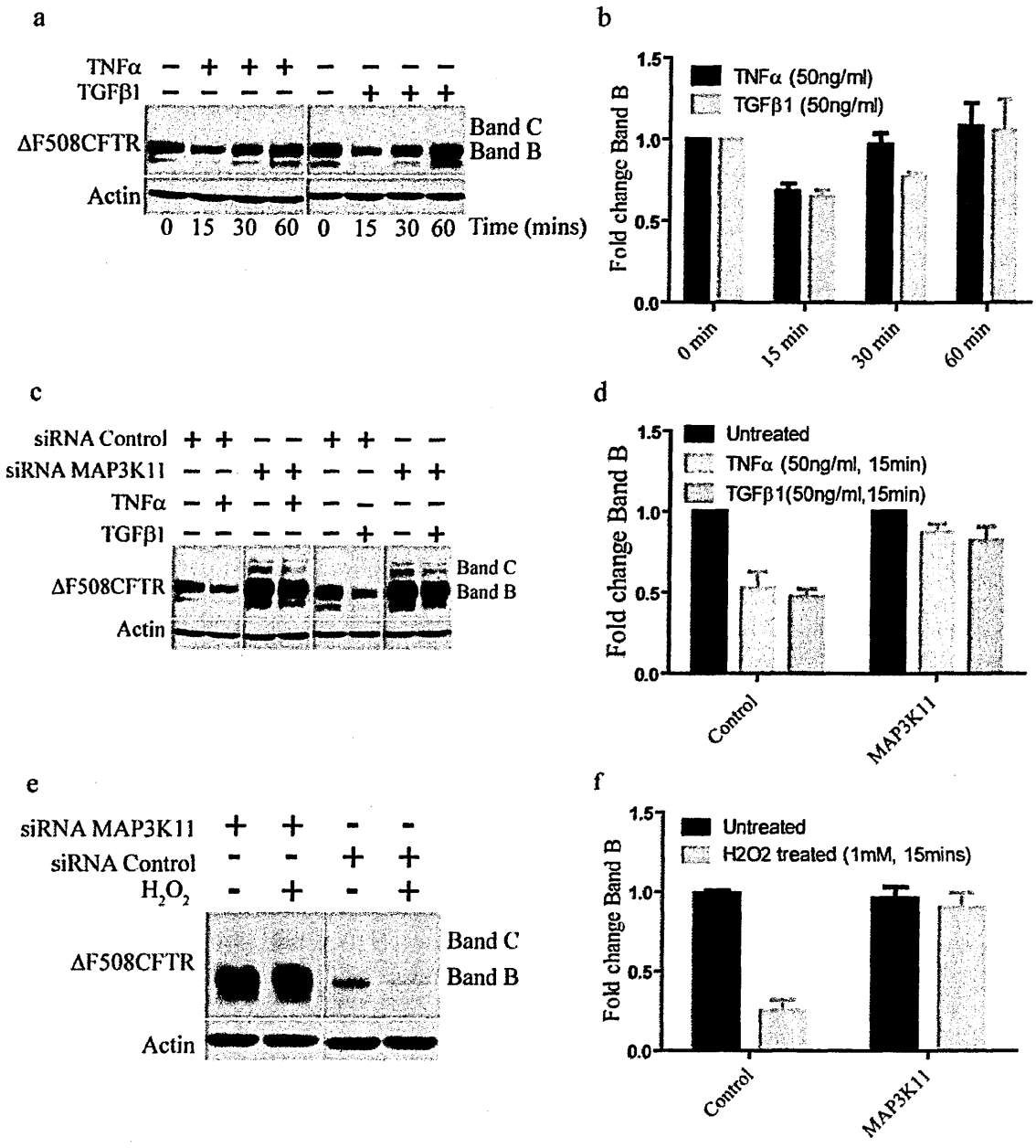

Figure 3.6. Inflammatory cytokines and ROS enhance ΔF508CFTR degradation.

a. CFBE cells were treated with 50 ng/ml TGF-β or TNF-α for the indicated times and lysed and immunoblotted for CFTR, **b**. Fold change of band b quantified and expressed as to initial amount (time-0) (n = 3) from the experiments in (a). **c.** Control and MAPK3K11-depleted CFBE cells were treated with 50 ng/ml TGF-β or TNF-α for 15 minutes, lysed, immunoblotted for CFTR, **d.** Band B levels of ΔF508CFTR were quantified from the experiments in (c), expressed as fold change compared to initial amount (time-0) (n = 3), **e.** Control and MAPK3K11-depleted CFBE cells were treated with 1 mM H_2O_2 for 15 mins, lysed, immunoblotted for CFTR, **f.** The ΔF508CFTR band B levels were quantified from the experiments in (e), expressed as fold change compared to initial amount (time-0), (n = 3). Data represent mean ± SD.

CFBE cells were treated for 72 h with TNF-α or TGF-β, with the fresh addition of the cytokines every 24 h. This chronic treatment with physiologically relevant concentrations of TNF-α or TGF-β did not lead to detectable changes in ΔF508CFTR proteostasis.

Another group of potent activators of the SAPK pathway are the ROS (Hong and Kim 2007). Moreover, ROS have been reported to be enhanced in CF cells, and they are produced in large number by neutrophils and other cells during inflammatory reactions that are common in patients with CF (Hull et al. 1997). Thus, CFBE cells were treated with 1 mM H_2O_2 for 15 min, and strikingly, this enhanced degradation was nearly completely inhibited by the absence of MAP3K11 (Figure 3.6d,e). Thus, the SAPK pathway activated by inflammatory cytokines, and more significantly by ROS, via MAP3K11 is a potent controller of ΔF508CFTR proteostasis.

3.7. Small molecule inhibitors of the MAP3K11–JNK pathway can correct ΔF508CFTR

The MAP3K11–JNK signalling pathways have well-characterised inhibitors (Cui et al. 2007). As the down-regulation of the pathway is associated with the rescue of ΔF508CFTR, the effects of inhibitors that inhibit the kinase activity of the MAP3K11–JNK pathway components were analysed, considering the rescue of ΔF508CFTR and the potential for therapeutic use. Moreover, a recent study where kinase inhibitors were screened for the correction of the ΔF508CFTR defect identified inhibitors that also target the MAP3K11–JNK pathway, which included oxozeaenol and kenpaullone (Trzcinska-Daneluti et al. 2012). Oxozeaenol targets MAP3Ks mainly through TAK1 (Ninomiya-Tsuji et al. 2003), and kenpaullone targets GSK3B. So batteries of inhibitors of the MAP3K11–JNK pathway were tested, using CFBE cells over 24 h, and then their effects on ΔF508CFTR were analysed. The well-characterised corrector VX-809 was used as the control for ΔF508CFTR rescue, which demonstrated very robust correction and increased the levels of band C to about 4-8-fold in the biochemical assay (as described in section 6.12). When ΔF508CFTR-expressing CFBE cells were treated with the JNK inhibitors (JNKi) a very robust increase in the levels of band C was obtained with the treatment of JNKi II (or SP600125), JNKi IX and JNKi XI (Figure 3.7b,c); oxozeaenol and kenpaullone also rescued ΔF508CFTR efficiently (Figure 3.7b,c), as has been reported (Trzcinska-Daneluti et al. 2012). The fold-increase in the levels of band C was comparable to that obtained with VX-809 (~4-8-fold). All

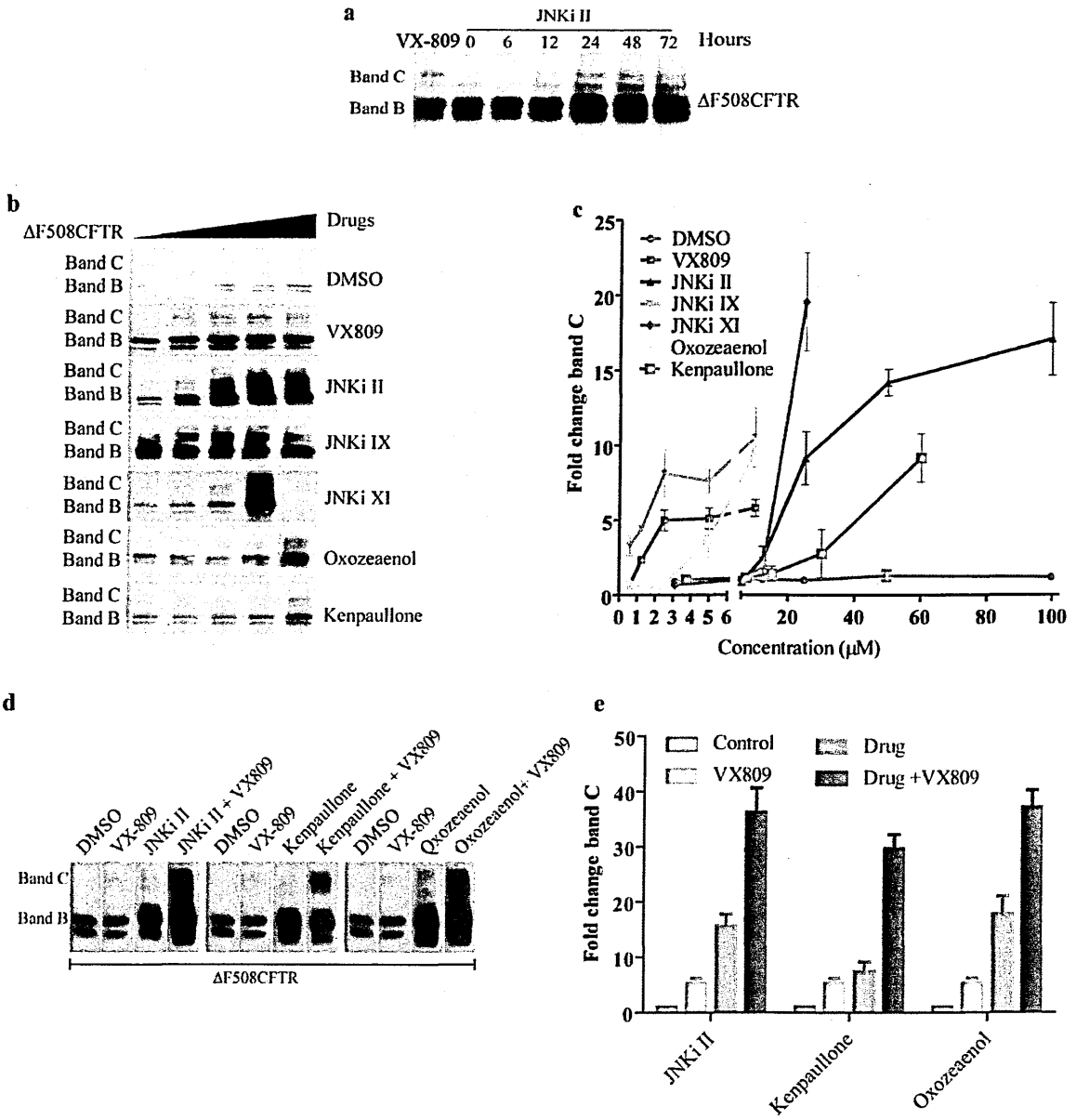

Figure 3.7. Small-molecule inhibitors of the MAP3K11–JNK pathway correct ΔF508CFTR.

a. CFBE cells treated with JNKi II for the indicated times, lysed, and ΔF508CFTR correction was analysed by immunoblot (representative of three separate experiments). **b.** Representative immunoblot of CFBE cells that were treated with indicated drugs for 48 h and immunoblotted for ΔF508CFTR. **c.** Immunoblot quantified fold change band C levels from the experiments in (b), at indicated drug concentration (x-axis), fold change expressed as compared to DMSO treatment (n=3). **d.** Representative immunoblot of ΔF508CFTR from CFBE cells that were treated with the indicated drugs (25 μM JNKi II, 30 μM Kenpaullone, 10 μM Oxozeaenol) alone or in combination with 5 μM VX-809 for 48 hours. **e.** Immunoblot quantified fold change band C levels from the experiments in (d) expressed as compared to DMSO treatment (n=3). Data represent mean ± SD.

of these three inhibitors of JNKi have different chemical structures, and while JNKi II and JNKi IX are ATP-competitive inhibitors of JNK, JNKi XI is an inhibitor of the substrate/ scaffold binding to JNK. This suggests that the rescue is not mediated by compounds with similar chemical structures, but rather due to specific inhibition of JNK. As oxozeaenol is reported to be a major Tak1 inhibitor (Ninomiya-Tsuji et al. 2003), *TAK1* knock-down was also examined, but it did not have any effects on ΔF508CFTR proteostasis, so the corrective effect of oxozeaenol which is known to also inhibit other MAP3Ks at higher concentration (Ninomiya-Tsuji et al. 2003) might be mediated by its effect on other MAP3Ks including MAP3K11. The other MAP3K11 inhibitors K252a (Pan et al. 2005) and URMC-099 (Marker et al. 2013), and JNK inhibitors JNK I, JNK VII and JNK XIII were tested, these did not correct the ΔF508CFTR; the reason for the lack of action of these other inhibitors remains unknown.

Importantly the levels of correction obtained with the JNK inhibitors were better than the corrector compounds (Table 2.1a) from which the pathway was derived. The corrector drugs (Table 2.1a) were obtained by random screening procedures, and this process of determining their mechanisms of action to specifically target the relevant network/pathway like MAP3K11-JNK pathway is justified by the increased rescue obtained. The effect of one of the inhibitors, JNKi II (SP600125), was also tested in HeLa cells expressing ΔF508CFTR, and this led to an increase in the levels of band C, although this increase was not as robust as for CFBE cells. The increase in band C levels started at about 25 μM JNKi II and reached a plateau at about 50 μM JNKi II. Again, as for the siRNA treatments, the increases in the levels of band C were accompanied by increases in the levels of band B. To study the time course of action of the JNKi on the correction of ΔF508CFTR, CFBE cells were treated with 50 μM JNKi II from 6 h to 72 h. A detectable increase in band C required at least 24 h of JNKi II treatment (Figure 3.7a), and this effect reached a peak level by around 24 h to 48 h. There was then no further detectable change in band C levels up to 72 h. Thus, inhibitors of the potential MAP3K11-regulated, MAP3K11–JNK pathway can correct the basic defect of the folding/ trafficking of the mutant ΔF508CFTR.

During the course of above study, it was also noted that the MAP3K11–JNK pathway inhibitor treatment using JNKi II, oxozeaenol and kenpaullone led to an increase in band B levels that was accompanied by an increase in band C levels, which was similar to that obtained by the

siRNA-mediated knock-down of the MAP3K11 pathway. In contrast, the treatment with VX-809, which is a known pharmacochaperone, allowed increased exit from the ER with little or no change in band B levels, which resulted in an increased band C/B ratio. This suggested that JNKi II, oxozeaenol and kenpaullone act at different steps of ΔF508CFTR biosynthesis, as they mainly increased the stability in the ER. Thus, it was hypothesised that combining these would lead to increased stability of band B mediated by JNKi II that can be efficiently rescued by VX-809. Indeed, when JNKi II, oxozeaenol and kenpaullone were individually combined with VX-809 for 48 h, this led to very efficient synergy between the drugs, and a rescue that reached nearly 8-fold greater than the effects of VX-809 alone (Figure 3.7d), as measured by the levels of band C in the biochemical assay (as described in section 6.12). Given that in a phase IIa clinical study, VX-809 was reported not to show statistically significant changes in lung function or patient-reported outcomes (Clancy et al. 2012), the observed additive/ synergistic effects here provides an exciting opportunity to explore this further.

3.8. The MAP3K11–JNK pathway depletion partially restores functional ΔF508CFTR

To determine whether the rescued ΔF508CFTR is indeed functional, the chloride conductance in CFBE cells after siRNA-mediated knock-down of MAP3K11 and JNK was investigated using an SPQ fluorescence assay; this indicated that the rescued ΔF508CFTR is indeed functional (Figure 3.8a, b, c, d). Then the conductance was also analysed by a halide sensitive (HS) yellow fluorescent protein (YFP) assay (Pedemonte et al. 2011) using HS-YFP stably transfected into CFBE cells (see section 6.16). This assay also showed that JNKi II, oxozeaenol and kenpaullone indeed increased the conductance (Figure 3.8e). JNKi II, oxozeaenol and kenpaullone were also examined in polarised CFBE cells for the correction of ΔF508CFTR by measuring the trans-epithelial short-circuit current using an Ussing chamber system (see section 6.17). The Ussing chamber system showed an increase in the chloride current upon treatment with oxozeaenol and kenpaullone (Figure 3.8f, g, h), but not with JNKi II (Figure 3.8h). In summary, the inhibitors targeting the MAP3K11–JNK pathway corrected ΔF508CFTR, which is then functionally active in gating the chloride through the PM even in polarised CFBE cells.

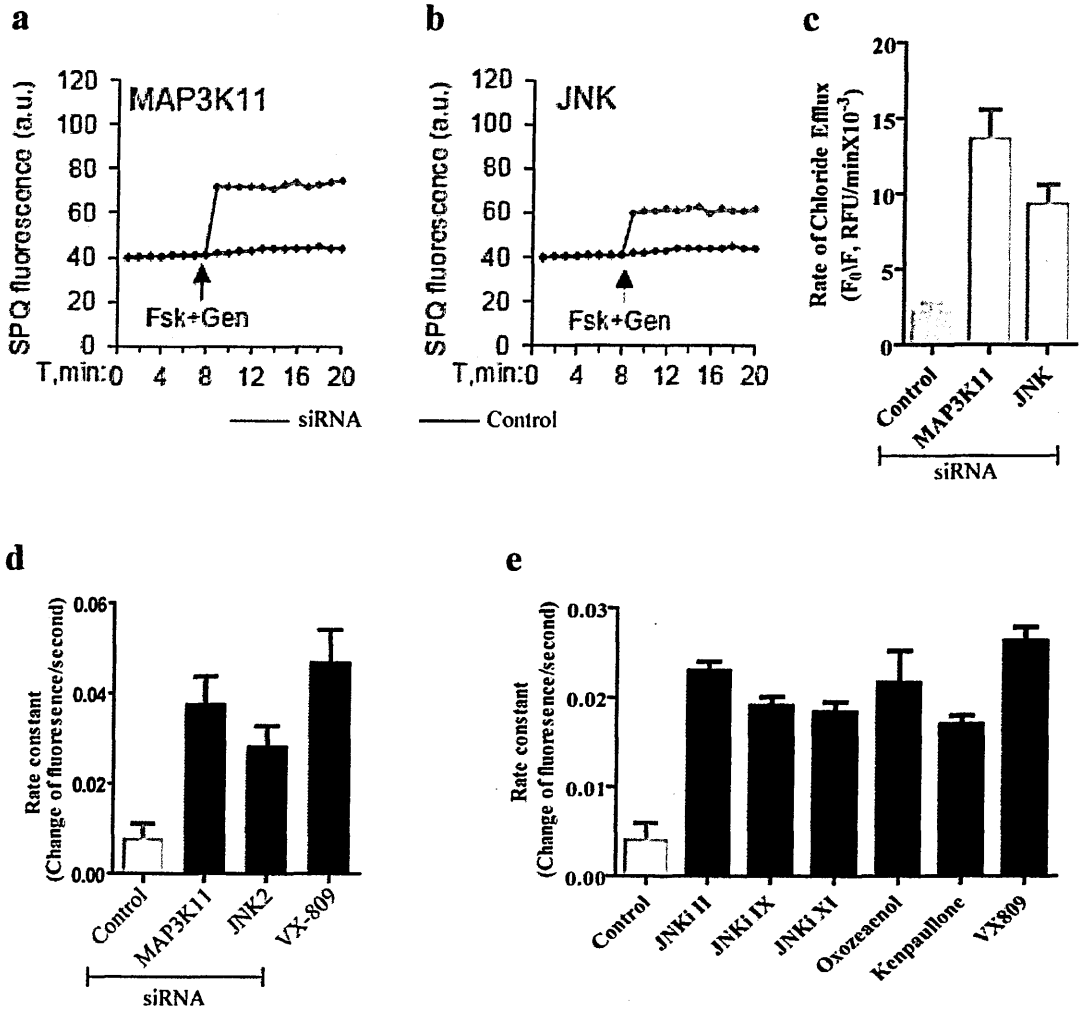

Figure 3.8. MAP3K11–JNK pathway depletion partially restores functional ΔF508CFTR.

a, b, c. CFBE cells were treated with the indicated siRNAs for 72 hour and the iodide efflux was measured using SPQ, an iodide sensitive fluorescent dye. The change in fluorescence was plotted until 20 mins for a control and siRNA treatment. The CFTR channel was stimulated with Fsk (forskolin) and Gen (genestin) after 8 Mins **a.** MAP3K11 siRNA-treated and **b.** JNK siRNA-treated CFBE cells **c.** Calculated rate of iodide efflux (n=50 cells). **d.** Rate constant measured by the changes in the fluorescence of iodide-sensitive YFP expressed in CFBE cells after cAMP stimulation after the pre-treatment with the indicated siRNA for 72 hour (n=50 cells). **e.** Rate constant measured by the changes in the fluorescence of iodide-sensitive YFP expressed in CFBE cells after cAMP stimulation after the pre-treatment with the indicated drugs for 48 hour (n=50 cells). VX-809 was used as positive control for the functional rescue.

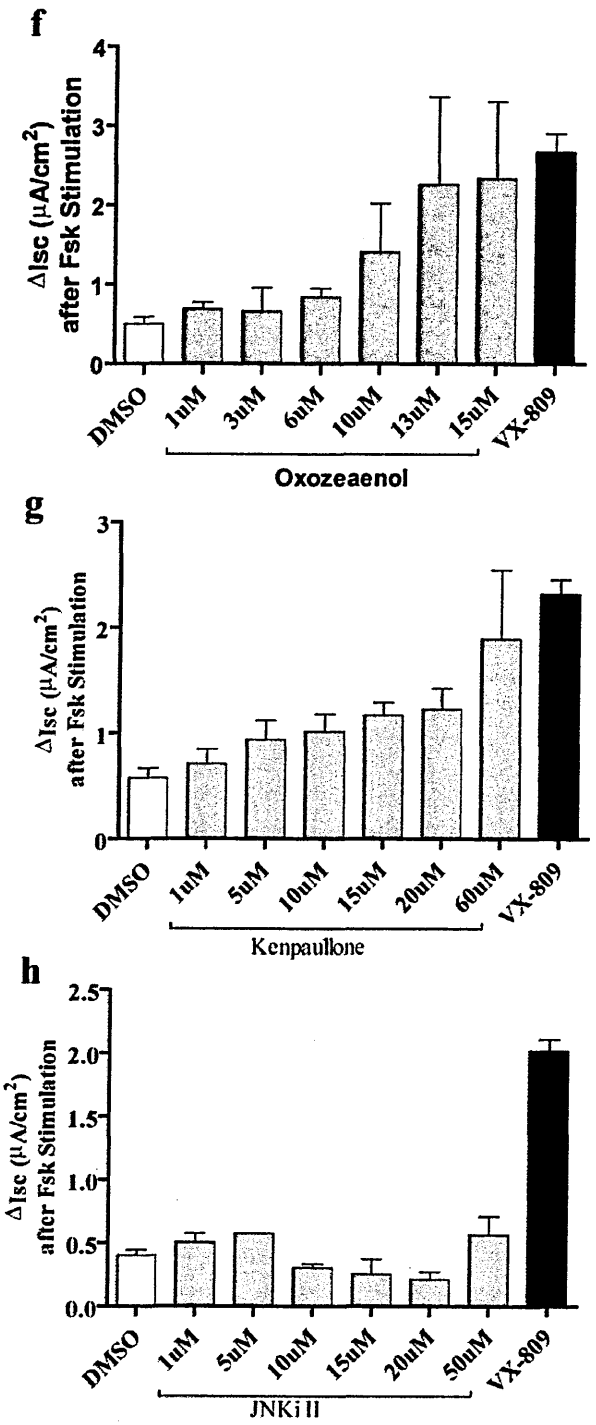

Figure 3.8. MAP3K11–JNK pathway depletion partially restores functional ΔF508CFTR (continued).

Polarised CFBE cells expressing ΔF508CFTR were treated with indicated drugs for 48 hours, and short-circuit current (Isc) was measured using the Ussing chamber assay system (n=3). **f.** Oxozeaenol, **g.** Kenpaullone, **h.** JNKi II were treated at indicated concentration. VX-809 was used as positive control for the functional rescue. Data represent mean ± SEM (n=3).

3.9. The MAP3K11–JNK pathway modifies the interactome of ΔF508CFTR

To understand how the MAP3K11-mediated SAPK pathway regulates ΔF508CFTR proteostasis, the interactome of ΔF508CFTR after treatment with JNKi II for 24 h was analysed by mass spectrometry and compared to the interactome of wtCFTR and ΔF508CFTR, which were also analysed in parallel. For this study, HeLa cells expressing an HA-tagged version of the wtCFTR or ΔF508CFTR were used. The wtCFTR interactome had 90 components, while that of ΔF508CFTR had 107, and ΔF508CFTR after JNKi II treatment had 141 components (Table 3.9). Comparison with the earlier published CFTR interactome (Wang et al. 2006) showed very minimal overlap, with only 12 common interactors of the ΔF508CFTR and six common interactors in the wtCFTR interactome. Given that two different heterologous systems were used for the studies (the earlier published study used BHK cells), the minimal overlap suggests that there are large differences in the proteostatic machinery and/or their regulation between these cell lines. Comparison of the wtCFTR and ΔF508CFTR interactomes obtained from HeLa cells pointed to several interesting observations (Table 3.9).

Nearly two-thirds of the components were common to both the wtCFTR and ΔF508CFTR interactomes (quantitative information based on the peptide count is not considered), and even the nature of the components were the same; e.g., ribosomal proteins, folding degradation machinery, and RNA processing machinery. This is surprising, given that the majority of the proteins are ER localised in the case of ΔF508CFTR, while the majority are Golgi processed and localised to the PM for wtCFTR. Nevertheless, the number of cytosolic proteostatic components associated with wtCFTR was nearly half of that associated with ΔF508CFTR, as expected. In spite of the absence of quantitative information that would help in the interpretation of the interactome data, the observation that the wtCFTR interactome (localised mainly in the post-ER compartments) had as many ER luminal components as that of the ΔF508CFTR suggests that wtCFTR has more affinity for these components than ΔF508CFTR. Considering the qualitative information the interactome of ΔF508CFTR after JNKi II treatment showed substantial increases in components of the ribosomal/ translational machinery and RNA-processing components, compared to the untreated conditions. Among the folding/ degradation machinery, there was a slight reduction in the cytosolic folding/

Table 3.9. Interactome of CFTR

The HeLa cells expressing wtCFTR, ΔF508CFTR or ΔF508CFTR were treated with JNKi II for 24 h. Then the CFTR-interacting proteins were determined by co-immunoprecipitation followed by mass spectrometry.

Total			Lost compared to ΔF508CFTR		Gained compared to ΔF508CFTR	
ΔF508CFTR	wtCFTR	ΔF508CFTR^{JNKi}	wtCFTR	ΔF508CFTR^{JNKi}	wtCFTR	ΔF508CFTR^{JNKi}
ACLY	ACLY	HSPE1	AKR1C3	AKR1C2	ADRM1	ADRM1
ACTN4	ACTN4	YWHAE	ANXA5	ANXA3	ANXA7	ANXA7
ADRM1	AHCY	PSMC4	CANX	ANXA5	ATAD3A	ATAD3A
AHCY	AKR1C3	RPS2	CCT2	CAD	ATIC	CCT3
ALDOA	ALDOA	RPS3	CFL1	CALR	BAG2	CCT5
ANXA1	ANXA1	RPS3A	DNAJC10	CANX	CAPRIN1	CKAP4
ANXA2	ANXA2	RPS4X	ELAVL1	CAPZA1	CCT3	CLTC
ANXA7	ANXA5	RPS8	FUBP1	CBR1	CCT5	CSE1L
ATAD3A	CANX	RPSA	HIST2H2AA4	CFL1	CCT6A	EEF1A1
ATIC	CCT2	RPLP0	HIST4H4	CPS1	CCT7	EIF4A1
BAG2	CCT4	RPL12	HNRNPF	DHX15	CCT8	EZR
CAPRIN1	CFL1	RPL14	HNRNPH3	DNAJC10	CKAP4	FAF2
CCT3	CKB	RPL23A	KPNB1	EEF1G	CSE1L	FKBP4
CCT4	CLTC	RPL3	MDH2	ELAVL1	EEF1A1	FSCN1
CCT5	DDX3X	RPL7A	MSN	FLNB	EEF1D	GPI
CCT6A	DDX5	RPL8	PCBP1	FLNC	ERLIN2	GSTP1
CCT7	DHX9	HSPA5	PRDX2	G3BP1	EZR	HLA-C
CCT8	DNAJC10	AHCY	PRDX6	HNRNPA1	FAF2	ILF2
CKAP4	EIF4A1	AKR1C2	RPL10A	HNRNPAB	FKBP4	IMPDH2
CKB	ELAVL1	ACTN4	RPS12	HNRNPD	FSCN1	MAT2A
CLTC	ENO1	ENO1	RPS2	HNRNPF	HLA-C	PPIA
CSE1L	ERLIN1	ANXA1	RPS29	HNRNPH3	HNRNPH1	PPIB
DDX3X	EWSR1	ANXA2	RPS8	HNRNPU	HSP90AA1	PSMD11
DDX5	FASN	ANXA3	SF3B3	HUWE1	HSPE1	PSMD3
DHX9	FUBP1	ANXA5	UBC	ILF3	IGF2BP3	PTBP1
EEF1A1	FUS	ACLY	VARS	KHSRP	MAT2A	RPL23
EEF1D	GPI	DHX9	XRCC5	KPNB1	MYH9	RPS18
EIF4A1	GSTP1	DDX3X	ZYX	LARS	P4HB	RPS25
ENO1	HIST2H2AA4	BAG2		MCM7	PABPC4	RPS27
ERLIN1	HIST4H4	ATIC		MDH2	PHB2	SFPQ
ERLIN2	HNRNPA2B1	CANX		MSN	PPIB	SLC25A5
EWSR1	HNRNPC	CALR		NONO	PSMB6	SND1
EZR	HNRNPF	CAPRIN1		PCBP1	PSMD11	STIP1
FAF2	HNRNPH3	CFL1		PCBP2	PSMD3	TCP1
FASN	HNRNPM	CKB		PDIA4	RPL12	
FKBP4	HNRNPUL1	MCM7		PRDX6	RPL23	

Table 3.9. Interactome of CFTR (continued)

Total			Lost compared to ΔF508CFTR		Gained compared to ΔF508CFTR	
ΔF508CFTR	wtCFTR	ΔF508CFTR^{INKI}	wtCFTR	ΔF508CFTR^{INKI}	wtCFTR	ΔF508CFTR^{INKI}
FSCN1	HSP90B1	DNAJC10		PSMC4	RPS18	
FUS	HSPA1A	RPN1		RBM14	RPS27	
GPI	HSPA5	TRIM21		RPL14	RUVBL2	
GSTP1	HSPA8	ELAVL1		RPL23A	SFPQ	
HLA-C	HSPB1	EEF1D		RPL24	SLC25A5	
HNRNPA2B1	ILF2	EEF1G		RPL27A	SND1	
HNRNPC	IMPDH2	TUFM		RPL3	TCP1	
HNRNPH1	KPNB1	HSP90B1		RPL5	UFD1L	
HNRNPM	LGALS3BP	ERLIN1		RPL7A	VDAC2	
HNRNPUL1	LMNA	FASN		RPL8		
HSP90AA1	MDH2	FLNB		RPN1		
HSP90B1	MSN	FLNC		RPS2		
HSPA1A	MVP	ALDOA		RPS21		
HSPA5	NCL	LGALS3BP		RPS3A		
HSPA8	PABPC1	HSPA1A		RPS4X		
HSPB1	PCBP1	HSPA8		RPS5		
HSPE1	PDIA3	TRAP1		RPS8		
IGF2BP3	PDIA6	HSPB1		RPS9		
ILF2	PFN1	HSP90AA1		SLC3A2		
IMPDH2	PGK1	HNRNPA2B1		SNRPA		
LGALS3BP	PLS3	HNRNPC		SYNCRIP		
LMNA	PPIA	HNRNPD		TAF15		
MAT2A	PRDX2	HNRNPF		TARS		
MVP	PRDX6	HNRNPH1		TFRC		
MYH9	PTBP1	HNRNPH3		TLN1		
NCL	RPL10A	HNRNPUL1		TRAP1		
P4HB	RPLP0	HNRNPU		TXNDC5		
PABPC1	RPS12	SYNCRIP		UBA1		
PABPC4	RPS2	KPNB1		UBAC2		
PDIA3	RPS25	IGF2BP3		VDAC1		
PDIA6	RPS29	ILF3		XRCC5		
PFN1	RPS3	MVP		YBX1		
PGK1	RPS8	MDH2				
PHB2	RPSA	MSN				
PLS3	SDHA	MYH9				
PPIA	SEC23A	NONO				
PPIB	SERPINH1	YBX1				
PSMB6	SF3B3	NCL				

Table 3.9. Interactome of CFTR (continued)

Total			Lost compared to ΔF508CFTR		Gained compared to ΔF508CFTR	
ΔF508CFTR	wtCFTR	ΔF508CFTR^{JNK1}	wtCFTR	ΔF508CFTR^{JNK1}	wtCFTR	ΔF508CFTR^{JNK1}
PSMD11	SRI	PGK1				
PSMD3	STIP1	PLS3				
PTBP1	TAGLN2	PCBP1				
RPL12	TFG	PCBP2				
RPL23	TKT	PABPC1				
RPLP0	TPI1	PABPC4				
RPS18	TRIM21	LMNA				
RPS25	TUFM	DDX5				
RPS27	UBC	PHB2				
RPS3	VARS	P4HB				
RPSA	VCL	PDIA3				
RUVBL2	VCP	PDIA4				
SDHA	XRCC5	PDIA6				
SEC23A	XRCC6	TFG				
SERPINH1	YWHAE	DHX15				
SFPQ	ZYX	G3BP1				
SLC25A5		RBM14				
SND1		EWSR1				
SRI		FUS				
STIP1		RUVBL2				
TAGLN2		SERPINH1				
TCP1		SDHA				
TFG		CCT7				
TKT		CCT8				
TPI1		CCT6A				
TRIM21		TLN1				
TUFM		TXNDC5				
UFD1L		TARS				
VCP		TAGLN2				
VDAC2		VCP				
XRCC6		TKT				
YWHAE		TPI1				
		UFD1L				
		UBA1				
		VCL				
		VDAC1				
		VDAC2				
		XRCC6				

Table 3.9. Interactome of CFTR (continued)

Total			Lost compared to ΔF508CFTR		Gained compared to ΔF508CFTR	
ΔF508CFTR	wtCFTR	ΔF508CFTR^{INKI}	wtCFTR	ΔF508CFTR^{INKI}	wtCFTR	ΔF508CFTR^{INKI}
		XRCC5				
		RPS21				
		RPS5				
		RPS9				
		SLC3A2				
		RPL24				
		RPL27A				
		RPL5				
		CAD				
		CPS1				
		CBR1				
		HUWE1				
		ERLIN2				
		CAPZA1				
		KHSRP				
		HNRNPAB				
		HNRNPA1				
		HNRNPM				
		LARS				
		PRDX6				
		PFN1				
		PSMB6				
		SEC23A				
		SRI				
		CCT4				
		TAF15				
		SNRPA				
		UBAC2				

degradation machinery (from 15 in untreated, to 12 after JNKi II treatment), while there was a slight increase in the ER luminal folding/ degradation machinery (from 9 to 13 components after treatment), which reflects the behaviour of the wtCFTR, as discussed above. Next, to determine whether the interactome of ΔF508CFTR treated with JNKi (ΔF508CFTR^{JNKi}) resembles that of wtCFTR, these were compared. For the proteins that were present in the ΔF508CFTR^{JNKi} interactome but absent in the ΔF508CFTR interactome, there was little overlap with that of the wtCFTR-specific proteins. An interesting candidate among the overlapping components was calnexin, as it has been shown that while wtCFTR is sensitive to modulation through calnexin dependent proteostasis; ΔF508CFTR is insensitive, with any such modulation suggesting that wtCFTR is probably in an advanced stage of folding/quality control, which ΔF508CFTR does not reach.

The presence of calnexin in the ΔF508CFTR^{JNKi} interactome suggests that the JNKi II treatment promotes ΔF508CFTR to an advanced folding/quality control stage. Among the proteins that were absent in the comparison of untreated ΔF508CFTR, the wtCFTR and ΔF508CFTR^{JNKi} interactomes showed substantial overlap. Among these components there were known proteostatic components involved in ERAD, including proteasomal subunits (PSMD3 and PSMD11) and FAF2 (or UBXD8), a known regulator of proteostasis of apolipoprotein B (ApoB) and also a regulator of triglyceride synthesis. Interesting components that had no previous established roles in ERAD included chaperonin subunits and ribosomal subunits. When the differences between the ΔF508CFTR and ΔF508CFTR^{JNKi} interactomes were scrutinised, in addition to differences that were similar to those seen between the wtCFTR and ΔF508CFTR interactome, it was noted that the ΔF508CFTR^{JNKi} interactome lost interactions with STIP1 (HOP), unlike the wtCFTR interactome. HOP has been reported to be involved in ΔF508CFTR proteostasis, and reduction in its levels by siRNA-mediated knock-down has been reported to rescue ΔF508CFTR (Marozkina et al. 2010). Moreover, siRNA-mediated depletion of HOP was also known to partially correct the ΔF508CFTR (Marozkina et al. 2010).

To summarise, the JNKi II treatment transforms the ΔF508CFTR interactome slightly, to mimic the wtCFTR interactome, and results in several changes in the interactome of ΔF508CFTR.

These changes lead to a reshaping of the proteostasis content for resemblance to that of wtCFTR, and probably explain the escape of ΔF508CFTR from the ERQC.

Discussion

This study identified a novel role for the MAP3K11–JNK pathway in the regulation of the quality control of ΔF508CFTR at the ER and the PM. Characterised inhibitors of this pathway led to a rescue of ΔF508CFTR from the ERQC. Moreover, initial investigations of this pathway revealed a relationship between mainly oxidative stress, inflammation and intracellular proteostasis, providing a possible link to integrate cellular proteostasis with cellular homeostasis. The inactivation of the pathway affected the ERAD of ΔF508CFTR and partially rescued the channel function. Most importantly, a previous study has demonstrated that the MAP3K11–JNK pathway inhibitors used in the present study, namely oxozeaenol and kenpaullone, are active in the correction of conductance in primary cells from CF patients (Trzcinska-Daneluti et al. 2012), which further supports the therapeutic potential of targeting this pathway.

MAP3K11-mediated control of ΔF508CFTR proteostasis is mediated through the JNK (JNK2) arm of the pathway. Nevertheless, the knock-down of MAP3K11 leads to quantitatively more rescue than down-regulation of JNK, which suggested that other MAP3K11-activated pathways also contribute to the regulation of ΔF508CFTR proteostasis in additive or synergistic ways. The JNK pathway is known to activate the ubiquitin ligase ITCH, which controls the proteostasis of phosphorylated c-jun and thus acts as a negative feedback loop in the JNK pathway (Gallagher et al. 2006). Although ITCH does not regulate ΔF508CFTR proteostasis (Okiyoneda et al. 2010), this example provides a precedent as to how the JNK pathway might control protein degradation via the ubiquitin-proteasome pathway. The JNK pathway is also known to activate downstream transcription factors that are known to control processes relevant to proteostasis, like the HSR (HSF1) (Park and Liu 2001), and it is also known to target some proteins, like MFN2 (Leboucher et al. 2012) and BimEL (Leung et al. 2008), to proteasomal degradation by direct phosphorylation.

The depletion of downstream transcriptional regulators of the JNK pathway e.g., HSF1 and ATF1, at least partially reproduces the rescue obtained with MAP3K11 or JNK depletion, which

suggests a transcriptional programme downstream of the JNK pathway that resets the proteostatic environment of the cell. On the other hand, the swift MAP3K11-dependent effects on the levels of ΔF508CFTR observed after the treatment with ROS or inflammatory cytokines suggests a post-transcriptional regulation of proteostatic components involved in the control of ΔF508CFTR by this pathway. The MAP3K11–JNK pathway appears to control the degradation of ΔF508CFTR at the level of both the ER and the PM. Whether multiple components of the proteostatic environment are affected to achieve this regulation at two subcellular locations, or whether the same components can act at both levels, is not clear. A recent study has shown that many components of the ubiquitin-proteasome system that regulate ΔF508CFTR proteostasis at the level of the ER are also involved in the regulation of degradation of ΔF508CFTR at the level of the PM (Okiyoneda et al. 2010), which suggests that the same proteostatic regulators might be involved in both locations.

In addition, it is possible that changes in the ERAD of ΔF508CFTR allow sufficient time for ΔF508CFTR to fold (although this was not detectable in these assays here), which reduces the targeting of the protein by the PM quality control system. Which of these proteostasis machinery components are regulated by post-translational or transcriptional means by the MAP3K11–JNK pathway remains unclear. To address the corrector mechanisms of the pathway, the present study used interactome analysis of ΔF508CFTR with and without corrector (JNKi II) treatment. This analysis suggested several changes, which include a probable advancement in the folding pathway, as indicated by the increased interaction with the calreticulin/ calnexin pathway, and the reduction in the association of HOP with ΔF508CFTR. Interestingly it is already known that reduction in the levels of HOP can rescue ΔF508CFTR from the quality control (Marozkina et al. 2010). Further validation is necessary to examine the importance of other changes that were seen to either gain or lose upon the JNKi II treatment. Further investigations using microarrays and phosphoproteomics are necessary to understand the molecular targets of the MAP3K11–JNK pathway.

The MAP3K11–JNK pathway appears to be under the control of mainly ROS and inflammatory cytokines. The reduction mediated by ROS was robust compared to that of the cytokines TNF-α or TGF-β, which were transient. The role of ROS/ oxidative stress in the control of ΔF508CFTR proteostasis is interesting, as the increased inflammatory response due to the presence of neutrophils in the CF lung leads to increased ROS levels (Hull et al. 1997) that can lead

to further worsening of the phenotype, by a reduction of ΔF508CFTR levels. Both TNF-α and TGF-β act as genetic modifiers in the case of CF, and their increased levels have been correlated with the worsening of lung function (Davies et al. 2005). How the increased levels of TNF-α and TGF-β lead to a probable worsening of lung function is not clear at present. The present study suggests a role for these cytokines in maintaining the intracellular levels of ΔF508CFTR, and it provides a possible molecular link between the levels of TNF-α and TGF-β and the worsening of lung function. The ROS and inflammatory cytokines produced by the immune cells present in the inflammed lungs can be seen as activators of the pathway.

Recent studies have also shown that the CF cells in isolation continue to show a hyper-inflammatory phenotype with increased intracellular ROS (Luciani et al. 2010), which might act in a cell-autonomous way to activate this pathway, or maintain tonically active levels of the pathway. In line with this, there is the observation that a reduction in the levels of the pathway components (MAP3K11 and JNK) under steady-state conditions with no addition of exogenous cytokines or ROS can still lead to increases in the levels of ΔF508CFTR, which suggests that this pathway is tonically active in the cell. It was also shown that ROS scavenging agents, like N-acetylcysteine or cystamine, can act as correctors (Luciani et al. 2010), further validating the importance of ROS management in ΔF508CFTR proteostasis. These observations indicate that the increased inflammatory and oxidative stress phenotype caused by the absence of ΔF508CFTR further reduces the levels of ΔF508CFTR; as such a vicious cycle of inflammation, ROS and intracellular proteostasis might operate under the CF conditions. This study provides an example of where the tonically active pathway controls intracellular proteostasis in a cell autonomous way, and can be coupled or integrated with the physiology/ pathology of the organism.

MAP3K11 and JNK inhibition has been shown to be neuroprotective in neurodegenerative misfolding diseases like Alzheimer's, Parkinson's and Huntington's diseases (Borsello and Forloni 2007). The present study has established the relevance of the MAP3K11–JNK pathway for the correction of the basic folding and trafficking defects of ΔF508CFTR. Furthermore, the MAP3K11–JNK pathway might be a target in many other misfolding mutations that are subjected to ERAD, like mutants of ATP7B, ATP8B1, alpha-1-antitrypsin, and others, which is an open avenue for further exploration.

Chapter 4

The calcium/ calmodulin-dependent kinase cascade regulates ΔF508CFTR proteostasis

Introduction

Calcium calmodulin dependent kinases (CaMKs) are activated by the intracellular second messenger calcium (Ca^{2+}) and are important in processes like growth-factor and hormone signaling, cell-cycle regulation, gene expression, and apoptosis (Berridge 2001; Hook and Means 2001). Calcium functions in signalling by forming a complex with calmodulin (CaM), which serves as a ubiquitous intracellular Ca^{2+} receptor. CaM increases its affinity for a large number of CaM-binding proteins upon Ca^{2+} binding, like CaMKs (CaMKI, CaMKII, and CaMKIV). For full activation of CaMKI and CaMKIV, phosphorylation by upstream CAMKK1 or CAMKK2 (CaMKKα or CaMKKβ, respectively) is also required, which leads to the concept of a CaMK cascade like that of the MAPK cascade (Hook and Means 2001). In addition to a role in cascades, CAMKK2 is also a physiologically relevant upstream activator of AMP-activated protein kinase (AMPK) (Hawley et al. 1995), which is known to be hyperactivated in CF (Hallows et al. 2006). CaMKII is a very important regulatory kinase, but it is not a component of a CaMK cascade (Colomer and Means 2007). The CaMKII substrates are implicated in homeostatic regulation of the cell, and in neuronal function (Hudmon and Schulman 2002).

CaMKI and CaMKII are ubiquitously expressed; CAMKK2 is expressed mainly in the brain, and also at low levels in testis, spleen and lung (Racioppi and Means 2012). CAMKK2 is known to function in both autonomous and Ca^{2+}/CaM (Ca/CaM)-dependent manners, which involves a wide variety of stimuli, including LPS-mediated TLR4 activation, ghrelin-mediated Gq-coupled growth-hormone secretagogue activation (Racioppi and Means 2012), and hypoxia-mediated ROS accumulation (Mungai et al. 2011). GSK3β and CDK5 are known to control the autonomous activity of CAMKK2 by phosphorylation (Green et al. 2011). The signals along the CAMKK2 pathway are reported to control cytoskeletal remodelling, energy homeostasis (Racioppi and Means 2012), autophagy (Hoyer-Hansen et al. 2007), and inflammation (Racioppi et al. 2012).

There is evidence that the intracellular Ca^{2+} concentration ($[Ca^{2+}]_i$) is enhanced in CF cells, and that this enhanced $[Ca^{2+}]_i$ also appears to contribute to the pathology (Ribeiro 2006; Antigny et al. 2011). Calcium signalling is also postulated to influence the proteostasis network (Powers et al. 2009). Drugs inhibiting L-type Ca^{2+} channels in the PM, like diltiazem and verapamil, lead to increased transcription and translation of numerous cytoplasmic and ER chaperones that controlled the proteostasis network to enhance the folding, trafficking, and activity of lysosomal enzymes (Mu et al. 2008). Moreover, drugs that inhibit Ca^{2+} pump, including thapsigargin and curcumin, have been shown to rescue ΔF508CFTR from the ERQC (Norez et al. 2006), thus motivating further characterisation of this pathway.

Interestingly, CAMKK2 is one of the drug down-regulated genes that upon down-regulation can rescue ΔF508CFTR. Further testing of the downstream kinases of the CAMKK2 cascade (Figure 4.1a) led to the identification of other kinases that can rescue ΔF508CFTR. The CAMKK2 cascade might also control the proteostasis of ΔF508CFTR.

Results

4.1. The CAMKK2–CAMK1, CAMKK2–AMPK cascades rescue ΔF508CFTR

As mentioned earlier in the introduction downstream kinases that are activated by CAMKK2 include CAMK4, CAMK1 and AMPK. While knockdown of CAMK4 did not show any effects on ΔF508CFTR, the down-regulation of CAMK1 and AMPK led to an increase in the ΔF508CFTR band C levels that was similar to that obtained with CAMKK2. This suggested that these two arms of the CAMKK2 pathway probably regulate CFTR proteostasis (Figure 4.1b, c). Moreover, the activation of AMPK using the treatment of CFBE cells with the well-known AMPK activator 2-deoxyglucose (Wang et al. 2011) led to a drastic decrease in band B of ΔF508CFTR (Figure 4.1d). CAMKK2 is also known to function in a Ca/CaM-dependent manner (Racioppi and Means 2012), so several upstream Ca^{2+}-binding calmodulin proteins and a few Ca^{2+} channels were tested by the siRNA-based approach. Among these, CALML5 is a CaM-like Ca^{2+}-binding protein, and ITPR2 is a receptor for inositol 1,4,5-trisphosphate (a second messenger that mediates the release of $[Ca^{2+}]$), and these marginally rescued ΔF508CFTR (Figure 4.1e). It appears that calcium

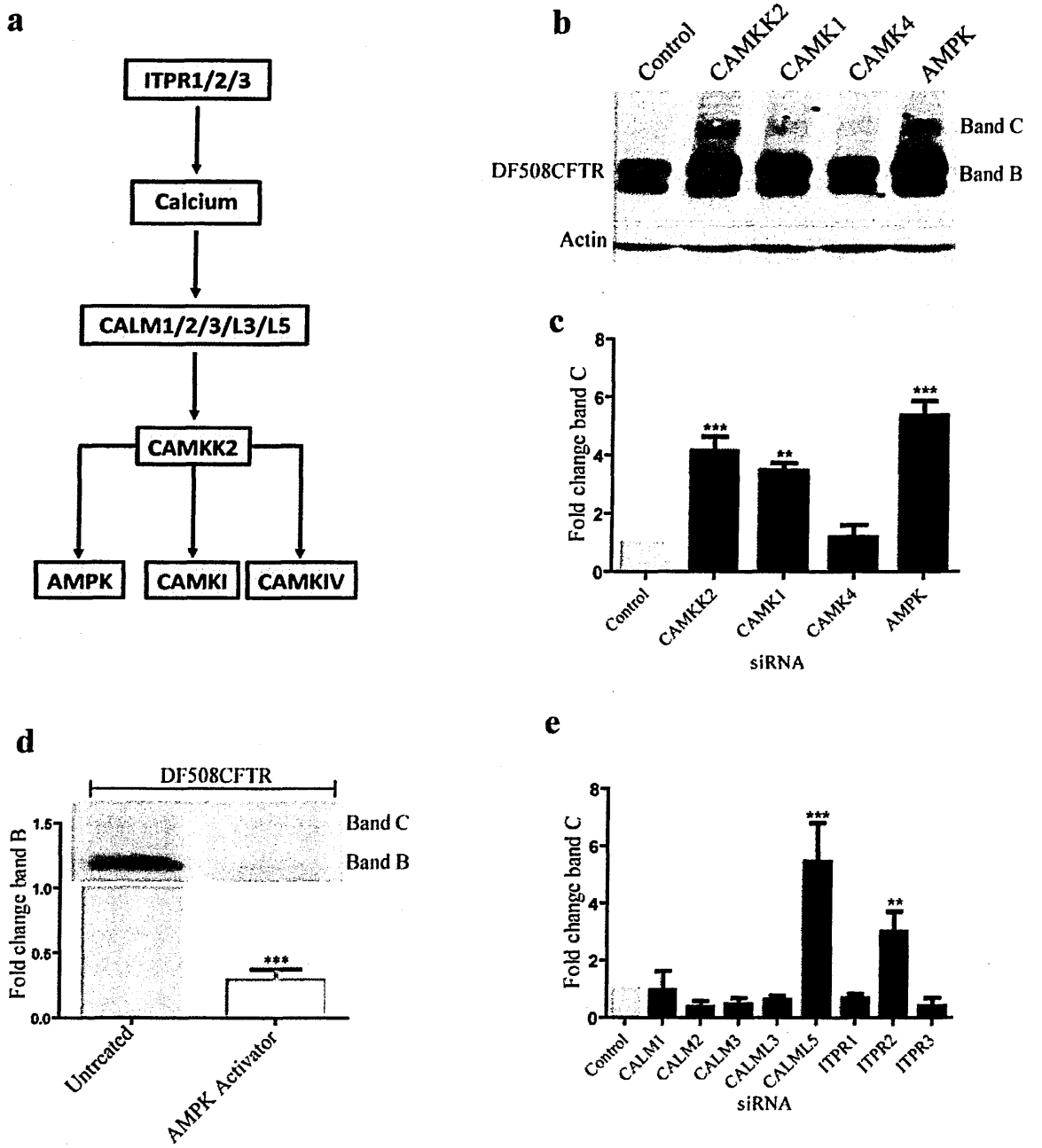

Figure 4.1. CAMKK2 cascade rescue ΔF508CFTR.

a. Model CaMKinase cascade. **b.** Representative immunoblot of the CFBE cells that were treated with siRNAs as indicated for 72 h and lysed and immunoblotted for CFTR. **c.** Fold change in band C quantified from immunoblots (n = 3) of the experiments in (a). **d.** CFBE cells were treated with AMPK activator (2-deoxyglucose 25 mM) for 3 hours, fold-change in band B quantified from immunoblots (n=3) and expressed and fold change compared to untreated, with representative immunoblot. **e.** The siRNAs targeting upstream activators of the CAMKK2 cascade were treated to CFBE cells as indicated for 72 h and fold-increases in band C were quantified from immunoblots (n = 3). Data represent mean ± SD (**P ≤ 0.01, ***P ≤ 0.001).

which is reported to be enhanced under CF conditions (Ribeiro 2006), can influence the quality control of ΔF508CFTR, and this process might be signalling dependent, with the participation of the upstream Ca^{2+}-binding CALML5 protein and the Ca^{2+}-releasing ITPR2 receptor, which confirms the role of the CaM kinase cascade in ΔF508CFTR proteostasis.

4.2. CAMKK2 and AMPK are connected to the CFTR proteostasis network

To determine the candidate downstream effectors of the CAMKK2 pathway that are involved in the control of CFTR proteostasis, bioinformatic analysis was used. The CAMKK2 pathway (Figure 4.2) components that were partially correcting the ΔF508CFTR and the CFTR proteostasis network (see table 2.5) components were combined, and the interactions between these were analysed using IPA analysis (see section 6.20). The CAMKK2 pathway signal transducer AMPK (PRKAA1 and PRKAA2) is shown to interact with several components of the ERAD machinery that is known to regulate ΔF508CFTR proteostasis, including VCP, UBE2I and HSPA4 (Figure 4.2). When the interactions between CAMKK2 and the CFTR proteostasis network were studied, it became obvious that the CAMKK2 pathway had connections with the components involved in intracellular protein degradation, the trafficking machinery.

Many ubiquitin ligases, the autophagy component (SQSTM1), the proteosomal component (PSMD11) and VCP are known to associate with AMPK, although whether they are phosphorylated by AMPK and if this phosphorylation regulates their activity in not known. One particular case, NEDD4L, is interesting, as AMPK is known to activate NEDD4L, an ubiquitin ligase that is involved in degradation of ΔF508CFTR at the post-ER level (Caohuy et al. 2009). The CAMKK2 pathway might regulate the NEDD4L which might contribute to the regulation of ΔF508CFTR proteostasis, along with the other potential modifications of protein degradation and trafficking machinery components. While for the membrane trafficking machinery, both SEC24A and AP2B1 are known to be phosphorylated by AMPK, again, the function of this modification is not known. Moreover, activation of the AMPK complex is reported to decrease the mRNA of STAT1 (Meares et al. 2013). A study has shown that STAT1 overexpression rescues ΔF508CFTR (Trzcinska-Daneluti et al. 2009). Therefore, the inhibition of AMPK might promote STAT1 activity, and this in turn might affect the proteostasis of ΔF508CFTR.

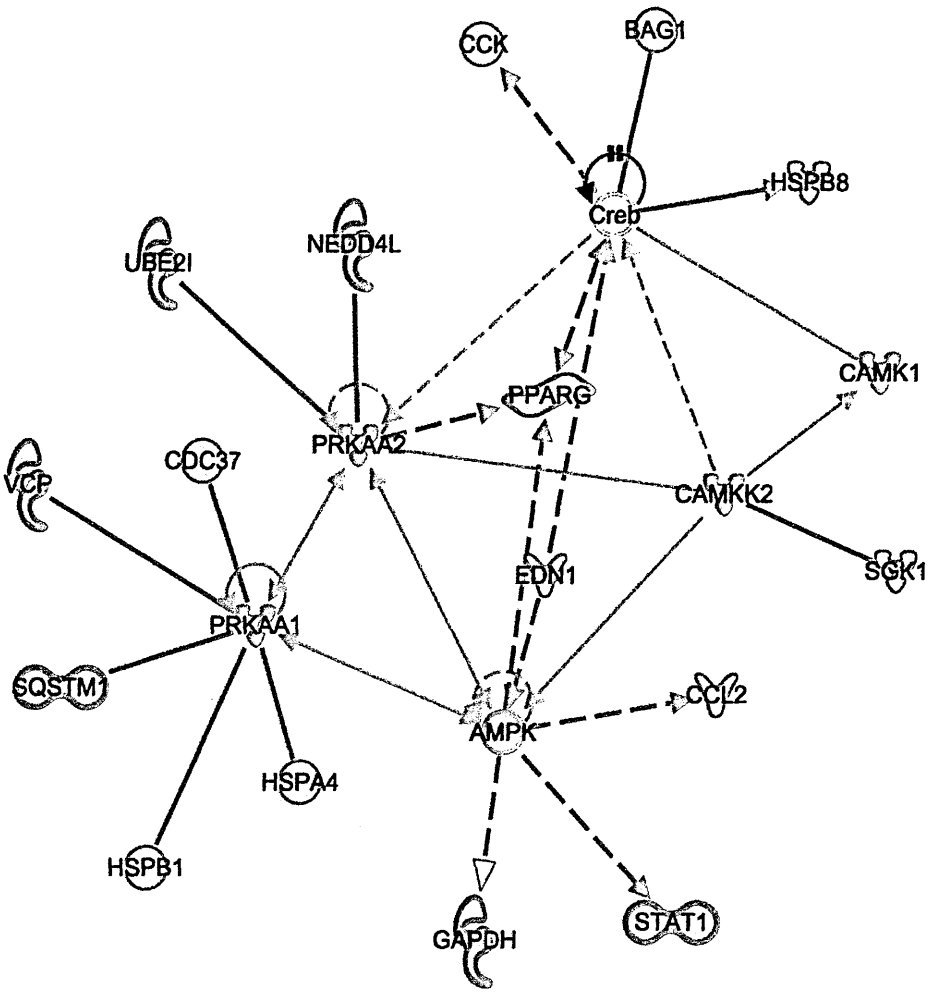

Figure 4.2. CAMKK2 and AMPK interact with the CFTR proteostasis network.

CAMKK2 cascade molecules (green) interact with known CFTR proteostasis network genes (grey), as predicted by the IPA analysis. (PRKAA1= AMPKa1, PRKAA2=AMPKa2 are catalytic subunits of AMPK)

Discussion

The present study reveals a role of the CaM kinase cascade dependent on CAMKK2 in rescuing ΔF508CFTR, through its CAMK1 and AMPK arms. Although CAMKK2 was the only kinase found in the commonly regulated genes, other CAMKK2 pathway components were inferred from the literature survey. Down-regulation of each of these genes showed that few of the downstream and upstream molecules of this pathway are also involved in the correction of ΔF508CFTR. This strategy potentially identified the other relevant genes of the same pathway, irrespective of whether or not they are modulated by the drugs.

Although the presence of ΔF508CFTR leads to increased intracellular calcium (Ribeiro 2006), it is not known whether Ca^{2+}-dependent signalling is hyperactivated in the ΔF508CFTR cells compared to wtCFTR. The $[Ca^{2+}]_i$ is known to be directly linked with the activity of Ca^{2+}-sensitive kinases. CAMKK2 (Hoyer-Hansen et al. 2007), and AMPK (Kroemer et al. 2010) will be activated by the abnormal $[Ca^{2+}]_i$ under stressed conditions, and these upstream sensors will immediately transmit the signals to downstream substrates for the adjustment of cellular metabolism in the new microenvironment. Furthermore, the CaM kinase cascade can also be activated by signalling through G_q-coupled receptors, inositol 1,4,5-trisphosphate-mediated release of Ca^{2+} via activation of the IP_3 receptor, and Ca^{2+} entry into cells via PM ion channels, and also by Toll-like receptors (Racioppi and Means 2012) and ROS (Mungai et al. 2011). Thus CAMKK2 might act as a signalling hub that can receive and decode signals transmitted by means of many diverse cellular regulatory pathways.

Therefore, higher levels of calcium might act as physiological activator of the CaM kinase cascade and maintain it at a tonically active state, to contribute to ΔF508CFTR proteostasis. Moreover, it is documented that ΔF508CFTR-mutant primary CF cells have higher AMPK activity (Hallows et al. 2006) , which suggests that the ΔF508CFTR condition might indeed have an active CaM kinase cascade. The siRNA-based knock-down of the members of this CaM kinase cascade, namely CAMKK2, AMPK and CAMKI, led to higher levels of band B, which indicates that there might be a compromise in the ERAD of ΔF508CFTR. However, whether up-regulation of this pathway enhances ERAD or ERQC was not explored, except that AMPK activation by drug led to

increased clearance of ΔF508CFTR. Another interesting point to be noted is that AMPK is also known to be activated by VEGF via CAMKK2 (Stahmann et al. 2010), VEGF is also reported to be over-produced under CF conditions (Martin et al. 2013). It is important to note that depletion of the VEGF receptor VEGFR2/ kinase insert domain receptor was found as one of the correctors in the present study (see section 2.6), which indicates further that the CaM kinase cascade might be physiologically important for ΔF508CFTR proteostasis. As AMPK phosphorylates the R domain on CFTR (King et al. 2009), which decreases its open probability, so another benefit of targeting AMPK or the CAMKK2 pathway might be that there will be an increase in the channel open probability.

There were interactions predicted between CAMKK2, AMPK and the known CFTR proteostasis network genes. Whether AMPK phosphorylates these components and modulates their activities is not known. While it is known that VCP is involved in the extraction of proteins from the ER for degradation and it is phosphorylated by the p38 MAPK pathway, and that this phosphorylation can regulate its activity, whether it is also phosphorylated by AMPK and if this phosphorylation can regulate its activity is not known. A recent study in *C. elegans* showed that increased $[Ca^{2+}]_i$ increased the activation of a known proteostasis regulator, HSF1, which is dependent on Ca^{2+}-dependent kinases (Silva et al. 2013). This indicates that the CaM kinase cascade might indeed be relevant in proteostasis. Moreover, the PM L-type calcium channel blockers diltiazem and verapamil helped the trafficking of N370S and L444P mutant glucocerebrosidase. Although the mechanism is not clear, these L-type calcium channel blockers diltiazem and verapamil led to increases in the expression of several chaperones (Mu et al. 2008), again indicating the ability of calcium-dependent signalling processes in the regulation of proteostasis. The ER calcium channel, SERCA, inhibitor thapsigargin has already been shown to correct ΔF508CFTR (Egan et al. 2002), but whether thapsigargin has any effect on the CaM kinase cascade is not clear. The CAMKK2 inhibitor STO609 (Tokumitsu et al. 2003) was tested, but it did not have any effects on ΔF508CFTR, probably because of the non-specific effects of STO609. Furthermore, the mechanistic insight into how this depletion of the CAMKK2-dependent CaM kinase cascade rescues ΔF508CFTR and influences its proteostasis and its physiological relevance is the topic for further investigation.

Chapter 5

General discussion

5.1. Meta-analysis method potentially identified novel links to ΔF508CFTR proteostasis.

The present study used meta-analysis/ fuzzy intersection analysis of gene expression to initially define the mode of action that is common to different corrector drugs for the correction of ΔF508CFTR. This thus focussed on the commonly regulated genes/ networks/ pathways that are important for the proteostasis and rescue of ΔF508CFTR. The gene expression data for many of the corrector drugs was obtained from the public Connectivity Map database (cMap; http://www.broadinstitute.org/ cmap/). Indeed, the biomedical field has been greatly influenced by the availability of various '-omics' technologies more recently. Moreover, public data repositories and databases like Gene Expression Omnibus (GEO; http://www.ncbi.nlm.nih.gov/geo/) and the Library of Integrated Network-based Cellular Signatures (LINCS; http://lincs.hms.harvard.edu/db/) now provide almost overwhelming datasets for many given drugs, physiological states, and disease conditions. These datasets can help to solve new hypotheses and might improve our overall biological understanding. Using these repositories, many meta-analyses has been carried out previously to identify common transcriptional effects of neoplastic transformation and progression (Rhodes et al. 2004), and the commonly dysregulated genes in pancreatic cancer (Grutzmann et al. 2005).

Although there are many instances where gene-expression meta-analyses have been used to understand the mechanisms in the context of disease, there have been very few examples of meta-analyses of the gene expression profiles that are promoted by many drugs, to reveal mechanisms that are common among these drugs. The present study is one such investigation, designed to dissect out the mechanisms of action that are common to many corrector drugs through an analysis of gene expression. More recently, an investigation into the mechanisms of action using gene expression among several anticancer drugs that are translation inhibitors revealed the commonly regulated HSF1 target (Santagata et al. 2013). Although this method allows the inclusion of pathways that are also not modulated by all of the drugs, there remains a high probability of

missing pathways that are common to a very few drugs, or those that are unique to individual drugs, which does not exclude the presence of other correction-relevant genes/ pathways/ networks that are particular to an individual drug. An alternative method might be useful for this purpose, where each drug is analysed individually for correction-relevant genes/ pathways/ networks. However, the currently used method of meta-analysis of microarray drugs followed by bio-informatic analysis has confirmed the potential to identify novel links to ΔF508CFTR proteostasis. Otherwise it would have been hard to arrive at the common mechanisms targeted by the many corrector drugs and link them to proteostasis by using more conventional hypothesis-driven studies. From the basic science perspective, although there is now a substantial body of data on the biophysics and cellular mechanisms of CFTR folding and ΔF508CFTR misfolding *in vitro,* there remain major gaps in our knowledge of how critical components of the quality control machinery recognize the folding defect in tissues (Lukacs and Verkman 2012). The present study employed a new strategy to shed lights on this gap and discovered several novel components that affect the quality control of ΔF508CFTR. This discovery may help to identify correctors with improved potency and efficacy.

The approach (Figure 5a) used in the present study returned several pathways/ molecules (Figure 5b) that are interesting from a therapeutic point of view (with many also being 'druggable'). A previous kinase inhibitor screening (Trzcinska-Daneluti et al. 2012) identified several hits that can correct ΔF508CFTR, and many of these drugs might target the genes that have been shown to rescue ΔF508CFTR in the present study. This evidence strongly supports the strength of the approach used in the present study. The present meta-analysis approach might be more efficient than small-molecule screening approaches for the identification of candidates for therapy. These corrector genes identified in the present study (Figure 5b) also emphasizes the further studies that seek to better understand the individual contribution of these proteins in CFTR folding.

The depletion of PIK3CB, PIK3CG, PDGFRA, PDGFRB, VEGFR2/KDR and VEGFR1/FLT1 were successful in correcting the basic ΔF508CFTR (section 2.6), and interestingly, inhibitors that can target these molecules have been identified also as rescuing ΔF508CFTR in a more cystic-fibrosis-relevant model: primary human bronchial epithelial cells

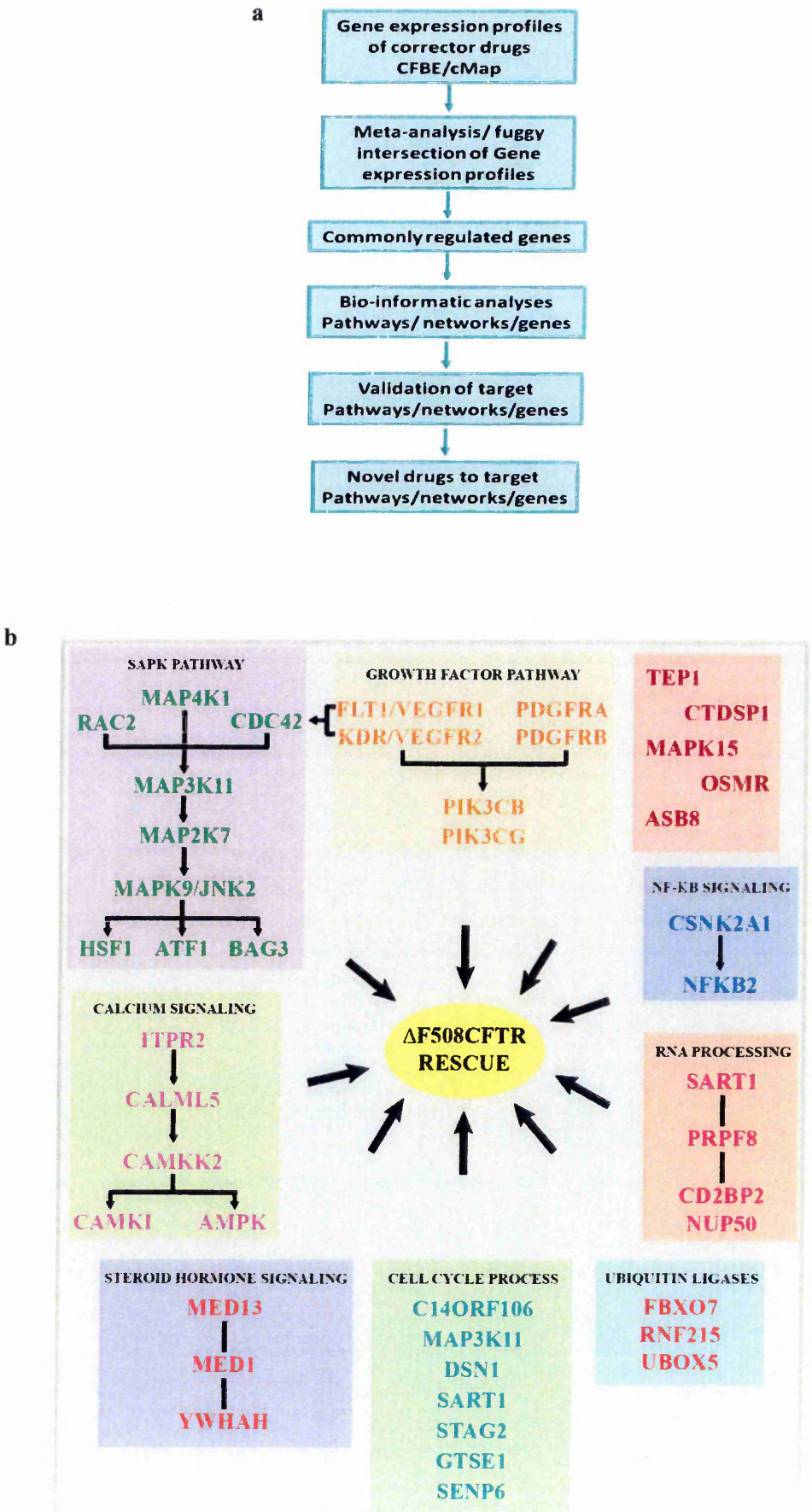

Figure 5.1. Strategy of meta-analysis yielded corrector pathways/ networks/ genes.

a. Flow diagram of the meta-analysis strategy. **b.** Pathways/networks that rescue ΔF508CFTR.

affected by cystic fibrosis (Trzcinska-Daneluti et al. 2012). There is an immediate need to test the battery of available inhibitors of the corrector genes, which might lead to the identification of many novel and efficient therapeutic candidate drugs.

5.2. The MAP3K11–JNK pathway is a new target to develop therapeutics for cystic fibrosis.

The hypothesis driven approaches led to the discovery of many molecules, such as PDE5 inhibitors (e.g. sildenafil) (Dormer et al. 2005), alpha-glucosidase inhibitors (e.g. miglustat) (Norez et al, 2006) and histone deacetylase inhibitors (e.g. SAHA) (Hutt et al, 2010), small molecule screening approaches led to the discovery of aminoarylthiazoles, quinazolinylaminopyrimidinones, bisaminomethylbithiazoles class chemical molecules (e.g. Corr-4a) (Pedemonte et al, 2005), quinazolines (e.g. VRT-325) (Loo et al, 2005), the sildenafil analogues like KM11060 (Robert et al, 2008), galfenine (Robert et al, 2010), chlorzoxazone (Carlile et al. 2007) and up to date the most potent corrector VX-809 (Van Goor et al, 2011), and CFTR model based virtual computational screening approaches has led to the discovery many more ΔF508CFTR correctors (Kalid et al. 2010; Odolczyk et al. 2013). After all these efforts there is no available efficient corrector for the ΔF508CFTR defect. The accumulating information on ΔF508CFTR indicate that it may not be possible to fully correct the trafficking defect with a single compound (Pedemonte and Galietta 2012). Several *in vitro* studies point out that a large rescue may be obtained only with a combination of correctors. More effective correctors may be identified by high-throughput screening of compounds with novel and unexplored structure, by exploiting the increasing information available on CFTR structure, or by taking advantage of the identification of important proteins of the CFTR interactome. In this respect, discovering the proteins with a high relevance for ΔF508CFTR quality control/ proteostasis has been highlighted (Pedemonte and Galietta 2012). The present study gives an example where the discovery of proteins that control the proteostasis has led to discovery of novel correctors drugs for ΔF508CFTR defect. The present study also opens a venue to try many more drugs that target the druggable proteins like PI3KCB/G, PDGFRA/B, KDR, FLT etc. which were potent ΔF508CFTR correctors.

Moreover, the MAP3K11–JNK cascade and the CAMKK2 cascade are also involved in proteostasis and rescue of ΔF508CFTR (section 3.1, section 4.1). There is evidence that these

cascades might be activated during the cystic fibrosis condition. In cystic fibrosis, reports have indicated increased p38 activity (a downstream target of MAP3K11) (Berube et al. 2010), increased Ca^{2+} levels (upstream of CAMKK2) (Ribeiro 2006), and hyperactivity of AMPK (downstream of CAMKK2) (Hallows et al. 2006). Inhibitors of JNK, and also oxozeaenol, which can reduce JNK activity (Ninomiya-Tsuji et al. 2003), can rescue ΔF508CFTR. In a clinical trial for cancer, oxozeaenol was also seen to correct ΔF508CFTR (Trzcinska-Daneluti et al. 2012). The present study provides the observation that ROS and cytokines can influence intracellular proteostasis of ΔF508CFTR (section 3.6). It will be interesting to test further whether the cystic fibrosis condition, which is known to involve high Ca^{2+} levels, has a hyperactive CAMKK2 cascade, which might influence proteostasis of ΔF508CFTR. The CAMKK2 cascade can also be targeted in the future using the many inhibitors that are available.

5.3. Increase in efficiency of ΔF508CFTR rescue by combination of correctors.

The development of correctors of the ΔF508CFTR defect has been hampered by an apparent upper limit of improvement (5%-10%), which is probably caused by the multiplicity of the steps/ factors involved in the folding/ trafficking of ΔF508CFTR. Recent studies have shown that simultaneously targeting multiple steps in the folding pathway of ΔF508CFTR can help to overcome this apparent limit (Okiyoneda et al. 2013). Okiyoneda et al. (2013) argued that to have ΔF508CFTR levels comparable to those of wt-CFTR, it is necessary to restore the inter-domain interactions. Ideally, any ΔF508CFTR corrector should enhance ΔF508CFTR folding and traficking from the ER, stablise it at the plasma membrane, and decrease the gating problem (increase the channel opening and closing capacity). This might be achieved by a combination of three classes of corrector compounds: class I, which target NBD1-MSD2 (VX-809); class II, which target NBD2 (corr-4a); and class III, which restore the energy defect (glycerol). Corr-4a is very toxic and therapeutically inapplicable. The concept of drug combination in CF (e.g., a corrector plus a potentiator) is already accepted (Pedemonte and Galietta 2012). So the search for compounds of class II and class III is still a need. Further efforts of screenings either of chemical libraries or CFTR model based computational are warranted to identify the highly efficient molecules under each class. Novel hypothesis driven approaches can also aid in this quest of new class of compounds.

While the studies of Okiyoneda et al. (2013) mainly focused on the use of pharmaceutical chaperones that bind and promote folding of ΔF508CFTR, here, in the present study, I targeted the modulation of the proteostatic machinery. This will not only allow ΔF508CFTR to overcome ER quality control, but also to stabilise the plasma membrane pool. The present observation of the different targets of the MAP3K11-JNK pathway and VX-809 along the ΔF508CFTR folding pathway, suggests that their therapeutic potential is complementary. The correction or rescue effects of the JNK inhibitor oxozeaenol in combination with VX-809 are highly synergistic in biochemical assays (section 3.7). Although the same synergistic effects must be tested further at the level of chloride conductance, this observation highlights a new strategy that can be used in combination with the above-mentioned classes of correctors. Whether this new strategy will lead to better inter-domain interactions and decrease the energetic defect has yet to be determined. The observations from the present study reveal many molecular targets, and it is now necessary to test molecules that target the corrector genes described in the present study, for the development of new therapies for cystic fibrosis caused by the ΔF508 mutation.

Chapter 6

Materials and methods

Materials

VX-809 was from Selleckchem (Houston, USA), oxozeaenol, and kenpaullone were from Tocris Bioscience (Bristol, UK). Puromycin, anti-CFTR M3A7 mouse monoclonal antibody, HRP-conjugated anti-mouse, anti-rabbit and anti-rat IgG antibodies, Luminata Crescendo Western HRP substrate, and PVDF membranes for protein blotting were from Merck Millipore (Massachusetts, USA). Nitrocellulose membranes for protein blotting were from Perkin Elmer (Massachusetts, USA). BCA protein estimation kits, SuperSignal West Femto Chemiluminescent Substrate, X-ray films, and coverslips for 24 well plates were from Thermo scientific (Waltham, USA). CellROX® Green, Lipofectamine 2000, Opti-MEM Glutamax, MEM, DMEM, MEM-NEAA 100×, G418, DPBS-10×, dithiothreitol, florescent tagged anti-mouse, anti-rabbit, and anti-rat IgG, Dynabeads protein A, G, and foetal bovine serum (FBS) were from Life Technologies (California, USA). The siRNAs used along with the provider are listed in Table 6.3. Glutamine 100×, penicillin/ streptomycin 100× and FBS were from Euroclone SPA (Milano Italy). Trypsin 10× for cell culture was from Biochrom (Cambridge USA). Protease inhibitor cocktails and phosphatase inhibitor (PhosSTOP) were from Roche (Basal Switzerland). Anti-JNK, anti-phosphoJNK, anti-cJUN, anti-phosphocJUN, anti-MAP3K11, and anti-ubiquitin antibodies were from Cell Signaling Technology (Danvers, Massachusetts, USA). The mouse anti-HA antibody was from Covance (Princeton, New Jersey, USA). Anti-Hsp70, anti-Hsp90, anti-Hop, and anti-Hsp40 antibodies were from Enzo Lifescienes (Farmingdale, NY, USA). The rabbit anti-Derlin1 antibody was from Abcam (Cambridge, UK). The mouse anti-hCFTR antibody clone 24.1 was from R&D Systems (Minnneapolis, USA). The rat anti-CFTR was kindly provided by CFTR Folding Consortium. Plasmid constructs containing mouse JNK2 (MKK7B2Jnk2a2-Plasmid #19727), MKK7 (Plasmid #14622) and GFP-Ub (GFP-ubiquitin) (Plasmid #11928) were from Addgene (Cambridge USA). The ZsProSensor-1 proteasome sensor was from Clontech (California, USA). The plasmid for temperature-sensitive VSVG tagged with GFP (VSVG-GFP) was a kind gift from Dr. Jennifer

Lippincott-Schwartz, NICHD, NIH, Bethesda, USA. The CDC42 plasmid was from A. Hall, Sloan-Kettering Institute, New York, NY, USA. The plasmid containing P-glycoprotein wt and the G268V and DY490 mutants were a kind gift from Dr. David M. Clarke, University of Toronto, Canada. hERG wt and the G601S mutant plasmids were a kind gift from Dr. Alvin Shrier, McGill University Life Sciences Complex, Montreal, Quebec, Canada. HiSpeed Plasmid Maxi kits for Plasmid DNA preparation, RNeasy Mini kits for RNA isolation, and QuantiTect Reverse Transcription kits were from Qiagen (Hilden, Germany). Anti-CFTR rat monoclonal (3G11) antibody was kindly provided by CFTR Folding Consortium, USA. Anti-α-actin, anti-α-tubulin antibodies, cell culture plastics, and all the other chemicals where purchased from Sigma Aldrich (St. Louis, USA). HeLa cells expressing HA-tagged wtCFTR and ΔF508CFTR (Okiyoneda et al. 2010) were a gift from Dr Gergely L. Lukacs, McGill University, Montreal, Quebec, H3G 1Y6, Canada. CFBE41o$^-$ cells expressing untagged wtCFTR and ΔF508CFTR (Bebok et al. 2005) (referred to as CFBE cells here) were a gift from Dr. J. P. Clancy, Gregory Fleming James Cystic Fibrosis Research Center, Birmingham, AL, USA. CFBE41o$^-$ cells expressing halide sensitive YFP (CFBE-YFP) were a kind gift from Dr. Luis Galietta, Istituto Giannina Gaslini, Italy.

Methods

6.1. Cell culture

All of the cells were grown in 95% air and 5% CO_2, and at 37 °C. The CFBE cells were cultured in MEM supplemented with 10% FBS, MEM NEAA, penicillin/ streptomycin, glutamine and 2 μg/ml puromycin. They were routinely grown on culture plates and flasks coated for 30 mins with a coating prepared as follows: 10 μg/ml fibronectin adhesion-promoting peptide (Sigma-Aldrich), 100 μg/ml albumin from bovine serum (Sigma-Aldrich), and 30 μg/ml bovine collagen type I ((BD Transduction Laboratories) dissolved in MEM (Lei et al. 1996). CFBE-YFP cells were cultured in the same medium as the CFBE cells, but supplemented with 50 μg/ml G418. HeLa cells expressing wtCFTR and ΔF508CFTR were cultured in DMEM supplemented with 10% FBS, penicillin/ streptomycin, glutamine and 1 μg/ml puromycin.

6.2. Plasmid preparation

Single colonies of bacteria transformed with the plasmid of interest or stored as a glycerol stock were inoculated into 2 ml LB containing the appropriate selective antibiotic(s), and grown at 37 °C under continuous shaking (200 rpm) for 6-8 h. This preculture was used to inoculate 200 ml LB containing the selective antibiotic(s) and grown overnight at 37 °C with continuous shaking. Then bacteria were collected by centrifugation at 4,000× *g* for 15 min at 4 °C, and processed using HiSpeed Plasmid Maxi kits, according to the manufacturer protocol. The plasmid DNA obtained was resuspended in Tris-EDTA (Ethylenediaminetetraacetic acid) (TE) buffer (10 mM Tris-HCl pH 8.0 and 1 mM EDTA) and stored at -20 °C.

6.3. Transfection of the siRNA and cDNA plasmids

The siRNAs used in the present study are listed in the table 6.3a. The silencer select siRNAs from Life Technologies were used at 20 nM, Sigma Aldrich and Qiagen siRNAs were used at 50 nM. For siRNA-mediated knock-down in CFBE cells, about 80,000 to 90,000 cells were plated in 12-well plates, and after 12 h they were transfected with the siRNAs using Lipofectamine 2000, according to the manufacturer protocol. The transfection mix was added to the cells in serum-free medium, i.e., opti-MEM, and 12 h after the transfection, the opti-MEM was replaced by normal CFBE cell medium.

For HeLa cells expressing ΔF508CFTR, about 35,000 to 40,000 cells were plated in 12-well plates, and after 12 h the cells were transfected with the Sigma siRNA at 50 nM, using Lipofectamine 2000, according to the manufacturer's protocol. The transfection mix was added to the cells in antibiotic-free medium, and after 12 h of transfection the medium was replaced by normal antibiotic-containing medium. The siRNA treatments were for 72 h, before processing the cells for analysis. The efficiency of depletion of only ΔF508CFTR corrector genes were determined by qRT-PCR (see section 6.21) of total RNAs isolated from ΔF508CFTR expressing CFBE cells (Figure 6.3). The primers used for the qRT-PCR is listed in table 6.3b.

For plasmid DNA expression, approximately 150,000 CFBE cells expressing ΔF508CFTR were plated in 12-well plates, and 12 h after plating they were transfected with 2 μg DNA, using the Lipofectamine 2000, according to the manufacturer's protocol.

Table 6.3a. The siRNAs used in the study.

Silencer select siRNA from Life Technologies (USA)

Gene Symbol	Sense siRNA Sequence 1	Sense siRNA Sequence 2	Sense siRNA Sequence 3
AKAP1	UCAACAUCAUGUAGACAAAtt	UCAACAUCAUGUAGACAAAtt	GGUGUACUAUUCUCCAGCAtt
AKAP8	GCAGUACAGUGAAUGCCGAtt	GCAGUACAGUGAAUGCCGAtt	CGGAAGCAGUUCCAACUUUtt
AKT1	GCGUGACCAUGAACGAGUUtt	GCGUGACCAUGAACGAGUUtt	GAACAAUCCGAUUCACGUAtt
AKT2	CAACUUCUCCGUAGCAGAAtt	CAACUUCUCCGUAGCAGAAtt	CGGGCUAAAGUGACCAUGAtt
AKT3	GUAACAUCUGAGACAGAUAtt	GUAACAUCUGAGACAGAUAtt	GGACUAUCUACAUUCCGGAtt
ALPK1	CCAUGAGCAAGAACGAUUAtt	CCAUGAGCAAGAACGAUUAtt	GGAAGUGAAUUAUCACGUUtt
ASB8	CUUCCCACAUGAUAAUGUAtt	CUUCCCACAUGAUAAUGUAtt	GGAUUACAACAAUGAUACAtt
BIN2	GGUCUCUCCUAAUCCAGAAtt	GGUCUCUCCUAAUCCAGAAtt	GAUGAACGAUUUGAACAAAtt
C14orf106	GGAUCUGAUAAGACAAAUAtt	GGAUCUGAUAAGACAAAUAtt	GGAUAUCCAAAUUAUCUCAtt
CALM1	AGGCAUUCCGAGUCUUUGAtt	AGGCAUUCCGAGUCUUUGAtt	UGACAAACUUAGGAGAAAAtt
CALM2	AAAGGAAUUGGGAACUGUAtt	AAAGGAAUUGGGAACUGUAtt	GCACAAUUGACUUCCCUGAtt
CALM3	AGAUGAUCAGGGAGGCUGAtt	AGAUGAUCAGGGAGGCUGAtt	GACUUCCCGGAGUUCCUGAtt
CALML3	GAGCUGACCUUAGGACCGAtt	GAGCUGACCUUAGGACCGAtt	GCUGUAACCUGUUCCUAUUtt
CALML5	GCCCAGCUAAGGAAACUCAtt	GCCCAGCUAAGGAAACUCAtt	CGGUUGACACGGAUGGAAAtt
CALML6	UAAUGGGAGUUUACCAUGAtt	UAAUGGGAGUUUACCAUGAtt	CCACCCUGCAGAAUCCUGUtt
CAMKK2	GGCACAUCAAGAUCGCUGAtt	GGCACAUCAAGAUCGCUGAtt	GCAUCGAGUACUUACACUAtt
CD2BP2	GAAUAUAAGUGGGAGAACAtt	GAAUAUAAGUGGGAGAACAtt	ACUACUUCCUGAACCGGGAtt
CENPA	GACUUUAGUUUGUGAGUUAtt	GACUUUAGUUUGUGAGUUAtt	UCAUAGAAGAUGUAUCAUAtt
CENPE	GGUUGACUCAGAUACUACAtt	GGUUGACUCAGAUACUACAtt	GGCUGUAAUAUAAAUCGAAtt
CSNK2A1	GGCUCGAAUGGGUUCAUCUtt	GGCUCGAAUGGGUUCAUCUtt	AGAUGUACGAUUAUAGUUUtt
CSNK2A2	GGAGUACAAUGUUCGUGUAtt	GGAGUACAAUGUUCGUGUAtt	GAUCCACACUUCAACGAUAtt
CSNK2B	AGAGUGACCUGAUUGAGCAtt	AGAGUGACCUGAUUGAGCAtt	GGCUCUACGGUUUCAAGAUtt
CTDSP1	GCCCAGGACUCAGACAAGAtt	GCCCAGGACUCAGACAAGAtt	CGGACUUCAUCAUCCCUGUtt
CYC1	CAGCUACCAUGUCCCAGAUtt	CAGCUACCAUGUCCCAGAUtt	GGGAAGCUGUUCGACUAUUtt
CYCS	AGUACAUCCCUGGAACAAAtt	AGUACAUCCCUGGAACAAAtt	UGAUCUUUGUCGGCAUUAAtt
DCLK1	CGAUAUAAAGUCGGAAGAAtt	CGAUAUAAAGUCGGAAGAAtt	GAUCGACUGCUAGAGAGUAtt
DGCR8	CCCUGUCUAUAAUUUCUUUtt	CCCUGUCUAUAAUUUCUUUtt	GGAUCAUGACAUUCCAUAAtt
DHX38	GAAGGAAUUUCAUUUGACAtt	GAAGGAAUUUCAUUUGACAtt	CGAUUCUGGUUAUUGCAAAtt
DICER1	GAUCCUAUGUUCAAUCUAAtt	GAUCCUAUGUUCAAUCUAAtt	CAGCAUACUUUAUCGCCUUtt
DNAJC2	GAACCAAGAUCAUUAUGCAtt	GAACCAAGAUCAUUAUGCAtt	CGAUUUGAAGGUCCAUAUAtt
DSN1	GGUGAUGGAUGAACUGCAAtt	GGUGAUGGAUGAACUGCAAtt	GUCUAUCAGUGUCGAUUUAtt
EHD1	AGAUCUACCAGAAGAUUGAtt	AGAUCUACCAGAAGAUUGAtt	AGACCACCUUCAUCCGACAtt
ELAVL1	ACUUAUUCGGGAUAAAGUAtt	ACUUAUUCGGGAUAAAGUAtt	UGAACUACGUGACCGCGAAtt
ERBB4	CCCUUUUGUUUCUCGGAGAtt	CCCUUUUGUUUCUCGGAGAtt	CCCUUACAAUGCAAUUGAAtt
EXOSC4	GGGCCCUAGUGAACUGUCAtt	GGGCCCUAGUGAACUGUCAtt	GGCAGAUGGUGGGACCUAUtt

Table 6.3a. The siRNAs used in the study (continued).

Silencer select siRNA from Life Technologies (USA)

Gene Symbol	Sense siRNA Sequence 1	Sense siRNA Sequence 2	Sense siRNA Sequence 3
FARSA	CCUUCACUCCGGUCAAGUAtt	CCUUCACUCCGGUCAAGUAtt	CGGAAAAACCUACUGCGAAtt
FBXO7	GAAUGACGACAGUAUGUUAtt	GAAUGACGACAGUAUGUUAtt	GGCUUUUACCCGACAAGCAtt
FGFBP1	CAAUUGGACCAUGAAUUUUtt	CAAUUGGACCAUGAAUUUUtt	GGAAACAAGUUGCCCGGAAtt
FLNB	GCACGGUCACUGUUAGAUAtt	GCACGGUCACUGUUAGAUAtt	GAUCGUGUGAUGUCAAAUAtt
FLT1	GGUGAGUAAGGAAAGCGAAtt	GGUGAGUAAGGAAAGCGAAtt	CCCUGAUGGAAAACGCAUAtt
FLT4	CCAGCAUCCUGACCAUCCAtt	CCAGCAUCCUGACCAUCCAtt	CGAGGUCAUUGUGCAUGAAtt
GEMIN4	CGUUGACACUUCUGCCGAAtt	CGUUGACACUUCUGCCGAAtt	CGGUGCCUCUCUUUGGAUAtt
GTSE1	GGAAUUAAAUAAUCCGGUUtt	GGAAUUAAAUAAUCCGGUUtt	CGGCCUCUGUCAAACAUCAtt
HNF4A	UGAGUAUGCCUACCUCAAAtt	UGAGUAUGCCUACCUCAAAtt	UCAUCUUCUUUGACCCAGAtt
ITPR1	GGUCAACCGUUACUAUGGAtt	GGUCAACCGUUACUAUGGAtt	GCACGACAGUGAAAACGCAtt
ITPR2	GCUUAAUCCUGAUUAUCGAtt	GCUUAAUCCUGAUUAUCGAtt	GGUGUCUAAUCAAGACGUAtt
ITPR3	GCAUCGUCACUGUCAUGAAtt	GCAUCGUCACUGUCAUGAAtt	CCACCUUGCAGAAAACCGAtt
IVL	CCAUCAAAGCAAGAGGAAAtt	CCAUCAAAGCAAGAGGAAAtt	CAGCAGGACGGACAACUAAtt
KDR	CAUGUUCUCUAAUAGCACAtt	CAUGUUCUCUAAUAGCACAtt	CCAUCGUCAUGGAUCCAGAtt
KIF20A	GGAACAUAGUCUUCAGGUAtt	GGAACAUAGUCUUCAGGUAtt	CGGCUAUGCGAGGAUCAAAtt
KRT34	GCAUACGCAGGAUCCUGGAtt	GCAUACGCAGGAUCCUGGAtt	CUUACCUGCUUUUCCAUUAtt
LMNB1	GGACUUGGAGUUUCGCAAAtt	GGACUUGGAGUUUCGCAAAtt	GAAUCGUUGUCAGAGCCUUtt
MAL	CUGUUGGUAUUGUCCACAAtt	CUGUUGGUAUUGUCCACAAtt	GGUCCAUGGUGGAAGACGAtt
MAP2K1	GGAACCAGAUCAUAAGGGAtt	GGAACCAGAUCAUAAGGGAtt	UGUUCAGUCUGGAAUUUCAtt
MAP2K2	GAUCAGCAUUUGCAUGGAAtt	GAUCAGCAUUUGCAUGGAAtt	GAACUUGACGAGCAGCAGAtt
MAP2K3	GGUCGACUGUUUCUACACUtt	GGUCGACUGUUUCUACACUtt	CCCGGACCUUCAUCACCAUtt
MAP2K4	GCAACUGUGAAAGCACUAAtt	GCAACUGUGAAAGCACUAAtt	GGUAAACGCAAAGCACUGAtt
MAP2K5	GCCCUCCAAUAUGCUAGUAtt	GCCCUCCAAUAUGCUAGUAtt	GUAAUGGAACAGCAAGUAAtt
MAP2K6	GGAUACAUCACUAGAUAAAtt	GGAUACAUCACUAGAUAAAtt	GGUGGACUCUGUUGCUAAAtt
MAP2K7	CGUCAUUGCCGUUAAGCAAtt	CGUCAUUGCCGUUAAGCAAtt	GACAGUUUCCCUACAAGAAtt
MAP3K11	CGUGAUCUCAAGUCCAACAtt	CGUGAUCUCAAGUCCAACAtt	GCGUAGCUGUUAACAAGCUtt
MAPK1	CAGGGUUCCUGACAGAAUAtt	CAGGGUUCCUGACAGAAUAtt	CAACCAUCGAGCAAAUGAAtt
MAPK15	AGAACGACAGGGACAUUUAtt	AGAACGACAGGGACAUUUAtt	UGAACGCAGUCAUCCGGAAtt
MAPK3	GGACCGGAUGUUAACCUUUtt	GGACCGGAUGUUAACCUUUtt	UGAUGGAGACUGACCUGUAtt
MAPK6	CCAUCCUUACAUGAGCAUAtt	CCAUCCUUACAUGAGCAUAtt	CUAGGUAUAUGGACUUAAAtt
MAPK7	GCUGAACAUCAGUACUUCAtt	GCUGAACAUCAGUACUUCAtt	GAGGAAUUCUUAAACCAGUtt
MED1	GCUGGUCCCUUGGAUAAGAtt	GCUGGUCCCUUGGAUAAGAtt	GACCAGUCCUUGUCUAUGAtt
MED13	GAAACGAUGUGAGUAUGCAtt	GAAACGAUGUGAGUAUGCAtt	CCUGCUAUGUCUUCGGUUAtt
MITF	CCGUGGACUAUAUCCGAAAtt	CCGUGGACUAUAUCCGAAAtt	GAAACUUGAUUGAUCUUUAtt
MKI67	CGUCGUGUCUCAAGAUCUAtt	CGUCGUGUCUCAAGAUCUAtt	CAUCAACGCGUUUAGGGAAtt
NFKB1	GGCUCAUGUUUACAGCUUUtt	GGCUCAUGUUUACAGCUUUtt	CCACCUUCAUUCUCAACUUtt

Table 6.3a. The siRNAs used in the study (continued).

Silencer select siRNA from Life Technologies (USA)

Gene Symbol	Sense siRNA Sequence 1	Sense siRNA Sequence 2	Sense siRNA Sequence 3
NFKB2	GGUUCUAUGAGGAUGAUGAtt	GGUUCUAUGAGGAUGAUGAtt	CCACAGAUGUGCAUAAACAtt
NOL3	GGUGACUUCUCUCCACAUAtt	GGUGACUUCUCUCCACAUAtt	AGGGAGGGCUUAGAGCUCAtt
NUP50	GAAGGACUGUCGAAUGGAAtt	GAAGGACUGUCGAAUGGAAtt	CUGUUUUACAAGAAAGACAtt
ONECUT1	GAAUUGCAAAUCACCAUUUtt	GAAUUGCAAAUCACCAUUUtt	GGUCAGCAAUGGAAGUAAUtt
OSMR	GUAACUGCAUUCAACUUGAtt	GUAACUGCAUUCAACUUGAtt	GACUCACAAGAAACCUAUAtt
PATZ1	GCGCCGAUAUAAUGCUCUUtt	GCGCCGAUAUAAUGCUCUUtt	GUGGUAAGGUGUUCACUGAtt
PDE11A	CCAUCGUGAUAUAUUUCGAtt	CCAUCGUGAUAUAUUUCGAtt	CGGGAGAGAUUAGAGCUCAtt
PDE3A	GCAGUGACAUUGUACAGAAtt	GCAGUGACAUUGUACAGAAtt	GUAUUCUCAAAAACGUAUAtt
PDGFRA	CUCUAGGAAUGACGGAUUAtt	CUCUAGGAAUGACGGAUUAtt	GGCCUUACUUUAUUGGAUUtt
PDGFRB	GGAACGUGCUCAUCUGUGAtt	GGAACGUGCUCAUCUGUGAtt	GAGCAACUUUGAUCAACGAtt
PIK3CA	GACUAGCUAGAGACAAUGAtt	GACUAGCUAGAGACAAUGAtt	GUAAUUACCCAGAUCCUAUtt
PIK3CB	CUCCAAAUGUUGCGCUUGAtt	CUCCAAAUGUUGCGCUUGAtt	GGGAAAGCUGGACUACUAAtt
PIK3CD	GUGAGAAAUUUGAACGGUUtt	GUGAGAAAUUUGAACGGUUtt	GACUAAUAAUAGUGAGAAAtt
PIK3CG	GCUUUAGAGUUCCAUAUGAtt	GCUUUAGAGUUCCAUAUGAtt	GCUGCACGACUUUACCCAAtt
PPAP2B	ACUGAAAACUGGUGAGACAtt	ACUGAAAACUGGUGAGACAtt	GGCUACAUUCAGAACUACAtt
PROKR1	AGACAGAGCAGAUCCGCAAtt	AGACAGAGCAGAUCCGCAAtt	AGAACGACACCGUCAAGUAtt
PROKR2	CCCUCUACGUCUCCACCAAtt	CCCUCUACGUCUCCACCAAtt	ACAGAAACGGUCCUCUUUAtt
PRPF4B	GGAAAUAGGUCUAGUACUAtt	GGAAAUAGGUCUAGUACUAtt	CAGUUGAUUUAAGAGGUAAtt
PRPF8	CCCUACAUGUGAACAACGAtt	CCCUACAUGUGAACAACGAtt	GCAGAUACAUUGAUCGCAUtt
PXN	CCUGGAGAACUAUAUCUCAtt	CCUGGAGAACUAUAUCUCAtt	GAACGACAAGCCUUACUGUtt
RBM7	CCACAUCUCCUAGCAGGUAtt	CCACAUCUCCUAGCAGGUAtt	CAAUUUAGAUCAGGAAGUAtt
RELA	CCCUUUACGUCAUCCCUGAtt	CCCUUUACGUCAUCCCUGAtt	GGAGUACCCUGAGGCUAUAtt
RELB	GCUACGGCGUGGACAAGAAtt	GCUACGGCGUGGACAAGAAtt	GGAUUUGCCGAAUUAACAAtt
RGS19	AGCAUGUGGUAGACGAGAAtt	AGCAUGUGGUAGACGAGAAtt	GGGAGGGCAUCAACAAGAAtt
RNF215	GAGUGGAAGUUGACCUUGUtt	GAGUGGAAGUUGACCUUGUtt	UGCCCACUGUGCAAAUUCAtt
S100A7	AGAAGAUUGAUUUUUCUGAtt	AGAAGAUUGAUUUUUCUGAtt	CCUUAGUGCCUGUGACAAAtt
SART1	GCUCUAUCCUGUCCAAGUAtt	GCUCUAUCCUGUCCAAGUAtt	GCAUCGAGGAGACUAACAAtt
SCO2	AGUUACCGCGUGUACUACAtt	AGUUACCGCGUGUACUACAtt	CGGCUGAGCAGAUCUCAGAtt
SENP6	CAACGACAGAACUAACAGAtt	CAACGACAGAACUAACAGAtt	GCACCUUUAGGCGAAGGAAtt
SHC3	GGACACGACUGACUAUGUUtt	GGACACGACUGACUAUGUUtt	CCAAACAGAUCAUAGCGAAtt
SPRR1A	GAAUCAUAAUCGCUCCUUUtt	GAAUCAUAAUCGCUCCUUUtt	GCUGUCACCCUGAAUCAUAtt
SPRR1B	GAAUGUGCUAUGAAGCUUUtt	GAAUGUGCUAUGAAGCUUUtt	AAGAGAGACUUAAGAUGAAtt
SPRR3	CAAAGUUCCUGAGCAAGGAtt	CAAAGUUCCUGAGCAAGGAtt	GCUACACCAAGGUCCCUGAtt
STAG2	GGUAGAUGAUUGGAUAGAAtt	GGUAGAUGAUUGGAUAGAAtt	CCACUGAUGUCUUACCGAAtt
TEP1	GUAGGACCCUAAUAUCGAUtt	GUAGGACCCUAAUAUCGAUtt	CUGAUGAGGCGGAUACUAAtt
TLR4	GAGCCGCUGGUGUAUCUUUtt	GAGCCGCUGGUGUAUCUUUtt	CAUUGAAGAAUUCCGAUUAtt
TOP3A	CGGCUUGCCUAGUUCUCUAtt	CGGCUUGCCUAGUUCUCUAtt	CAGGUUAAAGUUAAAGUUUtt

Table 6.3a. The siRNAs used in the study (continued).

Silencer select siRNA from Life Technologies (USA)

Gene Symbol	Sense siRNA Sequence 1	Sense siRNA Sequence 2	Sense siRNA Sequence 3
TP53	GUAAUCUACUGGGACGGAAtt	GUAAUCUACUGGGACGGAAtt	GAAAUUUGCGUGUGGAGUAtt
TROAP	CAGGCAGAGACAUCACAAAtt	CAGGCAGAGACAUCACAAAtt	CGUGGACCAGGAGAACCAAtt
UBOX5	ACAGUAACUUUGGUGUAAAtt	ACAGUAACUUUGGUGUAAAtt	GUCUUACUGAAAAACCAGAtt
VHL	CAUCCAUUCUACAUCCGUAtt	CAUCCAUUCUACAUCCGUAtt	GCUCUACGAAGAUCUGGAAtt
WDR6	GCAUCGGAUGGUUAAGGUAtt	GCAUCGGAUGGUUAAGGUAtt	AGGUCAAGCUUCUAGAGAAtt
WTAP	AGACUAAAGACAAACUGGAtt	AGACUAAAGACAAACUGGAtt	AGAUCUUAACUCUAAUGAUtt
YWHAH	CAAGGUGUUUUACCUGAAAtt	CAAGGUGUUUUACCUGAAAtt	CACUAAACGAGGAUUCCUAtt
ZAP70	AGAACUUUGUGCACCGUGAtt	AGAACUUUGUGCACCGUGAtt	GAACUGUACGCACUCAUGAtt
ZC3H3	ACGUGGUCAUCAAAGUUAAtt	ACGUGGUCAUCAAAGUUAAtt	AGAACGUGGUCAUCAAAGUtt
Control 1	CCGCACUCCUGAACUUGAAtt	GCACCGUCCUAAUCGUCGAtt	GCUGGGUGGCGGAUAAGUAtt
Control 2	CAGUCGAAGAAGAUGGUUAtt	CGAGUCCGUGGAUAUCGUUtt	ACCGCACUCCUGAACUUGAtt

The siRNA purchased from Sigma-Aldrich (USA)

Gene Symbol	Sense siRNA Sequence
MAP3K11	GGGCAGUGACGUCUGGAGUUU
MAPK8	GUGGAAAGAAUUGAUAUAUAA
MAPK9	AAGAGAGCUUAUCGUGAACUU
MAPK10	CCGCAUGUGUCUGUAUUCAUA
MAPK11	CAGGAUGGAGCUGAUCCAGUA
MAPK12	CUGGACGUAUUCACUCCUGAU
MAPK13	CCGGAGUGGCAUGAAGCUGUA
MAPK14	AACUGCGGUUACUUAAACAUA
MKK4	AUUGGACGAGGAGCUUAUG
MKK7	AGACUGCCUUACUAAAGAU
MKK6	AAGGCUUGCAUUUCUAUUGGA
MKK3	CCGGGCCACCGUGAACUCACA
ASK1	CCUGUGCUAACGACUUGCUUG
CAMK1	CAGGUGCUGGAUGCUGUGAAA
AKT1	AAUCACACCACCUGACCAAGA
PRKAA1(AMPK)	CCCACGAUAUUCUGUACACAA
PRKAA2(AMPK)	CCGAAGUCAGAGCAAACCGUA
RMA1-1	GCGCGACCUUCGAAUGUAA
RMA1-2	CGGCAAGAGUGUCCAGUAU
CAMKK2-1	GGAUCUGAUCAAAGGCAUC
CAMKK2-2	GCAUCGAGUACUUACACUA
MAP3K11-1	GCAGCGACGUGUCGAGCUU

Table 6.3a. The siRNAs used in the study (continued).

The siRNA purchased from Sigma-Aldrich (USA)

Gene Symbol	Sense siRNA Sequence
MAP3K11-2	GCAGUGACGUCUGGAGUUU
MAP3K11-3	GGGCAGUGACGUCUGGAGUUU
MAP3K11-4	CUGGAGGACUCAAGCAAUG
MAP3K11-5	GGAGGAGUCACAGCAUACATT
AHSA1(AHA1)-1	AUUGGUCCACGGAUAAGCU
HSF1	CGGAUUCAGGGAAGCAGCUGGUGCA
ATF2	AAUGAAGUGGCACAGCUGA
cMYC	AACAGAAAUGUCCUGAGCAAU
cJUN	UACCUCAGCAACUUCAACCCA
BAG3	AACAGGUGCAGUUUCUCGAUGGGUC
RAC1	UUUACCUACAGCUCCGUCUUU
RAC2	AACUACUCAGCCAAUGUGAUG
RAC3	CGCGCCCAUGCAGGCCAUCAA
GSK3B	GUAAUCCACCUCUGGCUAC
MAP4K1	CUGACUAAGAGUCCCAAGA
BRAF	AAGUGGCAUGGUGAUGUGGCA
MAP4K2	Not Available
CDC42	
ATF1	
ATF6	
ELK1	
TP53	
ASK1	
BAG1	
BAG2	
BAG3	
CHOP	
BCL2L1	
SQSTM1	
MDM2	
EIF2AK2	
XBP1	

The rest of the siRNAs used were purchased from Qiagen (Germany).

Table 6.3b. Primers used for qRT-PCR.

The Primers were collected from public database (http://pga.mgh.harvard.edu/primerbank/)

Gene	Forward Primer Sequence (5' 3')	Reverse Primer Sequence (5' 3')	Primer Bank ID
ASB8	CAGAGCAAATACTCTCTCTCCGA	TCTGACACCATACAGGCACAG	45333920c1
MIS18BP1	CAGGCACACTTACTCCTGTAAAA	GAGGTAGTAGCCTCTGTTAGCA	194473999c1
CALML5	GGTTGACACGGATGGAAACG	ACTCCTGGAAGCTGATTTCGC	8393159a1
CAMKK2	CATGAACGGACGCTGCATCT	ACAGTCCTGCATACCCGTGAT	259490264c2
CD2BP2	ACACTCTTTGGATAGCGATGAGG	GGTTAAAGGGTGTGATCCGAAC	343887346c1
CSNK2A1	GGTGGAATGGGGAAATCAAGAT	TGATGATGTTGGGACCTCCTC	29570791a1
CTDSP1	AGACCCCAGTCCAATACCTG	GACGCTTCAACACGTAGACCT	332308971c1
DSN1	CTCAGCCGGTCTATCAGTGTC	AGTGTCCCTTAGGAAAGGTTCAA	223890152c1
FBXO7	GATTCAGAGCATTCTTCACTCCA	GCCCTAACATACTGTCGTCATTC	74229026c1
FLT1	GAAAACGCATAATCTGGGACAGT	GCGTGGTGTGCTTATTTGGA	229892219c3
GTSE1	CAGGGGACGTGAACATGGATG	ATGTCCAAAGGGTCCGAAGAA	253970411c1
ITPR2	CACCTTGGGGTTAGTGGATGA	CTCGGTGTGGTTCCCTTGT	95147334c1
KDR	GTGATCGGAAATGACACTGGAG	CATGTTGGTCACTAACAGAAGCA	195546779c2
MAP2K7	GGGACGTTCATCACCAACAC	GCCACTGTCATCTTGCCCA	40806198c2
MAP3K11	GCAGCCCATTGAGAGTGAC	CACTGCCCTTAGAGAAGGTGG	56237030c1
MAPK15	AGAAGCCGTCCAATGTGCTC	CAAGGGTGTATCGGTGCGA	95147355c3
MED1	GAGGGCATCAACATTTGGTCA	AGATGAGAGCCCAGTCCATTC	154813205c2
MED13	TTGCTGGTGTCCGAATGATCT	CGTAACCGAAGACATAGCAGGAT	102468716c3
NFKB2	GGGCCGAAAGACCTATCCC	CAGCTCCGAGCATTGCTTG	117320530c3
NUP50	GGTAGCCTTTGGTTCTCTTGC	TGTGATAGGCATTTCCGACAC	82659110c2
OSMR	AATGTCAGTGAAGGCATGAAAGG	GAAGGTTGTTTAGACCACCCC	270288819c2
PDGFRA	TTGAAGGCAGGCACATTTACA	GCGACAAGGTATAATGGCAGAAT	172072625c3
PDGFRB	AGCACCTTCGTTCTGACCTG	TATTCTCCCGTGTCTAGCCCA	68216043c1
PIK3CB	TATTTGGACTTTGCGACAAGACT	TCGAACGTACTGGTCTGGATAG	365777410c1
PIK3CG	GGCGAAACGCCCATCAAAAA	GACTCCCGTGCAGTCATCC	21237724c1
PROKR1	TGGGGTTCATGGATGACAATG	AACGTCCTGGAATTGGTCACA	44921613c1
PRPF8	TGACAAAAGGGTTTACTTGGGTG	CTCATTGACGAAGGAAATGGCT	91208425c2
RNF215	GGAGACTGGCATCCCTCAAGA	GGTGAAACTCGTGCTTACAGG	63025219c2
SART1	CCAGCTCCAAAACTAGCTCAG	AAGGCCATAGGGTTGATGACA	119393884c1
SENP6	TCCTGTAAGGTTAAGTCGGCT	AGATAGAGGAGGAGTAGGCTGAT	156105702c1
STAG2	TGGCGTGTTAGTACGGCAATG	GCTTGTATGTCGAAATGCTCTGA	112789533c3
TEP1	ATTTGTACCGTGTGAACAACAGC	GAATCAAACCAACGACCCAAAG	225735570c2
UBOX5	GCCTCATCTAGCAGAGTGTCT	GTGGCTAAACACCACTTGGCT	40806195c2
YWHAH	GACATGGCCTCCGCTATGAAG	ATGCTGCTAATGACCCTCCAG	61744461c1
JNK2/MAPK9	GAAACTAAGCCGTCCTTTTCAGA	TCCAGCTCCATGTGAATAACCT	205277408c1
ATF1	CACAGATGGAGTACAGGGACT	GACCACCTGATTGCTGGGC	304361768c3
CAMK1	TGCTGTCCTGCACAAGATCAA	GCTCCGTGTAGAAGCCTTTTT	325995171c2
GSK3B	GGCAGCATGAAAGTTAGCAGA	GGCGACCAGTTCTCCTGAATC	225903415c1
HSF1	GCACATTCCATGCCCAAGTAT	GGCCTCTCGTCTATGCTCC	132626772c2
CDC42	CCATCGGAATATGTACCGACTG	CTCAGCGGTCGTAATCTGTCA	89903014c1
RAC2	CAACGCCTTTCCCGGAGAG	TCCGTCTGTGGATAGGAGAGC	27881480c1
MAP4K1/HPK1	ATCCCTCGGCGGATCAGAT	CACGTCGTCATAGTCATCGTC	110611904c3
PRKAA1	GGCACGCCATACCCTTGAT	TCTTCCTTCGTACACGCAAATAA	94557300c2
PRKAA2	CTGTAAGCATGGACGGGTTGA	AAATCGGCTATCTTGGCATTCA	157909838c2
HPRT1	ACCAGTCAACAGGGGACATAA	CTTCGTGGGGTCCTTTTCACC	164518913c2
CFTR	AAAAGGCCAGCGTTGTCTCC	AAACATCGCCGAAGGGCATTA	90421312c1

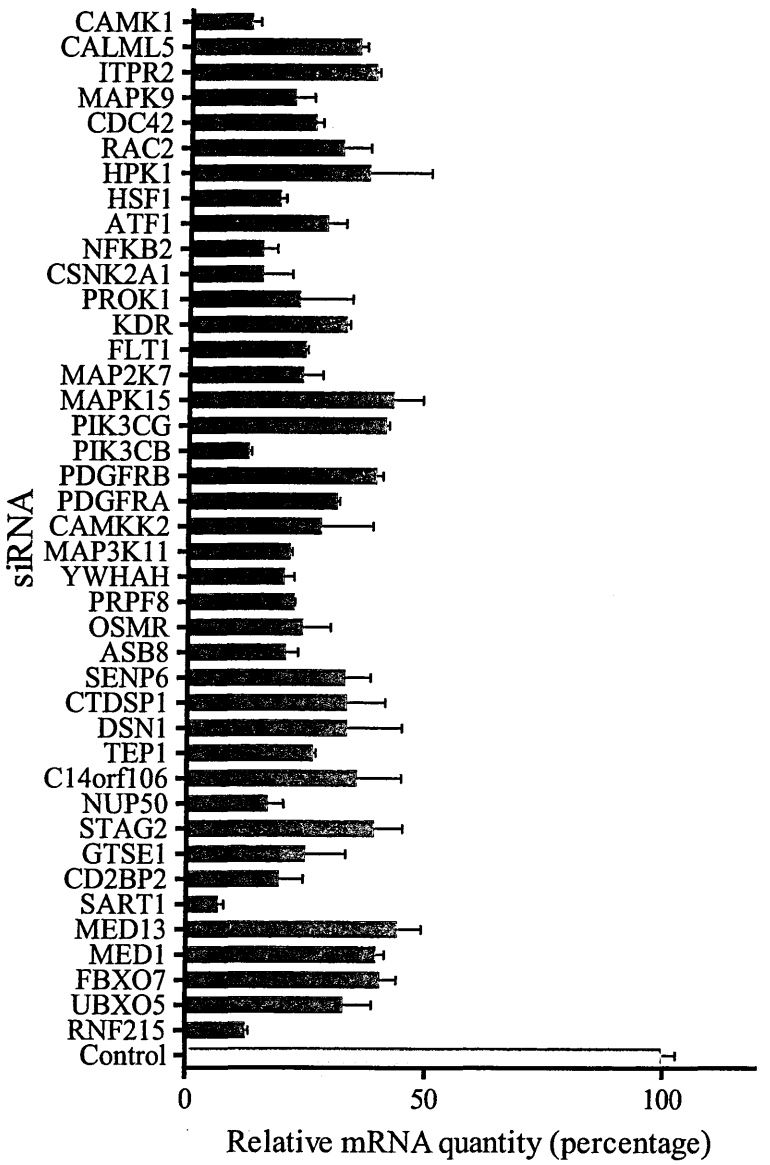

Figure 6.3. The siRNAs targeting the corrector genes reduce the mRNA of respective genes.

CFBE cells were transfected with mix of three silencer select siRNAs targeting the indicated genes for 72 hours, total RNA was isolated and subjected qRT-PCR. The relative mRNA quantity of indicated genes are plotted as a percentage compared to control treatment. Data represent mean ± SD (n=2).

6.4. Cell lysis

Cells were washed three times with pre-chilled DPBS, then the cells were lysed using radio-immunoprecipitation analysis (RIPA) buffer (150 mM NaCl, 1% Triton X-100, 0.5% deoxycholic acid, 0.1% SDS, 20 mM Tris-HCl, pH 7.4). The cells were lysed in the plate kept on ice by adding pre-chilled RIPA buffer supplemented with a protease inhibitor cocktail and a phosphatase inhibitor, while observing the phosphorylated proteins. The cell lysates were centrifuged at 15,000 rcf for 15 mins, before proceeding to SDS-PAGE analysis.

6.5. Protein estimation

Pierce BCA Protein Assay kits were used to quantify the protein concentrations in cell lysates, following the manufacturer's protocol.

6.6. SDS-PAGE

The SDS-PAGE apparatus was from Hoefer Scientific Instruments (Germany) and 16 cm × 18 cm gels were used. Protein from the cell lysates contained final concentrations of sample buffer (62.5 mM Tris-HCl, pH 6.8, 2% SDS, 10% glycerol, 0.001% bromophenol, 125 mM dithiothreitol). The samples were incubated at 37 °C for 30 min before loading onto the SDS-PAGE. Thirty millilitres of separating gel was prepared by mixing the reagents as shown in Table 5.6. Then 10 ml stacking gel was prepared (4% acrylamide, 5.6 ml water, 1.7 ml 30% acrylamide, 2.5 ml stacking buffer, 100 µl 10% SDS, and 100 µl 10% ammonium persulphate (APS), 10µl tetramethylethylenediamine (TEMED)). The protein samples were loaded into the wells in the polymerised gels and electroporated for 4 h at 35 mA, or overnight at 8 mA, using the running buffer of 25 mM TRIZMA base, 200 mM glycine, 0.1% (w/v) SDS.

6.7. Immunoblotting

The polyacrylamide gels and 3 mm Whatman papers were soaked for 15 min in chilled transfer buffer (25 mM TRIZMA base, 200 mM glycine, 20% (v/v) methanol). The gels were placed on a wet sheet of 3MM paper and covered with a nitrocellulose membrane that had been wetted in transfer buffer. This was then covered with another wet 3MM paper, to form a 'sandwich', and then this was assembled into the blotting apparatus (Hoefer Scientific Instruments,

Table 6.6. Separating gel composition

Ingredients for 30 ml separating gel for different percentage of SDS-PAGE.

SDS-PAGE (%)	Acryl amide 30% (ml)	Tris-HCl-1.5M pH-8.8 (ml)	Water (ml)	SDS-10% (µl)	APS-10% (µl)	TEMED (µl)
6	6	7.5	16.5	300	160	16
7	7	7.5	15.5	300	160	16
8	8	7.5	14.5	300	160	16
9	9	7.5	13.5	300	160	16
10	10	7.5	12.5	300	160	16
11	11	7.5	11.5	300	160	16
12	12	7.5	10.5	300	160	16
13	13	7.5	09.5	300	160	16
14	14	7.5	08.5	300	160	16
15	15	7.5	07.5	300	160	16

Germany). The protein transfer was carried out at 400 mA for 4 h. At the end of the transfer, the nitrocellulose filter was soaked in Ponceau red solution (0.2% Ponceau red in 5% (v/v) acetic acid) for 5 min, to visualise the protein, and then rinsed with 5% acetic acid to remove excess dye.

The nitrocellulose filters were cut into strips with a razor blade around the molecular weight of proteins of interest. These strips of nitrocellulose were incubated in the blocking solution (either 5% [w/v] bovine serum albumin or 5% skimmed milk in TBS-T (0.1% [w/v] Tween-20, 150 mM NaCl, 20 mM Tris-HCl, pH 7.5) for 1 hour at room temperature. The blocking solution was then replaced with the primary antibody in 5% (w/v) bovine serum albumin in TTBS for 2 h at room temperature or overnight at 4 °C. After this incubation, the antibody was removed and the strips were washed three times in TTBS, for 10 min each. Next, these washed strips were incubated for 1 h at room temperature with the appropriate HRP-conjugated secondary antibody in the blocking solution. After this, they were washed three times in TTBS, for 10 min each. After this washing, the strips were incubated with the ECL reagents, according to the manufacturer's instructions for ECL-based detection using X-ray film. The X-ray film was scanned between 200 dpi to 600 dpi and the protein bands were analysed using the ImageJ gel analysis tool (http://imagej.nih.gov/ij/).

6.8. Partial trypsin digestion of CFTR

Partial trypsin digestion of CFTR was carried our as described previously (Du et al. 2005; Rosser et al. 2008; Glozman et al. 2009). Cells were grown in 10-cm plates, and after the treatment, the cells were washed three times with 10 ml phosphate-buffered saline (PBS; 137 mM NaCl, 2.7 mM KCl, 8.1 mM Na_2HPO_4, 1.5 mM KH_2PO_4, 1 mM $CaCl_2$, 0.5 mM $MgCl_2$) and then scraped into 5 ml PBS. The cells were pelleted at 500 rcf for 5 min at 4 °C. The cell pellet was resuspended in 1 ml hypertonic buffer (250 mM sucrose, 10 mM Hepes, pH 7.2), and then homogenised using a ball bearing homogeniser. The nuclei and unbroken cells were removed by centrifugation at 600 rcf for 15 min. The membranes were then pelleted by centrifugation at 100,000 rcf for 30 min (Aleksandrov et al. 2001), and then they were resuspended in trypsin buffer (40 mM Tris, pH 7.4, 2 mM $MgCl_2$, 0.1 mM EDTA). Then, 50 µg proteins was added to different trypsin concentrations, and incubated for 15 min on ice. The reaction was stopped with the addition of

phenylmethylsulfonyl fluoride to 1 mM, and the samples were immediately denatured in sample buffer (62.5 mM Tris-HCl, pH 6.8, 2% SDS, 10% glycerol, 0.001% bromophenol, 125 mM dithiothreitol) at 37 °C for 30 min. The samples were run on 4% to 16% SDS-PAGE (Tris-glycine) and transferred onto nitrocellulose membranes. These membranes were blocked for 1 h in 5% milk with TBS-T. The membranes were then treated with the primary antibody overnight at 4 °C. NBD1 was probed using the 3G11 CFTR antibodies from the CFTR Folding Consortium; NBD2 was probed by using the M3A7 clone CFTR antibody from Millipore (Massachusetts, USA). Blots were developed by ECL, and quantified using NIH ImageJ analysis of the scanned films.

6.9. EndoH resistance assay

CFBE cells were treated with siRNA and after 48 hours VSVG-GFP was transfected for 24 hours and cells were kept at 40°C. Then the cells are shifted to 32°C for 15, 30, 60 and 120 minutes and after each time point the cells were lysed. Cells immediately lysed at 40°C were considered as 0 minute. VSVG transport through the Golgi can be followed by the processing of two oligosaccaride chains from the high mannose endoH-sensitive form to the endoH-resistant form. The processing intermediates can be easily distinguished by SDS-PAGE (Davidson and Balch 1993). The appearance of sequential processing intermediates allows the direct examination of ER-to-Golgi transport (Davidson and Balch 1993).

6.10. Plasma membrane quality control assay

Plasma membrane quality control was accessed using the previous described method (Okiyoneda et al. 2010). CFBE cells were treated with a control siRNA and siRNA against MAP3K11, and kept at low temperature (26 °C) for 36 h, to allow the mutant protein to reach the PM, which led to increased levels of band C. Then, the cells were shifted to 37 °C for 1.5 h with 100 μg/ml cycloheximide before turnover measurements were started (0 h), at 37 °C (the temperature at which the mutant protein at the PM is subjected to accelerated ubiquitination and degradation). The cells were lysed at 0, 1, 3 and 5 h, and the kinetics of degradation of band C was examined by immunoblotting.

6.11. Immunoprecipitation of CFTR

Cells expressing CFTR were washed in cold PBS, scraped into PBS, pelleted and resuspended in the Triton lysis buffer (25 mM Tris, pH 7.4, 150 mM NaCl, 1% Triton X-100 and protease inhibitors). The anti-CFTR antibodies were incubated with the cell lysate overnight with light agitation at 4 °C, and the anti-CFTR-antibody complex was pulled down using Dynabeads kits, according to manufacturer's protocol.

6.12. Biochemical assay for CFTR correction

Cells expressing either wtCFTR or ΔF508CFTR or ΔF508CFTR treated with correcting or test conditions were lysed and immunoblotted. On SDS-PAGE the wtCFTR shows two bands approximately at 140 kDa (band B) which is core glycosylated protein at ER, but when it passes through Golgi and secretory pathway it becomes modified by Golgi enzymes and runs at 170 kDa (band C) (Figure 6.12). But ΔF508CFTR usually shows only the 140 kDa (band B) as it fails to proceed through the secretory pathway, but when treated with corrective conditions like 26°C partial amount of ΔF508CFTR also pass along the secretory pathway through the Golgi and become modified by Golgi enzymes to shows considerable amounts of band C (Figure 6.12). This assay has proved very sensitive and robust to detect the small correction or changes in CFTR proteostasis (Farinha et al. 2004).

6.13. Interactome of CFTR upon treatment of drugs

CFTR-expressing Hela cells were grown in 150-mm plates. When the cells were about 80% confluent, 5 μM JNKi II (SP600125) was added to the ΔF508CFTR samples, with an equivalent amount of dimethylsulphoxide added to the wtCFTR and ΔF508CFTR control cells. The treatment was terminated at 24 h. The cells were then processed for the interactome study, by being lysed using Triton lysis buffer. Then, 8 mg protein of the HeLa cell lysates expressing either wtCFTR or ΔF508CFTR were incubated for 2 h with 500 μl settled resin of mouse IgG-agarose, for pre-cleaning. They were then incubated overnight with 500 μl mouse monoclonal anti-HA-agarose at 4 °C, and washed 3 times with RIPA buffer. CFTR was eluted by incubating the samples for 2 h at 4 °C with 250 μl RIPA buffer with 100 μg/ml of HA peptide. The non-specific interactome was the eluent of 8 mg of ΔF508CFTR-expressing cells incubated overnight with 500

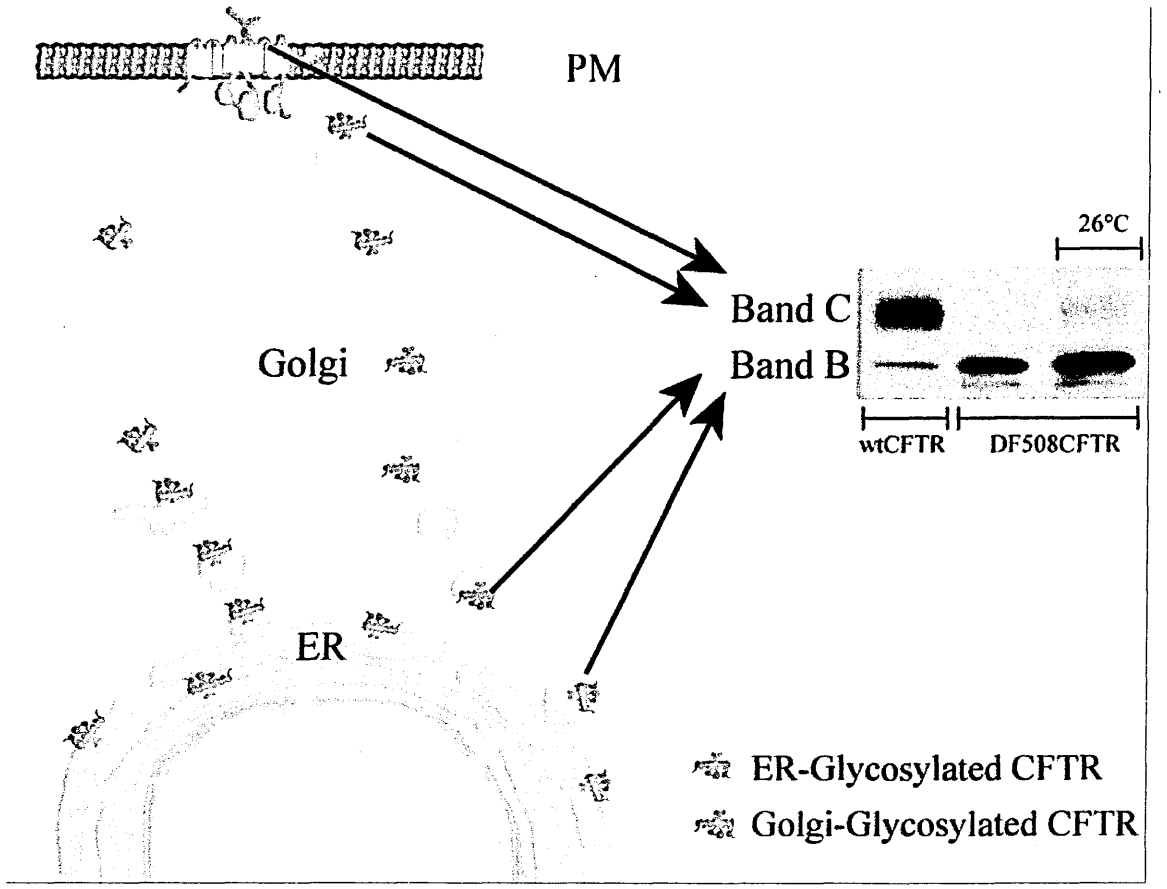

Figure 6.12. Biochemical assay of CFTR correction

wtCFTR at the ER after glycosylation shows approximately at 140 kDa (band B) and when it passes through the Golgi and secretory pathway it becomes modified by Golgi enzymes and runs at 170 kDa (band C) which is found at the PM. ΔF508CFTR usually undergoes ER glycosylation and shows 140 kDa (band B), but it fails to proceed through Golgi and secretory pathway. When treated with correctors like 26°C partial amounts of ΔF508CFTR pass through the Golgi and secretory pathway and become modified by Golgi enzymes and shows a significant amount of band C.

μl settled resin and mouse IgG-agarose eluted in the same manner as for CFTR. The interactome mass spectrometry was carried out by Dr. Maria Monti, Department of Chemical Sciences, "Federico II" University of Naples, Naples, and at CEINGE Biotecnologie Avanzate s.c.a r.l., Naples, Italy.

As previously published (Zito et al. 2007) the eluted samples were subjected to 12% SDS PAGE and stained with GelCode Blue Stain Reagent (Pierce). Protein bands were excised from the gel and destained by repeated washings with 50 mM NH_4HCO_3, pH 8.0, and acetonitrile. Samples were reduced and carboxyamidomethylated with 10 mM DTT and 55 mM iodoacetamide in 50 mM NH_4HCO_3 buffer, pH 8.0. Tryptic digestion of the alkylated samples was performed at 37 °C overnight, using 100 ng trypsin. MALDI mass spectra were recorded on an Applied Biosystems Voyager DE-PRO mass spectrometer equipped with a reflectron TOF analyser and used in delayed extraction mode. One μl of peptide mixture was mixed with an equal volume of α-cyano-4-hydroxycynnamic acid as matrix (in acetonitrile/50 mM citric acid [70:30, v/v]), applied to the metallic sample plate and air dried. Mass calibration was performed using the standard mixture provided by the manufacturer. Raw data, reported as monoisotopic masses, were then introduced into the MASCOT peptide mass fingerprinting search programme (Matrix Science, Boston, USA) and used for protein identification. It was decided to list the protein interactors based on the qualitative information without giving much importance to the quantitative information like peptide count. The proteins which were present in the nonspecific interactome sample were not considered. The proteins detected in test samples and that were not present at the nonspecific interactome are noted as test samples interacting partner. The proteins identified were listed in Table 3.9.

6.14. Immunofluorescence

The cells were grown on coverslips and fixed with 4% paraformaldehyde for 10 min at room temperature, and then permeabilised with 0.2% saponin in blocking solution (PBS containing 1% bovine serum albumin, 50 mM NH_4Cl). For the antibody-based detection, the fixing was followed by incubation with antibodies to the antigen of interest in the same blocking solution, for 1 h at room temperature, followed by the secondary antibodies labelled with Alexa Fluor dyes (Invitrogen). The coverslips were then mounted in the mounting media (16% [w/v] Mowiol 4–24

[EMD Millipore, USA] and 30% [v/v] glycerol in PBS), and examined under a confocal microscope (LSM710; Carl Zeiss). The images were then acquired with the pinhole set to 1 and under non-saturating conditions, using the 63× objective. The images were acquired using the Zen software system (Carl Zeiss).

6.15. SPQ iodide efflux

The iodide-sensitive fluorescent indicator, SPQ (Molecular Probes, Eugene, OR, USA) was introduced into the cells in a hypotonic solution of iodide buffer (130 mM NaI, 4 mM KNO_3, 1 mM $Ca(NO_3)_2$, 1 mM $Mg(NO_3)_2$, 10 mM glucose and 20 mM HEPES, pH 7.4) diluted 1:1 with water and containing a final concentration of 10 μM SPQ. The cells were loaded for 20 min at 37 °C in a humidified chamber with 5% CO_2. The SPQ-loaded cells were then mounted on a LSM510 Meta confocal microscope with a 37 °C heated stage, and perfused with iodide buffer. Changes in the CFTR-mediated SPQ fluorescence were monitored at the 445 nm in response to excitation at 340 nm during the perfusion at 37 °C in nitrate buffer (NaI replaced with 130 mM $NaNO_3$) for 10 min, with 20 μM forskolin plus 50 μM genistein or 20 μM forskolin plus 20 μM genistein. The peak iodide efflux rate (usually 12 min after the forskolin plus genistein addition) of untreated and treated cells was calculated according to the Stern-Volmer relationship, as follows: (Fo/F) - 1 = KCQ where F is the observed fluorescence, Fo is the fluorescence in the absence of a quenching anion, CQ is the concentration of the quenching anion, and K is the Stern-Volmer quench constant. The rates were calculated using Sigma Plot Version 7.1 for each mean fluorescence trace generated from 50 cells examined per population per coverslip.

6.16. HS-YFP assay for CFTR activity

Twenty-four hours after plating, the CFBE cells expressing ΔF508CFTR and HS-YFP were incubated with the test compounds at 37 °C for 24 h to 48 h. At the time of assay, the cells were washed with PBS and stimulated for 30 min with 20 μM forskolin in the absence or presence of 50 μM genistein. The cells were then transferred to Zeiss LSM 700 confocal microscope where the images were acquired using an open pinhole at a rate of 330msec/frame, at ambient temperature for CFTR activity determination. Each assay consisted of a continuous 300 s fluorescence reading with 30 s before and rest after injection of an iodide-containing solution (PBS with Cl^- replaced by

I^-; final I^- concentration in the well, 100 mM). To determine fluorescence quenching rate (QR) associated with I^- influx, the final 200 s of data for each well were fitted with a mono-exponential decay and decay constant K was calculated using GraphPad Prism software.

6.17. Ussing chamber assay for short-circuit current recordings

The Ussing chamber experiments were carried out using polarised CFBE epithelia performed 7-10 days after their seeding cells, when the transepithelial resistance was >1,000 $\Omega \cdot cm^2$, with the Snapwell inserts mounted in a self-contained Ussing chamber system (vertical diffusion chamber; Corning Life Sciences, (St. Louis, USA). The transepithelial short-circuit currents of the CFBE epithelia were measured. The apical and basolateral sides contained the same solution (126 mM NaCl, 0.38 mM KH_2PO_4, 2.1 mM K_2HPO_4, 1 mM $MgSO_4$, 1 mM $CaCl_2$, 24 mM $NaHCO_3$, 10 mM glucose), bubbled with 5% CO_2 in air. The hemichambers were connected to DVC-1000 voltage clamps (World Precision Instruments, Inc., Sarasota, FL, USA) via Ag/AgCl electrodes and 1 M KCl agar bridges. The transepithelial currents were digitised using PowerLab 4/25 data acquisition system, and stored on a computer. All of the measurements were carried out at 37 °C.

6.18. Meta-analysis of microarrays

The meta-analysis microarray profiles were carried out separately for the two gene sets. First, the cMap set was made up of 11 correctors (Table 2.1), the gene signatures of which were provided from the Prototype Ranked Lists obtained from Iorio et al. (Iorio et al. 2010) which was based on Affymetrix. The CFBE set was made up of 13 correctors, the gene signatures of which were obtained using the Agilent platform by treating CFBE41o$^-$ cells stably transfected with ΔF508CFTR, for 24 h. The CFBE dataset gene signature was obtained at Dr. D.Y. Thomas Laboratory, Department of Biochemistry, McGill University, Montréal, quality control, Canada, in collaboration with our Laboratory, and part of these microarray data have already been published (Zhang et al. 2012). The microarray data from the CFBE cells were then processed to obtain the ranked lists based on the fold-change of the probe; the highest up-regulated gene ranked first and lowest down-regulated gene ranked last. For each of the corresponding Prototype Ranked Lists or ranked lists, the top and bottom 20% of the probes were selected, which identifies the most up-

regulated and down-regulated probes, respectively. The 20% threshold was arbitrary, but it has been shown to represent most up-regulated and down-regulated probes for the cMap dataset (Iorio et al. 2010); a similar 20% threshold was used for the CFBE dataset. The common probes that lay in the top or bottom 20% of the cMap and CFBE drug sets were computed separately; there was one common down-regulated gene among the 11 cMap drugs, and there was one common up-regulated gene among the CFBE drugs. Then, a less stringent fuzzy intersection (Iorio et al. 2010) procedure was used to search for genes commonly up-regulated or down-regulated by a subset of the 11 cMap drugs and the 13 CFBE drugs. Keeping the up-regulated and down-regulated probes in each dataset separate, the probes that were common (=n) to any N number of drugs out of the 11 drugs of the cMap dataset and the 13 drugs of the CFBE dataset were computed (Figure 2.2); N ranging from 1 to 11 for the cMap data, and 1 to 13 for the CFBE data. The ideal cut-off would be when N corresponds to the best enrichment in the number of common probes in the specific drug set, $n_{observed}$, with respect to the ones due to random chance, n_{random}. Thus, a null hypothesis was built by sampling 1,000 configurations: for the cMap dataset, 11 Prototype Ranked Lists which were randomly selected from the 1,000 cMap drugs dataset; and for the CFBE dataset, 13 ranked lists which were randomly selected from 1,000 profiles computed by random shuffling of the total probes determined. For each value of N, the mean number of common probes by random chance n_{random} was computed (Figure 2.2). This process determined the number of common probes to be expected using a group of unrelated drugs. The first requirement for choosing the cut-off was that the corresponding $n_{observed}$ is unlikely to be due to chance, by selecting P values below 0.05. Taking the cMap drug dataset, no value of N had any significant increase in $n_{observed}/ n_{random}$ for the up-regulated genes; in contrast, the commonly down-regulated genes for cut-off 8 or 9 were statistically significant. The cMap dataset cut-off was set to 8, to increase the number of probes, and random probes (n_{random}) were less (better $n_{observed}/ n_{random}$). Although cut-offs of 7, 6 and 5, statically significant, they were not considered because of a poor $n_{observed}/ n_{random}$. For the CFBE dataset, the computed n_{random} was very small compared to the cMap dataset, and this might be due to the different statistical methods used, because 1,000 drug microarray profiles were not available using the Agilent platform, so that 13 random ranked lists could be picked for determining the n_{random}. The cut-off for the CFBE dataset was set to 9, which was almost the same percentage cut-

off (~70%) that was selected for the cMap dataset, and moreover, the calculated $n_{observed}/n_{random}$ was also statistically significant. This intersection procedure resulted in 541 up-regulated probes that corresponded to 402 genes (Table 2.2a), 191 down-regulated probes that corresponded to 117 genes from the CFBE dataset, and 108 down-regulated probes corresponding to 102 genes from the cMap dataset (Table 2.2b).

6.19. String protein-protein interactions

The gene set was the input to the string database (http://string-db.org/) (Franceschini et al. 2013) to identify the predicted interactions among the proteins. The required confidence was set to 0.7 and the active prediction methods used were neighbourhood, gene fusion, co-occurrence, co-expression, experiments, and databases.

6.20. Ingenuity pathway analysis

The gene sets were analysed using the core analysis (CA) application of the Ingenuity Pathway Analysis (IPA), a web-based software application. The IPA core analysis (IPACA) maps these genes onto canonical pathways, predicts the upstream regulators, and also converts them into a set of relevant networks of a maximum of 35 focus genes (can be changed to 70 or 140), based on the Ingenuity Pathways Knowledge Base of the Global Molecular Network (GMN), which is composed of thousands of genes and gene products that interact with each other. Each network has an assigned significance score based on the *P* value (calculated Fischer's exact test), the probability of finding focus genes in a set of genes randomly selected from GMN. The higher the number of focus genes in a network, the higher the score will be (a score of 53 means the respective *P* value 10E-53), and the higher the rank of the network will be. Each network also has predicted biological functions associated with it. The up-regulated and down-regulated genes of the CFBE dataset and the down-regulated genes of the cMap dataset were analysed separately and as a pool, to infer any common pathways or networks modulated among them.

6.21. QRT-PCR analysis

The total RNAs were isolated from samples using the GenElute™ 96 Well Total RNA Purification Kit (Sigma) according to the manufacturer's protocol. Then cDNAs were derived from these RNA

samples using the High Capacity cDNA Reverse Transcription Kit (Life Technologies) according to the manufacturer's protocol. Then these RNA samples were subjected to PCR using LightCycler® 480 SYBR Green I Master using LightCycler® 480 (Roche) according to the manufacturer's protocol. Then the relative amount of mRNA were calculated using 2(-Delta Delta C(T)) method (Livak and Schmittgen 2001).

References

Abcouwer, S. F., P. L. Marjon, R. K. Loper and D. L. Vander Jagt (2002). "Response of VEGF expression to amino acid deprivation and inducers of endoplasmic reticulum stress." Invest Ophthalmol Vis Sci **43**(8): 2791-2798.

Al-Awqati, Q. (2002). "Alternative treatment for secretory diarrhea revealed in a new class of CFTR inhibitors." J Clin Invest **110**(11): 1599-1601.

Alberti, S., K. Bohse, V. Arndt, A. Schmitz and J. Hohfeld (2004). "The cochaperone HspBP1 inhibits the CHIP ubiquitin ligase and stimulates the maturation of the cystic fibrosis transmembrane conductance regulator." Mol Biol Cell **15**(9): 4003-4010.

Aleksandrov, L., A. Mengos, X. Chang, A. Aleksandrov and J. R. Riordan (2001). "Differential interactions of nucleotides at the two nucleotide binding domains of the cystic fibrosis transmembrane conductance regulator." J Biol Chem **276**(16): 12918-12923.

Alvarez-Castelao, B., C. Ruiz-Rivas and J. G. Castano (2012). "A critical appraisal of quantitative studies of protein degradation in the framework of cellular proteostasis." Biochem Res Int **2012**: 823597.

Amaral, M. D. (2004). "CFTR and chaperones: processing and degradation." J Mol Neurosci **23**(1-2): 41-48.

Amaral, M. D. (2005). "Processing of CFTR: traversing the cellular maze--how much CFTR needs to go through to avoid cystic fibrosis?" Pediatr Pulmonol **39**(6): 479-491.

Amaral, M. D. and C. M. Farinha (2013). "Post-translational modifications of CFTR: insight into protein trafficking and cystic fibrosis disease." FEBS J.

An, H., H. Xu, M. Zhang, J. Zhou, T. Feng, C. Qian, R. Qi and X. Cao (2005). "Src homology 2 domain-containing inositol-5-phosphatase 1 (SHIP1) negatively regulates TLR4-mediated LPS response primarily through a phosphatase activity- and PI-3K-independent mechanism." Blood **105**(12): 4685-4692.

Andersen, D. H. (1938). "Cystic fibrosis of the pancreas and its relation to celiac disease." Am J Dis Child **56**.

Andersen, D. H. and R. G. Hodges (1946). "Celiac syndrome v. genetics of cystic fibrosis of the pancreaswith a consideration etiology." Am J Dis Child **72**: 62.

Anguiano, A., R. D. Oates, J. A. Amos, M. Dean, B. Gerrard, C. Stewart, T. A. Maher, M. B. White and A. Milunsky (1992). "Congenital bilateral absence of the vas deferens. A primarily genital form of cystic fibrosis." JAMA **267**(13): 1794-1797.

Anjos, S. M., R. Robert, D. Waller, D. L. Zhang, H. Balghi, H. M. Sampson, F. Ciciriello, P. Lesimple, G. W. Carlile, J. Goepp, J. Liao, P. Ferraro, R. Phillipe, F. Dantzer, J. W. Hanrahan and D. Y. Thomas (2012). "Decreasing Poly(ADP-Ribose) Polymerase Activity Restores DeltaF508 CFTR Trafficking." Front Pharmacol **3**: 165.

Antigny, F., C. Norez, F. Becq and C. Vandebrouck (2011). "CFTR and Ca Signaling in Cystic Fibrosis." Front Pharmacol **2**: 67.

Antonny, B. and R. Schekman (2001). "ER export: public transportation by the COPII coach." Curr Opin Cell Biol **13**(4): 438-443.

Arndt, V., C. Daniel, W. Nastainczyk, S. Alberti and J. Hohfeld (2005). "BAG-2 acts as an inhibitor of the chaperone-associated ubiquitin ligase CHIP." Mol Biol Cell **16**(12): 5891-5900.

Arnold, R., I. M. Patzak, B. Neuhaus, S. Vancauwenbergh, A. Veillette, J. Van Lint and F. Kiefer (2005). "Activation of hematopoietic progenitor kinase 1 involves relocation, autophosphorylation, and transphosphorylation by protein kinase D1." Mol Cell Biol **25**(6): 2364-2383.

Balch, W. E., R. I. Morimoto, A. Dillin and J. W. Kelly (2008). "Adapting proteostasis for disease intervention." Science **319**(5865): 916-919.

Balch, W. E., D. M. Roth and D. M. Hutt (2011). "Emergent properties of proteostasis in managing cystic fibrosis." Cold Spring Harb Perspect Biol **3**(2).

Ballar, P., A. U. Ors, H. Yang and S. Fang (2010). "Differential regulation of CFTRDeltaF508 degradation by ubiquitin ligases gp78 and Hrd1." Int J Biochem Cell Biol **42**(1): 167-173.

Bannykh, S. I., G. I. Bannykh, K. N. Fish, B. D. Moyer, J. R. Riordan and W. E. Balch (2000). "Traffic pattern of cystic fibrosis transmembrane regulator through the early exocytic pathway." Traffic **1**(11): 852-870.

Bartoszewski, R., A. Rab, L. Fu, S. Bartoszewska, J. Collawn and Z. Bebok (2011). "CFTR expression regulation by the unfolded protein response." Methods Enzymol **491**: 3-24.

Bartoszewski, R., A. Rab, A. Jurkuvenaite, M. Mazur, J. Wakefield, J. F. Collawn and Z. Bebok (2008). "Activation of the unfolded protein response by deltaF508 CFTR." Am J Respir Cell Mol Biol **39**(4): 448-457.

Basile, A., M. Pascale, S. Franceschelli, E. Nieddu, M. T. Mazzei, P. Fossa, M. C. Turco and M. Mazzei (2012). "Matrine modulates HSC70 levels and rescues DeltaF508-CFTR." J Cell Physiol **227**(9): 3317-3323.

Bebok, Z., J. F. Collawn, J. Wakefield, W. Parker, Y. Li, K. Varga, E. J. Sorscher and J. P. Clancy (2005). "Failure of cAMP agonists to activate rescued deltaF508 CFTR in CFBE41o- airway epithelial monolayers." J Physiol **569**(Pt 2): 601-615.

Benesch, S., S. Polo, F. P. Lai, K. I. Anderson, T. E. Stradal, J. Wehland and K. Rottner (2005). "N-WASP deficiency impairs EGF internalization and actin assembly at clathrin-coated pits." J Cell Sci **118**(Pt 14): 3103-3115.

Berridge, M. J. (2001). "The versatility and complexity of calcium signalling." Novartis Found Symp **239**: 52-64; discussion 64-57, 150-159.

Bertrand, C. A. and R. A. Frizzell (2003). "The role of regulated CFTR trafficking in epithelial secretion." Am J Physiol Cell Physiol **285**(1): C1-18.

Berube, J., L. Roussel, L. Nattagh and S. Rousseau (2010). "Loss of cystic fibrosis transmembrane conductance regulator function enhances activation of p38 and ERK MAPKs, increasing interleukin-6 synthesis in airway epithelial cells exposed to Pseudomonas aeruginosa." J Biol Chem **285**(29): 22299-22307.

Bhattacharyya, S., N. S. Balakathiresan, C. Dalgard, U. Gutti, D. Armistead, C. Jozwik, M. Srivastava, H. B. Pollard and R. Biswas (2011). "Elevated miR-155 promotes inflammation in cystic fibrosis by driving hyperexpression of interleukin-8." J Biol Chem **286**(13): 11604-11615.

Bicknell, A. A., J. Tourtellotte and M. Niwa (2010). "Late phase of the endoplasmic reticulum stress response pathway is regulated by Hog1 MAP kinase." J Biol Chem **285**(23): 17545-17555.

Blount, J. R., A. A. Burr, A. Denuc, G. Marfany and S. V. Todi (2012). "Ubiquitin-specific protease 25 functions in Endoplasmic Reticulum-associated degradation." PLoS One **7**(5): e36542.

Bodas, M. and N. Vij (2010). "The NF-kappaB signaling in cystic fibrosis lung disease: pathophysiology and therapeutic potential." Discov Med **9**(47): 346-356.

Bogoyevitch, M. A. and P. G. Arthur (2008). "Inhibitors of c-Jun N-terminal kinases: JuNK no more?" Biochim Biophys Acta **1784**(1): 76-93.

Bomberger, J. M., R. L. Barnaby and B. A. Stanton (2009). "The deubiquitinating enzyme USP10 regulates the post-endocytic sorting of cystic fibrosis transmembrane conductance regulator in airway epithelial cells." J Biol Chem **284**(28): 18778-18789.

Bombieri, C., M. Claustres, K. De Boeck, N. Derichs, J. Dodge, E. Girodon, I. Sermet, M. Schwarz, M. Tzetis, M. Wilschanski, C. Bareil, D. Bilton, C. Castellani, H. Cuppens, G. R. Cutting, P. Drevinek, P. Farrell, J. S. Elborn, K. Jarvi, B. Kerem, E. Kerem, M. Knowles, M. Macek, Jr., A. Munck, D. Radojkovic, M. Seia, D. N. Sheppard, K. W. Southern, M. Stuhrmann, E. Tullis, J. Zielenski, P. F. Pignatti and C. Ferec (2011). "Recommendations for the classification of diseases as CFTR-related disorders." J Cyst Fibros **10 Suppl 2**: S86-102.

Borsello, T. and G. Forloni (2007). "JNK signalling: a possible target to prevent neurodegeneration." Curr Pharm Des **13**(18): 1875-1886.

Bozoky, Z., M. Krzeminski, P. A. Chong and J. D. Forman-Kay (2013). "Structural changes of CFTR R region upon phosphorylation: a plastic platform for intramolecular and intermolecular interactions." FEBS J.

Bradbury, N. A. (1999). "Intracellular CFTR: localization and function." Physiol Rev **79**(1 Suppl): S175-191.

Brancho, D., J. J. Ventura, A. Jaeschke, B. Doran, R. A. Flavell and R. J. Davis (2005). "Role of MLK3 in the regulation of mitogen-activated protein kinase signaling cascades." Mol Cell Biol **25**(9): 3670-3681.

Brouillard, F., M. Bouthier, T. Leclerc, A. Clement, M. Baudouin-Legros and A. Edelman (2001). "NF-kappa B mediates up-regulation of CFTR gene expression in Calu-3 cells by interleukin-1beta." J Biol Chem **276**(12): 9486-9491.

Brown, C. R., L. Q. Hong-Brown, J. Biwersi, A. S. Verkman and W. J. Welch (1996). "Chemical chaperones correct the mutant phenotype of the delta F508 cystic fibrosis transmembrane conductance regulator protein." Cell Stress Chaperones **1**(2): 117-125.

Brown, R. K., H. Wyatt, J. F. Price and F. J. Kelly (1996). "Pulmonary dysfunction in cystic fibrosis is associated with oxidative stress." Eur Respir J **9**(2): 334-339.

Calamini, B., M. C. Silva, F. Madoux, D. M. Hutt, S. Khanna, M. A. Chalfant, S. A. Saldanha, P. Hodder, B. D. Tait, D. Garza, W. E. Balch and R. I. Morimoto (2012). "Small-molecule proteostasis regulators for protein conformational diseases." Nat Chem Biol **8**(2): 185-196.

Caohuy, H., C. Jozwik and H. B. Pollard (2009). "Rescue of DeltaF508-CFTR by the SGK1/Nedd4-2 signaling pathway." J Biol Chem **284**(37): 25241-25253.

Carlile, G. W., R. A. Keyzers, K. A. Teske, R. Robert, D. E. Williams, R. G. Linington, C. A. Gray, R. M. Centko, L. Yan, S. M. Anjos, H. M. Sampson, D. Zhang, J. Liao, J. W. Hanrahan, R. J. Andersen and D. Y. Thomas (2012). "Correction of F508del-CFTR trafficking by the sponge alkaloid latonduine is modulated by interaction with PARP." Chem Biol **19**(10): 1288-1299.

Carlile, G. W., R. Robert, D. Zhang, K. A. Teske, Y. Luo, J. W. Hanrahan and D. Y. Thomas (2007). "Correctors of protein trafficking defects identified by a novel high-throughput screening assay." Chembiochem **8**(9): 1012-1020.

Casals, T., J. De-Gracia, M. Gallego, J. Dorca, B. Rodriguez-Sanchon, M. D. Ramos, J. Gimenez, A. Cistero-Bahima, C. Olveira and X. Estivill (2004). "Bronchiectasis in adult patients: an expression of heterozygosity for CFTR gene mutations?" Clin Genet **65**(6): 490-495.

Chadee, D. N. and J. M. Kyriakis (2004). "MLK3 is required for mitogen activation of B-Raf, ERK and cell proliferation." Nat Cell Biol **6**(8): 770-776.

Chadee, D. N., T. Yuasa and J. M. Kyriakis (2002). "Direct activation of mitogen-activated protein kinase kinase kinase MEKK1 by the Ste20p homologue GCK and the adapter protein TRAF2." Mol Cell Biol **22**(3): 737-749.

Chang, X. B., A. Mengos, Y. X. Hou, L. Cui, T. J. Jensen, A. Aleksandrov, J. R. Riordan and M. Gentzsch (2008). "Role of N-linked oligosaccharides in the biosynthetic processing of the cystic fibrosis membrane conductance regulator." J Cell Sci **121**(Pt 17): 2814-2823.

Chang, X. B., J. A. Tabcharani, Y. X. Hou, T. J. Jensen, N. Kartner, N. Alon, J. W. Hanrahan and J. R. Riordan (1993). "Protein kinase A (PKA) still activates CFTR chloride channel after mutagenesis of all 10 PKA consensus phosphorylation sites." J Biol Chem **268**(15): 11304-11311.

Chanoux, R. A. and R. C. Rubenstein (2012). "Molecular Chaperones as Targets to Circumvent the CFTR Defect in Cystic Fibrosis." Front Pharmacol **3**: 137.

Chappe, V., D. A. Hinkson, L. D. Howell, A. Evagelidis, J. Liao, X. B. Chang, J. R. Riordan and J. W. Hanrahan (2004). "Stimulatory and inhibitory protein kinase C consensus sequences regulate the cystic fibrosis transmembrane conductance regulator." Proc Natl Acad Sci U S A **101**(1): 390-395.

Chen, J., E. M. Miller and K. A. Gallo (2010). "MLK3 is critical for breast cancer cell migration and promotes a malignant phenotype in mammary epithelial cells." Oncogene **29**(31): 4399-4411.

Chen, S. and D. F. Smith (1998). "Hop as an adaptor in the heat shock protein 70 (Hsp70) and hsp90 chaperone machinery." J Biol Chem **273**(52): 35194-35200.

Cheng, J., H. Wang and W. B. Guggino (2004). "Modulation of mature cystic fibrosis transmembrane regulator protein by the PDZ domain protein CAL." J Biol Chem **279**(3): 1892-1898.

Cheng, J., H. Wang and W. B. Guggino (2005). "Regulation of cystic fibrosis transmembrane regulator trafficking and protein expression by a Rho family small GTPase TC10." J Biol Chem **280**(5): 3731-3739.

Cheng, S. H., R. J. Gregory, J. Marshall, S. Paul, D. W. Souza, G. A. White, C. R. O'Riordan and A. E. Smith (1990). "Defective intracellular transport and processing of CFTR is the molecular basis of most cystic fibrosis." Cell **63**(4): 827-834.

Chmiel, J. F. and P. B. Davis (2003). "State of the art: why do the lungs of patients with cystic fibrosis become infected and why can't they clear the infection?" Respir Res **4**: 8.

Chmiel, J. F., M. W. Konstan and J. S. Elborn (2013). "Antibiotic and Anti-Inflammatory Therapies for Cystic Fibrosis." Cold Spring Harb Perspect Med.

Cho, H. J., H. Y. Gee, K. H. Baek, S. K. Ko, J. M. Park, H. Lee, N. D. Kim, M. G. Lee and I. Shin (2011). "A small molecule that binds to an ATPase domain of Hsc70 promotes membrane trafficking of mutant cystic fibrosis transmembrane conductance regulator." J Am Chem Soc **133**(50): 20267-20276.

Christianson, J. C., J. A. Olzmann, T. A. Shaler, M. E. Sowa, E. J. Bennett, C. M. Richter, R. E. Tyler, E. J. Greenblatt, J. W. Harper and R. R. Kopito (2012). "Defining human ERAD networks through an integrative mapping strategy." Nat Cell Biol **14**(1): 93-105.

Clancy, J. P., Z. Bebok, F. Ruiz, C. King, J. Jones, L. Walker, H. Greer, J. Hong, L. Wing, M. Macaluso, R. Lyrene, E. J. Sorscher and D. M. Bedwell (2001). "Evidence that systemic gentamicin suppresses premature stop mutations in patients with cystic fibrosis." Am J Respir Crit Care Med **163**(7): 1683-1692.

Clancy, J. P., S. M. Rowe, F. J. Accurso, M. L. Aitken, R. S. Amin, M. A. Ashlock, M. Ballmann, M. P. Boyle, I. Bronsveld, P. W. Campbell, K. De Boeck, S. H. Donaldson, H. L. Dorkin, J. M. Dunitz, P. R. Durie, M. Jain, A. Leonard, K. S. McCoy, R. B. Moss, J. M. Pilewski, D. B. Rosenbluth, R. C. Rubenstein, M. S. Schechter, M. Botfield, C. L. Ordonez, G. T. Spencer-Green, L. Vernillet, S. Wisseh, K. Yen and M. W. Konstan (2012). "Results of a phase IIa study of VX-809, an investigational CFTR corrector compound, in subjects with cystic fibrosis homozygous for the F508del-CFTR mutation." Thorax **67**(1): 12-18.

Clarke, L. A., L. Sousa, C. Barreto and M. D. Amaral (2013). "Changes in transcriptome of native nasal epithelium expressing F508del-CFTR and intersecting data from comparable studies." Respir Res **14**: 38.

Cohen, P. (2002). "Protein kinases--the major drug targets of the twenty-first century?" Nat Rev Drug Discov **1**(4): 309-315.

Colas, J., G. Faure, E. Saussereau, S. Trudel, W. M. Rabeh, S. Bitam, I. C. Guerrera, J. Fritsch, I. Sermet-Gaudelus, N. Davezac, F. Brouillard, G. L. Lukacs, H. Herrmann, M. Ollero and A. Edelman (2012). "Disruption of cytokeratin-8 interaction with F508del-CFTR corrects its functional defect." Hum Mol Genet **21**(3): 623-634.

Cole, E. T., Y. Zhan, W. F. Abi Saab, A. C. Korchnak, B. P. Ashburner and D. N. Chadee (2009). "Mixed lineage kinase 3 negatively regulates IKK activity and enhances etoposide-induced cell death." Biochim Biophys Acta **1793**(12): 1811-1818.

Collaco, J. M. and G. R. Cutting (2008). "Update on gene modifiers in cystic fibrosis." Curr Opin Pulm Med **14**(6): 559-566.

Collins, F. S. (1992). "Cystic fibrosis: molecular biology and therapeutic implications." Science **256**(5058): 774-779.

Colomer, J. and A. R. Means (2007). "Physiological roles of the Ca2+/CaM-dependent protein kinase cascade in health and disease." Subcell Biochem **45**: 169-214.

Consortium, T. C. F. G.-P. (1993). "Correlation between Genotype and Phenotype in Patients with Cystic Fibrosis." New England Journal of Medicine **329**(18): 1308-1313.

Cuevas, B. D., A. N. Abell and G. L. Johnson (2007). "Role of mitogen-activated protein kinase kinase kinases in signal integration." Oncogene **26**(22): 3159-3171.

Cui, J., M. Zhang, Y. Q. Zhang and Z. H. Xu (2007). "JNK pathway: diseases and therapeutic potential." Acta Pharmacol Sin **28**(5): 601-608.

Cyr, D. M., X. Lu and M. G. Douglas (1992). "Regulation of Hsp70 function by a eukaryotic DnaJ homolog." J Biol Chem **267**(29): 20927-20931.

Dalal, S., M. F. Rosser, D. M. Cyr and P. I. Hanson (2004). "Distinct roles for the AAA ATPases NSF and p97 in the secretory pathway." Mol Biol Cell **15**(2): 637-648.

Dalemans, W., P. Barbry, G. Champigny, S. Jallat, K. Dott, D. Dreyer, R. G. Crystal, A. Pavirani, J. P. Lecocq and M. Lazdunski (1991). "Altered chloride ion channel kinetics associated with the delta F508 cystic fibrosis mutation." Nature **354**(6354): 526-528.

Davezac, N., D. Tondelier, J. Lipecka, P. Fanen, F. Demaugre, J. Debski, M. Dadlez, A. Schrattenholz, M. A. Cahill and A. Edelman (2004). "Global proteomic approach unmasks involvement of keratins 8 and 18 in the delivery of cystic fibrosis transmembrane conductance regulator (CFTR)/deltaF508-CFTR to the plasma membrane." Proteomics **4**(12): 3833-3844.

Davidson, H. W. and W. E. Balch (1993). "Differential inhibition of multiple vesicular transport steps between the endoplasmic reticulum and trans Golgi network." J Biol Chem **268**(6): 4216-4226.

Davies, J., E. Alton and U. Griesenbach (2005). "Cystic fibrosis modifier genes." J R Soc Med **98 Suppl 45**: 47-54.

Davis, P. B. (2006). "Cystic fibrosis since 1938." Am J Respir Crit Care Med **173**(5): 475-482.

Denning, G. M., M. P. Anderson, J. F. Amara, J. Marshall, A. E. Smith and M. J. Welsh (1992). "Processing of mutant cystic fibrosis transmembrane conductance regulator is temperature-sensitive." Nature **358**(1380673): 761-764.

Denning, G. M., M. P. Anderson, J. F. Amara, J. Marshall, A. E. Smith and M. J. Welsh (1992). "Processing of mutant cystic fibrosis transmembrane conductance regulator is temperature-sensitive." Nature **358**(6389): 761-764.

di Sant'Agnese, P. A., R. C. Darling, G. A. Perera and E. Shea (1953). "Abnormal electrolyte composition of sweat in cystic fibrosis of the pancreas. Clinical significance and relationship to disease." Pediatrics **12**: 549–563.

Dorion, S. and J. Landry (2002). "Activation of the mitogen-activated protein kinase pathways by heat shock." Cell Stress Chaperones **7**(2): 200-206.

Dormer, R. L., C. M. Harris, Z. Clark, M. M. Pereira, I. J. Doull, C. Norez, F. Becq and M. A. McPherson (2005). "Sildenafil (Viagra) corrects DeltaF508-CFTR location in nasal epithelial cells from patients with cystic fibrosis." Thorax **60**(1): 55-59.

Doumanis, J., K. Wada, Y. Kino, A. W. Moore and N. Nukina (2009). "RNAi screening in Drosophila cells identifies new modifiers of mutant huntingtin aggregation." PLoS One **4**(9): e7275.

Drumm, M. L., D. J. Wilkinson, L. S. Smit, R. T. Worrell, T. V. Strong, R. A. Frizzell, D. C. Dawson and F. S. Collins (1991). "Chloride conductance expressed by delta F508 and other mutant CFTRs in Xenopus oocytes." Science **254**(5039): 1797-1799.

Du, K., M. Sharma and G. L. Lukacs (2005). "The DeltaF508 cystic fibrosis mutation impairs domain-domain interactions and arrests post-translational folding of CFTR." Nat Struct Mol Biol **12**(1): 17-25.

Egan, M. E., J. Glockner-Pagel, C. Ambrose, P. A. Cahill, L. Pappoe, N. Balamuth, E. Cho, S. Canny, C. A. Wagner, J. Geibel and M. J. Caplan (2002). "Calcium-pump inhibitors induce functional surface expression of Delta F508-CFTR protein in cystic fibrosis epithelial cells." Nat Med **8**(5): 485-492.

Farber, S. (1944). "Pancreatic function and disease in early life v. pathologic changes associated with pancreatic insufficiency in early life." Arch Pathol **37**: 238.

Faria, D., S. Dahimene, L. Alessio, T. Scott-Ward, R. Schreiber, K. Kunzelmann and M. D. Amaral (2011). "Effect of Annexin A5 on CFTR: regulated traffic or scaffolding?" Mol Membr Biol **28**(1): 14-29.

Farinha, C. M. and M. D. Amaral (2005). "Most F508del-CFTR is targeted to degradation at an early folding checkpoint and independently of calnexin." Mol Cell Biol **25**(12): 5242-5252.

Farinha, C. M., P. Matos and M. D. Amaral (2013). "Control of cystic fibrosis transmembrane conductance regulator membrane trafficking: not just from the endoplasmic reticulum to the Golgi." FEBS J.

Farinha, C. M., P. Nogueira, F. Mendes, D. Penque and M. D. Amaral (2002). "The human DnaJ homologue (Hdj)-1/heat-shock protein (Hsp) 40 co-chaperone is required for the in vivo stabilization of the cystic fibrosis transmembrane conductance regulator by Hsp70." Biochem J **366**(Pt 3): 797-806.

Farinha, C. M., D. Penque, M. Roxo-Rosa, G. Lukacs, R. Dormer, M. McPherson, M. Pereira, A. G. Bot, H. Jorna, R. Willemsen, H. Dejonge, G. D. Heda, C. R. Marino, P. Fanen, A. Hinzpeter, J. Lipecka, J. Fritsch, M. Gentzsch, A. Edelman and M. D. Amaral (2004). "Biochemical methods to assess CFTR expression and membrane localization." J Cyst Fibros **3 Suppl 2**: 73-77.

Fedorov, A. N. and T. O. Baldwin (1997). "Cotranslational protein folding." J Biol Chem **272**(52): 32715-32718.

Flattau, A., M. Olaywi, P. J. Gaglio, P. Marcus, P. Meissner, L. D. EB and J. F. Reinus (2011). "Social barriers to listing for adult liver transplantation: their prevalence and association with program characteristics." Liver Transpl **17**(10): 1167-1175.

Franceschini, A., D. Szklarczyk, S. Frankild, M. Kuhn, M. Simonovic, A. Roth, J. Lin, P. Minguez, P. Bork, C. von Mering and L. J. Jensen (2013). "STRING v9.1: protein-protein interaction networks, with increased coverage and integration." Nucleic Acids Res **41**(Database issue): D808-815.

Frizzell, R. A. (1999). "Ten years with CFTR." Physiol Rev **79**(1 Suppl): S1-2.

Fu, L. and E. Sztul (2003). "Traffic-independent function of the Sar1p/COPII machinery in proteasomal sorting of the cystic fibrosis transmembrane conductance regulator." J Cell Biol **160**(2): 157-163.

Fu, L. and E. Sztul (2009). "ER-associated complexes (ERACs) containing aggregated cystic fibrosis transmembrane conductance regulator (CFTR) are degraded by autophagy." Eur J Cell Biol **88**(4): 215-226.

Gadsby, D. C. and A. C. Nairn (1999). "Control of CFTR channel gating by phosphorylation and nucleotide hydrolysis." Physiol Rev **79**(1 Suppl): S77-S107.

Gadsby, D. C., P. Vergani and L. Csanady (2006). "The ABC protein turned chloride channel whose failure causes cystic fibrosis." Nature **440**(7083): 477-483.

Gallagher, E., M. Gao, Y. C. Liu and M. Karin (2006). "Activation of the E3 ubiquitin ligase Itch through a phosphorylation-induced conformational change." Proc Natl Acad Sci U S A **103**(6): 1717-1722.

Galy, A., M. J. Roux, J. A. Sahel, T. Leveillard and A. Giangrande (2005). "Rhodopsin maturation defects induce photoreceptor death by apoptosis: a fly model for RhodopsinPro23His human retinitis pigmentosa." Hum Mol Genet **14**(17): 2547-2557.

Ganeshan, R., K. Nowotarski, A. Di, D. J. Nelson and K. L. Kirk (2007). "CFTR surface expression and chloride currents are decreased by inhibitors of N-WASP and actin polymerization." Biochim Biophys Acta **1773**(2): 192-200.

Gardner, B. M., D. Pincus, K. Gotthardt, C. M. Gallagher and P. Walter (2013). "Endoplasmic reticulum stress sensing in the unfolded protein response." Cold Spring Harb Perspect Biol **5**(3): a013169.

Gee, H. Y., S. H. Noh, B. L. Tang, K. H. Kim and M. G. Lee (2011). "Rescue of DeltaF508-CFTR trafficking via a GRASP-dependent unconventional secretion pathway." Cell **146**(5): 746-760.

Gelman, M. S. and R. R. Kopito (2002). "Rescuing protein conformation: prospects for pharmacological therapy in cystic fibrosis." J Clin Invest **110**(11): 1591-1597.

Gentzsch, M., X. B. Chang, L. Cui, Y. Wu, V. V. Ozols, A. Choudhury, R. E. Pagano and J. R. Riordan (2004). "Endocytic trafficking routes of wild type and DeltaF508 cystic fibrosis transmembrane conductance regulator." Mol Biol Cell **15**(6): 2684-2696.

Gething, M. J. and J. Sambrook (1992). "Protein folding in the cell." Nature **355**(6355): 33-45.

Gilbert, A., M. Jadot, E. Leontieva, S. Wattiaux-De Coninck and R. Wattiaux (1998). "Delta F508 CFTR localizes in the endoplasmic reticulum-Golgi intermediate compartment in cystic fibrosis cells." Exp Cell Res **242**(1): 144-152.

Gillen, A. E., N. Gosalia, S. H. Leir and A. Harris (2011). "MicroRNA regulation of expression of the cystic fibrosis transmembrane conductance regulator gene." Biochem J **438**(1): 25-32.

Glozman, R., T. Okiyoneda, C. M. Mulvihill, J. M. Rini, H. Barriere and G. L. Lukacs (2009). "N-glycans are direct determinants of CFTR folding and stability in secretory and endocytic membrane traffic." J Cell Biol **184**(6): 847-862.

Gonda, R. L., R. A. Garlena and B. Stronach (2012). "Drosophila heat shock response requires the JNK pathway and phosphorylation of mixed lineage kinase at a conserved serine-proline motif." PLoS One **7**(7): e42369.

Graczyk, P. P. (2013). "JNK inhibitors as anti-inflammatory and neuroprotective agents." Future Med Chem **5**(5): 539-551.

Green, M. F., J. W. Scott, R. Steel, J. S. Oakhill, B. E. Kemp and A. R. Means (2011). "Ca2+/Calmodulin-dependent protein kinase kinase beta is regulated by multisite phosphorylation." J Biol Chem **286**(32): 28066-28079.

Gregory, R. J., S. H. Cheng, D. P. Rich, J. Marshall, S. Paul, K. Hehir, L. Ostedgaard, K. W. Klinger, M. J. Welsh and A. E. Smith (1990). "Expression and characterization of the cystic fibrosis transmembrane conductance regulator." Nature **347**(6291): 382-386.

Griesenbach, U. and E. W. Alton (2011). "Current status and future directions of gene and cell therapy for cystic fibrosis." BioDrugs **25**(2): 77-88.

Grove, D. E., C. Y. Fan, H. Y. Ren and D. M. Cyr (2011). "The endoplasmic reticulum-associated Hsp40 DNAJB12 and Hsc70 cooperate to facilitate RMA1 E3-dependent degradation of nascent CFTRDeltaF508." Mol Biol Cell **22**(3): 301-314.

Grutzmann, R., H. Boriss, O. Ammerpohl, J. Luttges, H. Kalthoff, H. K. Schackert, G. Kloppel, H. D. Saeger and C. Pilarsky (2005). "Meta-analysis of microarray data on pancreatic cancer defines a set of commonly dysregulated genes." Oncogene **24**(32): 5079-5088.

Guerra, L., T. Fanelli, M. Favia, S. M. Riccardi, G. Busco, R. A. Cardone, S. Carrabino, E. J. Weinman, S. J. Reshkin, M. Conese and V. Casavola (2005). "Na+/H+ exchanger regulatory factor isoform 1 overexpression modulates cystic fibrosis transmembrane conductance regulator (CFTR) expression and activity in human airway 16HBE14o- cells and rescues DeltaF508 CFTR functional expression in cystic fibrosis cells." J Biol Chem **280**(49): 40925-40933.

Haardt, M., M. Benharouga, D. Lechardeur, N. Kartner and G. L. Lukacs (1999). "C-terminal truncations destabilize the cystic fibrosis transmembrane conductance regulator without impairing its biogenesis. A novel class of mutation." J Biol Chem **274**(31): 21873-21877.

Haggie, P. M., J. K. Kim, G. L. Lukacs and A. S. Verkman (2006). "Tracking of quantum dot-labeled CFTR shows near immobilization by C-terminal PDZ interactions." Mol Biol Cell **17**(12): 4937-4945.

Hallows, K. R., A. C. Fitch, C. A. Richardson, P. R. Reynolds, J. P. Clancy, P. C. Dagher, L. A. Witters, J. K. Kolls and J. M. Pilewski (2006). "Up-regulation of AMP-activated kinase by dysfunctional cystic fibrosis transmembrane conductance regulator in cystic fibrosis airway epithelial cells mitigates excessive inflammation." J Biol Chem **281**(7): 4231-4241.

Hallows, K. R., V. Raghuram, B. E. Kemp, L. A. Witters and J. K. Foskett (2000). "Inhibition of cystic fibrosis transmembrane conductance regulator by novel interaction with the metabolic sensor AMP-activated protein kinase." J Clin Invest **105**(12): 1711-1721.

Hanrahan, J. W., Z. Kone, C. J. Mathews, J. Luo, Y. Jia and P. Linsdell (1998). "Patch-clamp studies of cystic fibrosis transmembrane conductance regulator chloride channel." Methods Enzymol **293**: 169-194.

Harada, K., T. Okiyoneda, Y. Hashimoto, K. Oyokawa, K. Nakamura, M. A. Suico, T. Shuto and H. Kai (2007). "Curcumin enhances cystic fibrosis transmembrane regulator expression by down-regulating calreticulin." Biochem Biophys Res Commun **353**(2): 351-356.

Harada, K., T. Okiyoneda, Y. Hashimoto, K. Ueno, K. Nakamura, K. Yamahira, T. Sugahara, T. Shuto, I. Wada, M. A. Suico and H. Kai (2006). "Calreticulin negatively regulates the cell surface expression of cystic fibrosis transmembrane conductance regulator." J Biol Chem **281**(18): 12841-12848.

Hartl, F. U., A. Bracher and M. Hayer-Hartl (2011). "Molecular chaperones in protein folding and proteostasis." Nature **475**(7356): 324-332.

Hassan, F., G. J. Nuovo, M. Crawford, P. N. Boyaka, S. Kirkby, S. P. Nana-Sinkam and E. Cormet-Boyaka (2012). "MiR-101 and miR-144 regulate the expression of the CFTR chloride channel in the lung." PLoS One **7**(11): e50837.

Hassink, G. C., B. Zhao, R. Sompallae, M. Altun, S. Gastaldello, N. V. Zinin, M. G. Masucci and K. Lindsten (2009). "The ER-resident ubiquitin-specific protease 19 participates in the UPR and rescues ERAD substrates." EMBO Rep **10**(7): 755-761.

Hawley, S. A., M. A. Selbert, E. G. Goldstein, A. M. Edelman, D. Carling and D. G. Hardie (1995). "5'-AMP activates the AMP-activated protein kinase cascade, and Ca2+/calmodulin activates the calmodulin-dependent protein kinase I cascade, via three independent mechanisms." J Biol Chem **270**(45): 27186-27191.

Hehner, S. P., T. G. Hofmann, A. Ushmorov, O. Dienz, I. Wing-Lan Leung, N. Lassam, C. Scheidereit, W. Droge and M. L. Schmitz (2000). "Mixed-lineage kinase 3 delivers CD3/CD28-derived signals into the IkappaB kinase complex." Mol Cell Biol **20**(7): 2556-2568.

Henderson, M. J., N. Vij and P. L. Zeitlin (2010). "Ubiquitin C-terminal hydrolase-L1 protects cystic fibrosis transmembrane conductance regulator from early stages of proteasomal degradation." J Biol Chem **285**(15): 11314-11325.

Hickson, J. A., B. Fong, P. H. Watson and A. J. Watson (2007). "PP2Cdelta (Ppm1d, WIP1), an endogenous inhibitor of p38 MAPK, is regulated along with Trp53 and Cdkn2a following p38 MAPK inhibition during mouse preimplantation development." Mol Reprod Dev **74**(7): 821-834.

Hollande, E., M. Fanjul, C. Chemin-Thomas, C. Devaux, S. Demolombe, J. Van Rietschoten, O. Guy-Crotte and C. Figarella (1998). "Targeting of CFTR protein is linked to the polarization of human pancreatic duct cells in culture." Eur J Cell Biol **76**(3): 220-227.

Hong, H. Y. and B. C. Kim (2007). "Mixed lineage kinase 3 connects reactive oxygen species to c-Jun NH2-terminal kinase-induced mitochondrial apoptosis in genipin-treated PC3 human prostate cancer cells." Biochem Biophys Res Commun **362**(2): 307-312.

Hook, S. S. and A. R. Means (2001). "Ca(2+)/CaM-dependent kinases: from activation to function." Annu Rev Pharmacol Toxicol **41**: 471-505.

Hosoi, T., K. Korematsu, N. Horie, T. Suezawa, Y. Okuma, Y. Nomura and K. Ozawa (2012). "Inhibition of casein kinase 2 modulates XBP1-GRP78 arm of unfolded protein responses in cultured glial cells." PLoS One **7**(6): e40144.

Hoyer-Hansen, M., L. Bastholm, P. Szyniarowski, M. Campanella, G. Szabadkai, T. Farkas, K. Bianchi, N. Fehrenbacher, F. Elling, R. Rizzuto, I. S. Mathiasen and M. Jaattela (2007). "Control of macroautophagy by calcium, calmodulin-dependent kinase kinase-beta, and Bcl-2." Mol Cell **25**(2): 193-205.

Hudmon, A. and H. Schulman (2002). "Neuronal CA2+/calmodulin-dependent protein kinase II: the role of structure and autoregulation in cellular function." Annu Rev Biochem **71**: 473-510.

Hull, J., P. Vervaart, K. Grimwood and P. Phelan (1997). "Pulmonary oxidative stress response in young children with cystic fibrosis." Thorax **52**(6): 557-560.

Hutt, D. M., D. Herman, A. P. Rodrigues, S. Noel, J. M. Pilewski, J. Matteson, B. Hoch, W. Kellner, J. W. Kelly, A. Schmidt, P. J. Thomas, Y. Matsumura, W. R. Skach, M. Gentzsch, J. R. Riordan, E. J. Sorscher, T. Okiyoneda, J. R. Yates, 3rd, G. L. Lukacs, R. A. Frizzell, G. Manning, J. M. Gottesfeld and W. E. Balch (2010). "Reduced histone deacetylase 7 activity restores function to misfolded CFTR in cystic fibrosis." Nat Chem Biol **6**(1): 25-33.

Hutt, D. M., D. M. Roth, M. A. Chalfant, R. T. Youker, J. Matteson, J. L. Brodsky and W. E. Balch (2012). "FK506 binding protein 8 peptidylprolyl isomerase activity manages a late stage of cystic fibrosis transmembrane conductance regulator (CFTR) folding and stability." J Biol Chem **287**(26): 21914-21925.

Hwang, T. C. and D. N. Sheppard (2009). "Gating of the CFTR Cl- channel by ATP-driven nucleotide-binding domain dimerisation." J Physiol **587**(Pt 10): 2151-2161.

Ichijo, H. (1999). "From receptors to stress-activated MAP kinases." Oncogene **18**(45): 6087-6093.

Illek, B., A. W. Tam, H. Fischer and T. E. Machen (1999). "Anion selectivity of apical membrane conductance of Calu 3 human airway epithelium." Pflugers Arch **437**(6): 812-822.

Iorio, F., R. Bosotti, E. Scacheri, V. Belcastro, P. Mithbaokar, R. Ferriero, L. Murino, R. Tagliaferri, N. Brunetti-Pierri, A. Isacchi and D. di Bernardo (2010). "Discovery of drug mode of action and drug repositioning from transcriptional responses." Proc Natl Acad Sci U S A **107**(33): 14621-14626.

Iorio, F., R. Tagliaferri and D. di Bernardo (2009). "Identifying network of drug mode of action by gene expression profiling." J Comput Biol **16**(2): 241-251.

Iskar, M., M. Campillos, M. Kuhn, L. J. Jensen, V. van Noort and P. Bork (2010). "Drug-induced regulation of target expression." PLoS Comput Biol **6**(9).

Jeon, Y. J., J. S. Choi, J. Y. Lee, K. R. Yu, S. H. Ka, Y. Cho, E. J. Choi, S. H. Baek, J. H. Seol, D. Park, O. S. Bang and C. H. Chung (2008). "Filamin B serves as a molecular scaffold for type I interferon-induced c-Jun NH2-terminal kinase signaling pathway." Mol Biol Cell **19**(12): 5116-5130.

Jia, Y., C. J. Mathews and J. W. Hanrahan (1997). "Phosphorylation by protein kinase C is required for acute activation of cystic fibrosis transmembrane conductance regulator by protein kinase A." J Biol Chem **272**(8): 4978-4984.

Johnston, J. A., C. L. Ward and R. R. Kopito (1998). "Aggresomes: a cellular response to misfolded proteins." J Cell Biol **143**(7): 1883-1898.

Jouret, F., A. Bernard, C. Hermans, G. Dom, S. Terryn, T. Leal, P. Lebecque, J. J. Cassiman, B. J. Scholte, H. R. de Jonge, P. J. Courtoy and O. Devuyst (2007). "Cystic fibrosis is associated with a defect in apical receptor-mediated endocytosis in mouse and human kidney." J Am Soc Nephrol **18**(3): 707-718.

Jovov, B., Ismailov, II, B. K. Berdiev, C. M. Fuller, E. J. Sorscher, J. R. Dedman, M. A. Kaetzel and D. J. Benos (1995). "Interaction between cystic fibrosis transmembrane conductance regulator and outwardly rectified chloride channels." J Biol Chem **270**(49): 29194-29200.

Kajino, T., H. Ren, S. Iemura, T. Natsume, B. Stefansson, D. L. Brautigan, K. Matsumoto and J. Ninomiya-Tsuji (2006). "Protein phosphatase 6 down-regulates TAK1 kinase activation in the IL-1 signaling pathway." J Biol Chem **281**(52): 39891-39896.

Kalid, O., M. Mense, S. Fischman, A. Shitrit, H. Bihler, E. Ben-Zeev, N. Schutz, N. Pedemonte, P. J. Thomas, R. J. Bridges, D. R. Wetmore, Y. Marantz and H. Senderowitz (2010). "Small molecule correctors of F508del-CFTR discovered by structure-based virtual screening." J Comput Aided Mol Des **24**(12): 971-991.

Kartner, N., O. Augustinas, T. J. Jensen, A. L. Naismith and J. R. Riordan (1992). "Mislocalization of delta F508 CFTR in cystic fibrosis sweat gland." Nat Genet **1**(5): 321-327.

Kaushal, S. (2006). "Effect of rapamycin on the fate of P23H opsin associated with retinitis pigmentosa (an American Ophthalmological Society thesis)." Trans Am Ophthalmol Soc **104**: 517-529.

Kerbiriou, M., M. A. Le Drevo, C. Ferec and P. Trouve (2007). "Coupling cystic fibrosis to endoplasmic reticulum stress: Differential role of Grp78 and ATF6." Biochim Biophys Acta **1772**(11-12): 1236-1249.

Kerem, B., J. M. Rommens, J. A. Buchanan, D. Markiewicz, T. K. Cox, A. Chakravarti, M. Buchwald and L. C. Tsui (1989). "Identification of the cystic fibrosis gene: genetic analysis." Science **245**(4922): 1073-1080.

Kerem, E., S. Hirawat, S. Armoni, Y. Yaakov, D. Shoseyov, M. Cohen, M. Nissim-Rafinia, H. Blau, J. Rivlin, M. Aviram, G. L. Elfring, V. J. Northcutt, L. L. Miller, B. Kerem and M. Wilschanski (2008). "Effectiveness of PTC124 treatment of cystic fibrosis caused by nonsense mutations: a prospective phase II trial." Lancet **372**(9640): 719-727.

Kim, I., W. Xu and J. C. Reed (2008). "Cell death and endoplasmic reticulum stress: disease relevance and therapeutic opportunities." Nat Rev Drug Discov **7**(12): 1013-1030.

Kim, K. Y., B. C. Kim, Z. Xu and S. J. Kim (2004). "Mixed lineage kinase 3 (MLK3)-activated p38 MAP kinase mediates transforming growth factor-beta-induced apoptosis in hepatoma cells." J Biol Chem **279**(28): 29478-29484.

King, J. D., Jr., A. C. Fitch, J. K. Lee, J. E. McCane, D. O. Mak, J. K. Foskett and K. R. Hallows (2009). "AMP-activated protein kinase phosphorylation of the R domain inhibits PKA stimulation of CFTR." Am J Physiol Cell Physiol **297**(1): C94-101.

Klegeris, A., S. Pelech, B. I. Giasson, J. Maguire, H. Zhang, E. G. McGeer and P. L. McGeer (2008). "Alpha-synuclein activates stress signaling protein kinases in THP-1 cells and microglia." Neurobiol Aging **29**(5): 739-752.

Kleizen, B., T. van Vlijmen, H. R. de Jonge and I. Braakman (2005). "Folding of CFTR is predominantly cotranslational." Mol Cell **20**(2): 277-287.

Kongsuphol, P., D. Cassidy, B. Hieke, K. J. Treharne, R. Schreiber, A. Mehta and K. Kunzelmann (2009). "Mechanistic insight into control of CFTR by AMPK." J Biol Chem **284**(9): 5645-5653.

Kopito, R. R. (1999). "Biosynthesis and degradation of CFTR." Physiol Rev **79**(1 Suppl): S167-173.

Koulov, A. V., P. LaPointe, B. Lu, A. Razvi, J. Coppinger, M. Q. Dong, J. Matteson, R. Laister, C. Arrowsmith, J. R. Yates, 3rd and W. E. Balch (2010). "Biological and structural basis for Aha1 regulation of Hsp90 ATPase activity in maintaining proteostasis in the human disease cystic fibrosis." Mol Biol Cell **21**(6): 871-884.

Kroemer, G., G. Marino and B. Levine (2010). "Autophagy and the integrated stress response." Mol Cell **40**(2): 280-293.

Kwon, S. H., H. Pollard and W. B. Guggino (2007). "Knockdown of NHERF1 enhances degradation of temperature rescued DeltaF508 CFTR from the cell surface of human airway cells." Cell Physiol Biochem **20**(6): 763-772.

Lamb, J., E. D. Crawford, D. Peck, J. W. Modell, I. C. Blat, M. J. Wrobel, J. Lerner, J. P. Brunet, A. Subramanian, K. N. Ross, M. Reich, H. Hieronymus, G. Wei, S. A. Armstrong, S. J. Haggarty, P. A. Clemons, R. Wei, S. A. Carr, E. S. Lander and T. R. Golub (2006). "The Connectivity Map: using gene-expression signatures to connect small molecules, genes, and disease." Science **313**(5795): 1929-1935.

Leboucher, G. P., Y. C. Tsai, M. Yang, K. C. Shaw, M. Zhou, T. D. Veenstra, M. H. Glickman and A. M. Weissman (2012). "Stress-induced phosphorylation and proteasomal degradation of mitofusin 2 facilitates mitochondrial fragmentation and apoptosis." Mol Cell **47**(4): 547-557.

Lei, D. C., K. Kunzelmann, T. Koslowsky, M. J. Yezzi, L. C. Escobar, Z. Xu, A. R. Ellison, J. M. Rommens, L. C. Tsui, M. Tykocinski and D. C. Gruenert (1996). "Episomal expression of wild-type CFTR corrects cAMP-dependent chloride transport in respiratory epithelial cells." Gene Ther **3**(5): 427-436.

Leonard, A., P. Lebecque, J. Dingemanse and T. Leal (2012). "A randomized placebo-controlled trial of miglustat in cystic fibrosis based on nasal potential difference." J Cyst Fibros **11**(3): 231-236.

Leung, K. T., K. K. Li, S. S. Sun, P. K. Chan, V. E. Ooi and L. C. Chiu (2008). "Activation of the JNK pathway promotes phosphorylation and degradation of BimEL--a novel mechanism of chemoresistance in T-cell acute lymphoblastic leukemia." Carcinogenesis **29**(3): 544-551.

Li, C., M. Ramjeesingh, E. Reyes, T. Jensen, X. Chang, J. M. Rommens and C. E. Bear (1993). "The cystic fibrosis mutation (delta F508) does not influence the chloride channel activity of CFTR." Nat Genet **3**(4): 311-316.

Lindquist, S. L. and J. W. Kelly (2011). "Chemical and biological approaches for adapting proteostasis to ameliorate protein misfolding and aggregation diseases: progress and prognosis." Cold Spring Harb Perspect Biol **3**(12).

Liu, G., J. Rogers, C. T. Murphy and C. Rongo (2011). "EGF signalling activates the ubiquitin proteasome system to modulate C. elegans lifespan." EMBO J **30**(15): 2990-3003.

Liu, Y. and Y. Ye (2011). "Proteostasis regulation at the endoplasmic reticulum: a new perturbation site for targeted cancer therapy." Cell Res **21**(6): 867-883.

Livak, K. J. and T. D. Schmittgen (2001). "Analysis of relative gene expression data using real-time quantitative PCR and the 2(-Delta Delta C(T)) Method." Methods **25**(4): 402-408.

Loo, M. A., T. J. Jensen, L. Cui, Y. Hou, X. B. Chang and J. R. Riordan (1998). "Perturbation of Hsp90 interaction with nascent CFTR prevents its maturation and accelerates its degradation by the proteasome." EMBO J **17**(23): 6879-6887.

Lu, Y., X. Xiong, A. Helm, K. Kimani, A. Bragin and W. R. Skach (1998). "Co- and posttranslational translocation mechanisms direct cystic fibrosis transmembrane conductance regulator N terminus transmembrane assembly." J Biol Chem **273**(1): 568-576.

Lubamba, B., B. Dhooghe, S. Noel and T. Leal (2012). "Cystic fibrosis: insight into CFTR pathophysiology and pharmacotherapy." Clin Biochem **45**(15): 1132-1144.

Lubamba, B., J. Lebacq, P. Lebecque, R. Vanbever, A. Leonard, P. Wallemacq and T. Leal (2009). "Airway delivery of low-dose miglustat normalizes nasal potential difference in F508del cystic fibrosis mice." Am J Respir Crit Care Med **179**(11): 1022-1028.

Luciani, A., V. R. Villella, S. Esposito, N. Brunetti-Pierri, D. Medina, C. Settembre, M. Gavina, L. Pulze, I. Giardino, M. Pettoello-Mantovani, M. D'Apolito, S. Guido, E. Masliah, B. Spencer, S. Quaratino, V. Raia, A. Ballabio and L. Maiuri (2010). "Defective CFTR induces aggresome formation and lung inflammation in cystic fibrosis through ROS-mediated autophagy inhibition." Nat Cell Biol **12**(9): 863-875.

Luciani, A., V. R. Villella, S. Esposito, M. Gavina, I. Russo, M. Silano, S. Guido, M. Pettoello-Mantovani, R. Carnuccio, B. Scholte, A. De Matteis, M. C. Maiuri, V. Raia, A. Luini, G. Kroemer and L. Maiuri (2012). "Targeting autophagy as a novel strategy for facilitating the therapeutic action of potentiators on DeltaF508 cystic fibrosis transmembrane conductance regulator." Autophagy **8**(11): 1657-1672.

Lukacs, G. L., X. B. Chang, C. Bear, N. Kartner, A. Mohamed, J. R. Riordan and S. Grinstein (1993). "The delta F508 mutation decreases the stability of cystic fibrosis transmembrane conductance regulator in the plasma membrane. Determination of functional half-lives on transfected cells." J Biol Chem **268**(29): 21592-21598.

Lukacs, G. L., X. B. Chang, N. Kartner, O. D. Rotstein, J. R. Riordan and S. Grinstein (1992). "The cystic fibrosis transmembrane regulator is present and functional in endosomes. Role as a determinant of endosomal pH." J Biol Chem **267**(21): 14568-14572.

Lukacs, G. L., A. Mohamed, N. Kartner, X. B. Chang, J. R. Riordan and S. Grinstein (1994). "Conformational maturation of CFTR but not its mutant counterpart (delta F508) occurs in the endoplasmic reticulum and requires ATP." EMBO J **13**(24): 6076-6086.

Lukacs, G. L. and A. S. Verkman (2012). "CFTR: folding, misfolding and correcting the DeltaF508 conformational defect." Trends Mol Med **18**(2): 81-91.

Luz, S., P. Kongsuphol, A. I. Mendes, F. Romeiras, M. Sousa, R. Schreiber, P. Matos, P. Jordan, A. Mehta, M. D. Amaral, K. Kunzelmann and C. M. Farinha (2011). "Contribution of casein kinase 2 and spleen tyrosine kinase to CFTR trafficking and protein kinase A-induced activity." Mol Cell Biol **31**(22): 4392-4404.

Maitra, R., C. M. Shaw, B. A. Stanton and J. W. Hamilton (2001). "Increased functional cell surface expression of CFTR and DeltaF508-CFTR by the anthracycline doxorubicin." Am J Physiol Cell Physiol **280**(5): C1031-1037.

Malik, S. and R. G. Roeder (2005). "Dynamic regulation of pol II transcription by the mammalian Mediator complex." Trends Biochem Sci **30**(5): 256-263.

Mall, M., A. Hipper, R. Greger and K. Kunzelmann (1996). "Wild type but not deltaF508 CFTR inhibits Na+ conductance when coexpressed in Xenopus oocytes." FEBS Lett **381**(1-2): 47-52.

Mall, M., K. Kunzelmann, A. Hipper, A. E. Busch and R. Greger (1996). "cAMP stimulation of CFTR-expressing Xenopus oocytes activates a chromanol-inhibitable K+ conductance." Pflugers Arch **432**(3): 516-522.

Marie, M., H. A. Dale, R. Sannerud and J. Saraste (2009). "The function of the intermediate compartment in pre-Golgi trafficking involves its stable connection with the centrosome." Mol Biol Cell **20**(20): 4458-4470.

Marker, D. F., M. E. Tremblay, J. M. Puccini, J. Barbieri, M. A. Gantz Marker, C. J. Loweth, E. C. Muly, S. M. Lu, V. S. Goodfellow, S. Dewhurst and H. A. Gelbard (2013). "The new small-molecule mixed-lineage kinase 3 inhibitor URMC-099 is neuroprotective and anti-inflammatory in models of human immunodeficiency virus-associated neurocognitive disorders." J Neurosci **33**(24): 9998-10010.

Marozkina, N. V., S. Yemen, M. Borowitz, L. Liu, M. Plapp, F. Sun, R. Islam, P. Erdmann-Gilmore, R. R. Townsend, C. F. Lichti, S. Mantri, P. W. Clapp, S. H. Randell, B. Gaston and K. Zaman (2010). "Hsp 70/Hsp 90 organizing protein as a nitrosylation target in cystic fibrosis therapy." Proc Natl Acad Sci U S A **107**(25): 11393-11398.

Martin, C., N. Coolen, Y. Wu, G. Thevenot, L. Touqui, V. Pruliere-Escabasse, J. Papon, A. Coste, E. Escudier, D. Dusser, I. Fajac and P. R. Burgel (2013). "CFTR dysfunction induces vascular endothelial growth factor synthesis in airway epithelium." Eur Respir J.

Matthews, R. P. and G. S. McKnight (1996). "Characterization of the cAMP response element of the cystic fibrosis transmembrane conductance regulator gene promoter." J Biol Chem **271**(50): 31869-31877.

Mayer, M. P. and B. Bukau (2005). "Hsp70 chaperones: cellular functions and molecular mechanism." Cell Mol Life Sci **62**(6): 670-684.

McDonald, R. A., R. P. Matthews, R. L. Idzerda and G. S. McKnight (1995). "Basal expression of the cystic fibrosis transmembrane conductance regulator gene is dependent on protein kinase A activity." Proc Natl Acad Sci U S A **92**(16): 7560-7564.

McNicholas, C. M., W. B. Guggino, E. M. Schwiebert, S. C. Hebert, G. Giebisch and M. E. Egan (1996). "Sensitivity of a renal K+ channel (ROMK2) to the inhibitory sulfonylurea compound glibenclamide is enhanced by coexpression with the ATP-binding cassette transporter cystic fibrosis transmembrane regulator." Proc Natl Acad Sci U S A **93**(15): 8083-8088.

Meacham, G. C., Z. Lu, S. King, E. Sorscher, A. Tousson and D. M. Cyr (1999). "The Hdj-2/Hsc70 chaperone pair facilitates early steps in CFTR biogenesis." EMBO J **18**(6): 1492-1505.

Meacham, G. C., C. Patterson, W. Zhang, J. M. Younger and D. M. Cyr (2001). "The Hsc70 co-chaperone CHIP targets immature CFTR for proteasomal degradation." Nat Cell Biol **3**(1): 100-105.

Meares, G. P., H. Qin, Y. Liu, A. T. Holdbrooks and E. N. Benveniste (2013). "AMP-activated protein kinase restricts IFN-gamma signaling." J Immunol **190**(1): 372-380.

Mendoza, J. L., A. Schmidt, Q. Li, E. Nuvaga, T. Barrett, R. J. Bridges, A. P. Feranchak, C. A. Brautigam and P. J. Thomas (2012). "Requirements for efficient correction of DeltaF508 CFTR revealed by analyses of evolved sequences." Cell **148**(1-2): 164-174.

Menon, M. B., C. Tiedje, J. Lafera, N. Ronkina, T. Konen, A. Kotlyarov and M. Gaestel (2013). "Endoplasmic reticulum-associated ubiquitin conjugating enzyme- Ube2j1 is a novel

substrate of MAPKAP kinase-2 involved in MK2-mediated TNFalpha production." Biochem J.

Mishra, R., M. K. Barthwal, G. Sondarva, B. Rana, L. Wong, M. Chatterjee, J. R. Woodgett and A. Rana (2007). "Glycogen synthase kinase-3beta induces neuronal cell death via direct phosphorylation of mixed lineage kinase 3." J Biol Chem **282**(42): 30393-30405.

Mitola, S., V. Sorbello, E. Ponte, E. Copreni, C. Mascia, M. Bardessono, M. Goia, F. Biasi, M. Conese, G. Poli, F. Bussolino and V. De Rose (2008). "Tumor necrosis factor-alpha in airway secretions from cystic fibrosis patients upregulate endothelial adhesion molecules and induce airway epithelial cell apoptosis: implications for cystic fibrosis lung disease." Int J Immunopathol Pharmacol **21**(4): 851-865.

Moniz, S., M. Sousa, B. J. Moraes, A. I. Mendes, M. Palma, C. Barreto, J. I. Fragata, M. D. Amaral and P. Matos (2013). "HGF stimulation of Rac1 signaling enhances pharmacological correction of the most prevalent cystic fibrosis mutant F508del-CFTR." ACS Chem Biol **8**(2): 432-442.

Morfini, G. A., Y. M. You, S. L. Pollema, A. Kaminska, K. Liu, K. Yoshioka, B. Bjorkblom, E. T. Coffey, C. Bagnato, D. Han, C. F. Huang, G. Banker, G. Pigino and S. T. Brady (2009). "Pathogenic huntingtin inhibits fast axonal transport by activating JNK3 and phosphorylating kinesin." Nat Neurosci **12**(7): 864-871.

Morito, D., K. Hirao, Y. Oda, N. Hosokawa, F. Tokunaga, D. M. Cyr, K. Tanaka, K. Iwai and K. Nagata (2008). "Gp78 cooperates with RMA1 in endoplasmic reticulum-associated degradation of CFTRDeltaF508." Mol Biol Cell **19**(4): 1328-1336.

Morris, A. P., S. A. Cunningham, D. J. Benos and R. A. Frizzell (1993). "Glycosylation status of endogenous CFTR does not affect cAMP-stimulated Cl- secretion in epithelial cells." Am J Physiol **265**(3 Pt 1): C688-694.

Mu, T. W., D. M. Fowler and J. W. Kelly (2008). "Partial restoration of mutant enzyme homeostasis in three distinct lysosomal storage disease cell lines by altering calcium homeostasis." PLoS Biol **6**(2): e26.

Mungai, P. T., G. B. Waypa, A. Jairaman, M. Prakriya, D. Dokic, M. K. Ball and P. T. Schumacker (2011). "Hypoxia triggers AMPK activation through reactive oxygen species-mediated activation of calcium release-activated calcium channels." Mol Cell Biol **31**(17): 3531-3545.

Namkung, W., Z. Yao, W. E. Finkbeiner and A. S. Verkman (2011). "Small-molecule activators of TMEM16A, a calcium-activated chloride channel, stimulate epithelial chloride secretion and intestinal contraction." FASEB J **25**(11): 4048-4062.

Ninomiya-Tsuji, J., T. Kajino, K. Ono, T. Ohtomo, M. Matsumoto, M. Shiina, M. Mihara, M. Tsuchiya and K. Matsumoto (2003). "A resorcylic acid lactone, 5Z-7-oxozeaenol, prevents inflammation by inhibiting the catalytic activity of TAK1 MAPK kinase kinase." J Biol Chem **278**(20): 18485-18490.

Norez, C., F. Antigny, F. Becq and C. Vandebrouck (2006). "Maintaining low Ca2+ level in the endoplasmic reticulum restores abnormal endogenous F508del-CFTR trafficking in airway epithelial cells." Traffic **7**(5): 562-573.

Norez, C., F. Antigny, S. Noel, C. Vandebrouck and F. Becq (2009). "A cystic fibrosis respiratory epithelial cell chronically treated by miglustat acquires a non-cystic fibrosis-like phenotype." Am J Respir Cell Mol Biol **41**(2): 217-225.

Odolczyk, N., J. Fritsch, C. Norez, N. Servel, M. F. da Cunha, S. Bitam, A. Kupniewska, L. Wiszniewski, J. Colas, K. Tarnowski, D. Tondelier, A. Roldan, E. L. Saussereau, P. Melin-Heschel, G. Wieczorek, G. L. Lukacs, M. Dadlez, G. Faure, H. Herrmann, M. Ollero, F. Becq, P. Zielenkiewicz and A. Edelman (2013). "Discovery of novel potent DeltaF508-CFTR correctors that target the nucleotide binding domain." EMBO Mol Med **5**(10): 1484-1501.

Oh, C., S. Park, E. K. Lee and Y. J. Yoo (2013). "Downregulation of ubiquitin level via knockdown of polyubiquitin gene Ubb as potential cancer therapeutic intervention." Sci Rep **3**: 2623.

Okiyoneda, T., P. M. Apaja and G. L. Lukacs (2011). "Protein quality control at the plasma membrane." Curr Opin Cell Biol **23**(4): 483-491.

Okiyoneda, T., H. Barriere, M. Bagdany, W. M. Rabeh, K. Du, J. Hohfeld, J. C. Young and G. L. Lukacs (2010). "Peripheral protein quality control removes unfolded CFTR from the plasma membrane." Science **329**(5993): 805-810.

Okiyoneda, T., G. Veit, J. F. Dekkers, M. Bagdany, N. Soya, H. Xu, A. Roldan, A. S. Verkman, M. Kurth, A. Simon, T. Hegedus, J. M. Beekman and G. L. Lukacs (2013). "Mechanism-based corrector combination restores DeltaF508-CFTR folding and function." Nat Chem Biol **9**(7): 444-454.

Olivari, S. and M. Molinari (2007). "Glycoprotein folding and the role of EDEM1, EDEM2 and EDEM3 in degradation of folding-defective glycoproteins." FEBS Lett **581**(19): 3658-3664.

Ostedgaard, L. S., O. Baldursson, D. W. Vermeer, M. J. Welsh and A. D. Robertson (2000). "A functional R domain from cystic fibrosis transmembrane conductance regulator is predominantly unstructured in solution." Proc Natl Acad Sci U S A **97**(10): 5657-5662.

Ostedgaard, L. S., O. Baldursson and M. J. Welsh (2001). "Regulation of the cystic fibrosis transmembrane conductance regulator Cl- channel by its R domain." J Biol Chem **276**(11): 7689-7692.

Ostedgaard, L. S., D. P. Rich, L. G. DeBerg and M. J. Welsh (1997). "Association of domains within the cystic fibrosis transmembrane conductance regulator." Biochemistry **36**(6): 1287-1294.

Pan, J., Q. G. Zhang and G. Y. Zhang (2005). "The neuroprotective effects of K252a through inhibiting MLK3/MKK7/JNK3 signaling pathway on ischemic brain injury in rat hippocampal CA1 region." Neuroscience **131**(1): 147-159.

Park, J. and A. Y. Liu (2001). "JNK phosphorylates the HSF1 transcriptional activation domain: role of JNK in the regulation of the heat shock response." J Cell Biochem **82**(2): 326-338.

Patrick, A. E. and P. J. Thomas (2012). "Development of CFTR Structure." Front Pharmacol **3**: 162.

Pedemonte, N. and L. J. Galietta (2012). "Pharmacological Correctors of Mutant CFTR Mistrafficking." Front Pharmacol **3**: 175.

Pedemonte, N., G. L. Lukacs, K. Du, E. Caci, O. Zegarra-Moran, L. J. Galietta and A. S. Verkman (2005). "Small-molecule correctors of defective DeltaF508-CFTR cellular processing identified by high-throughput screening." J Clin Invest **115**(9): 2564-2571.

Pedemonte, N., G. L. Lukacs, K. Du, E. Caci, O. Zegarra-Moran, L. J. V. Galietta and A. S. Verkman (2005). "Small-molecule correctors of defective DeltaF508-CFTR cellular processing identified by high-throughput screening." J Clin Invest **115**(16127463): 2564-2571.

Pedemonte, N., V. Tomati, E. Sondo, E. Caci, E. Millo, A. Armirotti, G. Damonte, O. Zegarra-Moran and L. J. Galietta (2011). "Dual activity of aminoarylthiazoles on the trafficking and gating defects of the cystic fibrosis transmembrane conductance regulator chloride channel caused by cystic fibrosis mutations." J Biol Chem **286**(17): 15215-15226.

Penmatsa, H., W. Zhang, S. Yarlagadda, C. Li, V. G. Conoley, J. Yue, S. W. Bahouth, R. K. Buddington, G. Zhang, D. J. Nelson, M. D. Sonecha, V. Manganiello, J. J. Wine and A. P. Naren (2010). "Compartmentalized cyclic adenosine 3',5'-monophosphate at the plasma membrane clusters PDE3A and cystic fibrosis transmembrane conductance regulator into microdomains." Mol Biol Cell **21**(6): 1097-1110.

Picciotto, M. R., J. A. Cohn, G. Bertuzzi, P. Greengard and A. C. Nairn (1992). "Phosphorylation of the cystic fibrosis transmembrane conductance regulator." J Biol Chem **267**(18): 12742-12752.

Pind, S., J. R. Riordan and D. B. Williams (1994). "Participation of the endoplasmic reticulum chaperone calnexin (p88, IP90) in the biogenesis of the cystic fibrosis transmembrane conductance regulator." J Biol Chem **269**(17): 12784-12788.

Pittman, N., G. Shue, N. S. LeLeiko and M. J. Walsh (1995). "Transcription of cystic fibrosis transmembrane conductance regulator requires a CCAAT-like element for both basal and cAMP-mediated regulation." J Biol Chem **270**(48): 28848-28857.

Powers, E. T., R. I. Morimoto, A. Dillin, J. W. Kelly and W. E. Balch (2009). "Biological and chemical approaches to diseases of proteostasis deficiency." Annu Rev Biochem **78**: 959-991.

Prodromou, C., G. Siligardi, R. O'Brien, D. N. Woolfson, L. Regan, B. Panaretou, J. E. Ladbury, P. W. Piper and L. H. Pearl (1999). "Regulation of Hsp90 ATPase activity by tetratricopeptide repeat (TPR)-domain co-chaperones." EMBO J **18**(3): 754-762.

Puchelle, E., D. Gaillard, D. Ploton, J. Hinnrasky, C. Fuchey, M. C. Boutterin, J. Jacquot, D. Dreyer, A. Pavirani and W. Dalemans (1992). "Differential localization of the cystic

fibrosis transmembrane conductance regulator in normal and cystic fibrosis airway epithelium." Am J Respir Cell Mol Biol 7(5): 485-491.
Qi, M. and E. A. Elion (2005). "MAP kinase pathways." J Cell Sci **118**(Pt 16): 3569-3572.
Qu, B. H. and P. J. Thomas (1996). "Alteration of the cystic fibrosis transmembrane conductance regulator folding pathway." J Biol Chem **271**(13): 7261-7264.
Quinton, P. M. (1983). "Chloride impermeability in cystic fibrosis." Nature **301**(5899): 421-422.
Rabeh, W. M., F. Bossard, H. Xu, T. Okiyoneda, M. Bagdany, C. M. Mulvihill, K. Du, S. di Bernardo, Y. Liu, L. Konermann, A. Roldan and G. L. Lukacs (2012). "Correction of both NBD1 energetics and domain interface is required to restore DeltaF508 CFTR folding and function." Cell **148**(1-2): 150-163.
Racioppi, L. and A. R. Means (2012). "Calcium/calmodulin-dependent protein kinase kinase 2: roles in signaling and pathophysiology." J Biol Chem **287**(38): 31658-31665.
Racioppi, L., P. K. Noeldner, F. Lin, S. Arvai and A. R. Means (2012). "Calcium/calmodulin-dependent protein kinase kinase 2 regulates macrophage-mediated inflammatory responses." J Biol Chem **287**(14): 11579-11591.
Rajalingam, K. and I. Dikic (2011). "Healthy ageing through regulated proteostasis." EMBO J **30**(15): 2983-2985.
Ramalho, A. S., S. Beck, M. Meyer, D. Penque, G. R. Cutting and M. D. Amaral (2002). "Five percent of normal cystic fibrosis transmembrane conductance regulator mRNA ameliorates the severity of pulmonary disease in cystic fibrosis." Am J Respir Cell Mol Biol **27**(5): 619-627.
Ramasamy, A., A. Mondry, C. C. Holmes and D. G. Altman (2008). "Key issues in conducting a meta-analysis of gene expression microarray datasets." PLoS Med **5**(9): e184.
Reijonen, S., J. P. Kukkonen, A. Hyrskyluoto, J. Kivinen, M. Kairisalo, N. Takei, D. Lindholm and L. Korhonen (2010). "Downregulation of NF-kappaB signaling by mutant huntingtin proteins induces oxidative stress and cell death." Cell Mol Life Sci **67**(11): 1929-1941.
Ren, H. Y., D. E. Grove, O. De La Rosa, S. A. Houck, P. Sopha, F. Van Goor, B. J. Hoffman and D. M. Cyr (2013). "VX-809 corrects folding defects in CFTR through action on membrane-spanning domain1 (MSD1)." Mol Biol Cell.
Rhodes, D. R., T. R. Barrette, M. A. Rubin, D. Ghosh and A. M. Chinnaiyan (2002). "Meta-analysis of microarrays: interstudy validation of gene expression profiles reveals pathway dysregulation in prostate cancer." Cancer Res **62**(15): 4427-4433.
Rhodes, D. R., J. Yu, K. Shanker, N. Deshpande, R. Varambally, D. Ghosh, T. Barrette, A. Pandey and A. M. Chinnaiyan (2004). "Large-scale meta-analysis of cancer microarray data identifies common transcriptional profiles of neoplastic transformation and progression." Proc Natl Acad Sci U S A **101**(25): 9309-9314.
Ribeiro, C. M. (2006). "The role of intracellular calcium signals in inflammatory responses of polarised cystic fibrosis human airway epithelia." Drugs R D 7(1): 17-31.
Riordan, J. R. (2008). "CFTR function and prospects for therapy." Annu Rev Biochem **77**: 701-726.
Riordan, J. R., J. M. Rommens, B. Kerem, N. Alon, R. Rozmahel, Z. Grzelczak, J. Zielenski, S. Lok, N. Plavsic and J. L. Chou (1989). "Identification of the cystic fibrosis gene: cloning and characterization of complementary DNA." Science **245**(2475911): 1066-1073.
Riordan, J. R., J. M. Rommens, B. Kerem, N. Alon, R. Rozmahel, Z. Grzelczak, J. Zielenski, S. Lok, N. Plavsic, J. L. Chou and et al. (1989). "Identification of the cystic fibrosis gene: cloning and characterization of complementary DNA." Science **245**(4922): 1066-1073.
Risco, A. and A. Cuenda (2012). "New Insights into the p38gamma and p38delta MAPK Pathways." J Signal Transduct **2012**: 520289.
Robert, R., G. W. Carlile, J. Liao, H. Balghi, P. Lesimple, N. Liu, B. Kus, D. Rotin, M. Wilke, H. R. de Jonge, B. J. Scholte, D. Y. Thomas and J. W. Hanrahan (2010). "Correction of the Delta phe508 cystic fibrosis transmembrane conductance regulator trafficking defect by the bioavailable compound glafenine." Mol Pharmacol **77**(6): 922-930.
Robert, R., G. W. Carlile, C. Pavel, N. Liu, S. M. Anjos, J. Liao, Y. Luo, D. Zhang, D. Y. Thomas and J. W. Hanrahan (2008). "Structural analog of sildenafil identified as a novel corrector of the F508del-CFTR trafficking defect." Mol Pharmacol **73**(2): 478-489.
Rommens, J. M., M. C. Iannuzzi, B. Kerem, M. L. Drumm, G. Melmer, M. Dean, R. Rozmahel, J. L. Cole, D. Kennedy, N. Hidaka and et al. (1989). "Identification of the cystic fibrosis gene: chromosome walking and jumping." Science **245**(4922): 1059-1065.

Rosenecker, J., S. Huth and C. Rudolph (2006). "Gene therapy for cystic fibrosis lung disease: current status and future perspectives." Curr Opin Mol Ther **8**(5): 439-445.

Rosser, M. F., D. E. Grove, L. Chen and D. M. Cyr (2008). "Assembly and misassembly of cystic fibrosis transmembrane conductance regulator: folding defects caused by deletion of F508 occur before and after the calnexin-dependent association of membrane spanning domain (MSD) 1 and MSD2." Mol Biol Cell **19**(11): 4570-4579.

Rubenstein, R. C., M. E. Egan and P. L. Zeitlin (1997). "In vitro pharmacologic restoration of CFTR-mediated chloride transport with sodium 4-phenylbutyrate in cystic fibrosis epithelial cells containing delta F508-CFTR." J Clin Invest **100**(10): 2457-2465.

Sampson, H. M., R. Robert, J. Liao, E. Matthes, G. W. Carlile, J. W. Hanrahan and D. Y. Thomas (2011). "Identification of a NBD1-binding pharmacological chaperone that corrects the trafficking defect of F508del-CFTR." Chem Biol **18**(2): 231-242.

Santagata, S., M. L. Mendillo, Y. C. Tang, A. Subramanian, C. C. Perley, S. P. Roche, B. Wong, R. Narayan, H. Kwon, M. Koeva, A. Amon, T. R. Golub, J. A. Porco, Jr., L. Whitesell and S. Lindquist (2013). "Tight coordination of protein translation and HSF1 activation supports the anabolic malignant state." Science **341**(6143): 1238303.

Savage, M. J., Y. G. Lin, J. R. Ciallella, D. G. Flood and R. W. Scott (2002). "Activation of c-Jun N-terminal kinase and p38 in an Alzheimer's disease model is associated with amyloid deposition." J Neurosci **22**(9): 3376-3385.

Sawyer, T. K., J. C. Wu, J. R. Sawyer and J. M. English (2013). "Protein kinase inhibitors: breakthrough medicines and the next generation." Expert Opin Investig Drugs **22**(6): 675-678.

Saxena, A., Y. K. Banasavadi-Siddegowda, Y. Fan, S. Bhattacharya, G. Roy, D. R. Giovannucci, R. A. Frizzell and X. Wang (2012). "Human heat shock protein 105/110 kDa (Hsp105/110) regulates biogenesis and quality control of misfolded cystic fibrosis transmembrane conductance regulator at multiple levels." J Biol Chem **287**(23): 19158-19170.

Saxena, S. K. and S. Kaur (2006). "Rab27a negatively regulates CFTR chloride channel function in colonic epithelia: involvement of the effector proteins in the regulatory mechanism." Biochem Biophys Res Commun **346**(1): 259-267.

Saxena, S. K., S. Kaur and C. George (2006). "Rab4GTPase modulates CFTR function by impairing channel expression at plasma membrane." Biochem Biophys Res Commun **341**(1): 184-191.

Schreiber, R., R. Greger, R. Nitschke and K. Kunzelmann (1997). "Cystic fibrosis transmembrane conductance regulator activates water conductance in Xenopus oocytes." Pflugers Arch **434**(6): 841-847.

Serohijos, A. W., T. Hegedus, A. A. Aleksandrov, L. He, L. Cui, N. V. Dokholyan and J. R. Riordan (2008). "Phenylalanine-508 mediates a cytoplasmic-membrane domain contact in the CFTR 3D structure crucial to assembly and channel function." Proc Natl Acad Sci U S A **105**(9): 3256-3261.

Shao, S. and R. S. Hegde (2011). "Membrane protein insertion at the endoplasmic reticulum." Annu Rev Cell Dev Biol **27**: 25-56.

Sharma, M., F. Pampinella, C. Nemes, M. Benharouga, J. So, K. Du, K. G. Bache, B. Papsin, N. Zerangue, H. Stenmark and G. L. Lukacs (2004). "Misfolding diverts CFTR from recycling to degradation: quality control at early endosomes." J Cell Biol **164**(6): 923-933.

Sheppard, D. N. (2011). "Cystic fibrosis: CFTR correctors to the rescue." Chem Biol **18**(2): 145-147.

Shigemizu, D., Z. Hu, J. H. Hung, C. L. Huang, Y. Wang and C. DeLisi (2012). "Using functional signatures to identify repositioned drugs for breast, myelogenous leukemia and prostate cancer." PLoS Comput Biol **8**(2): e1002347.

Short, D. B., K. W. Trotter, D. Reczek, S. M. Kreda, A. Bretscher, R. C. Boucher, M. J. Stutts and S. L. Milgram (1998). "An apical PDZ protein anchors the cystic fibrosis transmembrane conductance regulator to the cytoskeleton." J Biol Chem **273**(31): 19797-19801.

Shoulders, M. D., L. M. Ryno, J. C. Genereux, J. J. Moresco, P. G. Tu, C. Wu, J. R. Yates, 3rd, A. I. Su, J. W. Kelly and R. L. Wiseman (2013). "Stress-independent activation of XBP1s and/or ATF6 reveals three functionally diverse ER proteostasis environments." Cell Rep **3**(4): 1279-1292.

Silva, M. C., M. D. Amaral and R. I. Morimoto (2013). "Neuronal reprograming of protein homeostasis by calcium-dependent regulation of the heat shock response." PLoS Genet **9**(8): e1003711.

Silva, M. C., S. Fox, M. Beam, H. Thakkar, M. D. Amaral and R. I. Morimoto (2011). "A genetic screening strategy identifies novel regulators of the proteostasis network." PLoS Genet **7**(12): e1002438.

Silvis, M. R., C. A. Bertrand, N. Ameen, F. Golin-Bisello, M. B. Butterworth, R. A. Frizzell and N. A. Bradbury (2009). "Rab11b regulates the apical recycling of the cystic fibrosis transmembrane conductance regulator in polarized intestinal epithelial cells." Mol Biol Cell **20**(8): 2337-2350.

Sirota, M., J. T. Dudley, J. Kim, A. P. Chiang, A. A. Morgan, A. Sweet-Cordero, J. Sage and A. J. Butte (2011). "Discovery and preclinical validation of drug indications using compendia of public gene expression data." Sci Transl Med **3**(96): 96ra77.

Skach, W. R. (2000). "Defects in processing and trafficking of the cystic fibrosis transmembrane conductance regulator." Kidney Int **57**(3): 825-831.

Snodgrass, S. M., K. M. Cihil, P. K. Cornuet, M. M. Myerburg and A. Swiatecka-Urban (2013). "Tgf-beta1 inhibits Cftr biogenesis and prevents functional rescue of DeltaF508-Cftr in primary differentiated human bronchial epithelial cells." PLoS One **8**(5): e63167.

Son, Y., Y. K. Cheong, N. H. Kim, H. T. Chung, D. G. Kang and H. O. Pae (2011). "Mitogen-Activated Protein Kinases and Reactive Oxygen Species: How Can ROS Activate MAPK Pathways?" J Signal Transduct **2011**: 792639.

Stahmann, N., A. Woods, K. Spengler, A. Heslegrave, R. Bauer, S. Krause, B. Viollet, D. Carling and R. Heller (2010). "Activation of AMP-activated protein kinase by vascular endothelial growth factor mediates endothelial angiogenesis independently of nitric-oxide synthase." J Biol Chem **285**(14): 10638-10652.

Strickland, E., B. H. Qu, L. Millen and P. J. Thomas (1997). "The molecular chaperone Hsc70 assists the in vitro folding of the N-terminal nucleotide-binding domain of the cystic fibrosis transmembrane conductance regulator." J Biol Chem **272**(41): 25421-25424.

Stutts, M. J., C. M. Canessa, J. C. Olsen, M. Hamrick, J. A. Cohn, B. C. Rossier and R. C. Boucher (1995). "CFTR as a cAMP-dependent regulator of sodium channels." Science **269**(5225): 847-850.

Stutts, M. J., B. C. Rossier and R. C. Boucher (1997). "Cystic fibrosis transmembrane conductance regulator inverts protein kinase A-mediated regulation of epithelial sodium channel single channel kinetics." J Biol Chem **272**(22): 14037-14040.

Su, P. H., Y. W. Lin, R. L. Huang, Y. P. Liao, H. Y. Lee, H. C. Wang, T. K. Chao, C. K. Chen, M. W. Chan, T. Y. Chu, M. H. Yu and H. C. Lai (2013). "Epigenetic silencing of PTPRR activates MAPK signaling, promotes metastasis and serves as a biomarker of invasive cervical cancer." Oncogene **32**(1): 15-26.

Suaud, L., K. Miller, L. Alvey, W. Yan, A. Robay, C. Kebler, J. L. Kreindler, S. Guttentag, M. J. Hubbard and R. C. Rubenstein (2011). "ERp29 regulates DeltaF508 and wild-type cystic fibrosis transmembrane conductance regulator (CFTR) trafficking to the plasma membrane in cystic fibrosis (CF) and non-CF epithelial cells." J Biol Chem **286**(24): 21239-21253.

Sun, F., R. Zhang, X. Gong, X. Geng, P. F. Drain and R. A. Frizzell (2006). "Derlin-1 promotes the efficient degradation of the cystic fibrosis transmembrane conductance regulator (CFTR) and CFTR folding mutants." J Biol Chem **281**(48): 36856-36863.

Swenson-Fields, K. I., J. C. Sandquist, J. Rossol-Allison, I. C. Blat, K. Wennerberg, K. Burridge and A. R. Means (2008). "MLK3 limits activated Galphaq signaling to Rho by binding to p63RhoGEF." Mol Cell **32**(1): 43-56.

Swiatecka-Urban, A., M. Duhaime, B. Coutermarsh, K. H. Karlson, J. Collawn, M. Milewski, G. R. Cutting, W. B. Guggino, G. Langford and B. A. Stanton (2002). "PDZ domain interaction controls the endocytic recycling of the cystic fibrosis transmembrane conductance regulator." J Biol Chem **277**(42): 40099-40105.

Swiatecka-Urban, A., L. Talebian, E. Kanno, S. Moreau-Marquis, B. Coutermarsh, K. Hansen, K. H. Karlson, R. Barnaby, R. E. Cheney, G. M. Langford, M. Fukuda and B. A. Stanton (2007). "Myosin Vb is required for trafficking of the cystic fibrosis transmembrane conductance regulator in Rab11a-specific apical recycling endosomes in polarized human airway epithelial cells." J Biol Chem **282**(32): 23725-23736.

Tanaka, K., H. Minami, M. Kota, K. Kuwamura and E. Kohmura (2005). "Treatment of cerebral vasospasm with intra-arterial fasudil hydrochloride." Neurosurgery **56**(2): 214-223; discussion 214-223.

Terman, B. I., M. Dougher-Vermazen, M. E. Carrion, D. Dimitrov, D. C. Armellino, D. Gospodarowicz and P. Bohlen (1992). "Identification of the KDR tyrosine kinase as a receptor for vascular endothelial cell growth factor." Biochem Biophys Res Commun **187**(3): 1579-1586.

Thelin, W. R., M. Kesimer, R. Tarran, S. M. Kreda, B. R. Grubb, J. K. Sheehan, M. J. Stutts and S. L. Milgram (2005). "The cystic fibrosis transmembrane conductance regulator is regulated by a direct interaction with the protein phosphatase 2A." J Biol Chem **280**(50): 41512-41520.

Tisdale, E. J., J. R. Bourne, R. Khosravi-Far, C. J. Der and W. E. Balch (1992). "GTP-binding mutants of rab1 and rab2 are potent inhibitors of vesicular transport from the endoplasmic reticulum to the Golgi complex." J Cell Biol **119**(4): 749-761.

Tokumitsu, H., H. Inuzuka, Y. Ishikawa and R. Kobayashi (2003). "A single amino acid difference between alpha and beta Ca2+/calmodulin-dependent protein kinase kinase dictates sensitivity to the specific inhibitor, STO-609." J Biol Chem **278**(13): 10908-10913.

Trapnell, B. C., C. S. Chu, P. K. Paakko, T. C. Banks, K. Yoshimura, V. J. Ferrans, M. S. Chernick and R. G. Crystal (1991). "Expression of the cystic fibrosis transmembrane conductance regulator gene in the respiratory tract of normal individuals and individuals with cystic fibrosis." Proc Natl Acad Sci U S A **88**(15): 6565-6569.

Trouve, P., M. A. Le Drevo, M. Kerbiriou, G. Friocourt, Y. Fichou, D. Gillet and C. Ferec (2007). "Annexin V is directly involved in cystic fibrosis transmembrane conductance regulator's chloride channel function." Biochim Biophys Acta **1772**(10): 1121-1133.

Trzcinska-Daneluti, A. M., D. Ly, L. Huynh, C. Jiang, C. Fladd and D. Rotin (2009). "High-content functional screen to identify proteins that correct F508del-CFTR function." Mol Cell Proteomics **8**(4): 780-790.

Trzcinska-Daneluti, A. M., L. Nguyen, C. Jiang, C. Fladd, D. Uehling, M. Prakesch, R. Al-awar and D. Rotin (2012). "Use of kinase inhibitors to correct DeltaF508-CFTR function." Mol Cell Proteomics **11**(9): 745-757.

Urano, F., X. Wang, A. Bertolotti, Y. Zhang, P. Chung, H. P. Harding and D. Ron (2000). "Coupling of stress in the ER to activation of JNK protein kinases by transmembrane protein kinase IRE1." Science **287**(5453): 664-666.

Van Goor, F., S. Hadida, P. D. Grootenhuis, B. Burton, D. Cao, T. Neuberger, A. Turnbull, A. Singh, J. Joubran, A. Hazlewood, J. Zhou, J. McCartney, V. Arumugam, C. Decker, J. Yang, C. Young, E. R. Olson, J. J. Wine, R. A. Frizzell, M. Ashlock and P. Negulescu (2009). "Rescue of CF airway epithelial cell function in vitro by a CFTR potentiator, VX-770." Proc Natl Acad Sci U S A **106**(44): 18825-18830.

Van Goor, F., K. S. Straley, D. Cao, J. Gonzalez, S. Hadida, A. Hazlewood, J. Joubran, T. Knapp, L. R. Makings, M. Miller, T. Neuberger, E. Olson, V. Panchenko, J. Rader, A. Singh, J. H. Stack, R. Tung, P. D. Grootenhuis and P. Negulescu (2006). "Rescue of DeltaF508-CFTR trafficking and gating in human cystic fibrosis airway primary cultures by small molecules." Am J Physiol Lung Cell Mol Physiol **290**(6): L1117-1130.

Van Goor, F., K. S. Straley, D. Cao, J. Gonzalez, S. Hadida, A. Hazlewood, J. Joubran, T. Knapp, L. R. Makings, M. Miller, T. Neuberger, E. Olson, V. Panchenko, J. Rader, A. Singh, J. H. Stack, R. Tung, P. D. J. Grootenhuis and P. Negulescu (2006). "Rescue of DeltaF508-CFTR trafficking and gating in human cystic fibrosis airway primary cultures by small molecules." Am J Physiol Lung Cell Mol Physiol **290**(16443646): 1117-1130.

Vandivier, R. W., T. R. Richens, S. A. Horstmann, A. M. deCathelineau, M. Ghosh, S. D. Reynolds, Y. Q. Xiao, D. W. Riches, J. Plumb, E. Vachon, G. P. Downey and P. M. Henson (2009). "Dysfunctional cystic fibrosis transmembrane conductance regulator inhibits phagocytosis of apoptotic cells with proinflammatory consequences." Am J Physiol Lung Cell Mol Physiol **297**(4): L677-686.

Varga, K., A. Jurkuvenaite, J. Wakefield, J. S. Hong, J. S. Guimbellot, C. J. Venglarik, A. Niraj, M. Mazur, E. J. Sorscher, J. F. Collawn and Z. Bebok (2004). "Efficient intracellular processing of the endogenous cystic fibrosis transmembrane conductance regulator in epithelial cell lines." J Biol Chem **279**(21): 22578-22584.

Venglarik, C. J., B. D. Schultz, R. A. Frizzell and R. J. Bridges (1994). "ATP alters current fluctuations of cystic fibrosis transmembrane conductance regulator: evidence for a three-state activation mechanism." J Gen Physiol **104**(1): 123-146.

Venkatakrishnan, A., A. A. Stecenko, G. King, T. R. Blackwell, K. L. Brigham, J. W. Christman and T. S. Blackwell (2000). "Exaggerated activation of nuclear factor-kappaB and altered IkappaB-beta processing in cystic fibrosis bronchial epithelial cells." Am J Respir Cell Mol Biol **23**(3): 396-403.

Verhaeghe, C., K. Delbecque, L. de Leval, C. Oury and V. Bours (2007). "Early inflammation in the airways of a cystic fibrosis foetus." J Cyst Fibros **6**(4): 304-308.

Vij, N., S. Fang and P. L. Zeitlin (2006). "Selective inhibition of endoplasmic reticulum-associated degradation rescues DeltaF508-cystic fibrosis transmembrane regulator and suppresses interleukin-8 levels: therapeutic implications." J Biol Chem **281**(25): 17369-17378.

Wagner, E. F. and A. R. Nebreda (2009). "Signal integration by JNK and p38 MAPK pathways in cancer development." Nat Rev Cancer **9**(8): 537-549.

Wang, B., H. Heath-Engel, D. Zhang, N. Nguyen, D. Y. Thomas, J. W. Hanrahan and G. C. Shore (2008). "BAP31 interacts with Sec61 translocons and promotes retrotranslocation of CFTRDeltaF508 via the derlin-1 complex." Cell **133**(6): 1080-1092.

Wang, Q., B. Liang, N. A. Shirwany and M. H. Zou (2011). "2-Deoxy-D-glucose treatment of endothelial cells induces autophagy by reactive oxygen species-mediated activation of the AMP-activated protein kinase." PLoS One **6**(2): e17234.

Wang, X., J. Matteson, Y. An, B. Moyer, J. S. Yoo, S. Bannykh, I. A. Wilson, J. R. Riordan and W. E. Balch (2004). "COPII-dependent export of cystic fibrosis transmembrane conductance regulator from the ER uses a di-acidic exit code." J Cell Biol **167**(1): 65-74.

Wang, X., J. Venable, P. LaPointe, D. M. Hutt, A. V. Koulov, J. Coppinger, C. Gurkan, W. Kellner, J. Matteson, H. Plutner, J. R. Riordan, J. W. Kelly, J. R. Yates, 3rd and W. E. Balch (2006). "Hsp90 cochaperone Aha1 downregulation rescues misfolding of CFTR in cystic fibrosis." Cell **127**(4): 803-815.

Wang, Y., T. W. Loo, M. C. Bartlett and D. M. Clarke (2007). "Additive effect of multiple pharmacological chaperones on maturation of CFTR processing mutants." Biochem J **406**(2): 257-263.

Wang, Y., T. W. Loo, M. C. Bartlett and D. M. Clarke (2007). "Correctors promote maturation of cystic fibrosis transmembrane conductance regulator (CFTR)-processing mutants by binding to the protein." J Biol Chem **282**(46): 33247-33251.

Wang, Y., T. W. Loo, M. C. Bartlett and D. M. Clarke (2007). "Modulating the folding of P-glycoprotein and cystic fibrosis transmembrane conductance regulator truncation mutants with pharmacological chaperones." Mol Pharmacol **71**(3): 751-758.

Ward, C. L. and R. R. Kopito (1994). "Intracellular turnover of cystic fibrosis transmembrane conductance regulator. Inefficient processing and rapid degradation of wild-type and mutant proteins." J Biol Chem **269**(7523390): 25710-25718.

Ward, C. L., S. Omura and R. R. Kopito (1995). "Degradation of CFTR by the ubiquitin-proteasome pathway." Cell **83**(1): 121-127.

Wark, P. A. and V. McDonald (2003). "Nebulised hypertonic saline for cystic fibrosis." Cochrane Database Syst Rev(1): CD001506.

Weber, A. J., G. Soong, R. Bryan, S. Saba and A. Prince (2001). "Activation of NF-kappaB in airway epithelial cells is dependent on CFTR trafficking and Cl- channel function." Am J Physiol Lung Cell Mol Physiol **281**(1): L71-78.

Welsh, M. J. and A. E. Smith (1993). "Molecular mechanisms of CFTR chloride channel dysfunction in cystic fibrosis." Cell **73**(7): 1251-1254.

Wilkinson, D. J., T. V. Strong, M. K. Mansoura, D. L. Wood, S. S. Smith, F. S. Collins and D. C. Dawson (1997). "CFTR activation: additive effects of stimulatory and inhibitory phosphorylation sites in the R domain." Am J Physiol **273**(1 Pt 1): L127-133.

Wolde, M., A. Fellows, J. Cheng, A. Kivenson, B. Coutermarsh, L. Talebian, K. Karlson, A. Piserchio, D. F. Mierke, B. A. Stanton, W. B. Guggino and D. R. Madden (2007). "Targeting CAL as a negative regulator of DeltaF508-CFTR cell-surface expression: an RNA interference and structure-based mutagenetic approach." J Biol Chem **282**(11): 8099-8109.

Xu, G. W., M. Ali, T. E. Wood, D. Wong, N. Maclean, X. Wang, M. Gronda, M. Skrtic, X. Li, R. Hurren, X. Mao, M. Venkatesan, R. Beheshti Zavareh, T. Ketela, J. C. Reed, D. Rose, J.

Moffat, R. A. Batey, S. Dhe-Paganon and A. D. Schimmer (2010). "The ubiquitin-activating enzyme E1 as a therapeutic target for the treatment of leukemia and multiple myeloma." Blood **115**(11): 2251-2259.

Yamasaki, T., H. Kawasaki and H. Nishina (2012). "Diverse Roles of JNK and MKK Pathways in the Brain." J Signal Transduct **2012**: 459265.

Yang, Y., S. Janich, J. A. Cohn and J. M. Wilson (1993). "The common variant of cystic fibrosis transmembrane conductance regulator is recognized by hsp70 and degraded in a pre-Golgi nonlysosomal compartment." Proc Natl Acad Sci U S A **90**(20): 9480-9484.

Ye, S., K. Cihil, D. B. Stolz, J. M. Pilewski, B. A. Stanton and A. Swiatecka-Urban (2010). "c-Cbl facilitates endocytosis and lysosomal degradation of cystic fibrosis transmembrane conductance regulator in human airway epithelial cells." J Biol Chem **285**(35): 27008-27018.

Yoo, J. S., B. D. Moyer, S. Bannykh, H. M. Yoo, J. R. Riordan and W. E. Balch (2002). "Non-conventional trafficking of the cystic fibrosis transmembrane conductance regulator through the early secretory pathway." J Biol Chem **277**(13): 11401-11409.

Yoshida, Y., T. Chiba, F. Tokunaga, H. Kawasaki, K. Iwai, T. Suzuki, Y. Ito, K. Matsuoka, M. Yoshida, K. Tanaka and T. Tai (2002). "E3 ubiquitin ligase that recognizes sugar chains." Nature **418**(6896): 438-442.

Younger, J. M., L. Chen, H. Y. Ren, M. F. Rosser, E. L. Turnbull, C. Y. Fan, C. Patterson and D. M. Cyr (2006). "Sequential quality-control checkpoints triage misfolded cystic fibrosis transmembrane conductance regulator." Cell **126**(3): 571-582.

Zhang, D., F. Ciciriello, S. M. Anjos, A. Carissimo, J. Liao, G. W. Carlile, H. Balghi, R. Robert, A. Luini, J. W. Hanrahan and D. Y. Thomas (2012). "Ouabain Mimics Low Temperature Rescue of F508del-CFTR in Cystic Fibrosis Epithelial Cells." Front Pharmacol **3**: 176.

Zhang, T., H. Y. Hwang, H. Hao, C. Talbot, Jr. and J. Wang (2012). "Caenorhabditis elegans RNA-processing protein TDP-1 regulates protein homeostasis and life span." J Biol Chem **287**(11): 8371-8382.

Zhao, J., D. S. Pei, Q. G. Zhang and G. Y. Zhang (2007). "Down-regulation Cdc42 attenuates neuronal apoptosis through inhibiting MLK3/JNK3 cascade during ischemic reperfusion in rat hippocampus." Cell Signal **19**(4): 831-843.

Zielenski, J. and L. C. Tsui (1995). "Cystic fibrosis: genotypic and phenotypic variations." Annu Rev Genet **29**: 777-807.

Zito, E., M. Buono, S. Pepe, C. Settembre, I. Annunziata, E. M. Surace, T. Dierks, M. Monti, M. Cozzolino, P. Pucci, A. Ballabio and M. P. Cosma (2007). "Sulfatase modifying factor 1 trafficking through the cells: from endoplasmic reticulum to the endoplasmic reticulum." EMBO J **26**(10): 2443-2453.